

CO₂ as a monomer for the phosgene-free synthesis of new polycarbonates : catalyst development, mechanistic investigations and monomer screening

Citation for published version (APA):

Meerendonk, van, W. J. (2005). *CO₂ as a monomer for the phosgene-free synthesis of new polycarbonates : catalyst development, mechanistic investigations and monomer screening*. [Phd Thesis 1 (Research TU/e / Graduation TU/e), Chemical Engineering and Chemistry]. Technische Universiteit Eindhoven. <https://doi.org/10.6100/IR596016>

DOI:

[10.6100/IR596016](https://doi.org/10.6100/IR596016)

Document status and date:

Published: 01/01/2005

Document Version:

Publisher's PDF, also known as Version of Record (includes final page, issue and volume numbers)

Please check the document version of this publication:

- A submitted manuscript is the version of the article upon submission and before peer-review. There can be important differences between the submitted version and the official published version of record. People interested in the research are advised to contact the author for the final version of the publication, or visit the DOI to the publisher's website.
- The final author version and the galley proof are versions of the publication after peer review.
- The final published version features the final layout of the paper including the volume, issue and page numbers.

[Link to publication](#)

General rights

Copyright and moral rights for the publications made accessible in the public portal are retained by the authors and/or other copyright owners and it is a condition of accessing publications that users recognise and abide by the legal requirements associated with these rights.

- Users may download and print one copy of any publication from the public portal for the purpose of private study or research.
- You may not further distribute the material or use it for any profit-making activity or commercial gain
- You may freely distribute the URL identifying the publication in the public portal.

If the publication is distributed under the terms of Article 25fa of the Dutch Copyright Act, indicated by the "Taverne" license above, please follow below link for the End User Agreement:

www.tue.nl/taverne

Take down policy

If you believe that this document breaches copyright please contact us at:

openaccess@tue.nl

providing details and we will investigate your claim.

CO₂ as a Monomer for the Phosgene-free Synthesis of New Polycarbonates

Catalyst Development, Mechanistic Investigations and Monomer Screening

Wouter Johannes van Meerendonk

The cover picture shows the result of the first successful copolymerization of cyclohexene oxide and CO₂ in the high pressure reactor.

CIP-DATA LIBRARY TECHNISCHE UNIVERSITEIT EINDHOVEN

Meerendonk, Wouter J. van

CO₂ as a Monomer for the Phosgene-free Synthesis of New Polycarbonates : Catalyst Development, Mechanistic Investigations and Monomer Screening / by Wouter J. van Meerendonk. – Eindhoven : Technische Universiteit Eindhoven, 2005.

Proefschrift. – ISBN 90-386-2797-1

NUR 913

Subject headings: copolymerization / polycarbonate ; preparation / polymerization catalysts ; zinc / carbon dioxide / epoxides ; oxiranes / mass spectrometry ; MALDI-ToF-MS / chain transfer

Trefwoorden: copolymerizatie / polycarbonaat ; bereiding / polymerisatiekatalysatoren ; zinc / koolstof dioxide / epoxiden ; oxiranen / massaspectrometrie ; MALDI-ToF / ketenoverdracht

© 2005, Wouter J. van Meerendonk

Printed by PrintService Ipskamp, The Netherlands.

Cover design by Ronald Korporaal, Heerenveen, info@ronaldkorporaal.nl

This project forms part of the research program of the Dutch Polymer Institute (DPI), Engineering Plastics, DPI project #286.

An electronic copy of this thesis is available from the Eindhoven University Library in PDF format (www.tue.nl/bib).

CO₂ as a Monomer for the Phosgene-free Synthesis of New Polycarbonates

Catalyst Development, Mechanistic Investigations and Monomer Screening

PROEFSCHRIFT

ter verkrijging van de graad van doctor aan de Technische Universiteit Eindhoven, op
gezag van de Rector Magnificus, prof.dr.ir. C.J. van Duijn, voor een commissie
aangewezen door het College voor Promoties in het openbaar te verdedigen op maandag
17 oktober 2005 om 16.00 uur

door

Wouter Johannes van Meerendonk

geboren te Amersfoort

Dit proefschrift is goedgekeurd door de promotoren:

prof.dr. C.E. Koning
en
prof.dr. G.J.M. Gruter

Copromotor:
dr. R. Duchateau

“The most exciting phrase to hear in science, the one that heralds new discoveries, is not ‘Eureka!’ (I found it!) but
‘That's funny ...’”
- Isaac Asimov

Table of Contents

Glossary of symbols and abbreviations		9
Chapter 1	Introduction	11
1.1	Chemical routes to polycarbonates	11
1.2	Aim of this study	12
1.3	Outline of this thesis	13
1.4	References	15
Chapter 2	Literature overview	17
2.1	The monomers	17
2.2	Homopolymerization of oxiranes	19
2.3	Coupling of oxiranes with CO ₂	25
2.4	Copolymerization of oxiranes with CO ₂	26
2.5	Known catalysts for the copolymerizations of oxiranes with CO ₂	29
2.6	Other oxirane monomers	45
2.7	Summary and outlook	46
2.8	References	47
Chapter 3	Silsesquioxane zinc catalysts for the alternating copolymerization of cyclohexene oxide and carbon dioxide	55
3.1	Introduction	55
3.2	Results and discussion	58
3.3	Experimental section	70
3.4	Acknowledgements	74
3.5	References	74
Chapter 4	High throughput and mechanistic studies of zinc catalysts	79
4.1	Introduction	79
4.2	Results and discussion	81
4.3	Concluding remarks	96
4.4	Experimental section	97
4.5	Acknowledgements	100
4.6	References	101

Chapter 5	Alternative monomers for polycarbonate synthesis	105
5.1	Introduction	105
5.2	Results and discussion	107
5.3	Concluding remarks	127
5.4	Experimental section	128
5.5	Acknowledgements	132
5.6	References	133
Chapter 6	Physical properties of compression molded parts and coatings of aliphatic polycarbonates	135
6.1	Introduction	135
6.2	Results and discussion	137
6.3	Concluding remarks	146
6.4	Experimental section	146
6.5	Acknowledgements	149
6.6	References	149
Chapter 7	Epilogue and technology assessment	151
Appendix A	Lab scale reactor setup	153
A-1	Introduction	153
A-2	Communication and software setup	154
A-3	LabVIEW	155
A-4	Webcam	156
A-5	References	157
Summary		159
Samenvatting		161
Dankwoord		165
Curriculum Vitae		167
Scientific papers		167

Glossary of symbols and abbreviations

BDI	β -diketiminat ligand
CHO	Cyclohexene oxide
DCM	Dichloromethane
DMA (or DMTA)	Dynamic mechanical (thermal) analysis
DMSO	Dimethylsulfoxide
DSC	Differential Scanning Calorimetry
EO	Ethylene oxide
I	intensity (% or arbitrary units)
M ⁺	Cationization agent (MALDI-ToF-MS analyses)
MALDI-ToF-MS	Matrix-Assisted-Laser-Desorption-Ionization Time-of-Flight Mass-Spectrometry
MPVO	Meerwein-Ponndorf-Verley reduction/Oppenauer oxidation
MWD	Molecular weight distribution
\bar{M}_n	Number averaged molar mass
\bar{M}_w	Weight averaged molar mass
n	Number of repeating units in a polymer chain
PCHC	Poly(cyclohexene carbonate)
PCHO	Poly(cyclohexene oxide)
PCy ₃	Tricyclohexyl phosphine
PDI	Polydispersity index
PEO	Poly(ethylene oxide)
PO	Propylene oxide
PPC	Poly(propylene carbonate)
PPO	Poly(propylene oxide)
PS	Polystyrene
ROP	Ring-Opening Polymerization
SEC	Size Exclusion Chromatography
T	Temperature (°C)
TGA	Thermogravimetric analyses
Tpp	Tetraphenyl porphyrin
T _g	Polymer glass transition temperature (°C)
T _m	Polymer melt transition temperature (°C)

Chapter 1

Introduction

1.1 Chemical routes to polycarbonates

With a global annual demand exceeding 1.5 million tons, polycarbonates form a commercially important class of polymers.¹ Due to their toughness and optical clarity, they are widely used for structural parts, impact-resistant glazing, streetlight globes, household appliance parts, components of electrical/electronic devices, compact discs, automotive applications, reusable bottles, food and drink containers, and many other products.^{2,3} The most important polycarbonate is based on bisphenol-A. Currently, there are two different industrial routes for the synthesis of high molecular weight poly(bisphenol-A carbonate) (BA-PC). The first route involves the interfacial reaction between phosgene and the sodium salt of bisphenol-A in a heterogeneous system. The second route consists of a melt-phase transesterification between a bisphenol-A and diphenyl carbonate (Figure 1-1).¹

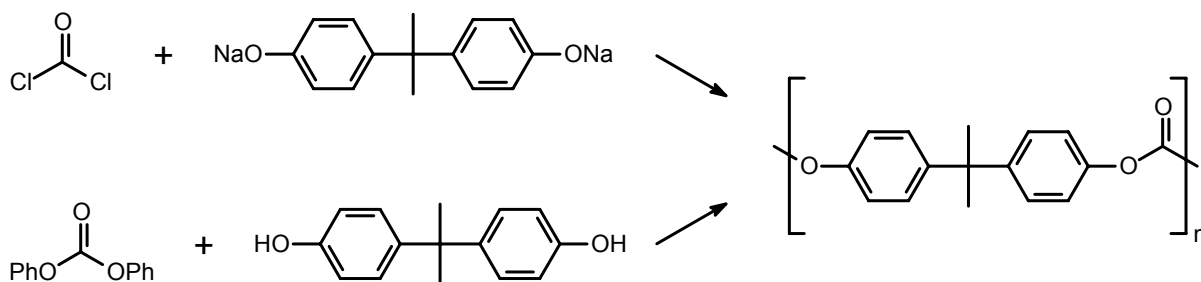


Figure 1-1. Industrial routes to poly(bisphenol-A carbonate).¹

The first route is environmentally undesirable due to the need of the hazardous dichloromethane and phosgene, and the production of large amounts of NaCl as a side product. The second route requires high temperature in order to remove phenol, the high boiling condensation product of this polymerization reaction.

A different approach in synthesizing polycarbonates was demonstrated by Inoue *et al.* in 1969.⁴ They reported the alternating copolymerization of an oxirane with carbon dioxide, resulting in an aliphatic polycarbonate as is depicted in Figure 1-2.

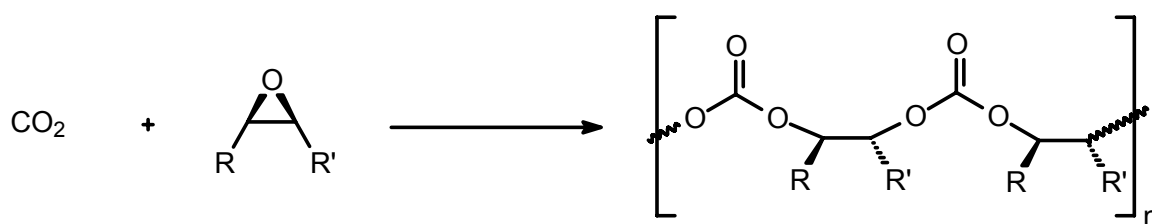


Figure 1-2. Polycarbonate from the copolymerization of an oxirane with CO₂

This approach has several advantages over the current industrial processes. In contrast to the step-growth mechanisms applied in the synthesis of BA-PC, the route reported by Inoue is a chain-growth process. Therefore, in theory, a much better control of molecular weight is feasible and monomer conversions do not have to approach unity in order to obtain high molecular weights. Another advantage is that the used monomers do not possess the safety hazards of the current industrial process based on phosgene. Furthermore, since carbon dioxide is as a renewable resource, a copolymerization process in which carbon dioxide is incorporated into the polymer can be regarded as green chemistry. Other advantages are that carbon dioxide is readily available, cheap, non-flammable and non-toxic.⁵ Unfortunately, the nature of these copolymerizations limits the type of backbone to an aliphatic C2 bridge. Consequently, the physical properties of the polymers are difficult to improve in order to match the good impact strength, heat resistance and transparency of commercially available poly(bisphenol-A carbonate).⁶ The use of larger cyclic ethers like oxetanes is difficult since they are usually not reactive enough, due to the lack of ring strain, to efficiently copolymerize with CO₂. Besides, such ethers are not expected to improve the physical properties.

1.2 Aim of this study

This project was initiated to develop more insight into the environmentally friendly process of preparing polycarbonates, to optimize the process and to obtain polycarbonates with desirable physical properties. To achieve this, different, potential property enhancing, monomers were chosen. To investigate the mechanistic aspects of these copolymerizations cyclohexene oxide, a known and easy to handle monomer, was used. Despite the significant amount of research already done on copolymerizations of oxiranes and CO₂ (see chapter 2), several intriguing questions still remain unanswered. The lack of conformity in copolymerization behavior of the different classes of catalysts as well as the exact mechanism of copolymerization are both still puzzles waiting to be solved.

As for the polymer characteristics of aliphatic polycarbonates, there is plenty of room for improvement. Poly(cyclohexene carbonate) (PCHC), which is often used by research groups investigating these copolymerizations, is a very brittle polymer with a T_g far below the value of the

T_g of poly(bisphenol-A carbonate) (118 °C versus 150 °C). Other aliphatic polycarbonates like poly(ethylene carbonate) (PEC) and poly(propylene carbonate) (PPC) have even lower T_g values (around 10 °C and 25 °C, respectively).⁷ Engineering plastics,⁸ however, are typically used below their T_g , and therefore the glass transition temperature should be as high as possible. To address these issues the following goals were defined at the start of the project, in addition to the already mentioned enhancements in mechanistic insight:

- 1) Development of suitable catalysts for the formation of new polycarbonates from bulky epoxides and CO₂.
- 2) Polymerization of CO₂ with bulky epoxides, resulting in relatively high T_g polycarbonates (and possible polyesters) suitable for engineering plastic and or coating applications. In order to establish structure-property relationships, the new polymers are to be molecularly and physically characterized.
- 3) Studying and modeling the phase behavior during polymerization in (high pressure) carbon dioxide with the aim of designing a preliminary, environmentally benign process for the production of new polycarbonates.

The third goal was tackled within the framework of a cooperation between the polymer chemistry group and the process development group, both at the Eindhoven University of Technology.

1.3 Outline of this thesis

This study can roughly be divided into three parts: a) Search for suitable catalysts and the investigation into their copolymerization behavior (chapters 2, 3 and 4). b) The design, synthesis and testing of T_g enhancing monomers (chapter 5). c) Discussion of polymer properties and potential applications (chapters 6 and 7).

In **chapter 2** a literature overview of catalysts for the copolymerization of oxiranes and CO₂ is presented. Relevant side reactions, like the homopolymerization of oxiranes and the formation of cyclic carbonates, as well as the different proposed copolymerization mechanisms will be discussed to give the reader a thorough understanding of the chemistry involved. Three classes of catalysts (β -diketiminato zinc, porphyrinato chromium and bis(phenoxy) zinc) were selected, synthesized and used for copolymerizations in chapters 4, 5 and 6.

In **chapter 3** the use of silsesquioxane zinc compounds as catalysts for the copolymerization of oxiranes with CO₂ will be discussed. Several complexes will be investigated and their phase behavior will be linked to the conversion. Since incompletely condensed silsesquioxanes can be regarded as realistic model systems for various types of silica surface silanol sites, the corresponding silsesquioxane zinc complexes serve as models for heterogeneous silica supported zinc catalysts. To confirm this, the copolymerization with both the silsesquioxane- and silica-based zinc catalysts have been studied and compared.

A detailed mechanistic study into the most promising class of catalysts (β -diketiminato zinc complexes) will be discussed in **chapter 4**. Together with the results of a high throughput validation with these complexes, several unprecedented side reactions that were observed will be addressed. It will be shown that rearrangement of cyclohexene oxides plays a significant role in the copolymerization under the reaction conditions used by us and that a very fast chain transfer takes place in the presence of alcohols. End group analyses with MALDI-ToF-MS proved to be a very powerful tool to investigate the mechanistic aspects of the copolymerization behavior with different catalysts.

In **chapter 5** the use of alternative monomers will be discussed. Several ester and amide substituted cyclohexene oxide monomers were synthesized and their copolymerization behavior is investigated. It will be shown that copolymers with CO₂ can be obtained and that several interesting side reactions occur during polymerization. Molecular weights obtained thus far are very low, hindering practical applications.

Chapter 6 will present a short discussion of the thermal and physical properties of poly(cyclohexene carbonate) (PCHC). The influence of the molecular weight distribution on the properties of PCHC will be investigated and compared to a commercial poly(Bisphenol-A carbonate) (BA-PC) sample. It will be shown that (molded) samples of PCHC are very brittle, but have a higher tensile modulus and UV transparency than BA-PC making them more suitable for coating applications. It will be shown that cross-linked PCHC-based coatings can indeed be prepared and their characteristics will be discussed.

In **chapter 7** a technology assessment of the industrial use of the aliphatic polycarbonates used in this thesis will be provided as well as some comments and suggestions for further research in this field.

Finally in the **appendix** a general description of the autoclave, used for most of the polymerizations discussed in this thesis, will be given.

1.4 References

- 1 Gross, S. M.; Flowers, D.; Roberts, G.; Kiserow, D. J.; DeSimone, J. M. *Macromol.* **1999**, *32*, 3167.
- 2 <http://www.bisphenol-a.org/>
- 3 Crivello, J. V.; Rajaraman, S.; Mowers, W. A.; Liu, S. *Macromol. Symp.* **2000**, *157*, 109.
- 4 Inoue, S.; Koinuma, H.; Tsuruta, T. *Polym. Lett.* **1969**, *7*, 287.
- 5 (a) Super, M. S.; Beckman, E. J. *Trends Polym. Sci.* **1997**, *5*, 236. (b) Beckman, E. J. *Science* **1999**, *283*, 946.
- 6 (a) Freitag, D; Grigo, U.; Müller, P. R.; Nouvertné, W. "Polymer carbonates", in: *Encyclopedia of Polymer Science and Engineering*, 2nd edition, Mark, H. F.; Bikales, N. M.; Overberger, C. G.; Menges, G.; Eds., John Wiley & Sons, New York 1998, Vol. 11, p. 648. (b) Freitag, D.; Fengler, L. *Angew. Chem. Int. Ed.* **1991**, *30*, 1598.
- 7 Thorat, S. D.; Phillips, P. J.; Semenov, V.; Gakh, A. *J. Appl. Pol. Sci.* **2003**, *89*, 1163.
- 8 A broad term covering those thermoplastics (with or without fillers or reinforcements) which retain their mechanical, chemical and thermal properties up to a temperature of around 200°C, and which are suitable for use under conditions of high impact, heat and/or moisture.

Chapter 2

Literature overview

Abstract

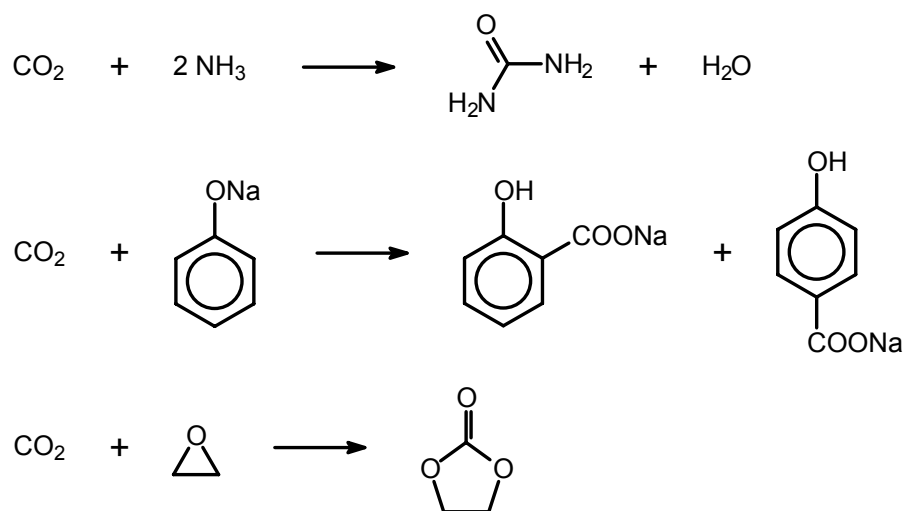
In this chapter the current state-of-the-art will be presented on the direct syntheses of polycarbonates from carbon dioxide and oxiranes. While some patents are mentioned in this review, it is not our intention to include all the available patent literature. More elaborate overviews can be found in some recent reviews.¹

2.1 The monomers

A short introduction of the chemistry related to the monomers used in the copolymerization of carbon dioxide and oxiranes is presented in this section.

2.1.1 Carbon dioxide

With the growing concern about the environmental impact of chemical substances, the chemical fixation of carbon dioxide has received increasing attention as a potential carbon source in industrial chemical processes.² Carbon dioxide is generally considered as a green, environmentally benign solvent and reactant that is cheap, non-toxic and renewable. Use of carbon dioxide could even result in more economical and/or efficient routes to existing products. Moreover, the production of chemicals and polymers from CO₂ might result in new materials. Nowadays there are three important industrial processes with carbon dioxide as a starting material: the synthesis of urea, salicylic acid and cyclic carbonates (Scheme 2-1).³ Approximately 110 megatons of carbon dioxide is currently used for chemical synthesis on a yearly base. The majority (90 megatons) is used for urea production (mainly used as a fertilizer). In addition to these commercial applications of carbon dioxide as a feedstock, several intriguing processes involving the chemical fixation of CO₂ are under investigation. The most promising processes are methanol synthesis and the production of aliphatic polycarbonates using carbon dioxide as feedstock.



Scheme 2-1. Several important uses of CO₂ in chemical industry; synthesis of, urea, salicylic acid and cyclic carbonates.

2.1.2 Oxiranes

Oxiranes, also known as epoxides, are three-membered cyclic ethers. This small ring is under a considerable strain (calculated around 27 kcal · mol⁻¹ for an epoxide) and is therefore very reactive towards a great number of nucleophiles (Figure 2-1).⁴

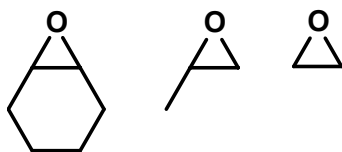
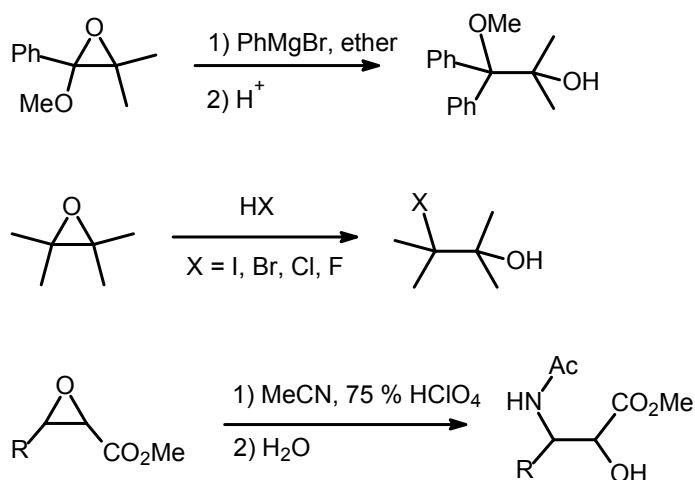


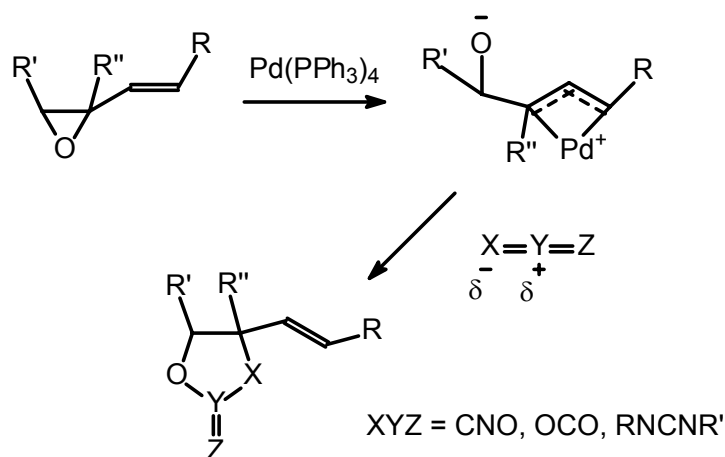
Figure 2-1. Cyclohexene oxide (CHO), propylene oxide (PO) and ethylene oxide (EO).

The use of oxiranes in organic chemistry is quite extensive⁵ and some examples are the addition reactions of oxiranes with Grignard and alkyl lithium reagents⁶, halide acids⁷ or nitriles⁸ (Scheme 2-2).



Scheme 2-2. Several organic reactions with oxiranes.

Cycloadditions are also possible. For example, Shim et al. reported the palladium catalyzed regioselective [3+2] cycloaddition of vinylic oxiranes with activated olefins (Scheme 2-3).⁹



Scheme 2-3. Palladium catalyzed cycloadditions.⁹

2.2 Homopolymerization of oxiranes

Oxiranes are fairly reactive organic compounds (vide supra) especially when compared to the relatively inert CO₂ molecule. When oxiranes are used as co-monomers in polycarbonate syntheses, the difference in reactivity can result in homopolymerization to polyethers due to an undesired side reaction. Since this homopolymerization can be a seriously competing reaction, this undesired process will be described first.

In 1863, Wurtz was one of the first researchers to make macromolecules via the oligomerization of oxiranes. About 64 years later, Levene reported the first successful polymerization of propylene-oxide (1927). After the Second World War the development of the petrochemical industry led to the large-scale production of ethylene-oxide and propylene-oxide.¹⁰ Most synthetic routes are based on the oxidation of double carbon bonds with oxygen or peroxides. The most important commercial processes involve the direct air oxidation of an olefin over a silver catalyst or through the halohydrin process.¹¹

Oxiranes can be polymerized by both anionic, cationic and coordination mechanisms due to the ring strain of the 3-membered ring (vide supra). Apart from these two mechanisms, a lot of research has been performed with coordination-type catalysts.

2.2.1 Stereochemistry

When using asymmetrical oxiranes as monomers in a (co)polymerization reaction, the stereochemistry of the obtained polymer is of large influence on the properties of the polymer, such as its melting point and crystallinity.¹² The stereochemical aspects of these ring opening

polymerizations are largely similar to the ones found in α -olefin polymerizations (propylene, 1-hexene, styrene etc.). The regio and stereo isomerism observed in the polymerization will be explained in the following paragraphs with poly(propylene oxide) (PPO) as an example.

2.2.2 Regio isomerism

For asymmetric oxiranes, like PO, the bond cleavage for the ring opening can occur at two different places (Figure 2-2). The cyclic ether can be cleaved at the methine-oxygen bond (α) or the methylene-oxygen bond (β).¹³

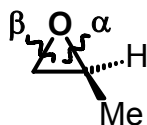


Figure 2-2. Ring opening of propylene-oxide.¹³

(Co)polymerization of asymmetric oxiranes can result in (co)polymers with different stereo isomers as depicted in Figure 2-3. These different isomers can be identified by ¹³C NMR as was shown by Goriot et al.¹⁴

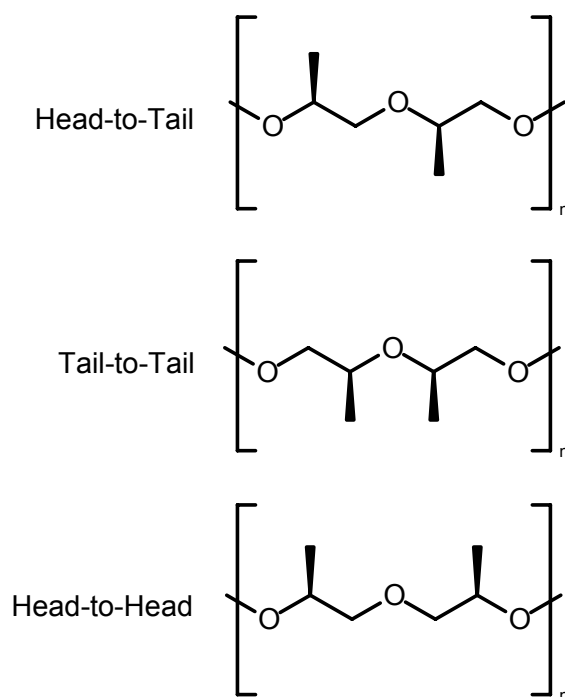


Figure 2-3. Regio isomers of poly(propylene oxide).

Usually an asymmetric monomer has a preferred direction for incorporation into a growing chain. Monomers like propylene, styrene or vinyl chloride have a large preference for head-to-tail

incorporation. For oxiranes this preference is much lower and gives rise to head-to-head and tail-to-tail units in the polymer chain. Usually ring opening takes place at the less hindered β -carbon atom.

2.2.3 Stereo isomerism

Another form of isomerism is stereo isomerism. Propylene-oxides exist in both the R- and S-optical form and the stereochemistry of the obtained polymers can be described in terms of tacticity (Figure 2-4). If all monomer units have the same optical configuration, the polymer is said to be isotactic. When monomer units have an alternating inverted optical configuration, the polymer is said to be syndiotactic. When the optical configuration is completely random, an atactic polymer is obtained.

In order to obtain an isotactic polymer, one option is to use only one enantiomer of the monomer, which is expensive or use a racemic mixture of chiral catalysts.¹⁵

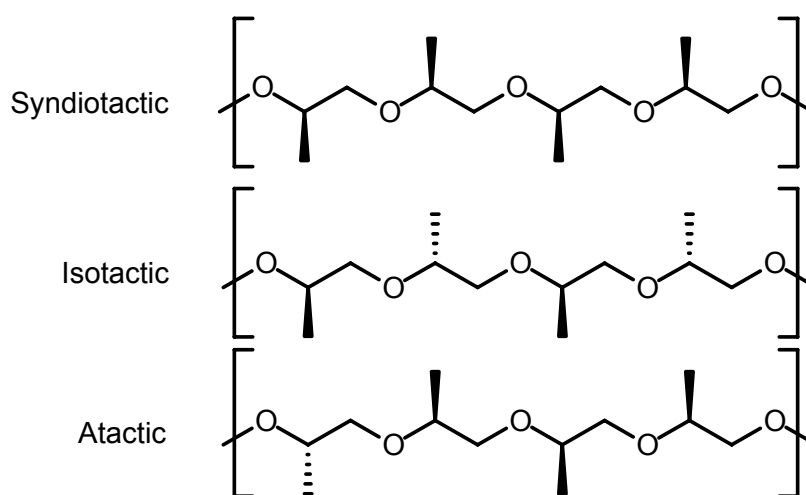
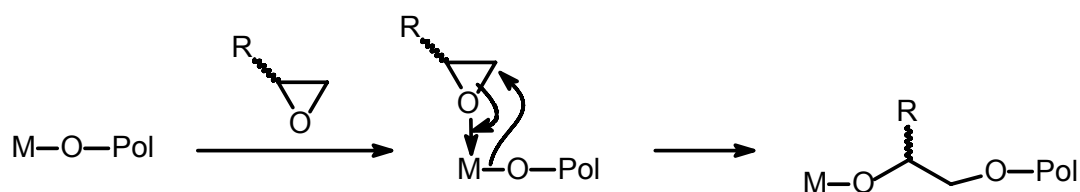


Figure 2-4. Tacticity of poly(propylene oxide).

Two types of stereochemical control exist: 1) Chain end control, where the growing chain induces selective incorporation of a monomer.¹⁶ 2) Enantiomeric site control, where the enantioselective incorporation is induced by ligands around the metal center.¹⁷

2.2.4 Homopolymerization of oxiranes, coordination mechanism

In the following section an overview will be given of the homopolymerization of oxiranes with coordination type catalysts. In a coordination mechanism, the propagation step occurs at the metal center by insertion of a pre-coordinated monomer in the metal-alkoxide bond of the growing chain (Scheme 2-4). This mechanism is comparable to the polymerization mechanism encountered in catalytic olefin polymerization, where a pre-coordinated olefin inserts into a metal-carbon bond.



Scheme 2-4. Coordination mechanism in the homopolymerization of PO.

One of the first catalyst systems, able to polymerize oxiranes through a coordination mechanism, was a FeCl_3/PO system.¹⁸ The most commonly used types of coordination catalysts are dialkyl zinc and trialkyl aluminum compounds in conjunction with an alcohol or water. Compared to cationic or anionic polymerization, these systems offer several advantages. The polymers formed via a coordination mechanism generally have a higher molecular weight. A coordination mechanism also has the potential to control the stereochemistry of the polymers because the propagation step occurs at the metal center and the ligand system can influence the orientation of the polymer chain and the monomer.

Unfortunately, most catalyst systems are only able to generate polymers with an isotacticity of about 40-70%.^{19,20} Another disadvantage is the rather low rate of polymerization compared to the anionic or cationic polymerization. An example of a commercial process using a coordination mechanism is the ring opening polymerization of propylene-oxide with a calcium amide/alkoxide catalyst.²¹

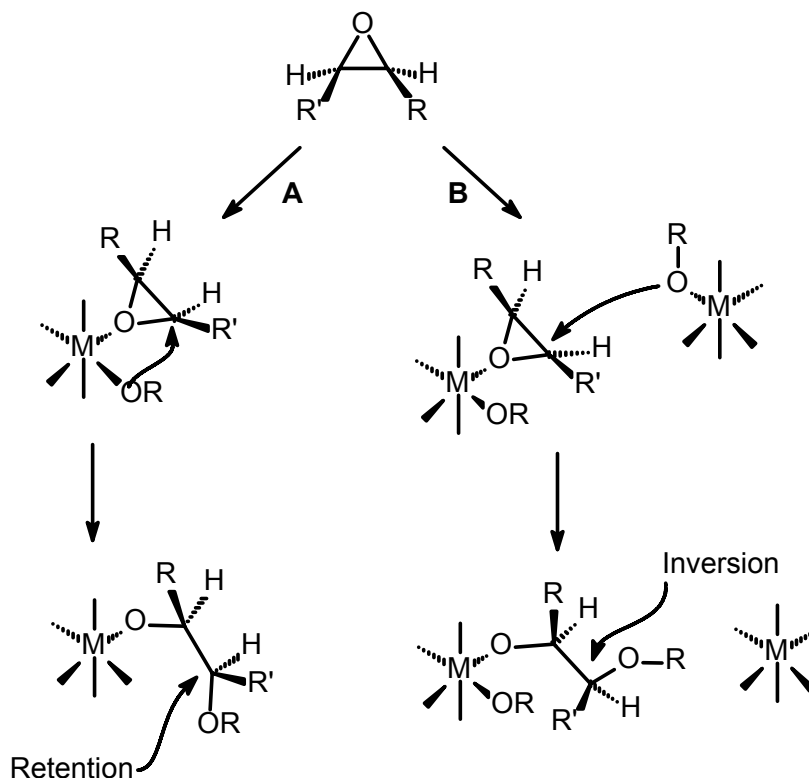
2.2.4.1 Initiation

Initiation of the polymerization requires a vacant coordination site at a Lewis acidic metal center and a reactive bond in which the oxirane can insert. This is usually a metal alkoxide bond. The initial formation of a catalyst-oxirane adduct can be a very exothermic reaction and can generate a lot of heat. Wu et al. found that sometimes the initial preparation of an oxirane adduct under controlled conditions is required to prevent overheating of the polymerization mixture, as is the case with an FeCl_3 catalyst.²⁰

2.2.4.2 Propagation

When a 1,2-bis-substituted monomer is used, the stereochemistry of the methane bond where the ring opening takes place depends on the type of coordination mechanism. Propagation can occur at either a single metal center (pathway A) or at two separate metal centers (pathway B) as depicted in Scheme 2-5.²² Pathway A involves a migratory insertion of the monomer, similar to the

mechanism for olefin polymerization²³, while the stereochemistry of the chiral methine carbon with the R' substituent is retained. In pathway B, another metal center activates the monomer and the nucleophilic attack of the polymer occurs at the other side of the monomer inducing an inversion of stereochemistry at the methine carbon. When a bimetallic metal complex is involved, where the metal centers are in close vicinity of each other, nucleophilic attack is more likely to take place at the same side of the monomer (pathway A-like, retention).

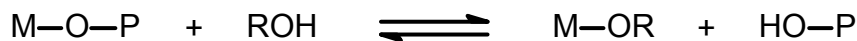


Scheme 2-5. Single (pathway A) vs. multiple (pathway B) metal sites involved in the propagation step of the coordination mechanism.²²

In contrast to the widely applied anionic polymerization of propylene-oxide, a coordination mechanism induces a larger amount of misinsertions (regio isomerism): i.e. insertion after an α -ring opening (see Figure 2-2). This can be explained by the enhanced polarization of the α -bond due to the cationic metal center. In addition, a methyl group can stabilize the formed cation after ring opening. The amount of misinsertions was studied in detail by Jacquier-Gonod et al. by ¹H and ¹³C NMR spectroscopy.¹³ They used several aluminum and rare earth alkoxides for the polymerization of PO.

During the normally living polymerizations only one chain per catalyst is produced. Therefore a chain transfer reagent (usually an alcohol) is often used to control molecular weight (Scheme 2-6).²⁴ This reversible reaction is used to induce the so-called ‘immortal’ polymerization. It is called ‘immortal’ since re-initiation and further polymerization of a chain-end remains possible after termination with a protic species like methanol or water. The termination leads to polymers with

hydroxyl chain-ends, which on their turn can also act as another chain transfer reagent. A clear advantage is the possibility to have a good control over the polymerization process.



Scheme 2-6. Schematic representation of a chain transfer reaction.

2.2.4.3 Recent developments

In 1999, Thiam et al. reported a new class of catalysts based on yttrium-isopropoxides and bimetallic isopropoxides of yttrium and aluminum.²⁵ These catalysts are able to polymerize cyclohexene oxide at room temperature.

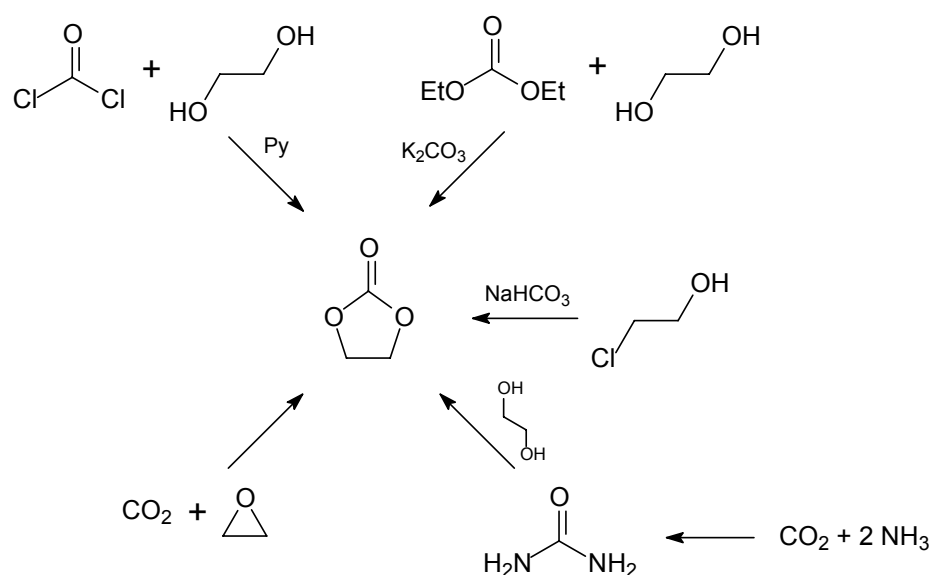
Another development is the use of supported catalysts. Hamaide et al. developed a heterogeneous system comprising a metal alkoxide grafted on silica or alumina support.²⁶ The positive effect of the support on the activity and kinetics of the polymerization of EO and PO was found to be quite strong. The best results were obtained for supported zirconium alkoxides. Another supporting material was introduced by Zeng et al. who used some chitosan supported rare earth metal complexes. In conjunction with a triisobutyl aluminum cocatalyst, this system is able to produce high molecular weight polymers of propylene-oxide with an isotactic content of about 40%.¹⁹

The use of a Lewis acidic cocatalyst to accelerate nucleophilic reactions is widely known in other areas, but its effect on the polymerization of oxiranes is usually low.²⁷ An example of a multicomponent system was reported by Ge et al.²⁸ They used two multicomponent rare earth catalytic systems for the ring opening polymerization of styrene-oxide. The exact structure and properties of these multicomponent systems is not fully known. The thus obtained poly(styrene-oxide) consisted of regular head-to-tail atactic polymers.

One of the most successful attempts to synthesize isotactic poly(propylene-oxide) was reported by Wu et al.²⁰ The polymerization of PO with an isobutylalumoxane-PO adduct yielded a polymer with a molecular weight of about $160 \text{ kg} \cdot \text{mol}^{-1}$ and with an isotactic content of 90-100%. Unfortunately, the structure of the catalyst is not fully characterized, as is the case with most aluminoxanes.²⁹ Therefore, the effect of modification of the catalyst system is unpredictable. Furthermore, it is unknown at present if the polymer has a stereo-block structure (i.e., copolymers with blocks of -RRRR- and -SSSS- connected by an -RS- or -SR-unit) or if a mixture of R- and S-polymers is formed.

2.3 Coupling of oxiranes with CO₂

Coupling of oxiranes and CO₂ can either result in polycarbonates or cyclic carbonates. Cyclic carbonates can be used as an alternative non-flammable solvent or monomer in ring opening polymerizations (ROP). The selective synthesis of these cyclic carbonates is under investigation since the early 1930s. In 1943, Vierling at I.G. Farbenindustrie was the first to report the synthesis of cyclic carbonates by the direct coupling of oxiranes with carbon dioxide.³⁰ The reaction was catalyzed by sodium hydroxide on activated charcoal, but the yields were low as the catalyst was short-lived. Many kinds of catalysts have been developed since to accelerate this reaction, including amines, onium salts, metal oxides, metal halides and several transition metal complexes. An excellent review on the synthesis and ring opening polymerization of cyclic carbonates was recently published by Rokicki and provides a good overview of this chemistry.³¹

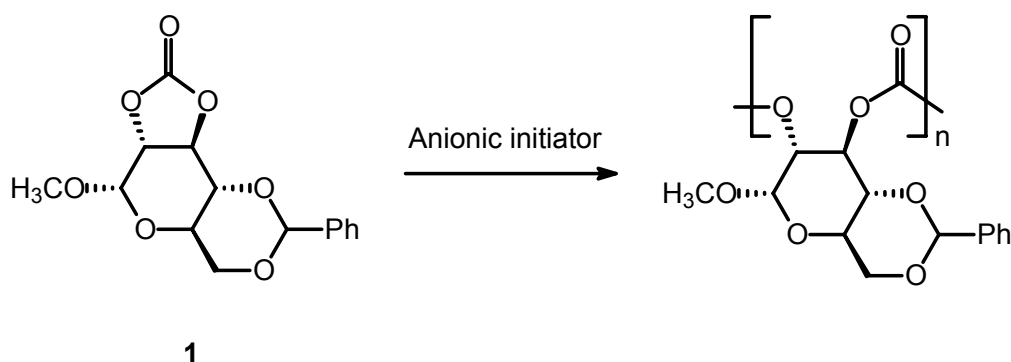


Scheme 2-7. Several routes to cyclic carbonates.

The ring opening polymerization of six- and larger membered cyclic carbonates is quite easy and shows potential for the controlled synthesis of aliphatic polycarbonates with C3 or longer alkyl chains in the backbone.³² These six-membered cyclic carbonates are harder to prepare, however, because they can normally not be prepared by the coupling reaction of CO₂ with a four-membered cyclic ether as these oxetanes have less ring-strain and are therefore less reactive.

Five-membered cyclic carbonates are easier to prepare, but are much harder to use for the production of polycarbonates via ring opening polymerizations since this is thermodynamically not favorable. The enthalpy of formation for the ring opening polymerization of ethylene carbonate is for example 125.6 kJ/mol and only partial release of CO₂ raises the entropy enough to compensate. As a consequence, the maximum content of CO₂ is around 50%³³ with the use of tin and zirconium metal alkoxides.³⁴ An exception to this case is the ring opening polymerization of compound **1**

(Scheme 2-8). This tricyclic compound can be anionically polymerized without the loss of CO₂ due to the abnormal ring strain which makes the ring opening polymerization thermodynamically possible.³⁵

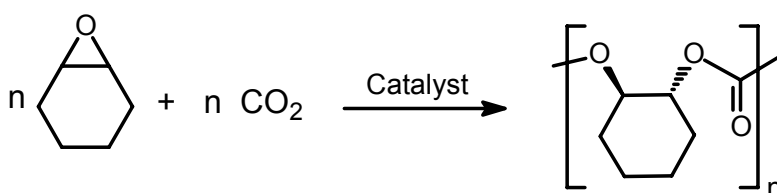


Scheme 2-8. Ring opening polymerization of a five membered cyclic carbonate with retention of CO₂.³⁵

2.4 Copolymerization of oxiranes with CO₂

2.4.1 Aliphatic polycarbonates

As discussed in the previous paragraph, aliphatic polycarbonates can be prepared by the ring opening polymerization of cyclic carbonates. In the case of 5-membered cyclic carbonates this is very difficult, but a more direct route to C2 bridged aliphatic polycarbonates is also possible. Originally discovered by Inoue et al. in 1969, the direct copolymerization of oxiranes with CO₂ has been extensively investigated (Scheme 2-9).³⁶ Reports on the copolymerization of carbon dioxide and four- or higher membered cyclic ethers are scarce due to the reduced reactivity as mentioned earlier (see paragraph 2.3). Baba, however, succeeded in the alternating copolymerization of oxetane with CO₂ with the use of organotin halide/PBu₃ catalysts.³⁷



Scheme 2-9. Copolymerization of carbon dioxide and cyclohexene oxide.

2.4.2 Stereochemistry

In the copolymerization of oxiranes, cyclohexene oxide (CHO) is frequently used. While cyclohexene oxide usually exists in the *cis* form, incorporation into a polymer chain can in principle lead to both *cis* and *trans* configurations of the cyclohexene unit (Figure 2-5). Investigations by Inoue et al. revealed the existence of only the *trans* configuration. During polymerization the stereochemistry of the CHO monomer is inverted with respect to the *cis* epoxide monomer.³⁸

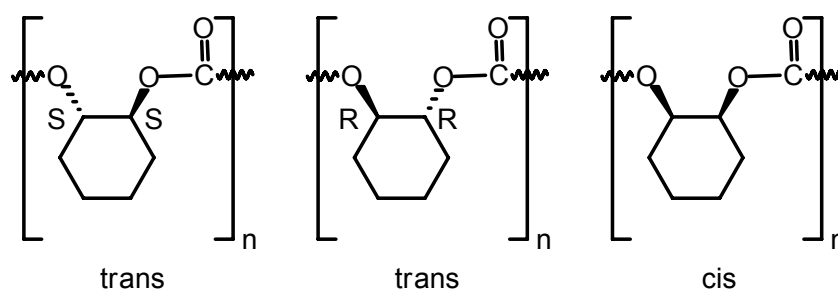
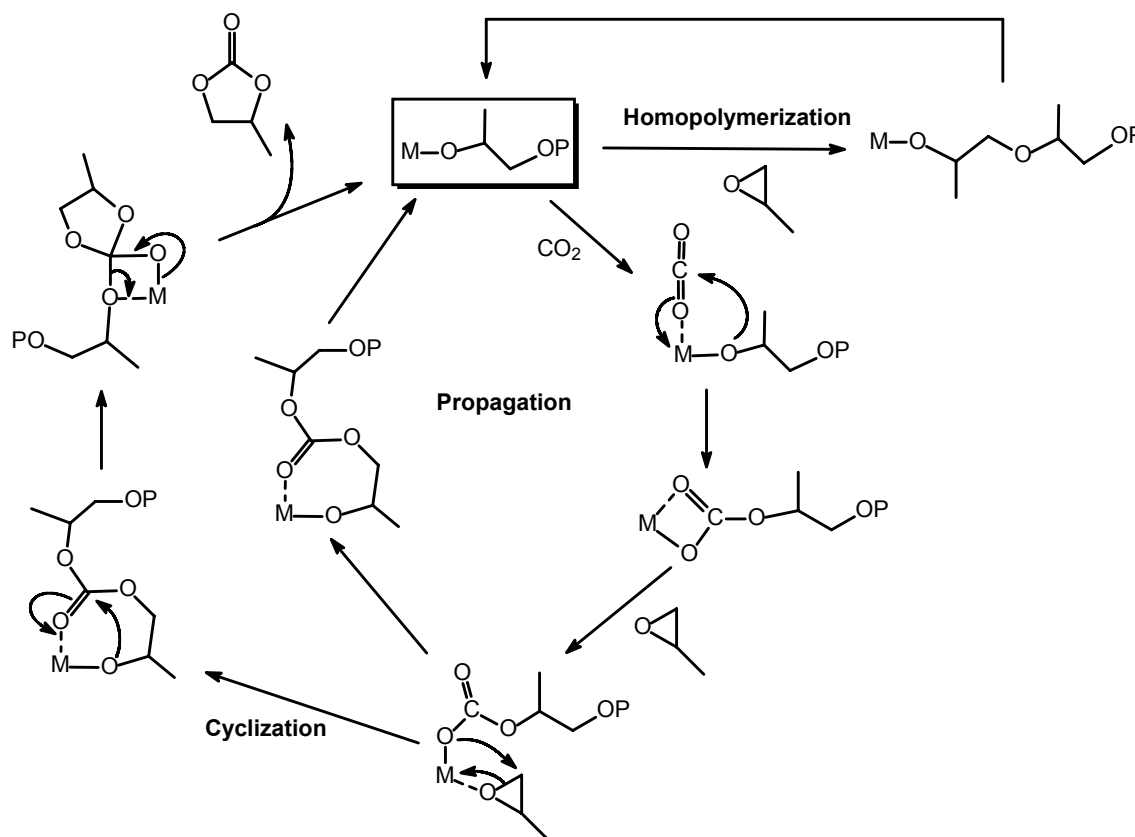


Figure 2-5. Stereochemistry in a poly(cyclohexene carbonate) chain.

2.4.3 General copolymerization mechanism

In the last decade a lot of effort has been put in the elucidation of the copolymerization mechanism. In general the copolymerization mechanism can be summarized as shown in Scheme 2-10. In a typical polymerization propagation cycle, the first step is the insertion of a carbon dioxide molecule into the metal-alkoxide bond. After insertion of an oxirane in the carbonate metal bond, either reinsertion of carbon dioxide can take place (propagation reaction), or cyclization occurs. If the polymer alkoxide end group reacts with an oxirane instead of a CO_2 unit, a less perfectly alternating polymer is formed.



Scheme 2-10. PO/ CO_2 Copolymerization mechanism and side-reactions.

2.4.4 *Supercritical carbon dioxide as both a solvent and monomer.*

In the search for new polymerization solvents supercritical fluids have received quite some attention lately.³⁹ A supercritical state is a hybrid state between fluid and gas. Like a liquid, a supercritical fluid can dissolve solutes and is relatively dense. Like a gas, it has a low viscosity, is easily compressed and can easily be mixed with other gasses. One of the earliest uses of a supercritical solvent for a chemical reaction was developed in the late 1930's for the production of low density poly(ethylene) (LDPE).⁴⁰ Of the supercritical fluids available, scCO₂ is one of the more popular choices. The critical conditions of CO₂ can be reached quite easily ($T_c = 31.1^\circ\text{C}$, $P_c = 73.8$ bar, $\rho_c = 0.47 \text{ g cm}^{-3}$) and CO₂ is a non-toxic, non-flammable, cheap and abundant gas to work with.⁴¹ Furthermore, as an ambient gas, CO₂ can easily be recycled after use as a solvent. Cooper wrote an extensive review in 2000 on the use of scCO₂ in polymer synthesis and processing.⁴¹

The use of supercritical CO₂ (scCO₂) as both solvent and monomer for the copolymerizations of oxiranes with CO₂ was first reported by Darensbourg et al.⁴² One of the major problems of using scCO₂ is its low polarity leading to low solubilities of the polymers and catalysts. A solution to this problem is the incorporation of fluoro substituted alkyl or silyl side groups in the catalysts or polymers, which increase the solubility drastically.^{43,44} A disadvantage, especially for the fluoro-substituted compounds, is their high cost. A detailed account on the effect of molecular architecture on the phase behavior was studied by Lepilleur et al. with some fluoroether-functional graft copolymers.⁴⁵

Recently Sarbu et al. reported the development of organic (C, H and O containing) CO₂-philics. The developed CO₂-philics consisted of either a polyether backbone with a number of carbonyl containing side groups, or a polyether chain with a number of carbonate groups incorporated.⁴⁶ Raising the carbonate contents above about 40% significantly raised the cloud point pressure. Sarbu et al. proposed that a requirement for a good CO₂-philic polymer chain is a flexible chain and therefore a low T_g .⁴⁷ The used polymers had a degree of polymerization of ± 25 , which resulted in an additional influence of the end groups on the solubility. Another way to increase the solubility of catalysts and polymers in scCO₂ is the addition of small amounts of organic co-solvents.

The phase behavior of carbon dioxide and CHO mixtures was extensively studied by Super et al.⁴⁸ They observed a sharp increase in the phase boundary between a one- and a two-phase system when small amounts of polymer were present. Another observation was the fact that homopolymerization of CHO was initiated by trace amounts of water above 383 K.

The outcome of a polymerization experiment depends greatly on the phase behavior during the polymerization.⁴⁴ In a binary system, it is possible to have an oxirane rich and an oxirane poor

layer. Depending on the preference of the catalyst for one of the layers, very different polymers and activities can be obtained. This behavior depends also on the ability of the oxirane to solubilize carbon dioxide and/or the catalyst.

Also for non-supercritical applications, CO₂ is a good choice for some reactions. Condensation of CO₂ in organic solvents (like toluene, acetonitrile, ethanol and ethyl acetate) at sub-critical conditions allows for an expanded solvent system with some clear advantages over their neat counterparts. Issues as reaction gas permeability (O₂ for example), solubility of catalysts and reactants, heat dissipation and workup procedures can all benefit from these expanded solvents without the need to go to supercritical conditions. Examples of successful application areas are homogeneous catalytic oxidations⁴⁹ and epoxidations.⁵⁰

2.5 Known catalysts for the copolymerizations of oxiranes with CO₂

Several systems are known to copolymerize oxiranes with other organic fragments, such as CO₂ or SO₂ (Figure 2-6). The majority of the work is focused on the copolymerization of oxiranes with CO₂ using zinc based catalyst systems, but more recently also aluminum, chromium, cobalt, manganese and iron catalysts were reported. A summary of the most interesting catalysts will be given in the following paragraphs. The most frequently used oxirane is cyclohexene oxide (CHO), which is one of the most reactive and easily handled oxiranes.

General notes: The activity of polymerization catalysts is usually expressed in gram(polymer) · gram(metal)⁻¹ which is the notation used in the industry. This value is of limited use, since it is not normalized for the reaction time. Furthermore, this value is normalized to 1 g of metal. For easier comparison of the different available system, it is better to express the activity per mol of catalyst. In this chapter it will be attempted to present the activities normalized to one hour and express them as a Turn Over Frequency, TOF = mol of monomer consumed · mol of catalyst used⁻¹ · hour⁻¹. Another point of consideration is that the copolymerization rates slow down dramatically at higher molecular weights and conversions (high viscosity limits mass transfer), making the comparison between different reports often difficult. Some articles only report the yield of polymerization, i.e. how much of the oxirane is used before the reaction is stopped. These values will not be taken into account.

1	H																	He
2	Li	Be										B	C	N	O	F		Ne
3	Na	Mg										Al	Si	P	S	Cl		Ar
4	K	Ca	Sc	Ti	V	Cr	Mn	Fe	Co	Ni	Cu	Zn	Ga	Ge	As	Se	Br	Kr
5	Rb	Sr	Y	Zr	Nb	Mo	Tc	Ru	Rh	Pd	Ag	Cd	In	Sn	Sb	Te	I	Xe
6	Cs	Ba		Hf	Ta	W	Re	Os	Ir	Pt	Au	Hg	Tl	Pb	Bi	Po	At	Rn
7	Fr	Ra		Rf	Ha	Sg	Ns	Hs	Mt	Uun								

(6)	La	Ce	Pr	Nd	Pm	Sm	Eu	Gd	Tb	Dy	Ho	Er	Tm	Yb	Lu
(7)	Ac	Th	Pa	U	Np	Pu	Am	Cm	Bk	Cf	Es	Fm	Md	No	Lr


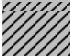
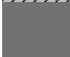
	Active
	Active in combination with other metals
	Co-catalyst required for best performance

Figure 2-6. Metals for catalysts reported to copolymerize oxiranes and CO₂.

2.5.1 Zinc catalysts

Various transition and main group metals are able to form cyclic carbonates from oxiranes and CO₂. With the exception of Al(III) complexes, only transition and rare earth metal complexes have been reported to make alternating CO₂/oxirane copolymers. Catalysts based on zinc form the most extensively studied class of catalysts for the copolymerization of carbon dioxide and oxiranes. Active zinc catalysts for the copolymerization of oxiranes with CO₂ can be split into a few main groups; i.e. partly hydrolyzed bis(alkyl), carboxylate, bis(phenoxy), and β -diketiminato zinc complexes. The hydrolyzed bis(alkyl) and the carboxylate zinc complexes are usually heterogeneous in nature, making them difficult to study in detail. However, their cheap and easy synthesis makes them industrially attractive. The β -diketiminato zinc complexes are the best defined catalysts and easier to study from a mechanistic point.

2.5.1.1 Partly hydrolyzed bis(alkyl) zinc complexes

The first group of zinc catalysts consists of partly hydrolyzed zinc bis(alkyls) and includes the first copolymerization system (ZnEt₂/H₂O) reported by Inoue et al.^{36,38,51} The catalysts are prepared by adding a certain amount (usually 0.5 equivalents) of an alcohol or water to a bis(alkyl) zinc

precursor. The result is an ill-defined mixture of different multinuclear catalytic species. Copolymers obtained with these catalysts tend to have a very broad molecular weight distribution. Furthermore, the turnover numbers of these catalysts are usually low. These disadvantages can be explained by the multinuclear nature of these catalysts. Different chemical sites produce different polymers as not every metal center is equally accessible for the monomers. An interesting observation with these systems was reported by Inoue et al. in 1975 when they copolymerized styrene oxide with CO₂. With this monomer, the ring opening takes place primarily at the methine oxygen bond in contrast to the methylene oxygen bond, which is more common with propylene oxide and derivatives.⁵²

Jansen et al. reported the use of zinc alkyl/water catalysts in the syntheses of side-chain liquid crystalline polycarbonates.⁵³ These polymeric liquid crystals have some interesting electrical and optical properties. Some novel oxiranes were used with biphenyl and with alkoxyphenyl benzoate mesogenic groups with alkoxy tails ranging from 1 to 8 carbon atoms. Polymerization yields were low and the carbonate content was around 70%. Mechanistic details of these (probably) multinuclear catalysts are not widely investigated.

2.5.1.2 Zinc carboxylates

In the second group of zinc catalysts, (di)carboxylic acids are used as ligands. In the early 90's some patents were filed by several companies, including ARCO Co. and Mitsui Petrochem. Ind., on the use of some polycarboxylate zinc complexes for the production of poly(propylene carbonate) (PPC).⁵⁴ The copolymerizations were performed in several organic solvents and some industrial processes are based on these patents.

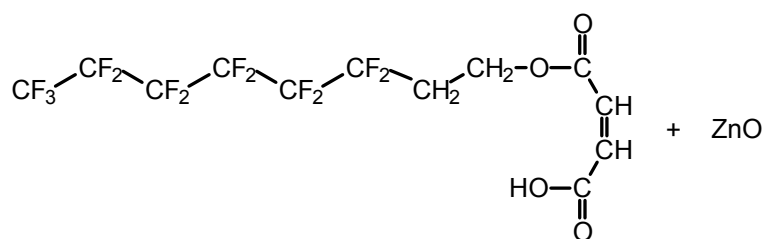


Figure 2-7. Fluorinated carboxylate zinc catalysts for the production of PPC.⁵⁴

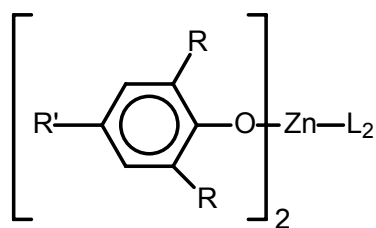
In 1995 Darenbourg et al. reported the use of heterogeneous zinc glutarate catalysts. These catalysts were synthesized by adding the corresponding (di)carboxylic acids to zinc oxide. After heating this solution in toluene, a white precipitate dropped out of solution that, after drying, was used as such.⁴² The exact structure of these catalysts has not been elucidated and the activity was rather low (TOF = 6 h⁻¹ with PO as a monomer). Zinc glutarate was also used for the synthesis of a

biodegradable polyester carbonate by Hwang et al. who terpolymerized CO₂ with PO and caprolactone.⁵⁵ Super et al. reported the use of a dicarboxylic ligand with a long fluorinated tail (Figure 2-7) for better solubility in scCO₂.⁵⁶ The maximum TOFs reached with these soluble carboxylate catalysts was 8 h⁻¹ with a carbonate content of about 90 % (reaction conditions: 100-110 °C, 133 bar). The molecular weight distributions obtained with these catalysts were generally high (> 4). Improvements in the synthesis of the zinc glutarate catalysts were reported by Wang et al. Ultrasonic stirring was used to achieve higher interdispersion of the powdery starting materials.⁵⁷ A large effect of the catalyst's crystallinity on the activity in the copolymerization of PO and CO₂ was found.⁵⁸ Another attempt to improve activity was the activation of the catalyst with SO₂.⁵⁹ A TOF of 3-6 h⁻¹ was reported with PO as a monomer.

A detailed study on the chain microstructure of PPC and PPO formed with these zinc glutarate catalysts was performed by Chrisholm et al. in 2002.⁶⁰ A preference of head-to-tail coupling was confirmed by ¹³C NMR. Zinc benzoate clusters were found to be moderately efficient catalysts for the copolymerization of CHO and CO₂ and the terpolymerization of PO, CHO and CO₂.⁶¹ Sarbu et al. reported the synthesis of a number of zinc and aluminum catalysts with mixed carboxylic, vinyl ether and cyclohexane ligands.⁶² These catalysts were tested as homopolymerization catalysts of CHO and copolymerization catalysts of CO₂ and CHO. However, the incorporation of CO₂ never exceeded 40% of the maximum amount possible in a completely alternating copolymer.

2.5.1.3 Bis(phenoxy) zinc complexes.

The first well-characterized soluble aryloxide zinc complexes were reported by Geerts et al. in 1986.⁶³ The complex (2,6-di-*t*-butylphenoxide)₂Zn(THF)₂ was obtained by the reaction of Zn[N(SiMe₃)₂]₂ with 2,6-di-*t*-butylphenol in THF. This catalyst performed well in the homopolymerization of oxiranes forming high molecular weight polyethers, but in a copolymerization the incorporation of carbon dioxide was very poor (53%).⁶⁴ The group of Darensbourg investigated a lot of complexes with a general formula as shown in Figure 2-8. The complexes were usually binuclear, except when very bulky substituents were used on the phenoxide ligands (like *t*-butyl).^{65,64} The activities of these catalysts were generally higher than those of the aliphatic bis-alkyl zinc/alcohol based systems, which probably existed as aggregates due to the reduced steric hindrance as compared to phenoxy ligands. Darensbourg et al. also claimed that the Lewis base binding affinity was found to be stronger when electron-donating *t*-butyl containing aryloxide ligands were used, as opposed to electron withdrawing substituents. This unexpected behavior was seen for a broad range of Lewis bases, but could not be explained. For all the complexes, the order of base-binding affinity was found to be pyridine > THF > epoxides.



R = Ph, *t*Bu, *i*Pr, Me, H, F

R' = Me, H

L = Et₂O, THF, Pyridine

Figure 2-8. Bis(phenoxy) zinc complexes.^{64,65}

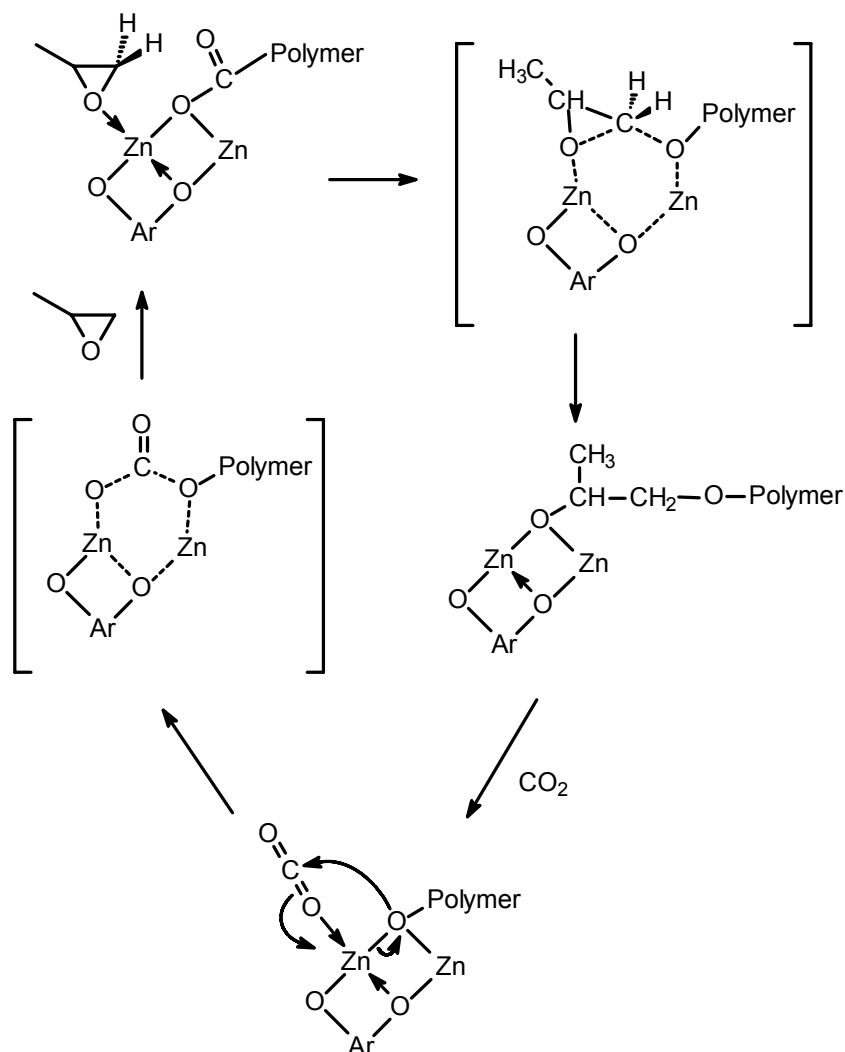
In 1995 Darensbourg et al. reported a mononuclear (2,6-diphenylphenoxy)₂Zn(Et₂O)₂ catalyst which was able to terpolymerize PO, CHO and CO₂.⁶⁵ An advantage of this terpolymerization was that the formation of a cyclic carbonate side product was inhibited by the presence of the third monomer (CHO) with respect to the normal copolymerization between propylene oxide and carbon dioxide.

One of the more promising variations of the zinc phenoxides, with respect to activity, are the fluoro substituted complexes. The dimeric complex [Zn(O-2,6-F₂C₆H₃)₂.THF]₂ was well characterized by Darensbourg et al. and was found to be the most active bis(phenoxy) zinc complex (TOF up to 7 h⁻¹).⁶⁶ The catalyst was active in the homopolymerization of CHO and in the presence of carbon dioxide the copolymer was formed almost exclusively. This was explained by the presence of only one available coordination site for an epoxide. In most systems, two free coordination sites are available and this increases the chance for two consecutive epoxide insertions (Section 2.4).⁶⁶ The polymers obtained with this catalyst system have been physically characterized by Koning et al.⁶⁷ Unfortunately, these polymers cannot withstand a direct comparison with commercially available poly(bisphenol-A carbonate). Furthermore, these polymers have again very broad molecular weight distributions (Chapter 6).

The requirement of two free coordination sites for the formation of polyethers was also demonstrated by Darensbourg et al. with bis(2,4,6-tri-*t*-butylphenoxy) zinc catalysts. The amount of ether bonds normally produced by this catalyst was significantly reduced from > 50 % to about 2 % upon the addition of tricyclohexyl phosphine PCy₃, while TOFs remained about 6 h⁻¹.⁶⁸ The phosphine seems to effectively block one of the coordination sites.

Polyhydric phenoxy zinc complexes were also tested for their activity in the copolymerization of oxiranes and CO₂, but no improvement in activity and selectivity was observed.⁶⁹ In 1994, Kuran et al. reported a possible mechanism for the copolymerization of PO with CO₂ involving a bimetallic active zinc species prepared from the reaction of a polyhydric phenol and ZnEt₂ (Scheme

2-11).^{69c} In this mechanism, two zinc centers stabilize the reaction intermediates. This stabilization was thought to inhibit the formation of cyclic carbonates, which is a major side reaction in a lot of copolymerizations (thermodynamically favored product).



Scheme 2-11. A proposed mechanism for the copolymerization involving a binuclear active species.^{69c}

Recently Xiao et al. reported a well-defined intramolecular dinuclear zinc catalyst. This in situ generated catalyst proved to be very active in the copolymerization of CHO and CO₂ with a maximum TOF of 142 h⁻¹ at 20 bar and 80°C. The intramolecular proximity of the second metal centrum enhanced the copolymerization rate, further indicating a binuclear mechanism.⁷⁰

To study the mechanism of copolymerization and in particular the coordination chemistry during the polymerization, Darensbourg studied several bulky bis(phenoxy) cadmium complexes.⁷¹ Cadmium complexes were usually less active than zinc complexes. The relative softness of Cd(II) in comparison to Zn(II) has led to the isolation and characterization of some cadmium epoxide carboxylates.⁷² Although a variety of Lewis bases like ether and THF were present in the solid-state zinc complexes, the extent of base binding in solution was strongly dependent on the temperature, solvent, type of Lewis base and electronic and steric characteristics of the ligands. Epoxide adducts

have not yet been isolated for zinc complexes. Either the binding affinity is too low or ring opening is too fast. An important conclusion of this work is the observation that with very bulky ligands, there has to be an initial insertion of an epoxide in the Zn-aryloxide bond before carbon dioxide can be inserted due to the steric hindrance of the ligands.⁷³ Another important conclusion was that only one coordination site was necessary for copolymerization, while two sites are needed for a consecutive epoxide insertion.^{68,82} Usually catalysts that were able to perform a homopolymerization of oxiranes, are not very suitable for the polymerization of completely alternating copolymers. Even when carbon dioxide was also used as the solvent (e.g. supercritical carbon dioxide) and was available in large excess, completely alternating copolymers were often not feasible with these catalysts.

2.5.1.4 β -Diketiminato zinc complexes

A new successful class of ligands was introduced by Cheng et al. The used β -diketiminato zinc complexes showed much higher TOFs (up to 257 h^{-1}) than other reported catalysts (Figure 2-9) for the copolymerization of CHO with CO_2 .⁷⁴ Molecular weights were reported up to $31 \text{ kg} \cdot \text{mol}^{-1}$. Some molecular weight distributions were as narrow as 1.07, indicating a living nature of the catalysts. With an asymmetrical ligand (right side of Figure 2-9), an enantiomeric excess of 86:14 (RR:SS) was observed in the poly(cyclohexene carbonate) chain. In 1999 Cheng et al. also reported the successful polymerization of lactide with these β -diketiminato zinc catalysts.⁷⁵ A more recently published article reports the modification of the ligands with CN groups on the backbone to further increase TOFs up to 2290 h^{-1} making them the most active catalysts available to date. With the addition of CF_3 groups on the phenyl moieties, high activities (TOF up to 235 h^{-1}) could also be obtained in the alternating copolymerization of PO and CO_2 , making them far more active than the zinc glutarates discussed earlier (section 2.5.1.2).

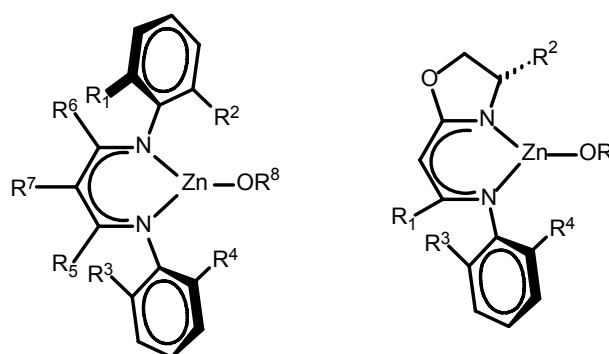
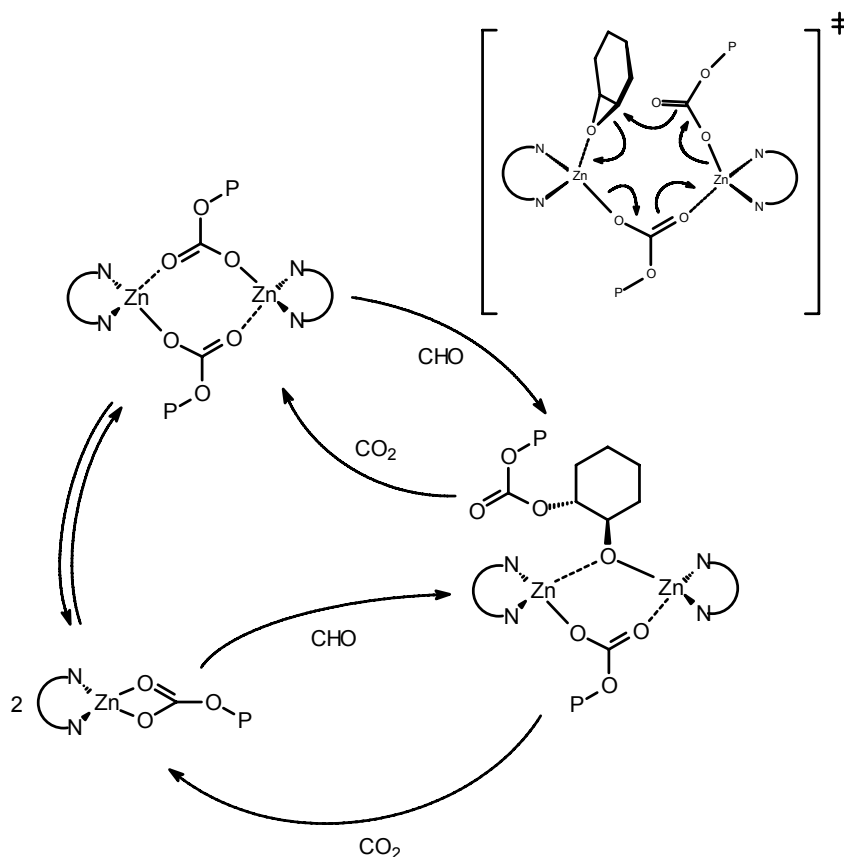


Figure 2-9. Highly adaptable β -diketiminato zinc complexes.⁷⁴

The mechanism of copolymerization of these single site β -diketiminato zinc catalysts has been extensively studied and the proposed bimetallic mechanism is shown in Scheme 2-12. In this mechanism, the bimetallic intermediates are in equilibrium with their monometallic species and the insertion of both monomers is a reversible process.



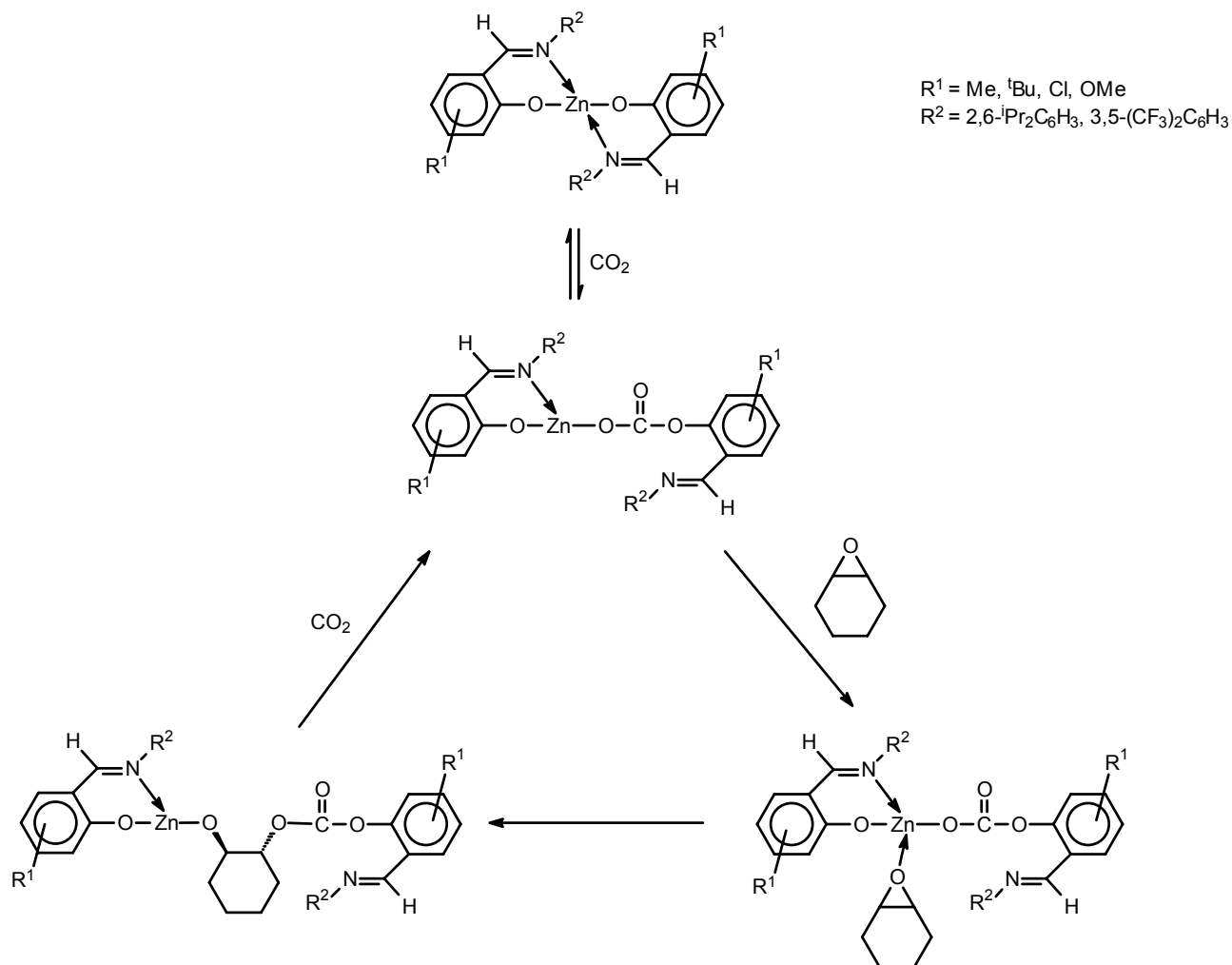
Scheme 2-12. Proposed copolymerization mechanism using β -diketiminato zinc catalysts including the epoxide ring opening transition state.⁷⁴

Reaction kinetics were also investigated and showed a first order dependence on the epoxide concentration and between first and second order dependence on the catalyst concentration (depending on the R groups used in the ligand).⁷⁴

2.5.1.5 Other zinc complexes

Nozaki et al. also reported the synthesis of optically active polycarbonates, which were prepared with asymmetrical amide-alkoxide zinc catalyst.⁷⁶ A maximum enantiomeric excess of 73% was reported. The exact structure of the catalyst is still under investigation.

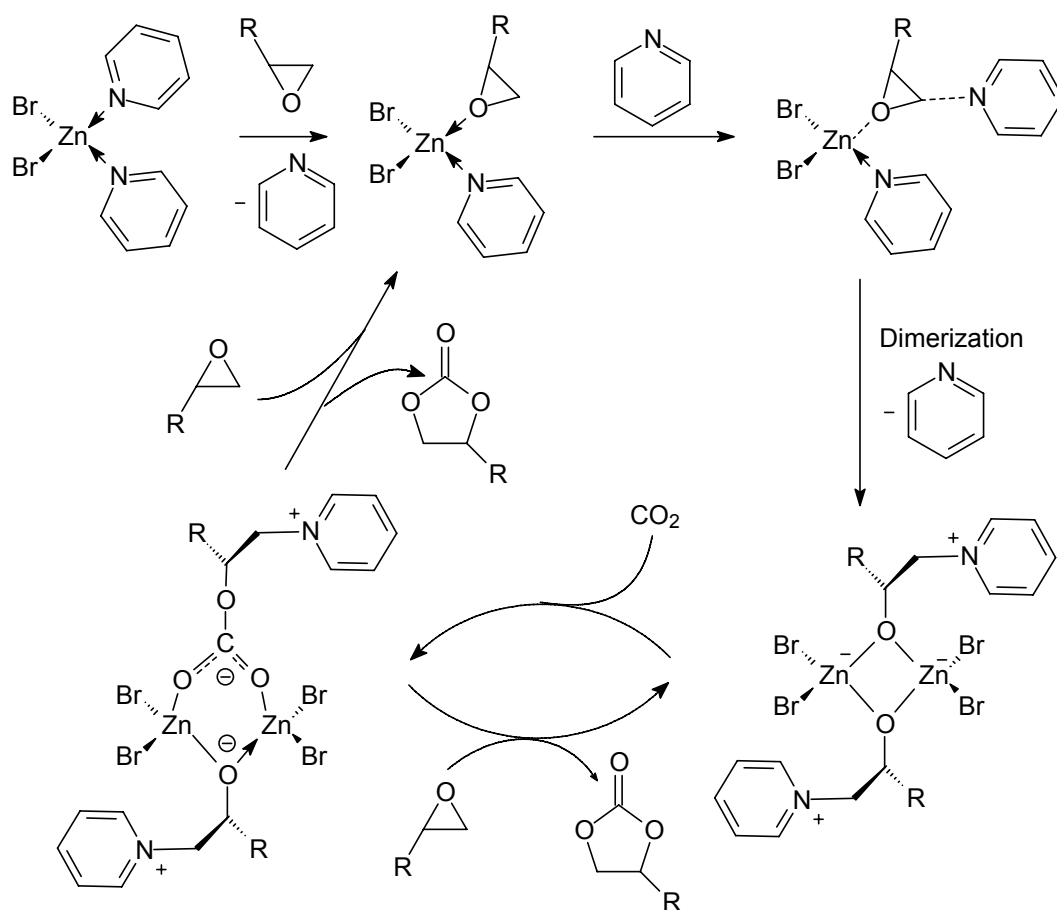
Recently Darensbourg et al. reported a bis-salicylamidinato zinc complex.⁷⁷ In contrast to a lot of bis-phenoxide zinc complexes, this complex is monomeric and the proposed mechanism is shown in Scheme 2-13.



Scheme 2-13. Copolymerization mechanism for the mononuclear bis-salicylamidinato zinc catalyst.⁷⁷

Although the activity was low (TOFs < 7.5 h⁻¹), ¹H NMR spectroscopy showed no ether linkages in the formed polymers, which further supports the theory that at least two available coordination sites are needed for two consecutive oxirane insertions. Furthermore, this mechanism also supports the fact that an initial carbon dioxide insertion is needed before an oxirane can be inserted.

Kim et al. reported the syntheses and isolation of a pyridinium alkoxy bridged dimeric zinc complex with which they studied the formation of cyclic carbonates from CO₂ and epoxides.⁷⁸ The proposed mechanism of this reaction is depicted in Scheme 2-14. In this mechanism the cyclization reaction is actually promoted by a bimetallic center.



Scheme 2-14. Selective formation of cyclic carbonates.⁷⁸

Recently, a new class of hetero metallic catalysts, the so-called double metal cyanides (DMC), was shown to be effective in the synthesis of cyclic carbonates and polycarbonates. And although the activity for the used complexes like $Zn_3[Co(CN)_6]_2$ and zinc hexacyanoferrate(III) can be high, incorporating high percentages of CO₂ proved to be difficult.⁷⁹ Addition of a complexing agent like *t*-butyl alcohol has a great influence on the activity and for the copolymerization of CHO with CO₂ a maximum TOF of 1653 h⁻¹ was reported by Chen et al. with a CO₂ incorporation of around 96%.⁸⁰ Nano-sized double metal cyanide catalyst clusters, composed of several combinations of zinc, cobalt, iron and cobalt clusters with CN ligands, were also found to copolymerize CHO with CO₂, although the activity and carbonate contents are rather low.⁸¹

In 1992 Chen reported the use of polymer supported zinc catalysts, which were reported as being slightly more active than the unsupported analogues.⁸² TOFs up till 6.5 h⁻¹ were reported when a polymer chelated bimetallic catalyst was employed, for example: $Pol_{2,2}-Zn(Fe(CN)_6)_{0.5}C_{10.5}(H_2O)_{0.76}(KCl)_{0.2}$.

2.5.2 Aluminum complexes

The capability of aluminum complexes to efficiently homopolymerize epoxides has triggered a number of research groups to investigate their potential as copolymerization catalysts. However, simple catalysts prepared by partly hydrolyzing aluminum alkyls are not efficient at incorporating CO₂ and maximum CO₂ contents of around 20%³³ were reported. The addition of a Lewis base increased the CO₂ contents to 80%, further supporting the theory that multiple active sites favor homopolymerization and blocking them with a ligand or Lewis base helps to favor copolymerization. Other aluminum complexes, including a calix[4]arene aluminum chloride, were also shown to copolymerize PO/CHO with CO₂ but although they are active, TOFs are very low.⁸³

The use of porphyrinato aluminum complexes (Figure 2-10) was first explored by Takeda et al. in 1978 but CO₂ incorporation was still below 40%.⁸⁴ The breakthrough came with the addition of cocatalysts like quaternary ammonium salt or triphenylphosphine, after which completely alternating copolymers could be obtained. In addition this was the first example of a copolymerization of carbon dioxide and epoxides in a living manner (PDI < 1.1). This reaction at room temperature with 50 bar of CO₂ pressure is very slow, however, as reaction times between 12 and 23 days are reported. The living nature was further demonstrated by the synthesis of AB- and ABA-type block copolymers with poly(propylene oxide) (PPO) and poly(propylene carbonate) (PPC) segments.⁸⁵

As is the case with the homopolymerization of oxiranes,²⁴ these porphyrinato complexes induce a living copolymerization of cyclohexene oxide and CO₂. Unfortunately, the formation of cyclic carbonates (up to 40%) during the polymerization could not be prevented.

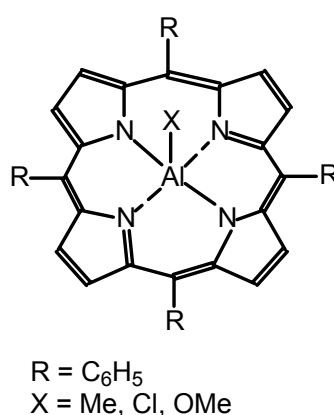


Figure 2-10. Porphyrinato aluminum catalyst.⁸⁴

Porphyrinato aluminum complexes were reported to be active in the copolymerization of PO and CO₂. Detailed investigation of the mechanism of the ring opening of propylene oxide in the copolymerization of propylene oxide and carbon dioxide, by Chrisholm et al. revealed a first order dependence on [Al].⁸⁶ This suggests a monometallic mechanism, in contrast to the mechanistic

proposals for the zinc catalysts mentioned earlier (section 2.5.1). The actual ring opening takes place via an interchange associative pathway with an almost ion-like behavior of the polymer-Al bond due to the trans-activation of the cocatalyst (DMAP in this case). The second important role of the cocatalyst is to promote the insertion of CO₂ into the polymer alkoxide aluminum bond, which inhibits the formation of polyether bonds.

Salen aluminum complexes were recently reported to be very active in the coupling reaction of CO₂ with epoxides (EO) thereby forming cyclic carbonates. With *n*-Bu₄NBr as a cocatalyst a maximum TOF of 2220 h⁻¹ was observed.⁸⁷ Other metal salen complexes were also tested and the order of activity was as follows: SalenAlCl > SalenCrCl > SalenCo > SalenNi > SalenMg, SalenCu, SalenZn. The use of scCO₂ as a solvent further increased the activity to 3070 h⁻¹ for the formation of ethylene carbonate.⁸⁸ Lu et al. reported the synthesis of propylene carbonate, using potassium iodide in conjunction with a crown ether (18-crown-6) as a cocatalyst, with SalenAlEt at room temperature. The proposed mechanism does not involve any bond breaking/making reactions on the SalenAlEt but only a free coordination site is used to activate PO.⁸⁹ This observation is in line with the activity of the e.g. the SalenCo(II) catalyst mentioned above, which only has sites for dative bonding.

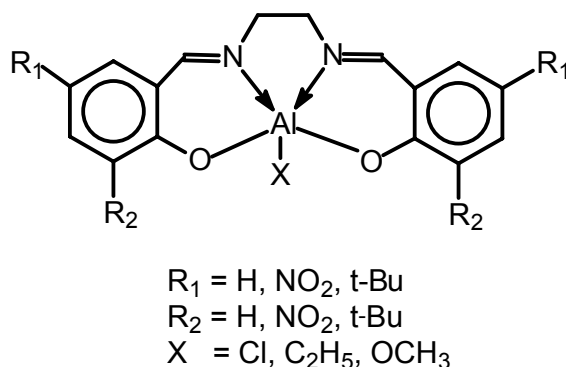


Figure 2-11. Salen aluminum catalysts.⁸⁷

2.5.3 Chromium complexes

The first report of the use of active porphyrinato chromium/DMAP catalysts came in 1995 by Kruper et al.⁹⁰ They used the chromium catalyst for the coupling of CO₂ with a wide range of epoxides and found that the reaction of CO₂ with CHO yielded low molecular weight polycarbonate instead of the predicted cyclic carbonate. TONs up to 10,000 were observed and the catalyst was reported to be recyclable. Shortly thereafter Paddock et al. reported that Cr(III) salen complexes were also very active in the coupling of terminal epoxides and CO₂ under mild conditions (7 bar, 75 °C) although not as active as the previously discussed aluminum analogues (section 2.5.2). The first use of chromium, specifically as a copolymerization catalyst, came in the year 2000 when Mang et

al. reported some interesting porphyrinato chromium complexes (Figure 2-12).⁹¹ The addition of some fluorinated substituents made these systems scCO_2 soluble and TOFs up to 72 h^{-1} were reached. The obtained polymers had a molecular weight of about $3500 \text{ g} \cdot \text{mol}^{-1}$ with a polydispersity index lower than 1.4 and a carbonate contents of 90-94%. Shortly thereafter, Stamp and coworkers demonstrated that these porphyrinato chromium catalysts could be supported on Aerogel beads and successfully recycled.⁹²

The salen chromium/DMAP system received a lot of interest lately. While first used for the selective synthesis of cyclic carbonates, polycarbonate synthesis was also possible with the right amount of cocatalyst, as was reported by Eberhardt et al.⁹³ A small increase in cocatalyst (DMAP) concentration from 0.5 to 2 equivalents could force the formation of almost exclusively poly(propylene carbonate) (PPC) to the formation of propylene carbonate (PC) as the major product.

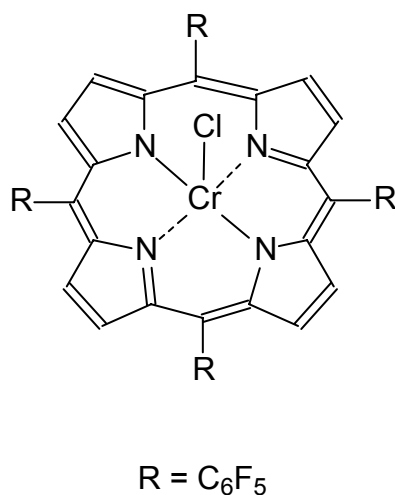
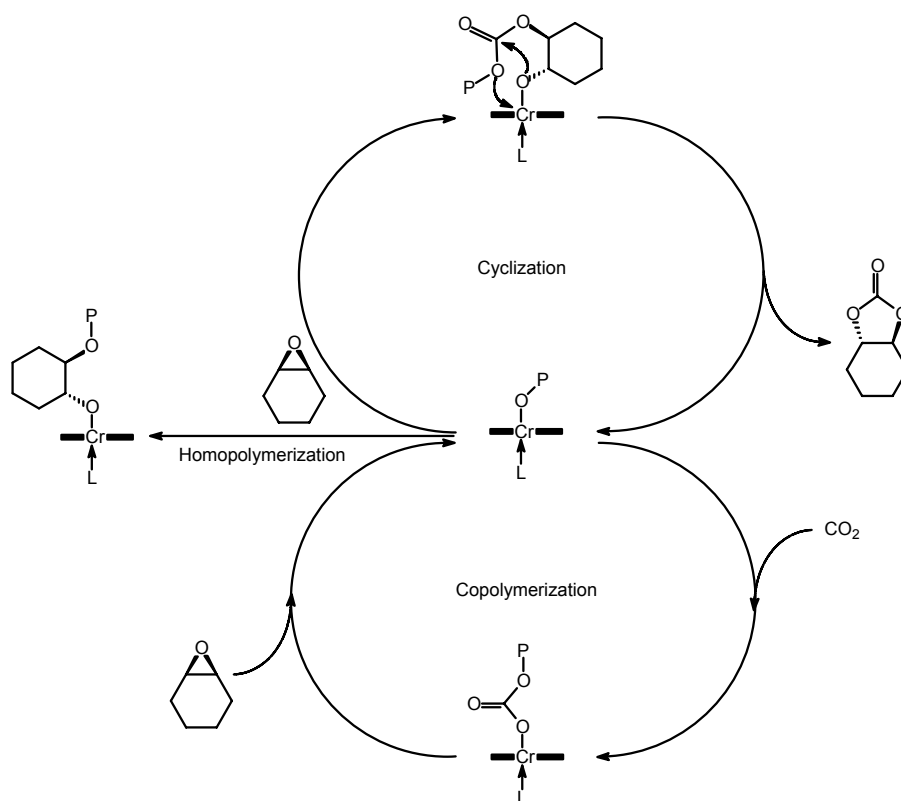


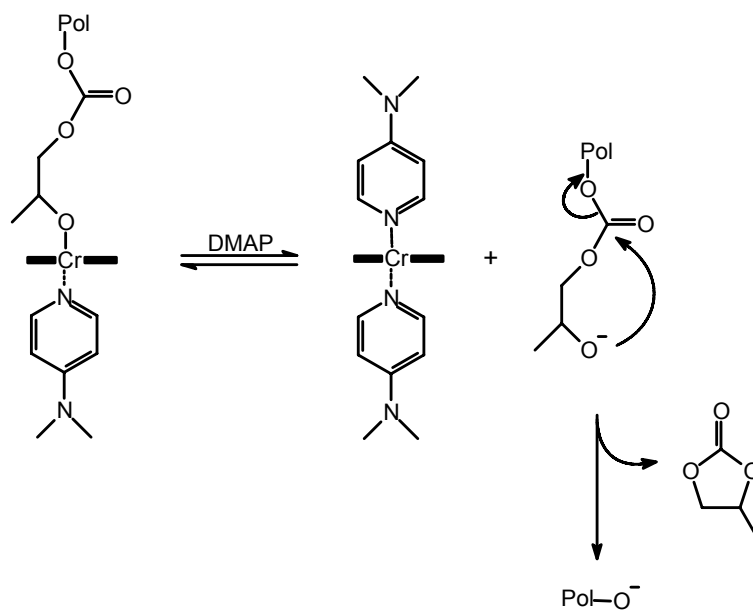
Figure 2-12. scCO_2 soluble porphyrinato chromium complex.⁹¹

Thereafter, the effects of other bases, initiating groups and monomers (CHO) on salen chromium(III) compounds were extensively studied by Darensbourg et al. who also developed an in situ ATR/FTIR probe to follow reaction kinetics.⁹⁴ The past few years several mechanisms have been reported, differing in the role of the cocatalyst and whether or not a bimetallic species plays a role in the copolymerization mechanism.^{1e,94} The most recent mechanism reported by Darensbourg et al. is depicted in Scheme 2-15 and presumes a monometallic active species.^{94e}



Scheme 2-15. Copolymerization mechanism of Salen chromium catalysts including side reactions.^{94e}

A possible mechanistic explanation of the role of the cocatalyst in the selectivity of the salen chromium catalysts was proposed earlier by Eberhardt et al., who suggested displacement of the growing polymer chain by the Lewis base (Scheme 2-16). The liberated anionic chain end would then be far more susceptible to backbiting and therefore the cyclic carbonates are the major product.⁹³



Scheme 2-16. Displacement of polymer chain by DMAP leading to cyclic carbonate formation.⁹³

2.5.4 Cobalt catalysts

The earliest report of the use of cobalt catalysts was published in 1978 by Soga and coworkers with a cobalt acetate catalyst that could copolymerize PO and CO₂, but yields were extremely low.⁹⁵ Later Shi et al. reported that salen cobalt could make propylene carbonate,⁹⁶ and recently Coates and coworkers reported moderate activities in the copolymerizations of PO and CO₂ at room temperatures. Well defined copolymers with a CO₂ contents > 95% were obtained and, in contrast to the related chromium analogues, there was no need for an additional cocatalyst. Furthermore, there was hardly any cyclic carbonate formation, which is quite rare when PO is used as a monomer.⁹⁷ Unfortunately, high pressures were required (55 bar) but with the addition of a cocatalyst (*N,N*-dimethylaminoquinoline) the required pressure could be lowered to 10-20 bar without sacrificing selectivity and activity.⁹⁸ As was reported by Cohen et al., the use of bis(triphenylphosphine-iminium)chloride as a cocatalyst proved the most active combination to date with a maximum TOF of 620 h⁻¹ in the copolymerization of *rac*-PO with CO₂.⁹⁹ Higher temperatures (> 100°C) led primarily to the formation of cyclic carbonates while at lower temperatures the initiating group and cocatalyst have a large influence as well.¹⁰⁰

2.5.5 Manganese catalysts

Recently, the first alternating copolymerization of CHO and CO₂ was reported with CO₂ pressures as low as 1 bar and 80 °C with the use of a porphyrinato manganese system.¹⁰¹ Although the TOF of 3 h⁻¹ was not very high, the extremely mild reaction conditions make these complexes interesting. Furthermore, a high CO₂ contents was obtained (> 95%) and the low polydispersities (1.3 to 1.9) indicated a living polymerization. Raising the pressure increased the activity to around 16 h⁻¹ and when PO was used as a monomer, only PC was obtained without any polyether bonds. Darensbourg performed a more detailed investigation into the insertion/deinsertion mechanism of both CO₂ and the epoxide.¹⁰² A strong influence of the initiating group was observed on the initial insertion of CO₂ (Mn-OR, fast when R = CH₃, slow when R = CH₂CF₃).

2.5.6 Lanthanides and group 3 metal catalysts

Several other metals have been used in the past years to prepare catalysts (usually bimetallic) that can copolymerize epoxides and CO₂. A selection of the most interesting combinations is reviewed here. A number of the catalysts contain at least one of the metals already known to be active (mostly zinc), so the added value of exotic lanthanides and other compounds is not always clear. For example the exotic Ln(CCl₃COO)₃/ZnEt₃/glycerol ternary catalytic systems reported by

Liu et al. are very active.¹⁰³ These systems produced poly(propylene carbonate) with number average molecular weights up to $73 \text{ kg} \cdot \text{mol}^{-1}$, and a maximum TOF of 67 h^{-1} was reported for the $\text{Nd}(\text{CCl}_3\text{COO})_3/\text{ZnEt}_2/\text{glycerol}$ system with a carbonate content of 95.6% at $90 \text{ }^\circ\text{C}$ and 3 bar CO_2 in dioxane. Yttrium analogues were slightly less active.^{104,103} $\text{Y}(\text{CF}_3\text{CO}_2)_3\text{-Zn}(\text{Et})_2\text{-}m\text{-hydroxybenzoic acid}$ clusters were used to make block-copolymers with highly alternating PPC with CHO and 4-vinyl substituted CHO copolymers.¹⁰⁵

Other exotic compounds like $\text{M}(\text{P}_{204})\text{-Al}[\text{CH}_2\text{CH}(\text{CH}_3)_2]_3$ (with $\text{M} = \text{La, Eu, Gd, Dy, Ho, Nd, Er, Yb, Lu, Y}$; $\text{P}_{204} = (\text{RO})_2\text{POO-}$, $\text{R} = \text{CH}_3(\text{CH}_2)_3\text{CH}(\text{C}_2\text{H}_5)\text{CH}_2\text{-}$) were reported to be active in the copolymerization of epichlorohydrin with CO_2 to form high molecular weight polymers, but the CO_2 content was rather low (30%) and the polydispersities were very broad. However, the thermal stability of the polymers was excellent ($T_d > 320 \text{ }^\circ\text{C}$).¹⁰⁶ Several allyl glycidol ethers were also copolymerized, but no further data on polymer composition, molecular weights and activities are reported.¹⁰⁷

Several mono(cyclopentadienyl)-M-bis(alkyl) complexes ($\text{M} = \text{Y, Dy, Lu, Sc}$) and some polyhydric analogues were reported by Cui et al. to be moderately active in the homo- and copolymerization of CHO and CO_2 .¹⁰⁸ TOFs of $7\text{-}14 \text{ h}^{-1}$ were obtained with carbonate contents between 90-99%. Molecular weights from $14\text{-}40 \text{ kg} \cdot \text{mol}^{-1}$ were measured with a polydispersity of 4-6.

2.5.7 Copolymerization of oxiranes with CO_2 analogues

Several other CO_2 related compounds are known to react with oxiranes and literature examples can be found for, amongst other, carbodiimides, isocyanates, SO_2 and CS_2 . Discussing the chemistry of all the compounds is outside the scope of this thesis, but the use of SO_2 will be discussed briefly since this is the most studied alternative monomer for copolymer synthesis.

In the late 1960s, Schaefer et al. reported the cationic copolymerization of SO_2 with propylene-oxide¹⁰⁹ The copolymerization can also be catalyzed according to an anionic mechanism, but the molecular weight of the obtained polymers (either by the anionic or the cationic mechanism) never exceeded $2000 \text{ g} \cdot \text{mol}^{-1}$. Recently, the copolymerization of SO_2 and propylene-oxide was reported by Lee et al using a zinc glutarate catalyst.¹¹⁰ With this catalyst, it was possible to obtain molecular weights up to $49 \text{ kg} \cdot \text{mol}^{-1}$. The coupling of PO and SO_2 to the corresponding oxathiolane-2-thione has also recently been described by Shen et al. A combination of a phenol and an organic base was used as catalyst.


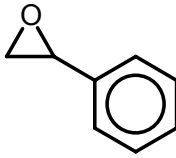
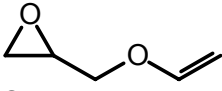
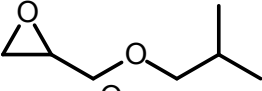
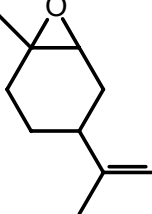
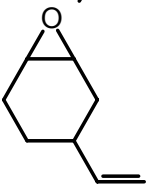
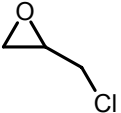
2.6 Other oxirane monomers

Several reports can be found in the literature where alternative monomers (other than EO, PO and CHO) are used (Table 2-1). As was already mentioned in paragraph 2.5.1.1, styrene oxide was one of the first alternative monomers used and was already reported in 1975 by Inoue and coworkers. Along with other monomers, styrene oxide was also used by Rätzsch and Haubold in 1977 and a T_g of 76 °C was found for the formed copolymer.¹¹¹ Other monomers tested were cyclopentene oxide, allyl glycidyl ether and *i*-butyl glycidyl ether, but a high carbonate content of the formed polymers could not be achieved. Allyl glycidyl ether was also used by Lukaszczyk et al. in the synthesis of biodegradable polycarbonates, which can be modified after polymerization to for example poly(epoxycarbonate). The used catalyst is a zinc pyrogallol (1,3,5 trihydroxybenzene) complex of undefined structure.¹¹² The activity of the catalyst was not reported. Tan et al. modified such a copolymer with 3-(trimethoxysilyl)propyl methacrylate via a free radical reaction and used the resulting alkoxy silane-containing copolymer in a sol-gel process resulting in a polyether carbonate – silica nanocomposite, which showed enhanced mechanical properties over the normal copolymer.¹¹³

In 2004, Byrne et al. reported the use of limonene oxide as a monomer in the synthesis of aliphatic polycarbonates.¹¹⁴ With the help of a β -diketiminato zinc catalyst they were able to produce highly region- and stereoregular polycarbonates from a renewable resource.

Hsu et al. used 4-vinyl cyclohexene oxide (VCHO) in their studies because of the possibility of a post-polymerization step on the double bonds, similar to the allyl glycidyl ethers. PVCHC and block copolymers with PPC were prepared (see section 2.5.6).¹⁰⁵ The epichlorohydrin monomer, also discussed in section 2.5.6, resulted in a much more thermally stable polymer.

Table 2-1. Alternative monomers used in polycarbonate synthesis.

Entry	Monomer	Name	References
1		Cyclopentene oxide (CPO)	111
2		Styrene oxide	52, 111, 115
3		Allyl glycidyl ether (AGE)	111, 112, 113
4		<i>I</i> so-butyl glycidyl ether	111
5		Limonene oxide	114
6		4-vinyl cyclohexene oxide (VCHO)	105
7		Epichlorohydrin (ECH)	106

2.7 Summary and outlook

For almost four decades now the copolymerization of carbon dioxide with epoxides has been studied by research groups all over the world. Still it remains a fascinating subject and the activation of carbon dioxide remains a hot topic. A shift from the early heterogeneous catalytic systems to the current homogeneous systems led to significant increases in activity and selectivity, however, industrial interest is still lacking. The low thermal stability and less than optimal physical properties have thus far prevented a breakthrough for these novel polycarbonates. In the last few years, research aimed towards milder reactions conditions and the use of novel monomers for improved physical properties might increase industrial interest again, but there is still a long road to go. In the following chapters our own research in this challenging will be presented.

2.8 References

- 1 (a) Darensbourg, D. J.; Holtcamp, M. W. *Coord. Chem. Rev.* **1996**, *153*, 155. (b) Super, M. S.; Beckman, E. J. *Trends Polym. Sci.* **1997**, *5*, 236. (c) Beckman, E. J. *Science* **1999**, *283*, 946. (d) Sugimoto, H.; Inoue, S. *J. Polym. Sci., Part A* **2004**, *42*, 5561. (e) Coates, G. W.; Moore, D. R. *Angew. Chem. Int. Ed. Engl.* **2004**, *43*, 6618. (f) Ochiai, B.; Endo, T. *Prog. Polym. Sci.* **2005**, *30*, 183.
- 2 (a) Behr, A. In *Catalysis in CI Chemistry*; Keim, W. Ed.; D. Reidel Publ. Co.: Dordrecht, the Netherlands, **1983**; p 169. (b) Behr, A. *Angew. Chem. Int. Ed. Engl.* **1988**, *27*, 661. (c) Braunstein, P.; Matt, D.; Nobel, D. *Chem. Rev.* **1988**, *88*, 747.
- 3 (a) Behr, A. *Chem. Ing. Tech.* **1985**, *57*, 893. (b) Behr, A. *Chem. Eng. Tech.* **1987**, *10*, 16. (c) Arakawa, H.; Aresta, M.; Armor, J. N.; Barteau, M. A.; Beckman, E. J.; Bell, A. T.; Bercaw, J. E.; Creutz, C.; Dinjus, E.; Dixon, D. A.; Domen, K.; DuBois, D. L.; Eckert, J.; Fujita, E.; Gibson, D. H.; Goddard, W. A.; Goodman, D. W.; Keller, J.; Kubas, G. J.; Kung, H. H.; Lyons, J. E.; Manzer, L. E.; Marks, T. J.; Morokuma, K.; Nicholas, K. M.; Periana, R.; Que, L.; Rostrup-Nielson, J.; Sachtler, W. M. H.; Schmidt, L. D.; Sen, A.; Somorjai, G. A.; Stair, P. C.; Stults, B. R.; Tumas, W. *Chem. Rev.* **2001**, *101*, 953 and references cited therein.
- 4 Sasaki, H.; Rudzinski, J. M.; Kakuchi, T. *J. Polym. Sci.* **1995**, *33*, 1807.
- 5 March, J. In *Advanced Organic Chemistry*, 4th ed., Wiley-Interscience, New York **1992**.
- 6 Smith, M. B. in *Organic Syntheses*, McGraw-Hill inc., New York **1994**.
- 7 (a) Alt, G. M.; Berton, O. H. R. *J. Chem. Soc.* **1954**, 4284. (b) Lucas, H. J.; Games, H. K. *J. Am. Chem. Soc.* **1950**, *72*, 2145.
- 8 Zvonkova, E. N.; Vevstigneeva, R. P. *J. Org. Chem. USSR* (Engl. transl.) **1974**, *10*, 883.
- 9 Shim, J. G.; Yamamoto, Y. *J. Org. Chem.* **1919**, *63*, 3067.
- 10 Crivello, J. V.; Rajaraman, S.; Mowers, W. A.; Liu, S. *Macromol. Symp.* **2000**, *157*, 109.
- 11 Pine, S. H. in *Organic Chemistry*, 5th ed., McGraw-Hill inc., New York **1987**, p. 544.
- 12 Coates, G. W. *Chem. Rev.* **2000**, *100*, 1223.
- 13 Jacquier-Gonod, V.; Llauro, M. F.; Hamaide, T. *Macromol. Chem. Phys.* **2000**, *201*, 12.
- 14 Goriot, R.; Petiaud, R.; Llauro, M. F.; Hamaide, T. *Macromol. Symp.* **1997**, *119*, 173.
- 15 Baar, C. R.; Levy, C. J.; Min, E. Y. J.; Henling, L. M.; Day, M. W.; Bercaw, J. E. *J. Am. Chem. Soc.* **2004**, *126*, 821

- 16 Sato, A.; Hirano, T.; Tsuruta, T.; *Makrom. Chem.* **1975**, *176*, 1187.
- 17 (a) Tsuruta, T. *J. Appl. Chem.* **1981**, *53*, 1745. (b) Tsuruta, T. *J. Polym. Sci.: Polym. Symp.* **1980**, *67*, 73.
- 18 U.S. Patent 2,706,181 1955 to Pruitt, M. E.; Bagget, I. M., Dow Chemical Co.
- 19 Zeng, X.; Zhang, Y.; Shen, Z. *J. Polym. Sci.* **1997**, *35*, 2177.
- 20 Wu, B.; Harlan, J.; Lenz, R.W.; Barron, A. R. *Macromolecules* **1997**, *30*, 316.
- 21 (a) U.S. patent 4,193,892 1980 to Goeke, G. L.; Park, K.; Karol, F. L.; Mead, B., Union Carbide Corp. (b) U.S. patent 4,667,013 1987 to Reichle, W.T.; Warren, N. J., Union Carbide Corp.
- 22 (a) Price, C. C.; Spector, R. *J. Am. Chem. Soc.* **1966**, *88*, 4171. (b) Price, C. C.; Akkapeddi, M. K.; DeBona, B. T.; Furie, B. C. *J. Am. Chem. Soc.* **1972**, *94*, 3964. (c) Kuran, W.; Rokicki, A.; Pienkowski, J. *J. Polym. Sci.: Part A* **1979**, *17*, 1235. (d) Watanabe, Y.; Yasuda, T.; Aida, T.; Inoue, S. *Macromolecules* **1992**, *25*, 1396.
- 23 (a) Arlman, E. J.; Cossee, P. *J. Cat.* **1964**, *3*, 99. (b) Arlman, E. J. *J. Cat.* **1964**, *3*, 89. (c) Cossee, P. *J. Cat.* **1964**, *3*, 80.
- 24 (a) Asano, S.; Aida, T.; Inoue, S. *J. Chem. Soc., Chem. Commun.* **1985**, 1148. (b) Aida, T.; Maekawa, Y.; Asano, S.; Inoue, S. *Macromolecules* **1988**, *21*, 1195 (c) Aida, T.; Inoue, S. *Acc. Chem. Res.* **1996**, *29*, 39.
- 25 Thiam, M.; Spassky, N. *Macromol. Chem. Phys.* **1999**, *200*, 2107.
- 26 Miola-Delaite, C.; Colomb, E.; Pollet, E.; Hamaide, T. *Macromol. Symp.* **2000**, *153*, 275.
- 27 (a) Sugimoto, H.; Kawamura, C.; Kuroki, M.; Aida, T.; Inoue, S. *Macromolecules* **1994**, *27*, 2013. (b) Takeuchi, D.; Watanabe, T.; Aida, T.; Inoue, S. *Macromolecules* **1995**, *28*, 651.
- 28 Ge, L.; Huang, Q.; Zhang, Y.; Shen, Z. *Eur. Polym. J.* **2000**, *36*, 2699.
- 29 See for example: Ystenes, M.; Eilertsen, J. L.; Liu, J.; Ott, M.; Rytter, E.; Stovng, J. A. *J. Polym. Sci., Part A: Polym. Chem.* **2000**, *38*, 3106.
- 30 German Patent 740,366 to Vierling, K., I.G. Farbenindustrie (1943)
- 31 Rokicki, G. *Prog. Polym. Sci.* **2000**, *25*, 259.
- 32 Endo, T.; Shibasaki, Y.; Sanda, F. *J. Polym. Sci., Part A* **2002**, *40*, 2190.
- 33 Of the theoretical maximum in a completely alternating copolymer.

- 34 (a) Vogdanis, L.; Martens, B.; Uchtmann, H.; Hensel, F.; Heitz, W. *Makromol. Chem.* **1990**, *191*, 465-472. (b) Vogdanis, L.; Heitz, W. *Makromol. Chem., Rapid Commun.* **1986**, *7*, 543.
- 35 Haba, O.; Tomizuka, H.; Endo, T. *Macromolecules* **2005**, *38*, 3562.
- 36 Inoue, S.; Koinuma, H.; Tsuruta, T. *Polymer Lett.* **1969**, *7*, 287.
- 37 (a) Baba, A.; Meishou, H.; Matsuda, H. *Makromol. Chem., Rapid Commun.* **1984**, *5*, 665. (b) Baba, A.; Kashiwagi, H.; Matsuda, H. *Organometallics* **1987**, *6*, 137.
- 38 Inoue, S.; Koinuma, H.; Yokoo, Y.; Tsuruta, T. *Makromol. Chem.* **1971**, *143*, 97.
- 39 In 1999 a complete issue of chemical reviews (volume 99, issue 2) was devoted to the use of supercritical fluids.
- 40 McHugh, M. A.; Krukoni, V. J. "Supercritical Fluid Extraction Principles and Practices" Butterworth Publishing Co., Boston, **1986**.
- 41 Cooper, A. I. *J. Mater. Chem.* **2000**, *10*, 207.
- 42 Darensbourg, D. J.; Stafford, N. W.; Katsurao, T. *J. Mol. Cat.: Part A* **1995**, *104*, L1.
- 43 Fink, R.; Hancu, D.; Valentine, R.; Beckman, E. J. *J Phys. Chem.* **1999**, *103*, 6441.
- 44 Super, M.; Beckman, E. J. *Macromol. Symp.* **1998**, *127*, 89.
- 45 Lepilleur, C.; Beckman, E. J.; Schonemann, H.; Krukoni, V. J. *Fluid Phase Equilib.* **1997**, *134*, 285.
- 46 Sarbu, T.; Styranec, T. J.; Beckman, E. J. *Ind. Eng. Chem. Res.* **2000**, *39*, 4678.
- 47 Fink, R.; Hancu, D.; Valentine, R.; Beckman, E. J. *J. Phys. Chem.* **1999**, *103*, 6441.
- 48 Super, M. S.; Enick, R. M.; Beckman, E. J. *J. Chem. Eng. Data* **1997**, *42*, 664.
- 49 (a) Musie, G.; Wei, M.; Subramaniam, B.; Busch, D. H. *Coord. Chem. Rev.* **2001**, *219-221*, 789. (b) Wei, M.; Musie, G. T.; Busch, D. H.; Subramaniam, B. *J. Am. Chem. Soc.* **2002**, *124*, 2513.
- 50 Rajagopalan, B.; Wei, M.; Musie, G. T.; Subramaniam, B.; Busch, D. H. *Ind. Eng. Chem. Res.* **2003**, *42*, 6505.
- 51 Inoue, S.; Kobayashi, M.; Koinuma, H.; Tsuruta, T. *Makromol. Chem.* **1972**, *155*, 61.
- 52 Hirano, T.; Inoue, S.; Tsuruta, T. *Makromol. Chem.* **1975**, *176*, 1913.
- 53 Jansen, J. C.; Addink, R.; Te Nijenhuis, K.; Mijs, W. *J. Macromol. Chem. Phys.* **1999**, *200*, 1407.

- 54 (a) U.S. Patent 4,783,445 1988 to S. Hsiang-ning, Arco Chemical Company. (b) U.S. Patents 5,026,676 1991 to S. Motika, Air Products and Chemicals, Inc., Arco Chemical Company and Mitsui Petrochemical Industries Ltd. (c) U.S. Patent 4,943,677 1990 to A. Rokicki, Air products and Chemicals, Inc. and Arco Chemical Company.
- 55 Hwang, Y.; Jung, J.; Ree, M.; Kim, H. *Macromolecules* **2003**, *36*, 8210.
- 56 Super, M.; Berluce, E.; Costello, C.; Beckman, E. *Macromolecules* **1997**, *30*, 368.
- 57 Wang, S. J.; Du, L. C.; Zhao, X. S.; Meng, Y. Z.; Tjong, S. C. *J. Appl. Pol. Sci.* **2002**, *85*, 2327.
- 58 Meng, Y. Z.; Du, L. C.; Tjong, S. C.; Zhu, Q.; Hay, A. S. *J. Polym. Sci., Part A* **2002**, *40*, 3579.
- 59 Eberhardt, R.; Allmendinger, M.; Zintl, M.; Troll, C.; Luinstra, G. A.; Rieger, B. *Macromol. Chem. Phys.* **2004**, *205*, 42.
- 60 Chisholm, M. H.; Navarro-Llobet, D.; Zhou, Z. *Macromolecules* **2002**, *35*, 6494.
- 61 Darensbourg, D. J.; Wildeson, J. R.; Yarbrough, J. C. *Inorg. Chem.* **2002**, *41*, 973.
- 62 Sarbu, T.; Beckman, E. J. *Macromolecules* **1999**, *32*, 6904.
- 63 Geerts, R. L.; Huffman, J. C.; Caulton, K. G. *Inorg. Chem.* **1986**, *25*, 1803-1805.
- 64 Darensbourg, D. J.; Holtcamp, M. W.; Struck, G. E.; Zimmer, M. S.; Niezgodna, S. A.; Rainey, P.; Robertson, J. B.; Draper, J. D.; Reibenspies, J. H. *J. Am. Chem. Soc.* **1999**, *121*, 107.
- 65 Darensbourg, D. J.; Holtcamp, M. W. *Macromolecules* **1995**, *28*, 7577.
- 66 Darensbourg, D. J.; Wildeson, J. R.; Yarbrough, J. C.; Reibenspies, J. H. *J. Am. Chem. Soc.* **2000**, *122*, 12487.
- 67 Koning, C. E.; Wildeson, J.; Parton, R.; Plum, B.; Steeman, P.; Darensbourg, D. J. *Polymer* **2001**, *42*, 3995.
- 68 Darensbourg, D. J.; Zimmer, M. S.; Rainey, P.; Larkins, D. L. *Inorg. Chem.* **2000**, *39*, 1578.
- 69 (a) Kobayashi, M.; Tang, Y.-L.; Tsuruta, T.; Inoue, S. *Makromol. Chem.* **1973**, *169*, 69. (b) Rokicki, A.; Kuran, W. *Makromol. Chem.* **1979**, *180*, 2153-2161. (c) Kuran, W.; Listos, T. *Macromol. Chem. Phys.* **1994**, *195*, 977. (d) Lukaszczyk, J.; Jaszcz, K.; Kuran, W.; Listos, T. *Macromol. Rapid Commun.* **2000**, *21*, 754.
- 70 Xiao, Y.; Wang, Z.; Ding, K. *Chem. Eur. J.* **2005**, *11*, 3668.

- 71 Darensbourg, D. J.; Niezgoda, S. A.; Draper, J. D.; Reibenspies, J. H. *J. Am. Chem. Soc.* **1998**, *120*, 4690.
- 72 Darensbourg, D. J.; Holtcamp, M. W.; Khandelwal, B.; Klausmeyer, K. K.; Reibenspies, J. H. *J. Am. Chem. Soc.* **1995**, *117*, 538.
- 73 Darensbourg, D. J.; Niezgoda, S. A.; Holtcamp, M. W.; Draper, J. D.; Reibenspies, J. H. *Inorg. Chem.* **1997**, *36*, 2426.
- 74 (a) Cheng, M.; Lobkovsky, E. B.; Coates, G. W. *J. Am. Chem. Soc.* **1998**, *120*, 11018. (b) Beckman, E. J. *Science* **1999**, *283*, 946. (c) Cheng, M.; Moore, D. R.; Reczek, J. J.; Chamberlain, B. M.; Lobkovsky, E. B.; Coates, G. W. *J. Am. Chem. Soc.* **2001**, *123*, 8738.
- 75 Cheng, M.; Ovitt, T. M.; Hustad, P. D.; Coates, G. W. *Polym. Prepr.* **1999**, *40*, 542.
- 76 Nozaki, K.; Nakano, K.; Hiyama, T. *J. Am. Chem. Soc.* **1999**, *121*, 11008.
- 77 Darensbourg, D. J.; Rainey, P.; Yarbrough, J. C. *Inorg. Chem.* **2001**, *40*, 986.
- 78 (a) Kim, H. S.; Kim, J. J.; Lee, B. G.; Jung, O. S.; Jang, H. G.; Kang, S. O. *Ang. Chem. Int. Ed.* **2000**, *39*, 4096. (b) Kim, H. S.; Kim, J. J.; Lee, S. D.; Lah, M. S.; Moon, D.; Jang, H. G. *Chem. Eur. J.* **2003**, *9*, 678.
- 79 (a) Chen, L.-B. *Makromol. Chem., Macromol. Symp.* **1992**, *59*, 75. (b) Darensbourg, D. J.; Adams, M. J.; Yarbrough, J. C.; Phelps, A. L. *Inorg. Chem.* **2003**, *42*, 7809. (c) Aramendia, M. A.; Borau, V.; Jimenez, C.; Marinas, J. M.; Romero, F. J. *J. Cat.* **1999**, *183*, 119. (d) Darensbourg, D. J.; Phelps, A. L. *Inorg. Chim. Acta* **2004**, *357*, 1603. (e) Chen, S.; Hua, Z.; Fang, Z.; Qi, G. *Polymer* **2004**, *45*, 6519-.
- 80 Chen, S.; Qi, G.-R.; Hua, Z.-J.; Yan, H.-Q. *J. Polym. Sci., Part A* **2004**, *42*, 5284.
- 81 Yi, M. J.; Byun, S.-H.; Ha, C.-S.; Park, D.-W.; Kim, I. *Solid State Ionics* **2004**, *172*, 139.
- 82 (a) Chen, L.-B. *Makromol. Chem., Macromol. Symp.* **1992**, *59*, 75. (b) Yang, S.-Y.; Fang, X.-G.; Chen, L.-B. *Macromol. Symp.* **1996**, *105*, 17.
- 83 (a) Kuran, W.; Listos, T.; Abramczyk, M.; Dawidek, A. *J. Macromol. Sci. Pure Appl. Chem.* **1998**, *35*, 427-437. (b) Sarbu, T.; Styranec, T. J.; Beckman, E. J. *Polym. Prepr.* **2000**, *41*, 137.
- 84 (a) Takeda, N.; Inoue, S. *Makromol. Chem.* **1978**, *179*, 1377. (b) Takeda, N.; Inoue, S. *Bull. Chem. Soc. Jpn.* **1978**, *51*, 3564. (c) Aida, T.; Inoue, S. *Macromolecules* **1982**, *15*, 682.
- 85 Aida, T.; Ishikawa, M.; Inoue, S. *Macromolecules* **1986**, *19*, 8.
- 86 Chisholm, M. H.; Zhou, Z. *J. Am. Chem. Soc.* **2004**, *126*, 11030.

- 87 Lu, X.-B.; Feng, X.-J.; He, R. *Appl. Catal. A* **2002**, *234*, 25.
- 88 Lu, X.-B.; He, R.; Bai, C.-X. *J. Mol. Catal. A* **2002**, *186*, 1.
- 89 Lu, X.-B.; Zhang, Y.-J.; Jin, K.; Luo, L.-M.; Wang, H. *J. Catal.* **2004**, *227*, 537.
- 90 Kruper, W. J.; Dellar, D. D. *J. Org. Chem.* **1995**, *60*, 725.
- 91 Mang, S.; Cooper, A. I.; Colclough, M. E.; Chauhan, N.; Holmes, A. B. *Macromolecules* **2000**, *33*, 303.
- 92 Stamp, L. M.; Mang, S. A.; Holmes, A. B.; Knights, K. A.; de Miguel, Y. R.; McConvey, I. F. *Chem. Commun.* **2001**, 2502.
- 93 Eberhardt, R.; Allmendinger, M.; Rieger, B. *Macromol. Rapid Commun.* **2003**, *24*, 194.
- 94 (a) Darensbourg, D. J.; Yarbrough, J. C.; Ortiz, C.; Fang, C. C. *J. Am. Chem. Soc.* **2003**, *125*, 7586. (b) Darensbourg, D. J.; Mackiewicz, R. M.; Rodgers, J. L.; Phelps, A. L. *Inorg. Chem.* **2004**, *43*, 1831. (c) Darensbourg, D. J.; Mackiewicz, R. M.; Phelps, A. L.; Billodeaux, D. R. *Acc. Chem. Res.* **2004**, *37*, 836. (d) Darensbourg, D. J.; Mackiewicz, R. M.; Rodgers, J. L.; Fang, C. C.; Billodeaux, D. R.; Reibenspies, J. H. *Inorg. Chem.* **2004**, *43*, 6024. (e) Darensbourg, D. J.; Mackiewicz, R. M.; Billodeaux, D. R. *Organometallics* **2005**, *24*, 144. (f) Darensbourg, D. J.; Rodgers, J. L.; Mackiewicz, R. M.; Phelps, A. L. *Catal. Today* **2004**, *98*, 485.
- 95 Soga, K.; Hyakkoku, K.; Ikeda, S. *Makromol. Chem.* **1978**, *179*, 2837.
- 96 Shen, Y.-M.; Duan, W.-L.; Shi, M. *J. Org. Chem.* **2003**, *68*, 1559.
- 97 Qin, Z. Q., Thomas, C. M., Lee, S., Coates, G. W. *Angew. Chem. Int. Ed.* **2003**, *42*, 5484.
- 98 Paddock, R. L.; Nguyen, S. *Macromolecules* **2005**, *38*, 6251.
- 99 Cohen, C. T.; Chu, T.; Coates, G. W. *J. Am. Chem. Soc.* **2005**, *127*, 10869.
- 100 (a) Lu, X.-B.; Wang, Y. *Angew. Chem. Int. Ed. Engl.* **2004**, *43*, 3574. (b) Paddock, R. L.; Nguyen, S. T. *Chem. Comm.* **2004**, 1622. (c) Lu, X.-B.; Xiu, J.-H.; He, R.; Jin, K.; Luo, L.-M.; Feng, X.-J. *Appl. Catal., A* **2004**, *275*, 73. (d) Paddock, R. L.; Hiyama, Y.; McKay, J. M.; Nguyen, S. T. *Tetrahedron Lett.* **2004**, *45*, 2023.
- 101 Sugimoto, H.; Ohshima, H.; Inoue, S. *J. Polym. Sci., Part A* **2003**, *41*, 3549.
- 102 (a) Darensbourg, D. J.; Lee, W.-Z.; Phelps, A. L.; Guidry, E. *Organometallics* **2003**, *22*, 5585. (b) Darensbourg, D. J.; Ganguly, P.; Billodeaux, D. R. *Organometallics* **2004**, *23*, 6025.

-
- 103 (a) Liu, B.; Zhao, X.; Wang, X.; Wang, F. *J. Polym.Sci., Part A: Polym. Chem.* **2001**, *39*, 2751. (b) Liu, B.; Zhao, X.; Wang, X.; Wang, F. *Polymer* **2003**, *44*, 1803.
- 104 (a) Tan, C.-S.; Hsu, T.-J. *Macromolecules* **1997**, *30*, 3147. (b) Quan, Z.; Min, J.; Zhou, Q.; Xie, D.; Liu, J.; Wang, X.; Zhao, X.; Wang, F. *Macromol. Symp.* **2003**, *195*, 281. (c) Hsu, T. J.; Tan, C. S. *Polymer* **2001**, *42*, 5143. (d) Quan, Z.; Wang, X.; Zhao, X.; Wang, F. *Polymer* **2003**, *44*, 5605.
- 105 Hsu, T.-J.; Tan, C.-S. *Polymer* **2002**, *43*, 4535.
- 106 Shen, Z.; Chen, X.; Zhang, Y. *Macromol. Chem. Phys.* **1994**, *195*, 2003.
- 107 Guo, J.-T.; Wang, X.-Y.; Xu, Y.-S.; Sun, J.-W. *J. Appl. Pol. Sci.* **2003**, *87*, 2356.
- 108 Cui, D.; Nishiura, M.; Hou, Z. *Macromolecules* **2005**, *38*, 4089.
- 109 Schaeffer, J.; Kern, R. J.; Katnik, R. J. *Macromolecules* **1968**, *1*, 107. (b) Schaeffer, J. *Macromolecules* **1968**, *1*, 101.
- 110 Lee, B.; Jung, J. H.; Ree, M. *Macromol. Chem. Phys.* **2000**, *201*, 831.
- 111 Ratzsch, M.; Haubold, W. *Z. Polymerforsch.* **1977**, *28*, 15.
- 112 Lukaszczyk, J.; Jaszcz, K.; Kuran, W.; Listos, T. *Macromol. Rapid Commun.* **2000**, *21*, 754.
- 113 Tan, C.-S.; Juan, C.-C.; Kuo, T.-W. *Polymer* **2004**, *45*, 1805.
- 114 Byrne, C. M.; Allen, S. D.; Lobkovsky, E. B.; Coates, G. W. *J. Am. Chem. Soc.* **2004**, *126*, 11404.
- 115 Darensbourg, D. J.; Zimmer, M. S. *Macromolecules* **1999**, *32*, 2137.

Chapter 3

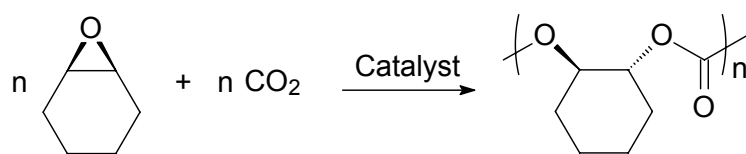
Silsesquioxane zinc catalysts for the alternating copolymerization of cyclohexene oxide and carbon dioxide

Abstract

Two novel silsesquioxane zinc complexes ($[(c-C_5H_9)_7Si_7O_{11}(OSiMePh_2)]_2Zn_4Me_4$ (**1a**) and $[(c-C_5H_9)_7Si_7O_{12}]_2Zn_4Me_2$ (**2a**)) have been used as model compounds for silica supported catalysts in the copolymerization of cyclohexene oxide and CO_2 . Both **1a** and **2a** exist as dimers in the solid phase. Complex **1a** has been characterized by X-ray diffraction. Two of the four zinc atoms in **1a** are distorted trigonal planar whereas the other two are tetrahedrally coordinated. Both complexes **1a** and **2a** were active in the copolymerization and poly(cyclohexene carbonate) was obtained with a carbonate content of 99% and a TOF of $15 \text{ mol CHO} \cdot \text{mol cat.}^{-1} \cdot \text{h}^{-1}$. Polymerizations with $ZnEt_2$ -treated silica particles in a precipitation polymerization resulted in polymer particles with \bar{M}_n and \bar{M}_w values comparable to the polymers obtained with their homogeneous analogues **1a** and **2a**. It was further demonstrated that CO_2 consumption can be followed on-line by monitoring the decrease of the system pressure during the reaction. CO_2 consumption was interpreted in relation to both polycarbonate as well as cyclic carbonate formation. These measurements represent the intrinsic kinetics of this reaction, which appear to be directly related to CO_2 pressure. Additionally, a significant difference between the two catalysts was found concerning their ability to homopolymerize CHO.

3.1 Introduction

In the search for new catalysts for the synthesis of aliphatic polycarbonates from carbon dioxide and oxiranes (Scheme 3-1) several classes have been developed over the years.¹ The focus of this research was mainly on discrete homogeneous systems such as the β -diketiminato zinc catalysts², the salen³/porphyrin⁴ chromium systems and porphyrin aluminum systems⁵.



Scheme 3-1. Copolymerization of carbon dioxide and cyclohexene oxide to poly(cyclohexene carbonate) (PCHC).

However, from an industrial viewpoint these homogeneous polymerizations are not ideal. Even with the addition of solvents, the reaction mixtures tend to get very viscous already at low conversions, which complicates processing and purification steps. Several methods can be used to suppress these high viscosities such as emulsion and precipitation polymerizations. During a precipitation polymerization the polymer precipitates from the non-solvent before contributing to the viscosity of the solution. Furthermore, provided that small particles are formed, precipitation polymerization offers better temperature control because heat is more easily dissipated through the low viscous reaction mixture. Moreover, a much higher solid content can be obtained. Precipitation also has its disadvantages, such as reactor fouling and poor morphology control. To prevent reactor fouling and to gain control over the polymer particle morphology, a heterogeneous catalyst is required.⁶ Several attempts have already been reported to support catalysts capable of copolymerizing oxiranes and carbon dioxide, including the tethering of β -diketiminato zinc complexes to silica by Yu and coworkers.⁷ Although this approach has led to a decrease in carbon dioxide content in the formed polycarbonate, it is close to the ideal of combining homogeneous and heterogeneous systems.

Another approach would be to go back to the original type of catalysts as developed by Inoue et al.⁸ Simply reacting dialkyl zinc with water or alcohols also produces a working catalyst. A significant difference is that in case of the β -diketiminato zinc complexes the ligands remain on the zinc during the polymerization, shielding the metal center, while there is a chance that in the case of the $\text{ZnEt}_2/\text{H}_2\text{O}$ catalyst a polymer chain can start growing from two sides. With the tendency of zinc to form clusters,⁹ several active sites with each a slightly different electronic and steric surrounding can be formed. This in turn will lead to an inhomogeneous polymer and the polydispersity will become broader than with single site catalysts. The bis(phenoxy) zinc catalysts developed by Darensbourg and coworkers behave in a similar manner and the phenoxide ligands become the end groups in the formed polymer.¹⁰ A potential use of this approach, where the polymer grows between the ligands and the zinc metal, is the ability to graft polymer chains directly on the surface of a support. Simple treatment of silica supports with ZnEt_2 would facilitate such a system, assuming that only the Zn-OSi bonds are active and not the (residual) ZnEt bonds.² Furthermore, this will only work if this results in a living system. Otherwise, only the first chain will be physically

Silsesquioxane zinc catalysts for the alternating copolymerization of cyclohexene oxide and carbon dioxide attached to the support. To study such a system, silsesquioxane zinc complexes can be used since silsesquioxane ligands are realistic homogeneous model compounds for silica silanol surface sites.¹¹

Little more than a decade ago silsesquioxane studies included laborious synthetic procedures and small scale work. Recent advances in the synthesis of silsesquioxanes have stimulated research in this area leading to a number of novel complexes based on several transition and main group metals.¹² Various heterogeneous catalytic processes such as olefin polymerizations¹³, alkene epoxidation¹⁴ and metathesis¹⁵ have already been mimicked successfully.

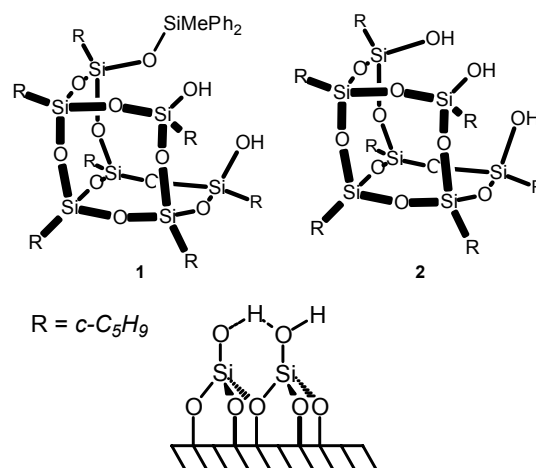


Figure 3-1. Silsesquioxane ligands with their silica surface silanol counterparts.

Here we report the use of two silsesquioxane ligands (Figure 3-1) for the synthesis of new epoxide/ CO_2 copolymerization catalysts. Incompletely condensed silsesquioxanes **1** and **2** were shown to structurally mimic vicinal disilanol sites present on silica surfaces.¹¹ With these ligands two different zinc complexes were synthesized (complexes **1a** and **2a**, Figure 3-2). Both complexes were tested for their activity in the copolymerization of CO_2 and cyclohexene oxide to form poly(cyclohexene carbonate) (PCHC). Furthermore the activity of mesoporous silica particles, treated with ZnEt_2 , was tested for comparison with the model compounds.

The kinetics of these copolymerizations were studied using a model that enables monitoring of the conversion via the pressure drop during polymerization. The model provides a mathematical description of the relation between system pressure, temperature, initial composition and actual composition.

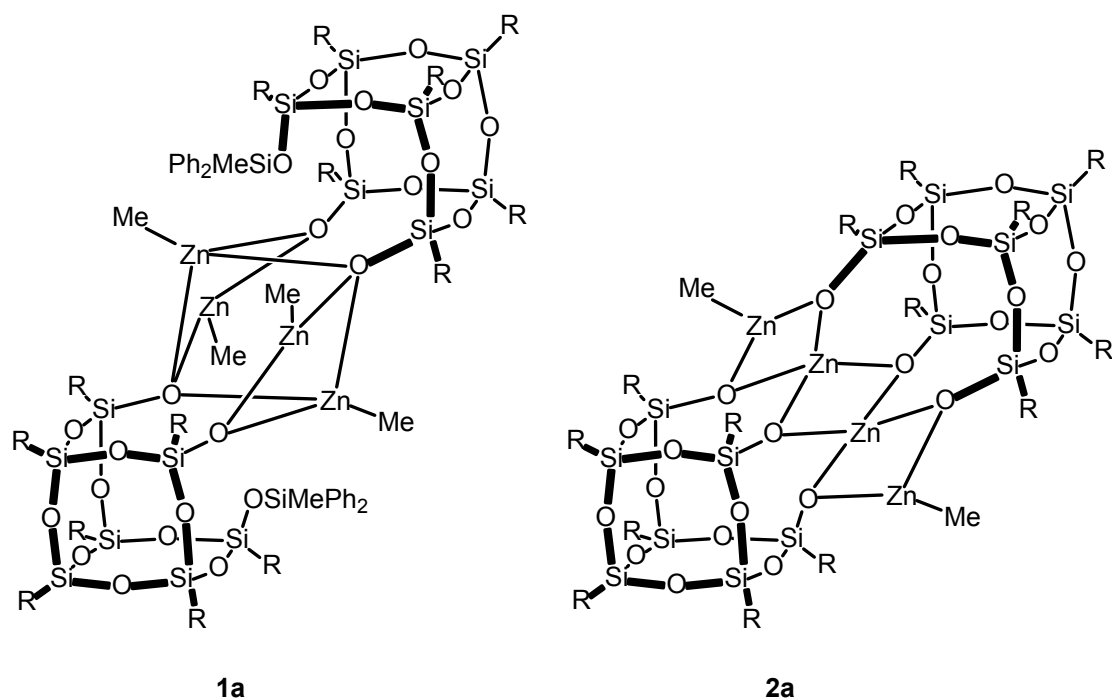


Figure 3-2. The silsesquioxane zinc catalysts $[(c\text{-C}_5\text{H}_9)_7\text{Si}_7\text{O}_{11}(\text{OSiMePh}_2)]_2\text{Zn}_4\text{Me}_4$ (**1a**) and $[(c\text{-C}_5\text{H}_9)_7\text{Si}_7\text{O}_{12}]_2\text{Zn}_2\text{Me}_4$ (**2a**).

3.2 Results and discussion

3.2.1 Synthesis of $[(c\text{-C}_5\text{H}_9)_7\text{Si}_7\text{O}_{11}(\text{OSiMePh}_2)]_2\text{Zn}_4\text{Me}_4$ (**1**)

Complex **1a** was obtained in moderate yield from the reaction of the silsesquioxane **1** with two equivalents of ZnMe_2 in toluene. Crystals of **1a** suitable for X-ray crystal structure determination were grown from a mixture of hexane/toluene. Figure 3-3 shows the molecular structure of $[(c\text{-C}_5\text{H}_9)_7\text{Si}_7\text{O}_{11}(\text{OSiMePh}_2)]_2\text{Zn}_4\text{Me}_4$ (**1a**).¹⁶ The X-ray structure of complex **2a** has been reported elsewhere.¹⁷ Complex **1a** is a dimeric species containing two silsesquioxane cages bound together by four zinc atoms. The molecule has a crystallographically imposed center of inversion in the center of the Zn1-O11-Zn1'-O11' plane. Two of the four zinc atoms are distorted trigonal planar whereas the other two are tetrahedrally coordinated similar to what was found in complex **2a**. Consequently, O1 is μ_2 -bridged and O11 is μ_3 -bridged between the zinc atoms. Accordingly, the $\text{Zn1-}\mu_2\text{-O1}$ (1.9767(11) Å), $\text{Zn1-}\mu_3\text{-O11}$ (2.1764(12) Å) and Zn1-C1 (1.948(2) Å) distances are longer than the corresponding $\text{Zn2-}\mu_2\text{-O1}$ (1.9254(12) Å), $\text{Zn2-}\mu_3\text{-O11'}$ (2.0518(11) Å) and Zn2-C2 (1.922(2) Å) bond lengths. The Zn2-C2 and $\text{Zn2-}\mu_2\text{-O1}$ bond lengths are significantly shorter than the corresponding Zn-C and $\text{Zn-}\mu_2\text{-O}$ distances of the trigonal planar zinc centers in $[(c\text{-C}_5\text{H}_9)_7\text{Si}_7\text{O}_{12}]_2\text{Zn}_4\text{Me}_2$ **2a** ($\text{Zn-C}_{\text{av}} = 1.942(5)$ Å, $\text{Zn-}\mu_2\text{-O}_{\text{av}} = 1.955(3)$ Å) and for example $[(\text{MeZn})_2\text{Zn}(\text{OSi}^i\text{Pr}_3)_4]$ ($\text{Zn-C}_{\text{av}} = 1.946(3)$ Å, $\text{Zn-}\mu_2\text{-O}_{\text{av}} = 1.975(2)$ Å).^{17,18} The $\text{Zn-}\mu_3\text{-O}$ bond

lengths in **1a** are similar to the Zn- μ_3 -O bond distances in e.g. [MeZn(μ_3 -OSiEt₃)₄] (Zn- μ_3 -O_{av} = 2.090(4) Å). The Si-O_{av} (1.6244(13) Å) is normal within the range found for silsesquioxane compounds. The C-Zn-O and O-Zn-O angles in **1a** are comparable to those in the abovementioned zinc silsesquioxane and siloxane complexes. The relative positioning of the zinc atoms between **1a** and **2a** differs significantly. In **2a** the four zinc atoms are located in a rough line, while in complex **1a** they are positioned at the corners of a square relative to each other.

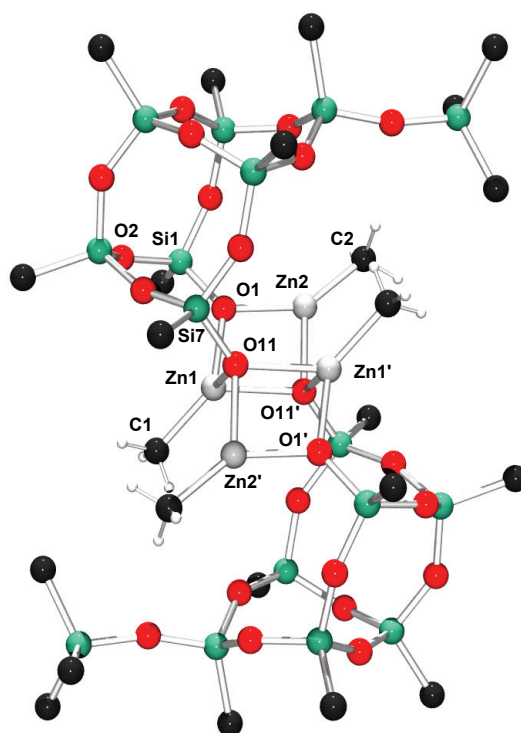


Figure 3-3. Molecular structure of [(c-C₅H₉)₇Si₇O₁₁(OSiMePh₂)₂]Zn₄Me₄ (**1a**). For clarity reasons, only the α -carbons and *i*-carbons of the cyclopentyl and phenyl groups are shown respectively. Selected bond distances (Å) Zn1-O1, 1.9767(11); Zn1-O11, 2.1764(12); Zn1-C1, 1.948(2); Zn1-O11, 2.1324(11); Zn2-O1, 1.9254(12); Zn2-C2, 1.922(2); Zn2-O11', 2.0518(11); Si1-O1, 1.6281(13); Si1-O2, 1.6307(13); Si7-O11, 1.6431(12). Selected bond angles (deg.): O1-Zn1-C1, 133.03(8); O11-Zn1-C1, 114.35(8); O11'-Zn1-C1, 129.73(7); O1-Zn1-O11, 100.81(5); O1-Zn1-O11', 82.28(5); O11-Zn1-O11', 83.76(4); O1-Zn2-C2, 141.76(8); O11'-Zn2-C2, 132.42(8); O1-Zn2-O11', 85.69(5); Zn1-O1-Zn2, 100.36(6); Zn1-O11-Zn1', 96.24(4); Zn1-O11-Zn2', 98.54(5); Zn1'-O11-Zn2', 91.48(4); Zn1-O1-Si1, 133.01(7); Zn2-O1-Si1, 126.03(7); Zn1-O11-Si7, 117.32(6); Zn1'-O11-Si7, 127.54(6); Zn2'-O11-Si7, 119.21(6).

3.2.2 Copolymerization of cyclohexene oxide and CO₂

The prepared silsesquioxane catalysts were tested for their activities in the copolymerization of cyclohexene oxide and carbon dioxide in a 380 mL stainless steel high pressure autoclave. The results of these experiments are summarized in Table 3-1. Conditions were chosen such that they mimic optimal conditions for two of the more commonly used catalysts: the β -diketiminato zinc systems (10 bar, 50 °C)^{2b} as well as the bis(phenoxy) zinc complexes (80 bar, 80 °C).^{10e}

Table 3-1. Copolymerization results with cyclohexene oxide and CO₂.

Entry	Complex ^{a)}	Time (h)	P (bar)	T (°C)	Conversion (%) ^{b)}	CHC (%) ^{b)}	Fraction CO ₂ (%)	TOF (h ⁻¹) ^{c)}	\overline{M}_n (g · mol ⁻¹) ^{d)}	$\overline{M}_w / \overline{M}_n$
1	None	24	80	120	1.75	0	0	-	-	-
2	[(2,6-F ₂ C ₆ H ₃ O) ₂ Zn·THF] ₂	28	80	80	19	0	98	15.4	25,800	18.4
3	1a	24	0	120	13	0	0	4.0	-	-
4	1a	24	10	50	9	2	79	2.8	- ^{e)}	-
5	1a	24	10	120	8	2	80	2.5	13,900	3.8
6	1a	24	80	120	44	14	91	13.5	11,600	10.0
7	1a	31	80	120	40	11	95	12.1	10,700	8.4
8	1a	24	80	80	34	2	92	10.1	10,600	10.8
9	2a	24	80	120	43	5	98	13.7	12,500	15.3
10	2a	28	80	120	44	7	85	13.5	12,900	7.8

a) All polymerizations were performed with 200 μmol of the catalyst (calculated for the monomeric form), 35 mL of toluene and 15 mL of CHO. b) Conversion determined by integration of methine peaks in ¹H NMR spectra. c) mol CHO · mol cat⁻¹ · h⁻¹ (referring to the monomeric catalyst species). d) PS equivalents. e) High molecular weight fraction of the distribution was outside the exclusion limit of the used SEC columns.

The effects of temperature and pressure on the activity and selectivity of complex **1a** are summarized in Figure 3-4 and in Figure 3-5. The PCHO in both figures represents the fraction of polyether bonds in the formed copolymer.

Without CO₂ at 120°C, **1a** is a moderately active catalyst for the homopolymerization of CHO to PCHO (Figure 3-4). Applying a moderate CO₂ pressure (10 bar) inhibits the formation of PCHO significantly and, although the activity is low, PCHC is formed with a carbonate content of around 80%. Increasing the pressure to 80 bar increases the activity significantly and PCHC with a carbonate content around 98% was obtained. Raising the temperature from 50 °C to 120 °C while maintaining the pressure at 10 bar has a negligible effect on the activity and selectivity of the catalyst (Table 3-1, entries 4 and 5). At higher pressures (80 bar), increasing the temperature has a positive effect on the activity, but the depolymerization reaction to CHC increases substantially as the formation of cyclic carbonates increases from 2% to 14% (Table 3-1, entries 6 and 7).

For the tested conditions, optimal conditions for complex **1a** were found to be 80 bar and 80 °C. The similarity in optimal polymerization conditions and broad polydispersities observed for the bis(phenoxy) zinc catalysts and the complex **1a** is probably caused by polymerization in the Zn-OSi

Silsesquioxane zinc catalysts for the alternating copolymerization of cyclohexene oxide and carbon dioxide bonds.¹⁰ After the initial insertions, the ligand is separated from the zinc center and any further influence of the ligand is negligible. This is of course not the case for the β -diketiminato zinc systems or the salen/porphyrin chromium complexes, where the ancillary ligand system remains firmly bound to the metal center during polymerization.^{2e,4b} With the very broad polydispersities, as is evident from Table 3-1, it is clear that no real control over the polymer chain growth can be obtained with these systems. This is similar to polymerizations catalyzed with ZnEt₂/H₂O mixtures or the bis(phenoxy) zinc systems, for which these very broad distribution have already been observed but not yet fully understood.^{10b,19} Such a distribution pattern is characteristic for multiple non-living active sites present in the system. These dimeric silsesquioxane zinc catalysts consist of four zinc centers with each two potential initiating sites and are likely to result in a multimodal distribution (see also Scheme 3-2). Furthermore, a possible dissociation of the dimer during polymerization will also lead to a multimodal distribution. As is the case of most heterogeneous systems, not every site is similar and differences in activity between these sites will lead to a large variety of chain lengths, resulting in large polydispersities as seen here.

For complex **1a** the number average molecular weight (\overline{M}_n) values ranging from 9,000 to 14,000 g · mol⁻¹ with polydispersities ranging from 4-19 were obtained. As expected, activities were found to be comparable to those of bis(phenoxy) zinc catalysts (TOFs around 15 mol CHO · mol cat.⁻¹ · h⁻¹). Similar activities and \overline{M}_n values were found for complex **2a**.

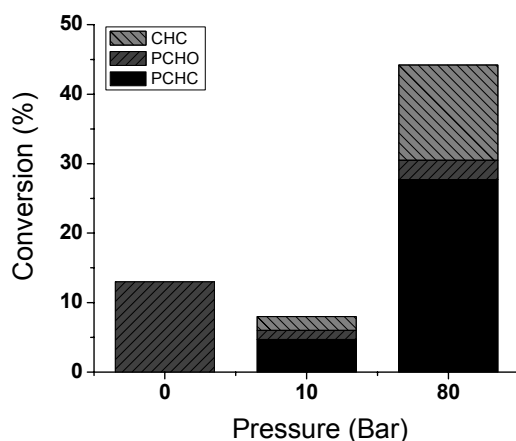


Figure 3-4. Influence of pressure at 120 °C for complex **1a**.

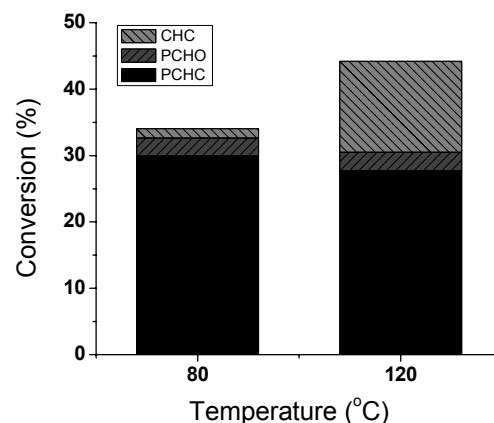
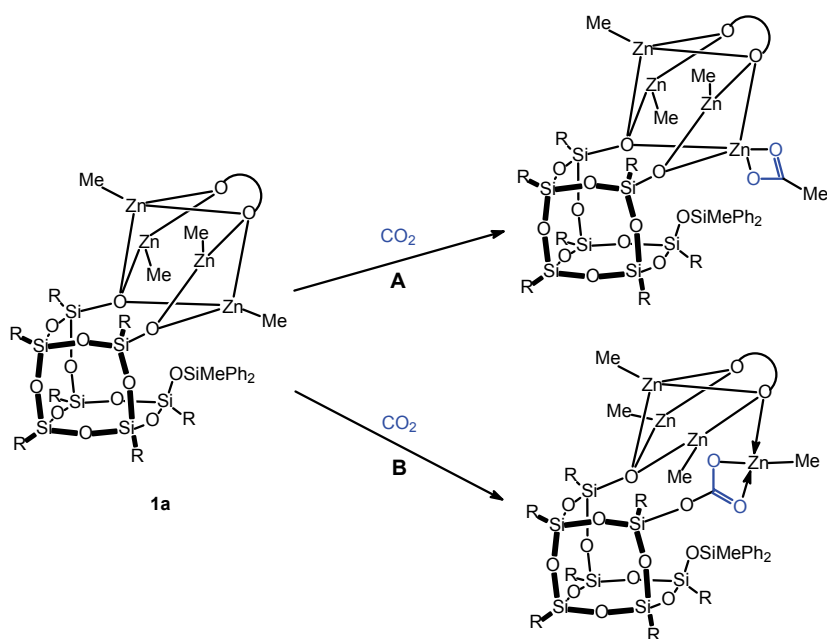


Figure 3-5. Influence of temperature at 80 bar for complex **1a**.

If we assume that initiation proceeds by an initial insertion of CO₂ (as also observed by MALDI-ToF-MS, vide infra), two possible pathways are envisaged (Scheme 3-2). Pathway A, where the CO₂ inserts in the Zn-Me bond, or pathway B, where the insertion takes place into the SiO-Zn bond. Microstructure analyses (vide infra) of the formed PCHC chains supports the

assumption that the initial initiation is facilitated by CO₂. The occurrence of pathway B could not be verified by microstructure analyses. The Si-O bonds are likely to be hydrolyzed during workup or analysis.



Scheme 3-2. Different insertion pathways for CO₂.

With the β -diketiminato zinc catalyst, the Zn-Me bond in itself was shown to be a very poor initiating group. Generally, treatment with an alcohol prior to the polymerization was required for good activity.² Pretreatment of the catalyst with a small excess of *i*-PrOH to replace the methyl groups of complex **1a** and **2a** to achieve faster initiation, however, did not improve activities.²⁰ A standard pretreatment with CO₂ (50 °C, 10 bar CO₂, 30 min) was always performed before the actual polymerization was started (by adding CHO) to give the catalyst a chance to react with CO₂. Sampling at regular intervals during polymerization allowed us to follow the conversion and molecular weight build up of a polymerization with **1a** and **2a** over a prolonged period of time (Table 3-1, entries 7 and 10).²¹

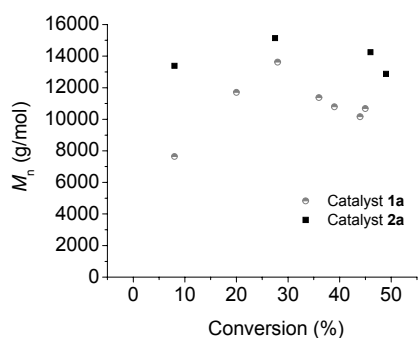


Figure 3-6. \overline{M}_n development plotted against the conversion for complexes **1a** and **2a**.

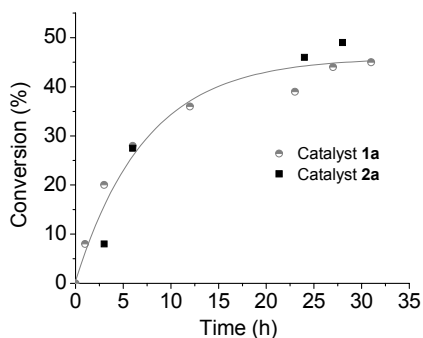


Figure 3-7. Conversion development over time for complexes **1a** and **2a**.

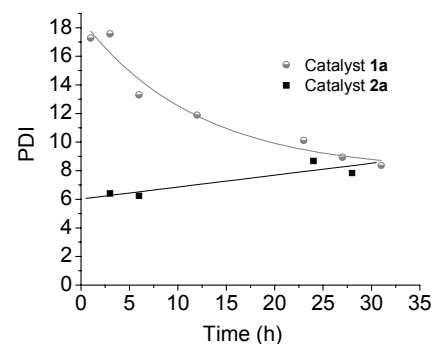


Figure 3-8. Polydispersity development over time for complexes **1a** and **2a**.

A good indication for the living character of a catalyst is the linear behavior of the \overline{M}_n plotted against the conversion. As is immediately clear from Figure 3-6, this is not the case for complexes **1a** and **2a**. \overline{M}_n values around 10,000 are already reached at the beginning of the polymerization and an ill-defined maximum value for both complexes can be seen at around 25% conversion. Figure 3-7 shows a typical development of conversion with time for complexes **1a** and **2a** with a large decrease in the polymerization rate when conversion approaches 50%. Mass transfer limitations due to the increased viscosity seem to inhibit the reaction rate above this point. The PDI development over time for catalyst **1a** (Figure 3-8) shows a maximum value in the beginning of the polymerization and a gradual decrease during polymerization. Surprisingly, this behavior was not observed for catalyst **2a**, but both polymerization runs converge to a polydispersity of about 9 after 30 hours. In contrast to complex **2a**, complex **1a** apparently has a tendency to make some very long chains in the beginning of the polymerization, while shorter chains are also produced. This leads to a high \overline{M}_w and a relatively low \overline{M}_n . Over time the lower molecular weight chains predominate, leading to a drop in the \overline{M}_w while the \overline{M}_n values still average around $11,000 \text{ g} \cdot \text{mol}^{-1}$ causing a reduction of the polydispersity index. This behavior can also be seen in Figure 3-9, showing the SEC plots of the same samples taken at selected time intervals for the construction of Figure 3-7 and Figure 3-8 (catalyst **1a**)

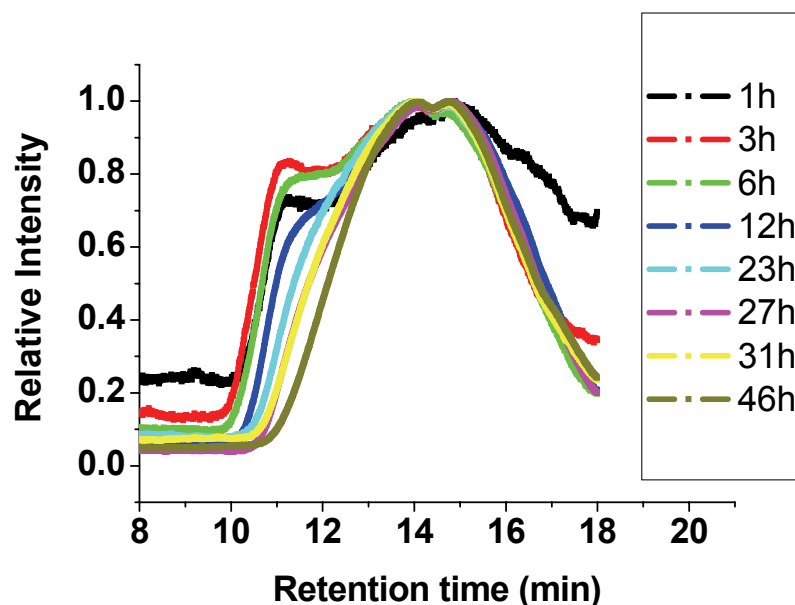


Figure 3-9. PCHC molecular weight development over time for a copolymerization of cyclohexene oxide and carbon dioxide with complex **1a** as catalyst.

Worth mentioning is the relative decrease in the fraction high molecular weight polymer over time. This could imply that the susceptibility towards chain transfer reactions increases with time, as a result of which the formation of lower molecular weight chains predominates at a later stage in the polymerization process. But, for the polymerization as displayed in entry 6 (Table 3-1), which was performed under similar conditions, about four chains per catalyst (monomeric species) were found. This corresponds exactly to the idea that two polymer chains per zinc centrum can be formed and this excludes a possible chain transfer reaction. On the other hand, as will be discussed later, MALDI-ToF-MS analysis reveals several different end groups strengthening the chain transfer hypothesis as stated earlier.

Another possible explanation for these broad distributions might be the presence of slow chain transesterification reactions. Fast chain transesterification reaction would lead to a Schulz-Flory distribution with a polydispersity of approximately 2. However, a prolonged polymerization with the $[(2,6\text{-F}_2\text{C}_6\text{H}_3\text{O})_2\text{Zn}\cdot\text{THF}]_2$ catalyst (which has similarly broad distributions) for two weeks, during which transesterification chains transfer reactions had ample opportunity to convert the broad polymer distribution into a Schulz-Flory distribution, did not show a tendency of the molecular weight distribution to go to a polydispersity of 2. In fact, no change at all could be seen in the SEC traces from a sample after 21 hours (35% conversion) versus a sample taken after the full two weeks (100% conversion), indicating that transesterification does not play a significant role.

3.2.3 MALDI-ToF-MS analyses

MALDI-ToF-MS analyses of the formed polycarbonates prepared with catalyst **1a** showed a non-perfect alternating behavior, as could also be seen in ^1H NMR. Three different end groups were discovered, but a silsesquioxane end group moiety was not detected. Since the silsesquioxane hydroxide moieties are good leaving groups, the polymer-silsesquioxane bonds are probably hydrolyzed during the workup procedure.²²

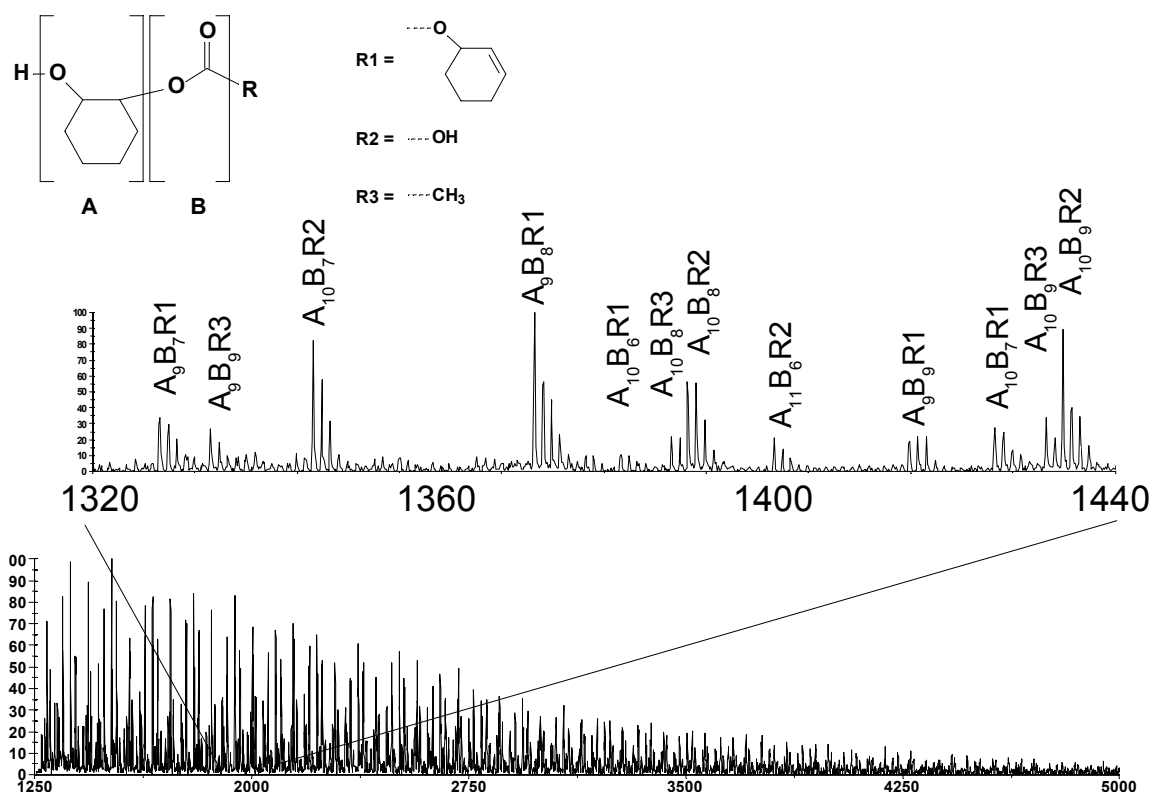
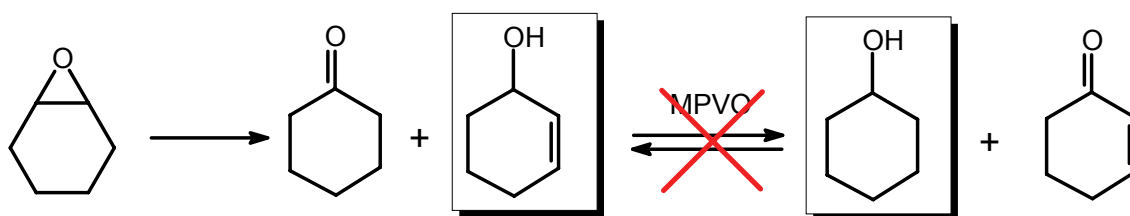


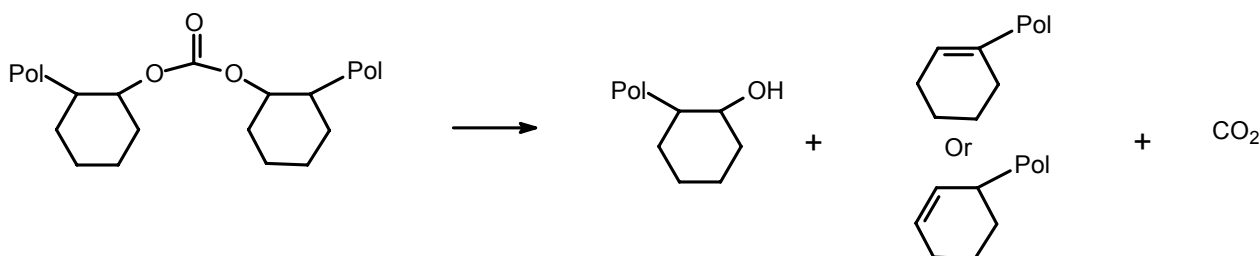
Figure 3-10. MALDI-ToF-MS spectrum of the K^+ adduct of PCHC obtained with catalyst **1a** (entry 7, Table 3-1) and an enlargement of a part of the spectrum.

End group *R1* represents a 2-cyclohexenyl moiety, which possibly originates from a cyclohexene oxide rearrangement, as was reported earlier for the β -diketiminato zinc systems and the bis(phenoxy) zinc catalysts.²³ Remarkable, unlike our previously published results, a cyclohexyl end group could not be found.²³ This indicates the absence of the Oppenauer oxidation/Meerwein-Ponndorf-Verley reduction²⁴ as was observed with for β -diketiminato zinc and bis(phenoxy) zinc catalyst (Scheme 3-3).



Scheme 3-3. Rearrangement reactions of cyclohexene oxide.²³

Another possible explanation for the presence of the 2-cyclohexenyl end groups is a chain scission as reported by Liu et al. for poly(propylene carbonate).²⁵ Due to the high polymerization temperature a carbon dioxide molecule might be released from the PCHC chain by a mechanism as depicted in Scheme 3-4. In this process, a cyclohexenyl and a cyclohexanol end group is formed, which can both be observed by MALDI-ToF-MS (Figure 3-10).



Scheme 3-4. Possible chain scission reaction of a PCHC chain.

At this point no conclusive evidence is present to favor one explanation over the other, but further degradation experiments should elucidate the chain scission mechanism. Chain scission could be partly responsible for the high polydispersities observed in SEC of the formed polymers. On the other hand, similar scission reactions were not observed with bis(phenoxy) zinc catalysts, displaying similar broad molecular weight distributions.²³ The lower temperature used during the copolymerizations with the bis(phenoxy) zinc catalyst (80°C versus the 120°C used for entry 7, Table 3-1) is probably the reason for the absence of the degradation reaction.

The R2 end groups can originate from hydrolyzed silsesquioxane end groups, chain scission as discussed above or water initiated chain transfer, as was also observed for the [(2,6-F₂C₆H₃O)₂Zn·THF]₂ catalyst.²³ Insertion of CO₂ into the Zn-Me bond was also observed (end group R3). Usually this bond is rather unreactive, but pretreating the catalyst with CO₂ (10 bar, 50 °C, 30 min) helps its activation.

3.2.4 Kinetics

A kinetic study on the copolymerization in neat cyclohexene oxide and carbon dioxide with catalysts **1a** and **2a** was performed. The pressure drop that was measured during the reactions was

Silsesquioxane zinc catalysts for the alternating copolymerization of cyclohexene oxide and carbon dioxide

interpreted in terms of a change in liquid phase composition, and was used to calculate the CHO and CO₂ conversion.²⁶ As the vapor pressure of the system is mainly determined by the CO₂ to CHO ratio in the liquid phase, it serves as a primary indication of the composition of this phase. The small influence of PCHC on the vapor pressure has been accurately determined over a wide range and was found to be negligible.²⁷ Consequently, the PCHC concentration can be readily calculated from the difference between the actual and initial CO₂ to CHO ratio. The use of this approach is restricted by the validity of the assumption of thermodynamic equilibrium between the vapor and liquid phases, knowledge of the stoichiometry of the reaction and knowledge of the initial composition. Additionally, the transfer of components between the liquid and vapor phase are assumed to be negligible, as the pressure drop and change in volume of the liquid phase are relatively small.

The experimental conditions and results of these experiments are summarized in Table 2. The results of these kinetic experiments are graphically presented in Figure 3-11. To improve the selectivity of these catalysts, PCy₃ was added (see also paragraph 2.5.1.3). The phosphine can block one of the coordination sites, preventing PCHO formation. Comparison of entry 1 with entries 2-7 indicates that addition of PCy₃ strongly improves the selectivity of polycarbonate over polyether formation. Addition of a stoichiometric ratio of PCy₃ to Zn (entries 2, 6 and 7) resulted in perfectly alternating copolymers for both catalysts **1a** and **2a**. For entry 2 the observed decrease in cyclic carbonate formation can be attributed to the lower reaction temperature. Entries 3-5 demonstrate that the formation of PCHO for catalyst **1a** can also be inhibited by adding PCy₃ to Zn in a 1:2 ratio. Entries 3-5 also demonstrate the positive effect of CO₂ pressure on catalyst activity, which indicates that CO₂ has a direct influence on the rate determining step of this reaction.

The results of the model calculations that provide a mathematical description of the relation between system pressure, temperature, initial composition and actual composition are presented in Figure 3-11. Although the model does not account for CHC formation, Figure 3-11 indicates that the total carbonate yield (PCHC + CHC), calculated from vapor pressure data, agrees well with the results of the ¹H NMR analysis. This is probably due to the very low vapor pressure of CHC and similar interaction towards CO₂, which allows us to treat CHC like carbonate fragments in the polymer chain. The development of conversion over time suggests that there is no significant change of the reaction rate. As diffusion coefficients are expected to decrease significantly in this regime, the absence of a change in the reaction rate indicates that reaction rates are not determined by mass transfer limitations and therefore represent intrinsic kinetics of this reaction.

Table 3-2. Results of kinetic experiments of the copolymerization of cyclohexene oxide and CO₂ by catalysts **1a** and **2a**.

Entry	Complex (μmol) ^{a)}	PCy ₃ :Zn (mol:mol)	Time (h)	P (bar)	T (°C)	Conversion (%) ^{b)}	CHC (%) ^{b)}	Fraction CO ₂ (%) ^{b)}	TOF (h ⁻¹) ^{c)}	\overline{M}_n (g · mol ⁻¹) ^{d)}	$\overline{M}_w / \overline{M}_n$
1	1a (227)	0.0	22	124	125	47	14	65	68.9	10,400	4.3
2	1a (222)	1.0	75	49	80	8.7	0.6	> 99	5.8	11,400	7.3
3	1a (189)	0.57	95	50	121	13	9.9	> 99	9.6	8,100	4.8
4	1a (188)	0.53	95	76	116	33	13	> 99	19.2	7,200	3.2
5	1a (189)	0.50	39	104	116	22	8.0	> 99	70.8	10,600	3.7
6	2a (96)	1.1	94	64	120	21	12	96	27.9	9,300	3.8
7	2a (96)	1.08	92	71	120	18	10	> 99	30.8	9,500	3.6

a) Referring to the monomeric catalyst species. b) As determined by integration of the methine peaks of the different species. c) mol CHO · mol cat⁻¹ · h⁻¹ (referring to the monomeric catalyst species). d) PS equivalents.

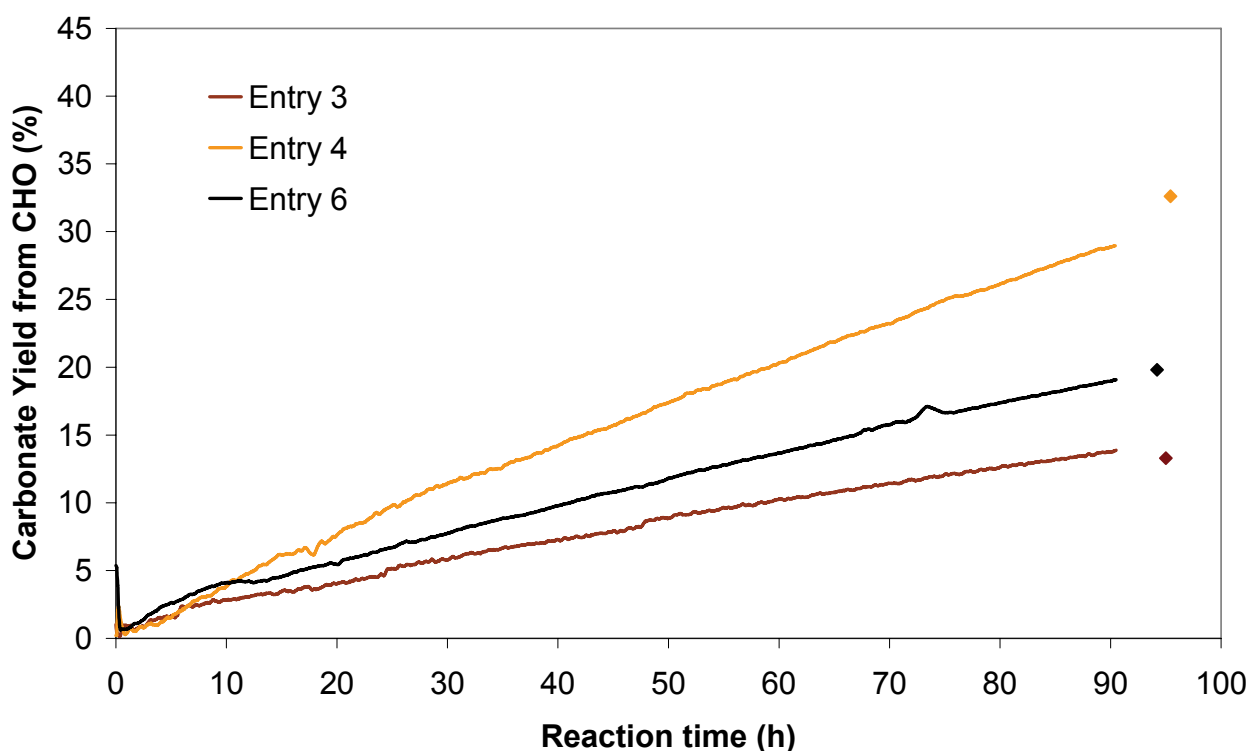


Figure 3-11. Carbonate yield as a function of reaction time for entries 3, 4 and 5 (Table 3-2). The lines are calculated from vapor pressure data, symbols represent results from ¹H NMR analysis.

3.2.5 Zinc modified silica particles

Mesoporous silica particles ($50 \mu\text{m}$, $304 \text{ m}^2 \cdot \text{g}^{-1}$) were modified with ZnEt_2 to prepare a heterogeneous zinc based catalyst. Analysis of the zinc contents of the catalyst by means of ICP-MS showed a contents of $1.82 \text{ mmol} \cdot \text{g}^{-1}$. Literature values of unmodified Sylopol 948 silica show a silanol content of $3.2 \text{ mmol} \cdot \text{g}^{-1}$, using the same drying conditions (250°C for 3 hours), which would imply a silanol conversion with zinc of around 56%. Several experiments were performed to compare the findings with the silsesquioxane model compounds with this silica supported zinc catalyst. If chain transfer can be suppressed, PCHC grafted silica particles could be obtained, which might offer better morphology control and less reactor fouling. Polymerizations with the supported catalyst were performed in a high pressure reactor equipped with a sapphire view-cell to visually follow the polymerizations. The first polymerization in toluene (good solvent for PCHC) showed a strong tendency of the support to stick to the side of the reactor after the polymer particles started to grow. To counter this stickiness, the following polymerizations were performed in a non solvent (either petroleum ether or heptane) to precipitate the polymer upon formation. Unfortunately, the monomer itself is a very good solvent for the polymer and still makes the particles sticky. Polymerizations under starved feed conditions might be more suitable for these systems. CO_2 may be considered as a non-solvent for PCHC, CHO on the other hand acts as an excellent solvent for PCHC. Keeping the CHO concentration relatively low and constant throughout the polymerization might be a useful way to control the precipitation of PCHC from the medium as well as the molecular weight. Provided that a concentration of 24 wt% CHO can be maintained, the maximum solubility of PCHC in CO_2 is below 1 wt% at pressures of approximately 1200 bar. This implies that above this concentration the driving force for phase separation increases.²⁸

Table 3-3. Copolymerization results with cyclohexene oxide and CO_2 with zinc modified silica particles.

Entry	Solvent	CHO (mL)	T ($^\circ\text{C}$)	P (bar)	Time (h)	mg catalyst (μmol zinc)	Yield (g)	Fraction CO_2 (%) ^{a)}	\overline{M}_n ($\text{g} \cdot \text{mol}^{-1}$) ^{b)}	TOF (h^{-1}) ^{c)}	$\overline{M}_w / \overline{M}_n$
1	Toluene (35 mL)	15	80	80	24	150 (273)	0.82	91	10,300	0.9	17.1
2	Heptane (200 mL)	15	120	80	48	200 (364)	0.7	85	8,400	0.6	5.0
3	Pet. Ether (200 mL)	15	120	80	24	200 (364)	0.9	93	9,000	0.7	5.3

a) As determined by integration of the methine peaks of the different species. b) PS equivalents. c) $\text{Mol CHO} \cdot \text{mol cat}^{-1} \cdot \text{h}^{-1}$ (referring to the monomeric catalyst species).

Although the modified silica particles are active in the copolymerization of carbon dioxide and cyclohexene oxide, activities and yields are lower than of their homogeneous analogues. This is a common phenomenon when homogeneous catalysts are being supported; see for example the

silica immobilization of metallocenes.²⁹ The low yield can further be explained by heterogenization of the system during polymerization. The formation and precipitation of the sticky particles will hamper the polymerization significantly and at least a part of the zinc catalysts will not participate in the polymerization anymore. The carbonate contents, however, remained at the same levels as with the silsesquioxane catalysts. This in contrast to the results obtained with the tethering of β -diketiminato zinc complexes to a silica support where a considerable drop in CO₂-content was observed compared to the homogeneous analogue.⁷ Due to starvation of CO₂ at the active site, the carbonate content was found to drop at the end of the polymerization. The morphology of the formed polymer is quite different from the one observed with the polymers obtained with complex **1a** and **2a**. The particles which are formed have a high bulk density in contrast to the light and fluffy polymers obtained after precipitation of a homogeneous reaction mixture in petroleum ether. Dissolution in THF for SEC analyses, however, did not present a problem.

3.2.6 Conclusion

It can be concluded that the silsesquioxane zinc complexes tested are active in the copolymerization of cyclohexene oxide and CO₂. Polydispersities are broad, which indicates a similar type of polymerization mechanism to what is seen with the bis(phenoxy) zinc catalysts. Following the polymerization over time showed a different polydispersity development between catalyst **1a** and **2a**, although the exact cause remains unknown. Precipitation polymerization with ZnEt₂-treated silica particles resulted in a lowering of the viscosity of the medium, but also led to fouling of the reactor wall with sticky polymer particles.

Reaction kinetics was determined by following the CO₂ pressure drop, which was related to the change of composition during the reaction. These measurements appear to represent the intrinsic kinetics of this reaction, which is directly influenced by CO₂ pressure. The addition of PCy₃ had a positive effect on the selectivity of the catalysts.

3.3 Experimental section

3.3.1 Materials

Cyclohexene oxide (Aldrich, 98%) was dried over CaH₂, distilled and stored under argon on molsieves (4Å) prior to use. Carbon dioxide (> 99.9993% pure) was purchased from HoekLoos and was used without any further purification. Toluene (AR) and petroleum ether (40-70, AR) were dried over an alumina column and stored on molsieves (4 Å). Heptane (AR) was dried by

Silsesquioxane zinc catalysts for the alternating copolymerization of cyclohexene oxide and carbon dioxide
distillation from Na/K alloy. Unless mentioned otherwise, all manipulations were performed under an inert atmosphere using standard Schlenk techniques or a in a nitrogen-filled glove-box. Commercial silica gel (Grace Davison, Sylopol 948, 50 μm , 304 $\text{m}^2 \cdot \text{g}^{-1}$) was used for the support experiments. All other chemicals were purchased from Aldrich and were used as received. Silsesquioxane ligands **1**³⁰ and **2**³¹ and the bis(phenoxy) zinc complex $[(2,6\text{-F}_2\text{C}_6\text{H}_3\text{O})_2\text{Zn}\cdot\text{THF}]_2$ ^{10e} were prepared according to literature procedures.

3.3.2 Analytical techniques

¹H NMR spectra were recorded on a Varian Gemini 2000 (300 MHz), a Varian Mercury Vx (400 MHz) and a Varian Mercury Plus (200 MHz) spectrometer. Size Exclusion Chromatography (SEC) spectra were recorded on a Waters GPC equipped with a Waters model 510 pump and a model 410 differential refractometer (40 °C). THF was used as the eluent at a flow rate of 1.0 $\text{mL} \cdot \text{min}^{-1}$. A set of two linear columns (Mixed C. Polymer Laboratories, 30 cm, 40 °C) were used. Molecular weights were calculated relative to polystyrene standards. Data acquisition and processing was performed using Waters Millennium32 software. MALDI-ToF-MS analysis was carried out on a Voyager DE-STR from Applied Biosystems. The matrix, DCTB (*trans*-2-[3-(4-*t*-butylphenyl)-2-methyl-2-propenylidene] malononitrile) was synthesized according to literature procedures.³² Potassium trifluoroacetate (Aldrich, > 99%) was added to the polymer samples as the cationization agent. The matrix was dissolved in THF at a concentration of 40 $\text{mg} \cdot \text{mL}^{-1}$. The potassium trifluoroacetate was added to THF at typical concentrations of 1 $\text{mg} \cdot \text{mL}^{-1}$. Polymer was dissolved in THF at approximately 1 $\text{mg} \cdot \text{mL}^{-1}$. In a typical MALDI-ToF-MS analysis, the matrix, potassium trifluoroacetate and the polymer solution were premixed in a ratio of 10:1:5. The premixed solutions were hand-spotted on the target well and left to dry. Spectra were recorded in both the linear and reflector mode.

3.3.3 Synthesis of $[(c\text{-C}_5\text{H}_9)_7\text{Si}_7\text{O}_{11}(\text{OSiMePh}_2)]_2\text{Zn}_4\text{Me}_4$ (**1a**)

To a cooled (-80 °C) solution of $(c\text{-C}_5\text{H}_9)_7\text{Si}_7\text{O}_9(\text{OSiMePh}_2)(\text{OH})_2$ (2.14 g, 2.0 mmol) in toluene (20 mL), ZnMe_2 (2.2 mL 2.0 M in toluene, 4.4 mmol) was added. The mixture was allowed to warm to room temperature, upon which evolution of gas was visible. After stirring for 30 min, the mixture was gently heated, and after gas evolution ceased, heated to reflux for 1 minute. After evaporation of the volatiles, the residue was dissolved in hot hexane (50 mL) and toluene (10 mL) and the solution was filtered. Colorless crystals, suitable for an X-ray diffraction study (1.27g, 0.52 mmol, 52%) were obtained after crystallization at -30°C. ¹H NMR ($[\text{D}_6]$ benzene): $\delta = 7.80$ (d, 8 H,

Ph), 7.25 (m, 12 H, Ph), 1.70 (m, 112 H, $CH_2-C_5H_9$), 1.25 (m, 14 H, $CH-C_5H_9$), 0.95 (s, 6 H, Si- CH_3), 0.05 (s, 12 H, ZnMe). $^{13}C\{^1H\}$ NMR ($[D_6]$ benzene): $\delta = 137.82, 134.73, 129.69, 128.14$ (Ph), 28.62, 28.43, 28.26, 28.17, 27.94, 27.89, 27.46, 27.42, 27.36, 27.33, 27.30, 27.17, 26.95, ($CH_2-C_5H_9$), 25.65, 25.17, 24.16, 23.04, 22.82 (1:2:2:1:1, $CH-C_5H_9$), 0.41 (Si- CH_3), -10.39 (Zn- CH_3). $^{29}Si\{^1H\}$ NMR ($[D_6]$ benzene vs. $SiMe_4$) $\delta = -10.77$ ($SiMePh_2$), -57.33, -63.26, -64.12, -65.20, -65.60 (2:1:1:1:2).

3.3.4 Synthesis of $[(c-C_5H_9)_7Si_7O_{12}]_2Zn_4Me_2$ (**2a**)

To a solution of $(c-C_5H_9)_7Si_7O_9(OH)_3$ (3.79 g, 4.32 mmol) in toluene (20 mL), $ZnMe_2$ (4.33 mL 2.0 M in toluene, 8.66 mmol) was slowly added at room temperature. After gas evolution ceased, the cloudy mixture was heated till everything was dissolved and then slowly cooled to $-18^\circ C$, resulting in the formation of a white crystalline compound. After decanting the liquid, traces of solvents were removed in vacuo yielding **2a** as a white solid (2.9 g, 1.4 mmol of the dimer, 65%). 1H NMR ($[D_6]$ benzene): $\delta = 2.3-1.4$ (m, CH_2 , C_5H_9 , 112H), 1.4-1.1 (m, CH , C_5H_9 , 14H), -0.07 (s, $ZnCH_3$, 6H); $^{13}C\{^1H\}$ NMR ($[D_6]$ benzene): $\delta = 28.75, 28.54, 28.39, 28.35, 27.96, 27.94, 27.82, 27.68, 27.58, 27.52, 27.46$ (s, CH_2 , C_5H_9), 24.82, 24.43, 24.32, 22.83, 22.73 (s, CH , C_5H_9 , relative intensities 1:1:2:2:1), -14.18 (s, $ZnCH_3$)

3.3.5 Treatment of silica-support with $ZnEt_2$

To a suspension of pre-dried silica ($250^\circ C$, 3h, vacuum) in heptane (25 mL), $ZnEt_2$ (25 mL, 1 M solution in hexane, 25 mmol) was slowly added. The suspension was stirred overnight, decanted, washed with heptane (2×10 mL) to remove unreacted $ZnEt_2$ and dried in vacuo. The samples were analyzed by ALControl BV, Hoogvliet the Netherlands, using the following method: silica catalyst (108.9 mg) was extracted in the course of 1 hour using HNO_3 (10 mL of a 1% solution). The solution was then filtered ($0.45 \mu m$) and analyzed by ICP-MS (according to NEN 6426). The concentration of zinc was found to be $1.82 \text{ mmol zinc} \cdot \text{g silica}^{-1}$.

3.3.6 Example of a typical copolymerization using catalyst **1a**

Catalyst **1a** (240 mg of the dimeric compound, 100 μmol) was dissolved in toluene (35 mL) and injected into the autoclave. The autoclave was pressurized to 10 bar and heated to $50^\circ C$ for 30 minutes. Next the CHO (15 mL) was injected into the reactor with a CO_2 overpressure (50 bar). All

Silsesquioxane zinc catalysts for the alternating copolymerization of cyclohexene oxide and carbon dioxide

valves were closed and the reactor was further heated to 120 °C resulting in a pressure of about 80 bar. After a set polymerization time, a sample was taken for ^1H NMR analysis (300 MHz, CDCl_3) to determine the conversion. Conversions were determined by integration of the methine peaks in the ^1H NMR spectra: ^1H NMR (300 MHz, CDCl_3): δ 4.65 (br, CH (PCHC), 2H), 3.11 (s, CH (CHO), 2H). The samples for SEC analysis were prepared as follows: About 0.5 mL of each of the reaction mixtures was added dropwise to a tenfold excess of petroleum-ether (40-70) upon which the poly(cyclohexene carbonate) (PCHC) precipitated. After separation, the polymer was redissolved in the SEC eluent (THF). Polymers needed for MALDI-ToF-MS analyses were prepared in a similar manner as described above.

3.3.7 Example of a typical copolymerization for kinetic measurements

These reactions were carried out in a set-up as depicted in Figure 3-12. The initial CO_2 to CHO ratio for the kinetic experiments was controlled by preparation of a liquid feed in a separate autoclave. For this purpose dry CHO (300 mL) was added to a dry 500 mL autoclave (feed reactor, Figure 3-12), which was subsequently pressurized with CO_2 . The composition of the liquid phase in this reactor was controlled by temperature and pressure.³³

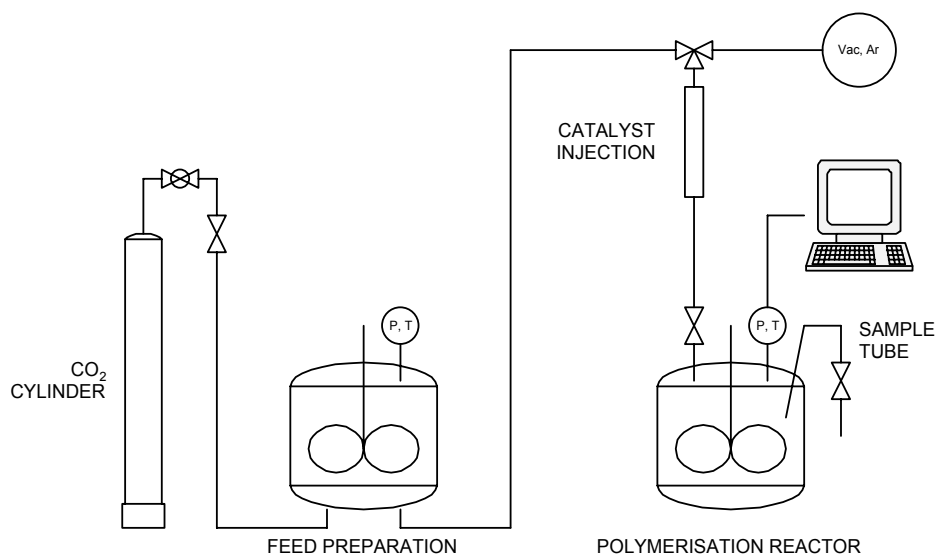


Figure 3-12. Schematic outline of set-up for on-line determination of conversion from pressure drop.

Thermodynamic equilibrium was assumed after 12 h of intensive mechanical stirring. Prior to the catalytic experiments, the 100 mL polymerization reactor was dried overnight at 120°C under argon flow. After transfer of a mixture of solid catalyst (**1a** or **2a**) and PCy_3 to the autoclave, the complete system was rinsed during three repetitive cycles of vacuum and CO_2 atmosphere. While maintaining the autoclave at room temperature, the liquid feed was added and subsequently heated

to the desired reaction temperature. It should be noted that for these copolymerizations no solvents were used. Typical catalyst loading, reaction temperature, pressure and reaction time for these experiments were 50-100 μmol (of the dimeric complex), 120°C, 50 to 75 bar and around 90 h, respectively. After each experiment the conversion as calculated from the vapor pressure was verified using ^1H NMR. The products were purified by the dropwise addition of a 10 fold volumetric dilution of the reaction mixture in THF to a 10 fold excess of petroleum ether. The precipitated poly(cyclohexene carbonate) was subsequently separated and dissolved in THF for analysis by SEC, as described earlier.

3.4 Acknowledgements

Marcus van Schilt is kindly acknowledged for the kinetic measurements experiments and the development of the model relating the CO_2 pressure drop to the CHO conversion. Gijsbert Gerritsen and Rob Hannsen are both kindly acknowledged for providing the catalysts and characterization thereof.

3.5 References

1. (a) Beckman, E. J. *Science* **1999**, 283, 946. (b) Darensbourg, D. J.; Holtcamp, M. W. *Coord. Chem. Rev.* **1996**, 153, 155. (c) Super, M. S.; Beckman, E. J. *Trends Polym. Sci.* **1997**, 5, 236. (d) Rokicki, G. *Prog. Polym. Sci.* **2000**, 25, 259. (e) Sugimoto, H.; Inoue, S. *J. Polym. Sci.: Part A* **2004**, 42, 5561. (f) Coates, G. W.; Moore, D. R. *Angew. Chem. Int. Ed.* **2004**, 43, 6618.
2. (a) Cheng, M.; Lobkovsky, E. B.; Coates, G. W. *J. Am. Chem. Soc.* **1998**, 120, 11018. (b) Cheng, M.; Moore, D. R.; Reczek, J. J.; Chamberlain, B. M.; Lobkovsky, E. B.; Coates, G. W. *J. Am. Chem. Soc.* **2001**, 23, 8738. (c) Allen, S. D.; Moore, D. R.; Lobkovsky, E. B.; Coates, G. W. *J. Am. Chem. Soc.* **2002**, 124, 14284. (d) Moore, D. R.; Cheng, M.; Lobkovsky, E. B.; Coates, G. W. *Angew. Chem. Int. Ed.* **2002**, 41, 2599. (e) Moore, D. R.; Cheng, M.; Lobkovsky, E. B.; Coates, G. W. *J. Am. Chem. Soc.* **2003**, 125, 11911.

- 3 (a) Darensbourg, D. J.; Yarbrough, J. C. *J. Am. Chem. Soc.* **2002**, *124*, 6335. (b) Eberhardt, R.; Allmendinger, M.; Rieger, B. *Macromol. Rapid Commun.* **2003**, *24*, 194. (c) Darensbourg, D. J.; Yarbrough, J. C.; Ortiz, C.; Fang, C. C. *J. Am. Chem. Soc.* **2003**, *125*, 7586. (d) Darensbourg, D. J.; Mackiewicz, R. M.; Rodgers, J. L.; Phelps, A. L. *Inorg. Chem.* **2004**, *43*, 1831. (e) Darensbourg, D. J.; Mackiewicz, R. M.; Phelps, A. L.; Billodeaux, D. R. *Acc. Chem. Res.* **2004**, *37*, 836. (f) Darensbourg, D. J.; Rodgers, J. L.; Mackiewicz, R. M.; Phelps, A. L. *Catal. Today* **2004**, *98*, 485. (g) Darensbourg, D. J.; Mackiewicz, R. M.; Rodgers, J. L.; Fang, C. C.; Billodeaux, D. R.; Reibenspies, J. H. *Inorg. Chem.* **2004**, *43*, 6024.
4. (a) Kruper, W. J.; Dellar, D. V. *J. Org. Chem.* **1995**, *60*, 725. (b) Chisholm, M. H.; Zhou, Z. *J. Am. Chem. Soc.* **2004**, *126*, 11030. (c) Stamp, L. M.; Mang, S. A.; Holmes, A. B.; Knights, K. A.; de Miguel, Y. R.; McConvey, I. F. *Chem. Commun.* **2001**, 2502. (d) Paddock, R. L.; Nguyen, S. T. *J. Am. Chem. Soc.* **2001**, *123*, 11498. (e) Mang, S.; Cooper, A. I.; Colclough, M. E.; Chauhan, N.; Holmes, A. B. *Macromolecules* **2000**, *33*, 303.
- 5 (a) Takeda, N.; Inoue, S. *Makromol. Chem.* **1978**, *179*, 1377. (b) Aida, T.; Inoue, S. *Macromolecules* **1982**, *15*, 682. (c) Aida, T.; Ishikawa, M.; Inoue, S. *Macromolecules* **1986**, *19*, 8. (d) Aida, T.; Inoue, S. *Acc. Chem. Res.* **1996**, *29*, 39.
- 6 See for example Hlatky, G. G. *Chem. Rev.* **2000**, *100*, 1347.
- 7 Yu, K.; Jones, C. W. *Organometallics* **2003**, *22*, 2571.
8. Inoue, S.; Koinuma, H.; Tsuruta, T. *Polymer Lett.* **1969**, *7*, 287.
- 9 Archibald, S. J. *Comprehensive Coordination Chemistry II* **2004**, *6*, 1147.
- 10 (a) Darensbourg, D. J.; Holtcamp, M. W.; Struck, G. E.; Zimmer, M. S.; Niezgoda, S. A.; Rainey, P.; Robertson, J. B.; Draper, J. D.; Reibenspies, J. H. *J. Am. Chem. Soc.* **1999**, *121*, 107. (b) Koning, C. E.; Wildeson, J.; Parton, R.; Plum, B.; Steeman, P.; Darensbourg, D. J. *Polymer* **2001**, *42*, 3995. (c) Darensbourg, D. J.; Wildeson, J. R.; Lewis, S. J.; Yarbrough, J. C. *J. Am. Chem. Soc.* **2002**, *124*, 7075. (d) Darensbourg, D. J.; Wildeson, J. R.; Yarbrough, J. C. *Inorg. Chem.* **2002**, *41*, 973. (e) Darensbourg, D. J.; Wildeson, J. R.; Yarbrough, J. C.; Reibenspies, J. H. *J. Am. Chem. Soc.* **2000**, *122*, 12487. (f) Darensbourg, D. J.; Zimmer, M. S.; Rainey, P.; Larkins, D. L. *Inorg. Chem.* **2000**, *39*, 1578. (g) Darensbourg, D. J.; Niezgoda, S. A.; Draper, J. D.; Reibenspies, J. H. *Inorg. Chem.* **1999**, *38*, 1356. (h) Darensbourg, D. J.; Niezgoda, S. A.; Draper, J. D.; Reibenspies, J. H. *J. Am. Chem. Soc.* **1998**, *120*, 4690. (i) Darensbourg, D. J.; Holtcamp, M. W. *Macromolecules* **1995**, *28*, 7577. (j) Dinger, M. B.; Scott, M. J. *Inorg. Chem.* **2001**, *40*, 1029.

- 11 (a) Vansant, E. F.; Van Der Voort, P.; Vrancken, K. C.; Characterization and chemical modification of the silica surface. In *Studies in Surface Science and Catalysis* Elsevier, Amsterdam **1995**, 93. (b) Morrow, B. A.; Gay, I. D. Infrared and NMR Characterization of the Silica Surface. In *Adsorption on Silica Surface*; Papirer, E., Ed.; Marcel Dekker: New York, 2000. pp 9-33. (c) Krijnen, S.; Harmsen, R. J.; Abbenhuis, H. C. L.; van Hooff, J. H. C.; van Santen, R. A. *Chem. Commun.* **1999**, 501.
- 12 See for example: (a) Feher, F. J.; Terroba, R.; Jin, R.-Z.; Lucker, S.; Nguyen, F.; Brutchey, R.; Wyndham, K. D. *Materials Research Society Symposium Proceedings* **2001**, 628, CC2 1 1-CC2 1 6. (b) Hanssen, R. W. J. M.; van Santen, R. A.; Abbenhuis, H. C. L. *Eur. J. Inorg. Chem.* **2004**, 675. (c) Marciniak, B.; Maciejewski, H. *Coord. Chem. Rev.* **2001**, 223, 301.
- 13 (a) Duchateau, R. *Chem. Rev.* **2002**, 102, 3525. (b) Duchateau, R.; Cremer, U.; Harmsen, R. J.; Mohamud, S. I.; Abbenhuis, H. C. L.; Van Santen, R. A.; Meetsma, A.; Thiele, S. K. H.; Van Tol, M. F. H.; Kranenburg, M. *Organometallics* **1999**, 18, 5447.
- 14 (a) Vorstenbosch, M. L. W. Alkene epoxidation with silsesquioxane-based chromium and titanium complexes. Ph. D. thesis, Eindhoven, **2002**, ISBN 90-386-2773-4. (b) Abbenhuis, H. C. L.; Krijnen, S.; van Santen, R. A. *Chem. Comm.* **1997**, 331. (c) Crocker, M.; Herold, R. H. M.; Orpen, A. G. *Chem. Comm.* **1997**, 2411. (d) Pescarmona, P. P.; Maschmeyer, T.; van der Waal, J. C. *Chem. Eng. Commun.* **2004**, 191, 68. (e) Smet, P.; Riondato, J.; Pauwels, T.; Moens, L.; Verdonck, L. *Inorg. Chem. Comm.* **2000**, 3, 557. (f) Skowronska-Ptasinska, M. D.; Vorstenbosch, M. L. W.; van Santen, R. A.; Abbenhuis, H. C. L. *Angew. Chem. Int. Ed. Engl.* **2002**, 41, 637.
- 15 (a) Feher, F. J.; Soulivong, D.; Eklund, A. G.; Wyndham, K. D. *Chem. Comm.* **1997**, 1185. (b) Feher, F. J.; Tajima, T. L. *J. Am. Chem. Soc.* **1994**, 116, 2145.
- 16 $(C_{50}H_{82}O_{12}Si_8Zn_2)_2$, $M_r = 2461.32$, monoclinic, $P21/n$, $a = 14.8772(6)$, $b = 17.9401(7)$, $c = 21.9733(8)$ Å, $\beta = 90.006(1)^\circ$, $V = 5864.6(4)$ Å³, $Z = 2$, $D_x = 1.394$ gcm⁻³, $F(000) = 2600$, $\mu = 10.38$ cm⁻¹, $T = 110$ K, 53279 reflections measured, $Goof = 1.041$, $wR(F^2) = 0.0869$, $R(F) = 0.0327$. Data were collected on a Nonius Kappa CCD area detector with a graphite monochromator ($\lambda = 0.71073$ Å).
- 17 Hanssen, R. W. J. M. *On the formation and reactivity of multinuclear silsesquioxane metal complexes*, Ph.D. Thesis, Eindhoven, **2003**, ISBN 90-386-2924-9.
- 18 Driess, M.; Merz, K.; Rell, S. *Eur. J. Inorg. Chem.* **2000**, 2000, 2517.
- 19 Darensbourg, D. J.; Rainey, P.; Yarbrough, J. C. *Inorg. Chem.* **2001**, 40, 986.

- 20 1 eq (to Zn-Me moieties) of *i*-PrOH was added to the solution of the catalyst in toluene and stirred for 30 minutes at room temperature (gas evolution was visible) prior to polymerization.
- 21 Reaction conditions: 100 μ mol of the dimeric catalyst, 15 mL of CHO, 35 mL of toluene, 120 $^{\circ}$ C, 80 bar.
- 22 A silanol group is more acidic than a cyclohexanol, which is a good indication that the silanol is a better leaving group. See: Dijkstra, T. W.; Duchateau, R.; van Santen, R. A.; Meetsma, A.; Yap, G. P. A. *J. Am. Chem. Soc.* **2002**, *124*, 9856.
- 23 Meerendonk, W. J. van; Duchateau, R.; Koning, C. E.; Gruter, G.-J. M. *Macromolecules* **2005**, *38*, 7306.
24. For some recent papers see: (a) Nishide, K.; Node, M. *Chirality* **2002**, *14*, 759. (b) de Graauw, C. F.; Peters, J. A.; van Bekkum, H.; Huskens, J. *Synthesis* **1994**, *10*, 1007. (c) Ooi, T.; Otsuka, H.; Miura, T.; Ichikawa, H.; Maruoka, K. *Org. Lett.* **2002**, *4*, 2669.
- 25 Liu, B.; Chen, L.; Zhang, M.; Yu, A. *Macromol. Rapid Commun.* **2002**, *23*, 881.
- 26 The assumption was made that the copolymer is perfectly alternating.
- 27 Investigated range: 0-140 bar, 0-50% CO₂ and 80-150 $^{\circ}$ C. The effect of PCHC on the vapor pressure of similar CHO/CO₂ mixtures at 120 $^{\circ}$ C and 20% conversion is typically lower than 2%.
- 28 Van Schilt, M. A.; Wering, R. M.; Van Meerendonk, W. J.; Kemmere, M. F.; Keurentjes, J. T. F.; Kleiner, M.; Sadowski, G.; De Loos, T. W. *Ind. Eng. Chem. Res.* **2005**, *44*, 3363.
- 29 Smit, M.; Zheng, X.; Loos, J.; Chadwick, J. C.; Koning, C. E. *J. Pol. Sci.:Part A.* **2005**, *43*, 2734.
- 30 Abbenhuis, H. C. L.; Burrows, A. D.; Kooijman, H.; Lutz, M.; Palmer, M. T.; van Santen, R. A.; Spek, A. L. *Chem. Commun.* **1998**, 2627.
- 31 (a) Feher, F. J.; Budzichowski, T. A.; Weller, K. J. *J. Am. Chem. Soc.* **1989**, *111*, 7288. (b) Feher, F. J.; Weller, K. J. *Organometallics* **1990**, *9*, 2638 (c) Feher, F. J.; Weller, K. J.; Ziller, J. W. *J. Am. Chem. Soc.* **1992**, *114*, 9686.
- 32 Ulmer, L.; Mattay, J.; Torres-Garcia, H. G.; Luftmann, H. *Eur. J. Mass Spectrom.* **2000**, *6*, 49.
- 33 Van Schilt, M. A.; Wering, R. M.; De Loos, Th. W.; Keurentjes, J. T. F. *Measurement and modelling of the high-pressure phase behavior of the binary system carbon dioxide and cyclohexene oxide*, *J. Chem. Eng. Data*, in press.

Chapter 4

High throughput and mechanistic studies of zinc catalysts

A high throughput parallel set-up has been validated for the copolymerization of CO₂ and cyclohexene oxide (CHO). Two β -diketiminato zinc complexes, [HC(C(Me)=N-2,6-C₆H₃R₂)₂]ZnN(SiMe₃)₂ (R = Et (1), i-Pr (2)), were tested for their activity at different catalyst concentrations. Molecular weights, polydispersities and activities were found to be comparable with literature values and lab scale reactions. For both the high throughput experiments (HTE) and the lab scale polymerizations, a deviation was discovered between the theoretical \overline{M}_n development versus conversion and the calculated values. Therefore, a detailed investigation was conducted into the chain microstructure and reaction mechanisms of the synthesis of poly(cyclohexene carbonate) (PCHC) prepared with two β -diketiminato zinc catalysts ((EtBDI)ZnOEt, (EtBDI)ZnOMe (EtBDI = 2-(2,6-diethylphenyl)amido-4-(2,6-diethylphenyl)imino-2-pentene) and a bis(phenoxy)zinc catalyst [(2,6-F₂C₆H₃O)₂Zn·THF]₂). The bis(phenoxy) zinc system yielded some ether linkages, while the β -diketiminato zinc catalyzed system produces perfectly alternating cyclohexene oxide – CO₂ copolymers. Besides the expected methoxy and ethoxy end groups, originating from the initiating group from the catalyst, the presence of a 1:1 mixture of cyclohexyl and cyclohexenyl end groups for all three catalyst systems points to an unexpected side reaction, most probably the result of trace amounts of water present in the system. Under these conditions the β -diketiminato zinc catalyst is not a truly living system, which explains the lower observed \overline{M}_n compared to the theoretical value. The, for a non-living system, surprisingly low polydispersity index, is the result of a rapid reversible chain transfer process (with respect to the propagation reaction) with alcohols and/or hydroxyl terminated polymer chains.

4.1 Introduction

Copolymerization of CO₂ and oxiranes using high pressure autoclaves typically allows one experiment per reactor per day. In this chapter we like to demonstrate that a high throughput approach towards further development and fine tuning of these copolymerizations is feasible with

the current state of the art equipment available on the market, allowing a significant efficiency increase. Two β -diketiminato zinc catalysts (**1** and **2**, Figure 4-1) were used for these experiments.

Although various catalysts have been developed for the oxirane-CO₂ copolymerization, the complete mechanism of the polymerization reaction is still not fully understood (see chapter 2). For example, there is still some debate about whether β -diketiminato zinc complexes have to be dimeric to be catalytically active.¹ Furthermore, termination or chain transfer reactions have never been seriously addressed in the past. In case of the β -diketiminato zinc catalysts, absence of any termination or chain transfer mechanism seemed justified, as the low polydispersities reported for this system and the linear relationship found between \overline{M}_n vs. monomer conversion are indicative for a living nature (vide infra). The bis(phenoxy)zinc catalysts (**5**, Figure 4-1), on the other hand, do give poly(cyclohexene carbonate) (PCHC) with extremely high polydispersities. The lack of conformity between these seemingly similar polymerizations triggered us to take a closer look at these systems. Some anomalies were found in the high throughput experiments, which could not be explained by the mechanism proposed previously (see chapter 2) and a more detailed investigation of the polymer microstructure was undertaken with triple-SEC and MALDI-ToF-MS. In this chapter we present our results on a mechanistic study of the cyclohexene oxide – CO₂ copolymerization catalyzed by β -diketiminato zinc species (**3** and **4**, Figure 4-1) and a bis(phenoxy)zinc catalyst (**5**, Figure 4-1), and we compare the poly(cyclohexene carbonate) products obtained using the two catalyst systems.

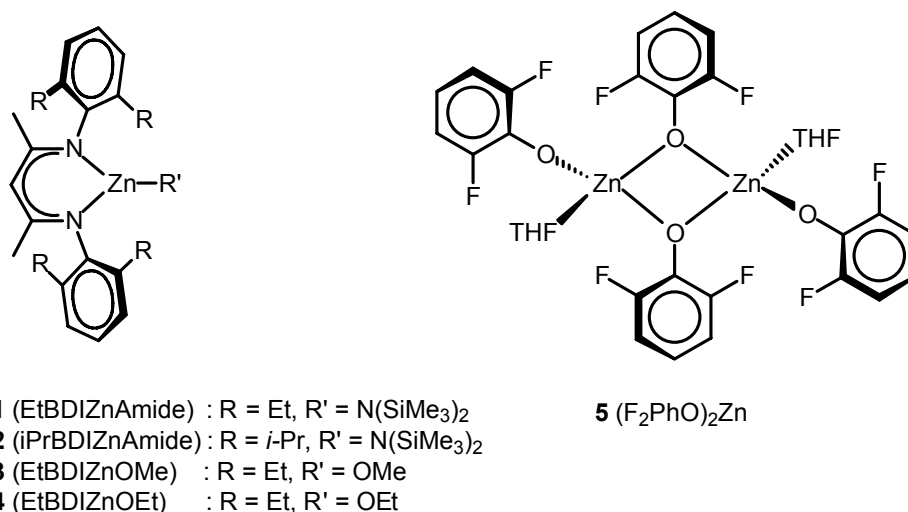


Figure 4-1. β -Diketiminato zinc and bis(phenoxy) zinc catalysts used in this study.

4.2 Results and discussion

4.2.1 High Throughput Automated Parallel Evaluation of Zinc Based Catalysts for the Copolymerization of CHO and CO₂ to Polycarbonates.

This viability study of the use of high throughput equipment for copolymerization of oxiranes with carbon dioxide was performed with catalysts **1** and **2** (Figure 4-1), first employed by Coates et al.² We have selected the β -diketiminato zinc amide catalysts with ethyl- and *iso*-propyl- substituted aryl groups for their proven high copolymerization activities.³ For the high throughput experiments, twelve copolymerization reactions were performed simultaneously. The two zinc catalysts (**1** and **2**, Figure 4-1) were applied in three different concentrations (0.03, 0.06 and 0.09 mol% with respect to the amount of CHO used). To test the reproducibility of the setup, each combination was performed in duplicate. Conversions were determined by integration of the polymeric versus the monomeric methine proton resonance in the ¹H NMR spectra. A summary of the obtained results is presented in Table 4-1.

Table 4-1. Polymerization results of high throughput experiments at 50°C for 3 hours.

Reaction Nr.	Catalyst	Mol-% catalyst ^{a)}	Conversion to PCHC ^{b)}		TOF ^{c)}		\overline{M}_w (kg · mol ⁻¹) ^{d)}		$\overline{M}_w / \overline{M}_n$	
			Exp 1	Exp 2	Exp 1	Exp 2	Exp 1	Exp 2	Exp 1	Exp 2
#1	1	0.03%	3%	0%	32	0	2.6	0	1.1	0
#2	1	0.06%	20%	21%	105	111	19.4	20.6	1.1	1.1
#3	1	0.09%	11%	25%	38	88	9.3	23.8	1.2	1.2
#4	2	0.03%	4%	5%	41	51	3.4	3.5	1.2	1.1
#5	2	0.06%	23%	25%	122	131	25.1	30.0	1.1	1.2
#6	2	0.09%	30%	27%	105	93	31.5	28.1	1.2	1.2

a) Mol-% of catalyst with respect to the monomer. b) Determined by ¹H NMR. c) Mol CHO · mol catalyst⁻¹ · hour⁻¹. d) Polystyrene equivalents.

Several interesting features can be derived from the results depicted in Table 4-1, Figure 4-2 and Figure 4-3. Let us first look at the reproducibility of the results. Except for experiment 2 of reaction #1 and experiment 1 of reaction #3, the conversions obtained are as expected and the duplicate runs are similar with only a small deviation of approximately 3%. The molecular weights nicely follow the same trend as the conversions. For example, the somewhat higher conversion in experiment 1 of reactions #2 and #6 or experiment 2 of reaction #5 is reflected in a slightly higher molecular weight. Reactions #1 and #3 clearly show different results for the duplicate experiments. The conversion of experiment 1 of reaction #3 is only half of what was expected, while no conversion at all was observed for experiment 2 of reaction #1. These observations are most likely

due to the poisonous effect of water² or oxygen,⁴ present in very small but different amounts in the reactors of the specific experiments, which most probably is the result of improper manual filling of the reactor block. With automated filling and sampling, pipetting errors may be avoided in the future.

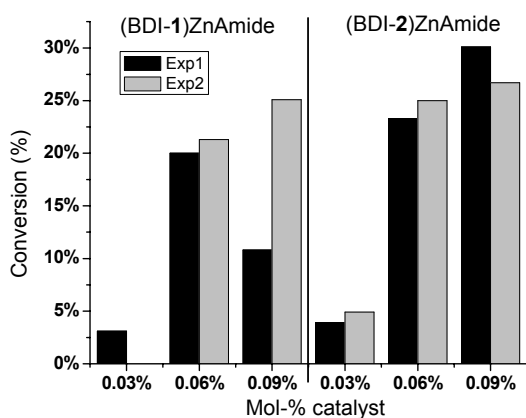


Figure 4-2. CHO conversions determined by ¹H NMR analyses.

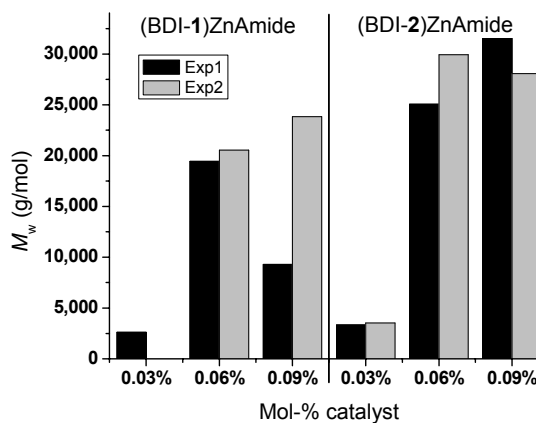


Figure 4-3. \overline{M}_w values determined SEC analyses.

Other interesting features are the observed conversion and molecular weights of the polymers obtained at different catalyst concentrations. For a living catalyst system (meaning a system with no chain termination or -transfer) like **1** and **2**, producing one chain per catalyst, one would expect a linear increase in conversion with increasing catalyst concentration at low conversions while the molecular weight of the polymer remains the same. At maximum conversions an overall decrease in molecular weight is expected with increasing catalyst concentration since the same amount of monomer is distributed over more active sites. As can be seen in Table 4-1, the CHO conversion strongly increases when going from a catalyst concentration of 0.03 mol-% to 0.06 mol-% but hardly increases when the catalyst concentration is increased further to 0.09 mol-%. Theoretically one would expect an increase of the conversion of 1.5 times going from a catalyst concentration of 0.06 % to 0.09 % and halving of the conversion when going from a catalyst concentration of 0.06 % to 0.03 %. The lower observed conversion for the system with a catalyst concentration of 0.03 % can readily be explained by the presence of traces of water or oxygen. For these low catalyst concentrations (30 ppm), which are at the lower limit of what is possible in the current setup, traces of water or oxygen kills most of the catalyst soon after the start of the polymerization. The reduced amount of active catalysts explains the lower conversion.

Both the conversions and the molecular weights for the systems with a catalyst concentration of 0.09 mol-% (reactions #3 and #6) are only slightly higher than observed for the systems with a catalyst concentration of 0.06 mol-% (reactions #2 and #5). For these polymerizations, the viscosity

rapidly increases with conversion, which has a pronounced retarding effect on the polymerization rate. However, it is not likely that mass transport limitation at higher conversion causes the relatively low conversion and molecular weight for the 0.09% system, since the effect is similarly strong for catalyst systems **1** and **2**. Since catalyst **1** results in both a lower conversion and a lower molecular weight, the reaction mixtures for catalyst system **1** are significantly less viscous than those for catalyst system **2**. Therefore one would expect a larger difference in conversion and molecular weight for reactions #2 and #3, compared to reactions #5 and #6, which is not observed.

To assess the scalability of the results, the viscosity behavior and the catalyst stability at longer reaction time and high conversion, reaction #5 was repeated on a larger scale (50 mL CHO, 0.06 mol-% Zn, 16.7 mL toluene for 24 hours, 10 bar) in a 380 mL stainless steel autoclave. During this lab-scale reaction, samples were taken at regular intervals to follow the conversion and molecular weight development in time (Figure 4-4 and Figure 4-5).

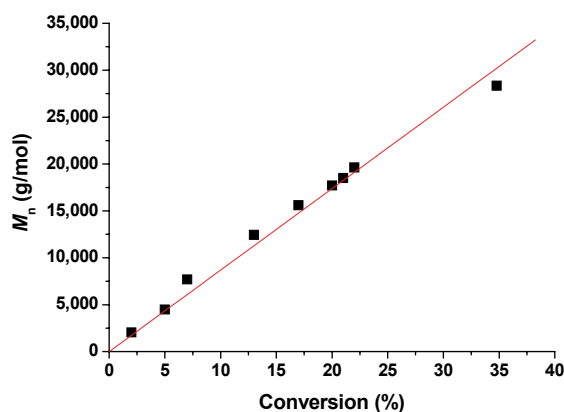
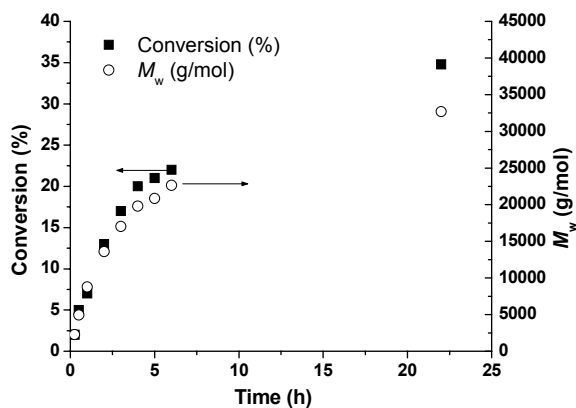


Figure 4-4. The conversion and molecular weight (\bar{M}_w) development with time.

Figure 4-5. The \bar{M}_n development plotted versus conversion.

For the CHO – CO₂ copolymerization the viscosity is known to rapidly increase with increasing conversion. Consequently, conversions higher than 40-50% are difficult to achieve as a result of severe mass transport limitation. Figure 4-4 clearly shows a decreasing activity at longer reaction times as a result of diffusion limitation, which also influences the expected linear correlation of \bar{M}_n versus time for a living system. However, the plot of \bar{M}_n versus the conversion (Figure 4-5) shows a straight line which is in agreement with a living nature of the catalyst and indicates that the catalyst is active for prolonged reaction time.

The catalyst activities in our high throughput experiments are in the same order as reported in the literature (a TOF of 219 h⁻¹ was reported by Coates et al. against the 126 (±5) h⁻¹ found here).²

The slightly lower values can be explained by the fact that in our study a more diluted system was used in combination with a somewhat longer reaction time (3 versus 2 hours).⁵

4.2.2 Mechanistic investigations

A closer look at the linear behavior represented in Figure 4-5, however, showed the \overline{M}_n values obtained by SEC (\overline{M}_n (experimental)) to be substantially lower than the values calculated using the ^1H NMR monomer conversion values and the catalyst concentration (\overline{M}_n (theory)). The SEC measurements were processed using a polystyrene calibration line, but due to the absence of Mark-Houwink parameters for PCHC, the \overline{M}_n values were validated by means of Triple-SEC and MALDI-ToF-MS measurements, which all gave very similar molecular weights. To rule out the occurrence of fortuitous events causing this deviation, similar polymerization experiments with (EtBDI)ZnOR (R = Me, Et) as the catalysts were carried out, which showed a similar (R = Et) or even larger (R = Me) deviation between \overline{M}_n (theory) and \overline{M}_n (experimental). The behavior of \overline{M}_n vs. time for both the (*i*-PrBDI)ZnN(SiMe₃)₂ and the (EtBDI)ZnOMe catalyst is shown in Figure 4-6 and Figure 4-7, respectively. The possibility that the formation of cyclic carbonate forms the origin of the deviation of theoretical from experimental molecular weight values could also be excluded as no cyclohexene carbonate was detected by ^1H NMR. Catalyst deactivation can also be excluded as a possible reason for the deviation between the experimental and theoretical \overline{M}_n values. Fast catalyst deactivation at the beginning of the polymerization would lead to a lower concentration of active catalysts. For a living system, the expected \overline{M}_n would therefore be higher instead of lower than the theoretical \overline{M}_n for the same conversion and yield. Slow deactivation during the polymerization process will not affect the number of chains much but is expected to broaden the molecular weight distribution, which was not observed either. Hence, the found deviation is most probably the result of a non-living behavior of the catalyst.

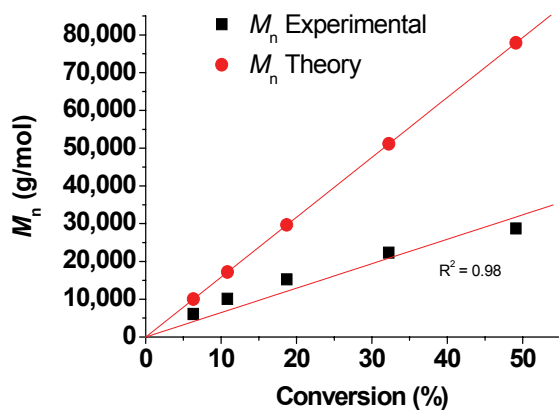


Figure 4-6. Deviation between \overline{M}_n (experimental) and \overline{M}_n (theory) for the $(i\text{-PrBDI})\text{ZnN}(\text{SiMe}_3)_2$ catalyst.

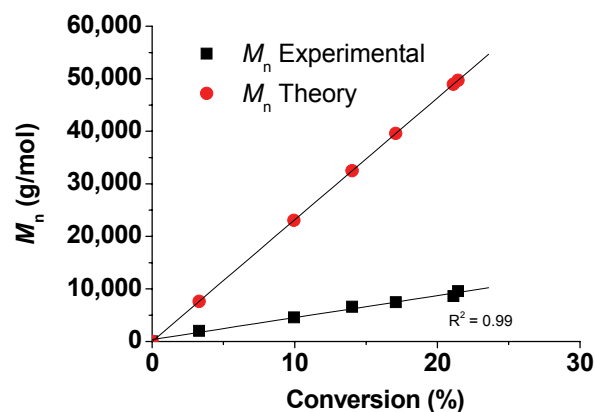


Figure 4-7. Deviation between \overline{M}_n (experimental) and \overline{M}_n (theory) for the $(\text{EtBDI})\text{ZnOMe}$ catalyst.

The next questions that arise are what kind of chain termination or chain transfer mechanism is playing a role, and how for example temperature, catalyst type and concentration affect these processes. The influence of temperature and catalyst concentration on the number of chains and the \overline{M}_n was investigated and the results are displayed in Table 4-2.

Table 4-2. Effect of catalyst $(\text{EtBDI})\text{ZnOEt}$ concentration and temperature on chain transfer.

Entry	catalyst (μmol)	Temperature ($^{\circ}\text{C}$)	Conversion to PCHC (%) ^a	TOF (h^{-1}) ^b	\overline{M}_n ($\text{g} \cdot \text{mol}^{-1}$) ^c	$\overline{M}_w / \overline{M}_n$	Chains per catalyst ^d
1	300	30	14.4	36	4,100	1.76	2.5
2	200	50	26.4	98	9,700	1.08	2.9
3	300	50	39.4	97	11,600	1.18	2.4
4	400	50	45.3	85	12,600	1.09	1.9
5	300	80	9.5 ^d	53	2,900	1.23	2.3

All polymerizations were performed with 15 mL of CHO and 35 mL of Toluene at 9 bar of CO_2 pressure for 2 hours. a) Conversion determined by integration of methine peaks in ^1H NMR spectra. b) $\text{mol CHO} \cdot \text{mol cat}^{-1} \cdot \text{h}^{-1}$. c) PS equivalents. d) As a result of backbiting around 11% of the CHO was converted to the cyclic carbonate (trans-CHC). d) Calculated based on both SEC data and conversion data from ^1H NMR, assuming that 100% of the catalyst is active.

As can be seen from Table 4-2, changing the temperature does not have a significant effect on the number of chains per active site. However, the temperature does have a considerable effect on the molecular weight and the selectivity of the reaction. At 30°C (entry 1) the activity is very low and raising the temperature to 50°C leads to a substantial improvement (entry 2).^{1,6} Further increasing the temperature to 80°C does not lead to a further increase in activity and severely affects the selectivity of the catalyst towards PCHC formation. Around 50% of the CHO is converted to the trans-cyclic carbonate by backbiting of the PCHC chain. This also severely reduces the molecular

weight, as can be seen from entry 5. A similar change in selectivity was observed by Allen and coworkers during CO₂ – propylene oxide copolymerization, which selectively afforded poly(propylene carbonate) at 25°C, while at 50°C exclusively propylene carbonate was formed.⁷ Kinetic studies performed by Coates et al. revealed a near second-order dependence in zinc for the copolymerization, which indicates the presence of dimeric active species.⁶ At higher temperature, the monomer-dimer equilibrium of the catalyst shifts towards the monomer form.^{1,6,7} Regardless whether or not the monomeric species is an active catalyst for the copolymerization, the monomeric zinc-polymer species can still undergo intramolecular backbiting yielding cyclohexene carbonate and lower molecular weight polycarbonates.

Increasing the catalyst concentration leads to a reduction of the number of chains per catalyst. Since the TOF is more or less constant, the same amount of CHO is now build into less chains leading to an increase in \overline{M}_n . The lowering of the number of chains is most likely caused by the relatively lower effect of poisoning impurities, present in the reactor or in the monomer, at higher catalyst concentrations (vide infra).

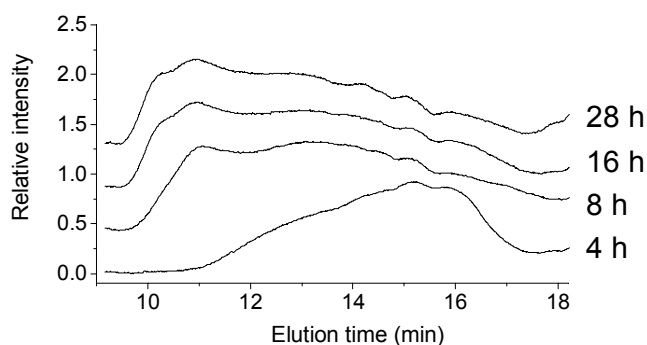


Figure 4-8. Characteristic SEC plots of polycarbonate samples synthesized with $[(2,6\text{-F}_2\text{C}_6\text{H}_3\text{O})_2\text{Zn}\cdot\text{THF}]_2$, taken at set time intervals. Polymerization performed at 80°C and 80 bar.

As was reported earlier, the bis(phenoxy)zinc system $[(2,6\text{-F}_2\text{C}_6\text{H}_3\text{O})_2\text{Zn}\cdot\text{THF}]_2$ shows very high polydispersities. This broad molecular weight distribution originates from multimodal Schulz-Flory distributions, which are hardly affected by temperature or catalyst concentration. Figure 4-8 shows characteristic SEC plots of polycarbonate samples taken at set time intervals during a polymerization. Already at the beginning of the polymerization the polydispersity is higher than 6 and increases during the polymerization to a value of 18. Although the polydispersity drops somewhat towards the end of the polymerization, it is clear that the shape of the SEC plots does not change significantly. Similar distributions were also found with the bis-salicylaldiminato zinc complexes made by Darensbourg and coworkers.⁸ Such a distribution pattern is characteristic for multiple active sites present in the system. Koning et al. already commented upon these broad polydispersities and postulated that different phases during a polymerization caused the increase in

polydispersity.⁹ Slow or incomplete initiation in combination with the formation of aggregates is another probable cause of the high polydispersities for this catalyst system.

To investigate the possible occurrence of transesterification reactions, for both catalytic systems (EtBDIZnOMe and [(2,6-F₂C₆H₃O)₂Zn·THF]₂) the reaction mixture was kept at polymerization conditions for a long time (10 days) after full conversion had already been reached. Although intermolecular transesterification does not affect the number of polymer chains, randomization should lead to a molecular weight distribution of around 2. However, for the bis(phenoxy)zinc system the PDI remained very high (~9), while for the β -diketiminato zinc catalysts, even after the prolonged polymerization, the polydispersities were still as low as 1.12 indicating that intramolecular transesterification is negligible. Intramolecular transesterification on the other hand would lead to cyclohexene carbonate or ring structures in combination with a smaller chain fragment, and thus indeed to an increase of the number of polymer molecules per active site. However, the molecular weight of the polymers did not decline and MALDI-ToF-MS analysis of polymer samples did not show any sign of ring structures nor randomization (head-to-head, tail-to-tail structures) of the polymer chains, ruling out significant random chain scission/recombination reactions. However, MALDI-ToF-MS did show some unexpected results.

4.2.3 MALDI-ToF-MS analysis.

Several polymers were produced with two β -diketiminato systems and a bis(phenoxy) zinc system. Experimental details and polymerization results are summarized in Table 4-3.

Table 4-3. Details of experimental conditions and results for polymers analyzed with MALDI-ToF-MS.

Entry	Catalyst	CHO (mL)	Toluene (mL)	T (°C)	P (bar)	Time (hour)	Conversion to PCHC (%) ^{a)}	TOF (h ⁻¹) ^{b)}	\overline{M}_n (g · mol ⁻¹) ^{c)}	$\overline{M}_w / \overline{M}_n$	Chains per catalyst ^{d)}	MALDI spectrum
1	(EtBDI)ZnOMe	50	16.7	50	9	2	9	55	3,700	1.11	5.6	Figure 4-9
2	(EtBDI)ZnOEt	50	0	50	9	2	40	97	11,600	1.18	2.4	
3	[(2,6-F ₂ C ₆ H ₃ O) ₂ Zn·THF] ₂	50	0	80	80	28	19	38	25,800	18.4	1.7	Figure 4-10

All polymerizations were performed with 300 μ mol of catalyst, 15 mL of CHO and 35 mL of toluene. a) Conversion determined by integration of methine peaks in ¹H NMR spectra. b) mol CHO · mol cat⁻¹ · h⁻¹ c) PS equivalents. d) Calculation based on both SEC data and conversion data from ¹H NMR, assuming that 100% of the catalyst is active.

MALDI-ToF-MS analyses of the polymers produced by the bis(phenoxy) zinc and β -diketiminato zinc systems reveal some interesting differences. In Figure 4-9 a Poisson type molecular weight distribution is found for the PCHC produced with the (EtBDI)ZnOMe zinc catalyst, while on the other hand, the PCHC formed with the [(2,6-F₂C₆H₃O)₂Zn·THF]₂ catalyst shows a Schulz-Flory type molecular weight distribution (Figure 4-10).

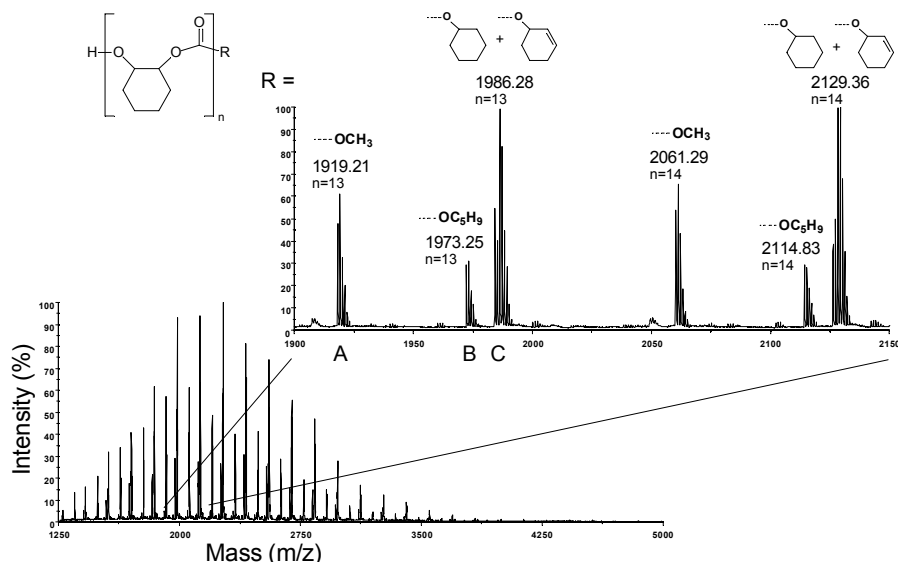


Figure 4-9. MALDI-ToF-MS spectrum of the K⁺ adduct of PCHC obtained with (EtBDI)ZnOMe and an enlargement of part of the spectrum (entry 1 in Table 4-3).

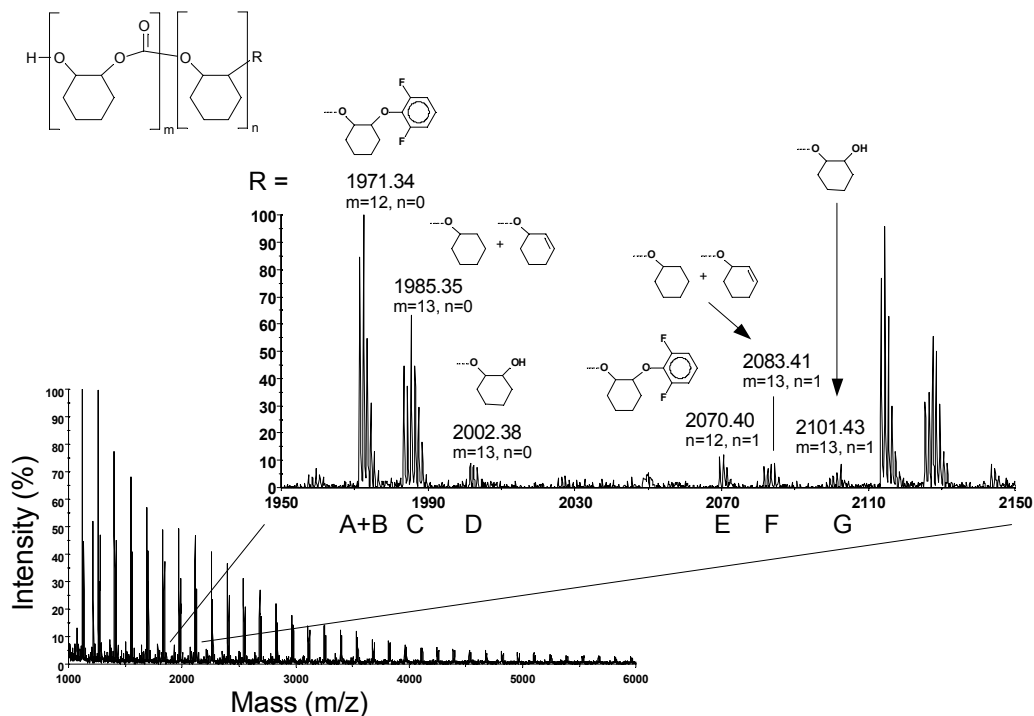


Figure 4-10. MALDI-ToF-MS spectrum of the K⁺ adduct of PCHC obtained with [(2,6-F₂C₆H₃O)₂Zn·THF]₂ and an enlargement of part of the spectrum (entry 3 in Table 4-3).

The repeating unit is 142 Dalton, which is the mass of a cyclohexene carbonate repeating unit. The various peaks (each peak, in turn, is split into its isotope pattern) within a repeating unit are the result of different end groups that are present in the polymer. Since, a priori, the formation of different end groups *after* polymerization could not be ruled out completely, various workup procedures were applied and the end groups were carefully analyzed.¹⁰ However, no changes were observed in either SEC or MALDI-ToF-MS spectra, indicating that the various end groups were

formed during the polymerization. In all polymers prepared with a β -diketiminato zinc catalyst, CO_2 is the first monomer to insert into the zinc-initiator bond. This is not surprising since homopolymerization of CHO is not possible with this catalyst under typical polymerization conditions. Correspondingly, perfectly alternating cyclohexene oxide – CO_2 copolymers are formed. Besides perfectly alternating copolymers, the MALDI-ToF-MS spectrum of the PCHC made with the Darensbourg catalyst $[(2,6\text{-F}_2\text{C}_6\text{H}_3\text{O})_2\text{Zn}\cdot\text{THF}]_2$ (Figure 4-10) also shows the presence of polymeric chains in which one or more CO_2 units are missing. Interestingly, the phenoxides first react selectively with cyclohexene oxide before inserting a carbon dioxide monomer. This is in agreement with the capability, albeit poor, of $[(2,6\text{-F}_2\text{C}_6\text{H}_3\text{O})_2\text{Zn}\cdot\text{THF}]_2$ to homopolymerize cyclohexene oxide to the corresponding polyether.

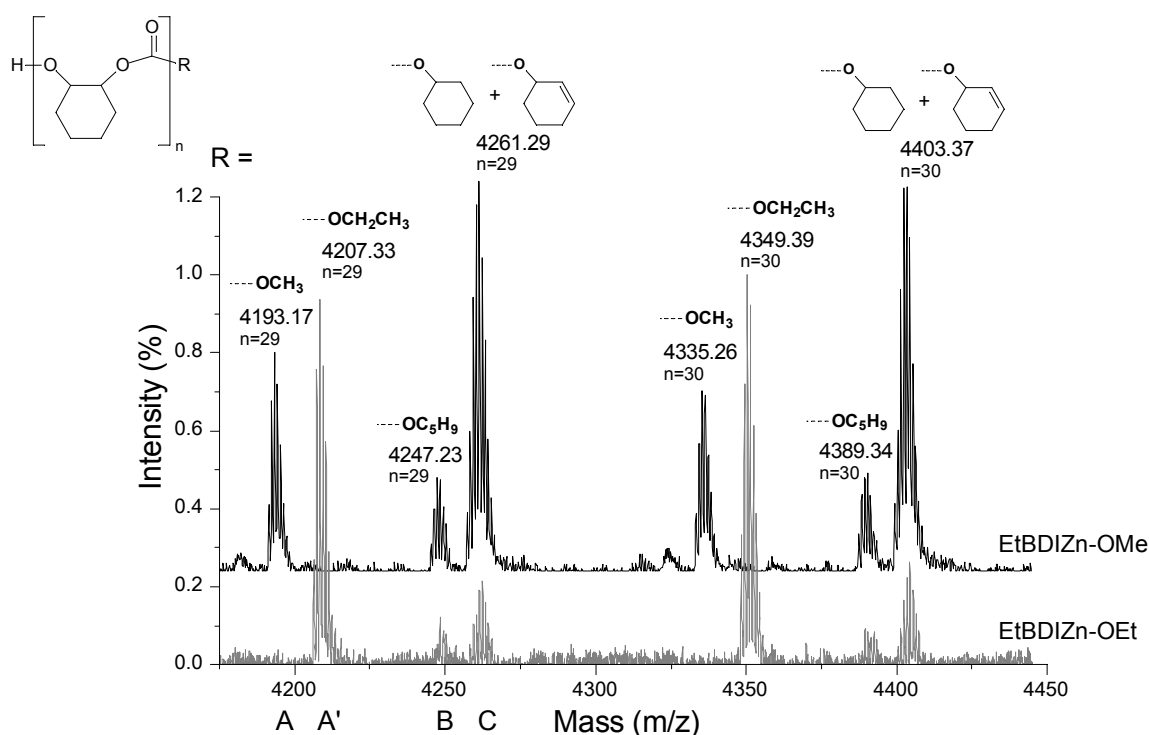


Figure 4-11. Comparison between MALDI-ToF-MS spectra of PCHC obtained with (EtBDI)ZnOMe (entry 1, Table 4-3) and (EtBDI)ZnOEt (entry 2, Table 4-3).

For the PCHC prepared with (EtBDI)ZnOMe (Figure 4-9), peak A is the expected chain-end originating from ionization by K^+ of a normal polymer consisting of thirteen cyclohexene carbonate repeating units carrying the methoxide group on one side (resulting from the catalyst initiating moiety) and a proton on the other side (originating from hydrolysis of the polymer-catalyst bond after quenching with MeOH/HCl). Similarly, peak A in Figure 4-10 corresponds to the expected K^+ ionized polymer that contains the initiating phenoxide group 2,6- $\text{F}_2\text{C}_6\text{H}_3\text{O}$ of $[(2,6\text{-F}_2\text{C}_6\text{H}_3\text{O})_2\text{Zn}\cdot\text{THF}]_2$ and is end-capped with a proton as a result of the hydrolysis after quenching.

The incorporation of the phenoxide ligand as an end group in the polymer chain was previously observed by ^{19}F NMR and UV spectroscopy.^{11,12} For the bis(phenoxy)zinc system (peak D, Figure 4-10), polymers with two hydroxyl end groups are also observed. Water, which can act as a chain transfer agent, possibly forms the origin of these end groups. Peaks E, F and G in Figure 4-10 correspond to polymers (peaks A-D, Figure 4-10) in which one carbon dioxide unit is missing. Such peaks were absent in the β -diketiminato zinc system, which formed completely alternating copolymers. More difficult to assign are peaks B and C. Peaks B and C do not appear to be influenced by the initiating group, as can be seen in Figure 4-11 where the spectra of PCHC prepared with the (EtBDI)ZnOEt and the (EtBDI)ZnOMe are shown. The peaks of the polymeric species initiated with the alkoxide groups can clearly be seen as peaks A and A' for the methoxide and ethoxide, respectively. However, peaks B and C do not shift. Moreover, both (EtBDI)ZnOR (R = Me, Et) and $[(2,6\text{-F}_2\text{C}_6\text{H}_3\text{O})_2\text{Zn}\cdot\text{THF}]_2$ (Figure 4-9 and Figure 4-10) show the same peaks B and C at the same mass, which indicates that the corresponding chain structures are catalyst independent. In the case of $[(2,6\text{-F}_2\text{C}_6\text{H}_3\text{O})_2\text{Zn}\cdot\text{THF}]_2$ peak B overlaps with peak A (Figure 4-10), but a similar analysis on the analogous dimethyl substituted zinc phenoxide $[(2,6\text{-Me}_2\text{C}_6\text{H}_3\text{O})_2\text{Zn}\cdot\text{THF}]_2$ clearly shows the presence of peak B. Interestingly, peaks B and C were exclusively found when zinc-based catalysts were used to catalyze the copolymerization. For example, when the porphyrinato chromium complex [TPP]CrCl was used as the catalyst, only polymers with two hydroxyl end groups ($\text{HO}[\text{C}_6\text{H}_{10}\text{OC}(=\text{O})\text{O}]_n\text{C}_6\text{H}_{10}\text{OH}$) were observed.

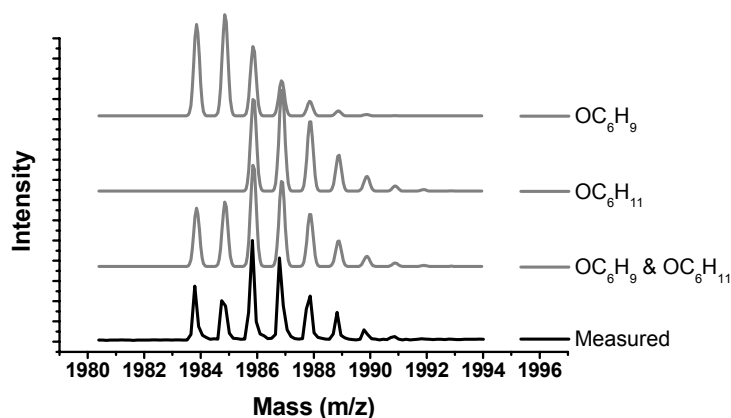
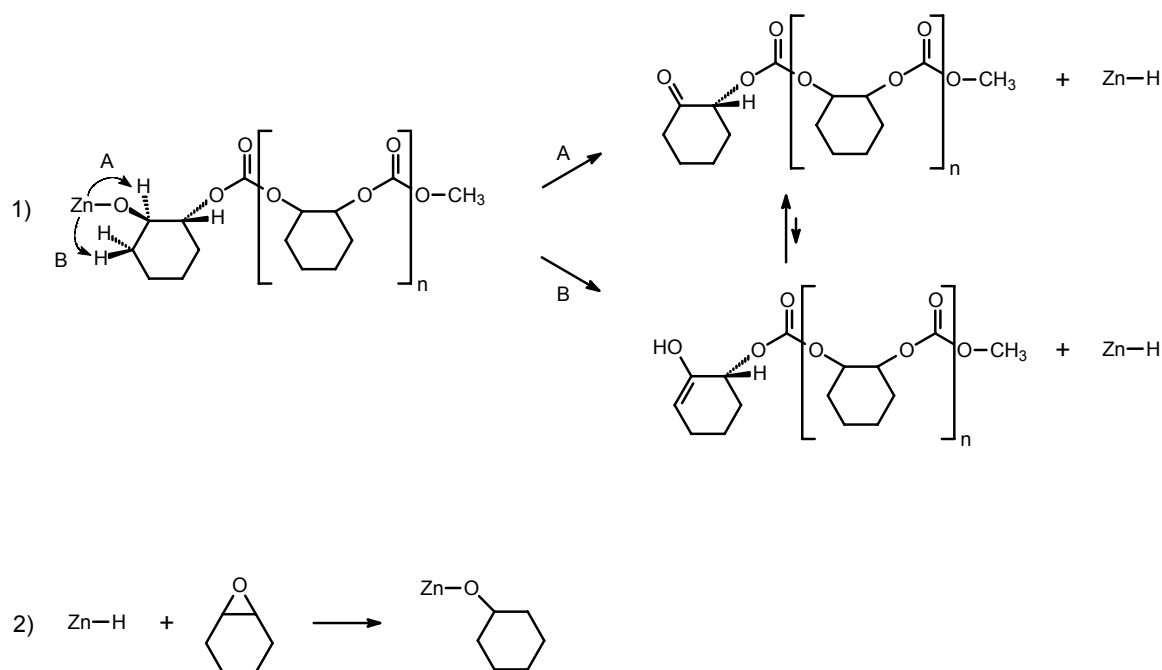


Figure 4-12. Simulated and measured isotope patterns of peak C in Figure 4-9.

The fact that the fragments B and C were formed, irrespective of the type of zinc catalyst, did point at a catalyst independent structure, like rings formed after transesterification. As already mentioned, no plausible ring structures could be modeled with the mass of peak B or C and SEC-DV measurements showed a linear Mark-Houwink plot typical for a linear polymer.⁹ Peak B corresponds to a polycarbonate with a $\text{C}_5\text{H}_9\text{O}$ -initiating group and a proton end group ($\text{HO}[\text{C}_6\text{H}_{10}\text{OC}(=\text{O})\text{O}]_n\text{C}_5\text{H}_9$). So far it is a complete mystery where the $\text{C}_5\text{H}_9\text{O}$ -fragment originates

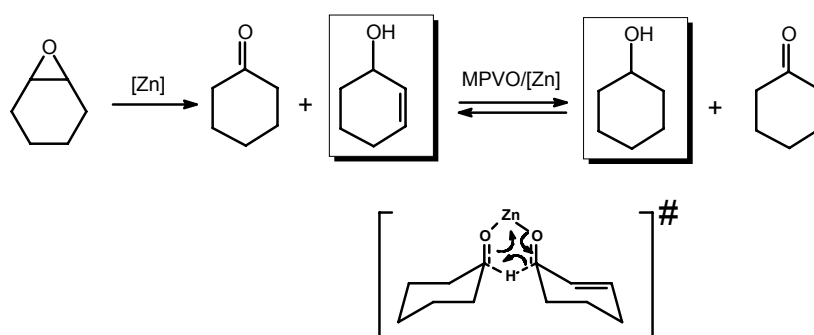
from. GC-MS analysis of the cyclohexene oxide and toluene showed no such impurities, and the fact that only the use of zinc catalysts gives rise to the formation of C_5H_9O end groups strongly suggests some kind of zinc-based side reaction. A careful analysis of the isomer patterns revealed that peak C is a combination of two overlapping isotope patterns with an end group mass corresponding to a $C_6H_{11}O$ and a C_6H_9O fragment, which indicates the presence of cyclohexyl and cyclohexenyl end groups in a 1:1 ratio (Figure 4-12). Although their presence is evident, the origin of the cyclohexyl and cyclohexenyl end groups is not obvious.¹³ The possibility of chain scission during MALDI-ToF-MS experiments can be excluded, since these peaks were not observed in the MALDI-ToF-MS spectra of PCHC samples prepared by using porphyrinato chromium catalyst systems.¹⁴ To exclude any zinc-based reactions during sample preparation or MALDI-ToF-MS measurements, some β -diketiminato zinc alkoxide was added to PCHC samples produced with the porphyrinato chromium/DMAP system. However, this led neither to the appearance of cyclohexyl/cyclohexenyl end groups (peak C) nor to the appearance of C_5H_9O - end groups (peak B). Hence, the cyclohexyl and cyclohexenyl end groups, as well as the cyclopentyl end group, are formed prior to or during the polymerization reaction as a side reaction where a zinc species plays a crucial role. A possible β -H transfer can be thought of that might explain the presence of a cyclohexenyl and a cyclohexyl (end)group (Scheme 4-1, reaction 1 and 2 respectively). However, in the MALDI-ToF-MS spectra no matching peaks, for the structures formed in reaction 1, could be observed.



Scheme 4-1. Possible β -hydrogen transfer reactions (1) and reinitiation (2).

Another possible origin of these cyclohexyl and cyclohexenyl moieties could be a combination of oxirane rearrangement and a “MPVO-type” reaction. In synthetic organic chemistry,

the base-mediated isomerization of oxiranes into ketones and allylic alcohols^{15,16,17} as well as the Meerwein-Ponndorf-Verley reduction/Oppenauer oxidation (collectively denoted as MPVO)¹⁸ are two well known synthetic transformations. Since zinc was reported to show catalytic activity in both of these reactions,¹⁹ it is not unlikely that the oxirane isomerization reaction in combination with MPVO is also catalyzed by the zinc catalysts (zinc-alkyl reagents or their hydrolysis products) used in these copolymerizations. Assuming this is indeed possible: the cyclohexene oxide rearranges to afford cyclohexanone and 2-cyclohexenol, which via MPVO are in equilibrium with cyclohexanol and 2-cyclohexenone (Scheme 4-2). This could also explain the fact that cyclohexyl and cyclohexenyl end groups were absent during the chromium ([Tpp]CrCl) catalyzed cyclohexene oxide – CO₂ copolymerization, since the abovementioned rearrangement reactions are not catalyzed by chromium.



Scheme 4-2. Schematic representation of the cyclohexene oxide rearrangements and MPVO reaction.

The presence of different end groups is most probably related to the formation of more chains per active site than expected for a living catalyst as a result of some sort of chain transfer process. However, this is only possible if alcohols, generated by the rearrangement reactions, can function as chain transfer agents similar as was found for the porphyrinato aluminum catalyzed ring opening polymerization of oxiranes.^{20,21} The observation that with time the molecular weight of all the polymer chains increases simultaneously, suggests that chain transfer is indeed taking place and is a reversible process (Scheme 4-3). Furthermore, since the polydispersities of the polymers are very narrow, this chain-transfer process appears has to be fast relative to propagation.

4.2.4 Reversible chain transfer.

In 1978 Soga showed that acetic acid could cause chain transfer in the copolymerization of PO and CO₂ with the use of a cobalt acetate catalyst.²² It is also known that silica-immobilized β -diketiminato zinc catalysts can give chain transfer in the polymerization of *L*-Lactide in the presence of the surface Si-OH groups.²³ However, when the same immobilized catalytic system was

used in the copolymerization of cyclohexene oxide and CO₂ it was concluded on the basis of observed \overline{M}_n values that chain transfer could not take place due to steric hindrance.

To prove that alcohols can indeed act as effective chain transfer agents in our case and that chain transfer is a fast and reversible process, two polymerizations with (EtBDI)ZnOMe were carried out in the presence of ethanol. In the first reaction ten equivalents of ethanol were present from the beginning of the polymerization.²⁴ As expected, MALDI-TOF-MS analyses showed that the polymerization mainly resulted in ethoxy end-capped polycarbonates. Although lower than the theoretical value of eleven chains per active site, the observed average value of 7.1 chains per catalyst proves that alcohols can indeed act as chain transfer agents. Moreover, the narrow molecular weight distribution of 1.1 proves that chain transfer is a reversible and much faster process than propagation. These characteristics are very typical for a quasi-living polymerization.²⁵ Further proof came from an experiment where 10 equivalents of ethanol were added after 2 hours of polymerization, after which the polymerization was continued for another 22 hours (Figure 4-13).

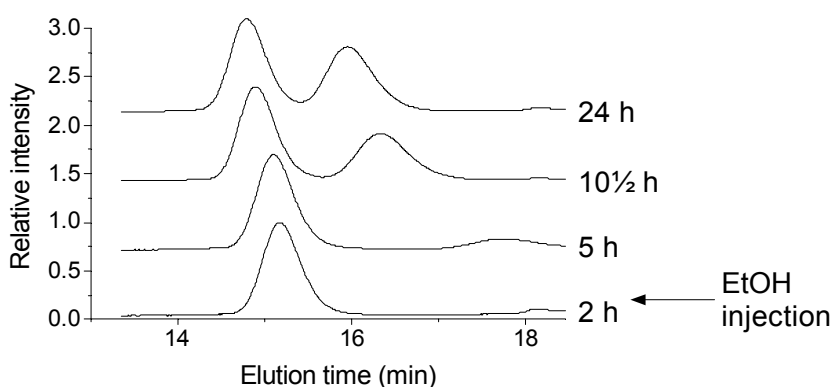


Figure 4-13. SEC plots of sample before and after EtOH addition.

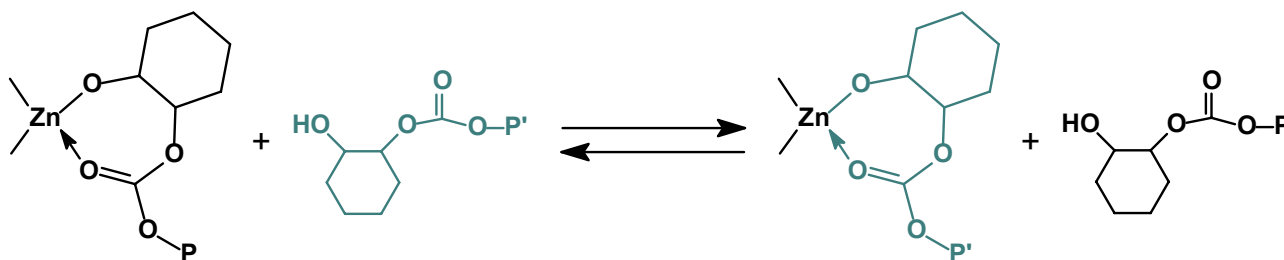
After the ethanol addition, a second distribution emerged in the SEC plot at lower molecular weight values (longer elution time, Figure 4-13). Both distributions continued shifting to a higher molecular weight with increasing polymerization time. The polydispersity index of both distributions remained very low (Table 4-4), which further supports a reversible and very fast chain transfer mechanism (Scheme 4-3). MALDI-ToF-MS analysis revealed that the low molecular weight fraction consisted exclusively of ethoxide initiated polymer chains. In the new distribution no cyclopentyl, cyclohexyl or cyclohexenyl end groups were observed, whereas they are present in the originally formed high molecular weight fraction. This indicates that formation of C₅H₉O, cyclohexyl and cyclohexenyl end groups exclusively takes place prior to or at the beginning of the polymerization. It is therefore assumed that traces of water or other impurities in the system play a crucial role in the formation of the zinc species that are active in the proposed rearrangement reactions and not a β -H elimination or chain scission process, as was seen in chapter 3, that should

occur throughout the polymerization. Since the formation of cyclopentyl, cyclohexyl and cyclohexenyl end groups is only observed at the beginning of the reaction, it seems that the reaction is stoichiometric rather than catalytic. The exact nature of the zinc species, responsible for these rearrangement reactions, is unfortunately still unknown.

Table 4-4. Molecular weight data from chain transfer experiment.

Time (hours) ^{a)}	Low molecular weight fraction			High molecular weight fraction			Conversion to PCHC (%) ^{c)}
	\overline{M}_n (g · mol ⁻¹) ^{b)}	\overline{M}_w (g · mol ⁻¹) ^{b)}	$\overline{M}_w/\overline{M}_n$	\overline{M}_n (g · mol ⁻¹) ^{b)}	\overline{M}_w (g · mol ⁻¹) ^{b)}	$\overline{M}_w/\overline{M}_n$	
2	-	-	-	12,635	13,573	1.08	40
5	1,088	1,283	1.18	13,438	14,872	1.11	46
10½	4,131	4,596	1.11	16,533	17,332	1.05	70
24	5,909	6,498	1.10	18,465	19,563	1.06	92

a) Ethanol was injected after 2 hours. b) PS equivalents. c) Conversion determined by integration of methine peaks in ¹H NMR spectra.



Scheme 4-3. Schematic representation of the fast reversible chain-transfer process. The hydroxyl terminated chains are dormant while the zinc-bonded polymers are the growing chains.

4.2.5 Chain coupling

The importance of a small catalytic trace of H₂O for the formation of cyclohexanone and 2-cyclohexenol was demonstrated by a NMR tube reaction in C₆D₆ with the EtBDIZnOMe catalyst and 10 equivalents of CHO. The reaction was done overnight at 50 °C and 10 bar of CO₂ pressure and yielded a quantitative amount of PCHC with no traces of cyclohexyl/cyclohexenyl end groups as could be observed by MALDI-ToF-MS (Figure 4-14). Interesting is the fact that a small amount of what appear to be coupled chains were found with two methoxide end groups.

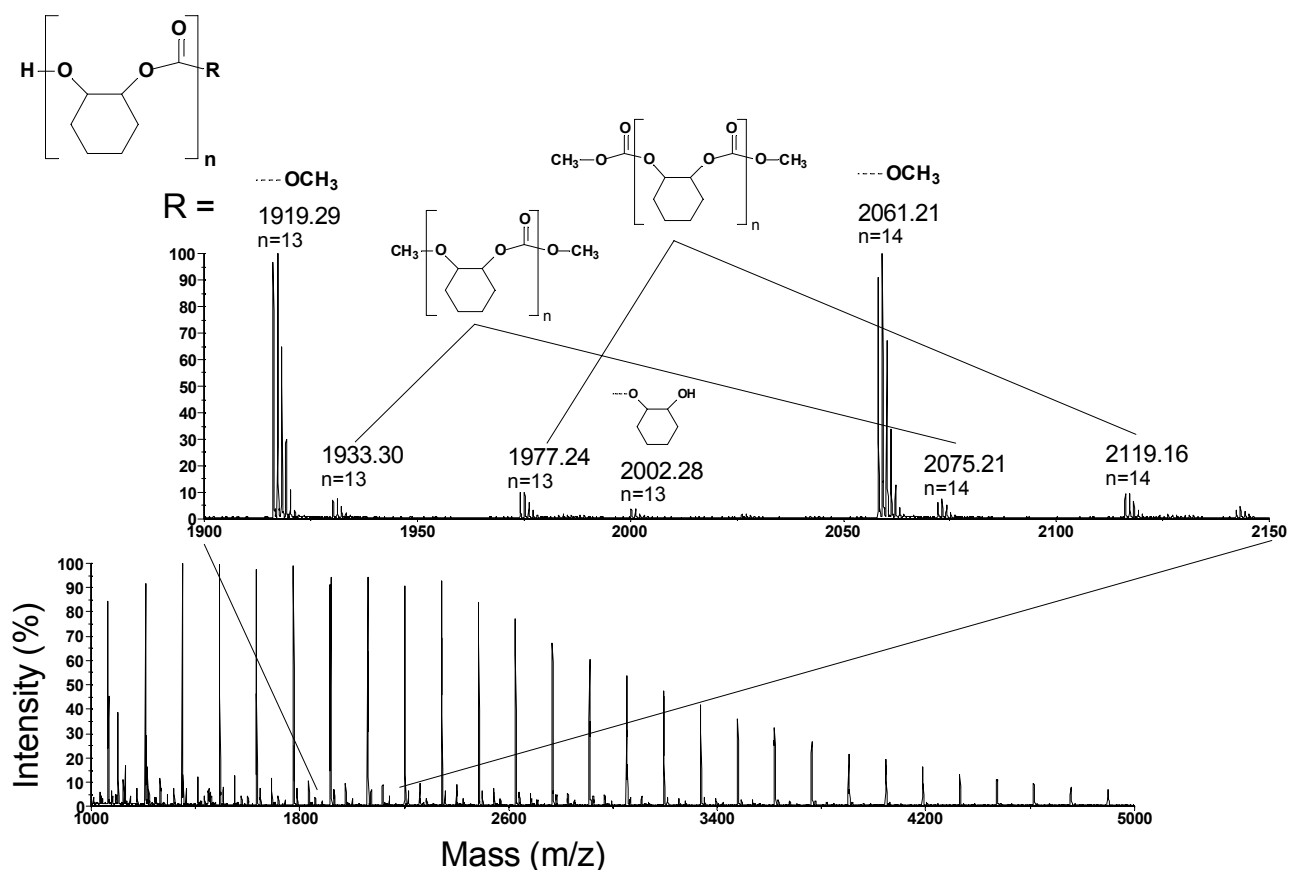
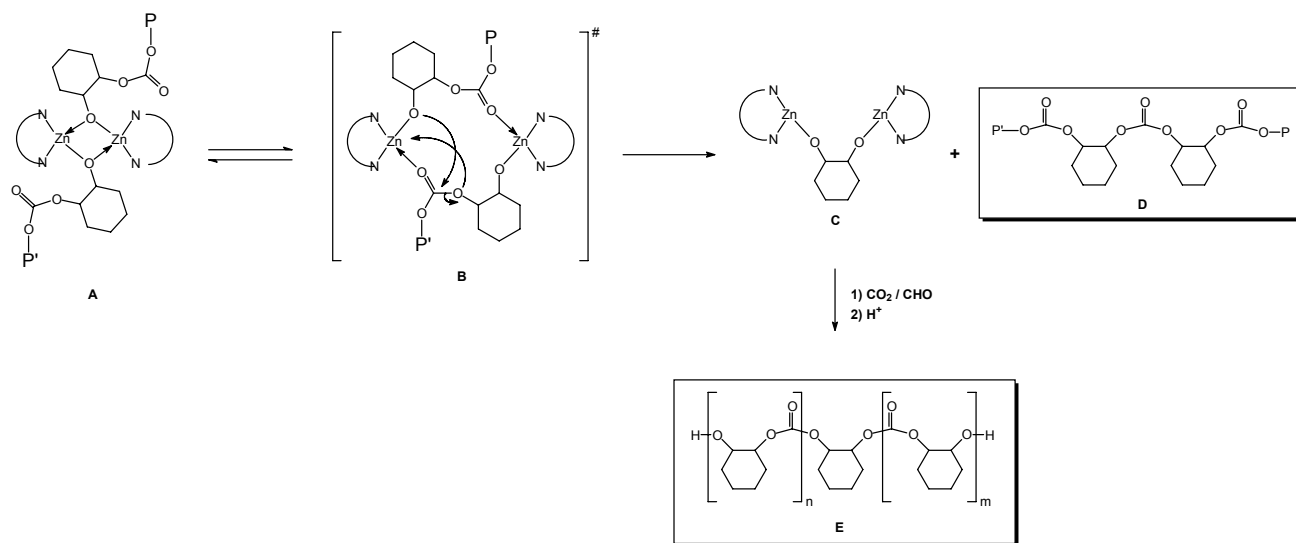


Figure 4-14. MALDI-ToF-MS spectrum of the polymer obtained in a NMR-tube polymerization of CHO and CO₂ (cationization ion: K⁺).

A possible mechanism for the coupling reaction is displayed in Scheme 4-4. A transesterification reaction, between two coordinated polymer chains (species B), would lead to the formation of the coupling of two chains (species D, peaks at 1977.24 and 2119.16 m/z) as observed by MALDI-ToF-MS (Figure 4-14). Species C, which should also be formed according to this mechanism, would lead to the formation of two hydroxide end groups and ultimately species E which was also observed in the MALDI-ToF-MS spectrum shown in Figure 4-14 (peak at 2002.28 m/z). Although not mechanistically explained in Scheme 4-4, the peaks at 1933.30 and 2075.21 m/z represent species D with the loss of one carbon dioxide moiety.

The coupled products were not previously observed during lab scale polymerizations. Even with the prolonged polymerization described previously (paragraph 4.2.2), no significant chain transfer reactions (like the chain coupling described here) were observed with MALDI-ToF-MS. Since the coupling effectively doubles the molecular weight and only very small amounts are present (Figure 4-14), it is difficult to observe these peaks with MALDI-ToF-MS. However, as was also mentioned by Eberhardt et al., in SEC chromatograms a small shoulder at higher molecular weights than the main polymer peak for can often be observed, which could not satisfactory be

explanation so far. It seems likely that the origin of this high molecular weight shoulder originates from the chain coupling as shown in Scheme 4-4.



Scheme 4-4. Possible chain coupling mechanism as observed in Figure 4-14.

4.3 Concluding remarks

In this chapter we reported the successful application of a high throughput approach for the copolymerization of carbon dioxide and cyclohexene oxide with two β -diketiminato zinc complexes. It was shown that the polymerizations were controlled and reproducible. However, not every reaction was successful. Until the reason for the failure is known (most likely a mistake in the addition or traces of moisture deactivating the very small catalyst amounts involved) duplicate experiments are obligatory. An up-scaled experiment to conventional lab scale, which was sampled and analyzed over time, showed a quasi-living system, with a comparable activity than in the high throughput experiment.

MALDI-ToF-MS proved to be a powerful tool to provide more insight into the mechanisms of the various reactions that take place during the zinc catalyzed cyclohexene oxide – CO₂ copolymerizations. Whereas the β -diketiminato zinc alkoxides first react with CO₂, the bis(phenoxy)zinc system is initiated by the reaction with cyclohexene oxide. This is in agreement with the observation that [(2,6-F₂C₆H₃O)₂Zn·THF]₂ is also capable of homopolymerizing cyclohexene oxide, whereas the β -diketiminato zinc system is not and produces perfectly alternating poly(cyclohexene carbonate). The results of the SEC measurements of the bis(phenoxy)zinc system suggest that either the initiation is very slow or different active species are formed that result in an extremely broad molecular weight distribution. Although the β -diketiminato zinc system is

intrinsically living, a closer look at the SEC and MALDI-ToF-MS data revealed a quasi-living nature of the catalyst, where alcohols can act as chain transfer agents in a reversible and relatively fast chain transfer process. This process allows the synthesis of multiple polycarbonate chains per active site with a very narrow molecular weight distribution, and overcomes the one chain per catalyst limitation of a living system, while retaining good molecular weight control. The number of chains per site depends on the amount of chain transfer agent added, while the molecular weight can be tuned by the polymerization time. MALDI-ToF-MS also revealed a thus far unrecognized side reaction leading to cyclopentyl, cyclohexyl and cyclohexenyl end groups. Although the origin of the cyclopentyl end group remains a mystery, the cyclohexyl and cyclohexenyl are likely to be formed by a zinc catalyzed rearrangement of oxiranes, in combination with a MPVO reaction. An experiment in which ethanol was added after two hours of polymerization time, showed that the cyclopentyl, cyclohexyl and cyclohexenyl end groups are exclusively formed prior to, or at the beginning of the polymerization. It is therefore believed that traces of water or other impurities present at the beginning of the reaction, in combination with some zinc species, play a crucial role in this process rather than some kind of β -H elimination or chain scission process that would be active throughout the polymerization. Further investigation in the nature of the zinc species involved is currently in progress.

4.4 Experimental section

4.4.1 Materials

Cyclohexene oxide (Aldrich, 98%) was dried over CaH_2 , distilled and stored under argon on molsieves (4Å) prior to use. Carbon dioxide (> 99.9993% pure) was purchased from HoekLoos. Toluene (AR) was dried over an alumina column and stored on molsieves. The β -diketiminato (BDI) zinc catalysts $[\text{HC}(\text{C}(\text{CH}_3)\text{N}-2,6-\text{R}-\text{C}_6\text{H}_3)_2]\text{Zn}-\text{N}(\text{SiMe}_3)_2$ (R = Et (**1**), *i*-Pr (**2**)) were synthesized according to literature procedures.² The (EtBDI)ZnOR catalysts (R = Me (**3**), Et (**4**); EtBDI = 2-(2,6-diethylphenyl)amido-4-(2,6-diethylphenyl)imino-2-pentene) and the bis(phenoxy)zinc catalyst $[(2,6-\text{F}_2\text{C}_6\text{H}_3\text{O})_2\text{Zn}\cdot\text{THF}]_2$ (**5**) were synthesized according to literature procedures.^{2,26}

4.4.2 Analytical techniques

¹H NMR spectra were recorded on a Varian Gemini 2000 (300 MHz) and a Varian Mercury Vx (400 MHz) spectrometer. Size Exclusion Chromatography (SEC) traces were recorded on a Waters GPC equipped with a Waters model 510 pump and a model 410 differential refractometer (40 °C). THF was used as the eluent at a flow rate of 1.0 mL · min⁻¹. A set of two linear columns

(Mixed C. Polymer Laboratories, 30 cm, 40 °C) was used. Molecular weights were calculated relative to polystyrene standards. Data acquisition and processing was performed using Waters Millennium32 software. Triple-SEC measurements were performed on a system consisting of a 3 column set (2 PLgel Mixed-C 5 μ columns and one PLgel Mixed-D 5 μ column from Polymer Laboratories), with a guard column (PLgel 5 μ Polymer Laboratories), a gradient pump (Waters Alliance 2695, flow rate of 1.0 mL \cdot min⁻¹ isocratic), a photodiode array detector (Waters 2996) and differential refractive index detector (Waters 2414) as concentration detectors, a light scattering detector (Viscotek), a viscosity detector (Viscotek, dual detector 250) and THF as a solvent. THF was filtered twice (0.2 μ filter) and stabilized with BHT (4-Me-2,6-(*t*-Bu)₂C₆H₂OH). Data acquisition and processing was performed with Viscotek TriSec GPC Software (version 3.0 Rev. B.03.04). MALDI-ToF-MS analysis was carried out on a Voyager DE-STR from Applied Biosystems. The matrix, DCTB (*trans*-2-[3-(4-*t*-butylphenyl)-2-methyl-2-propenylidene]malononitrile) was synthesized according to literature procedures.²⁷ Potassium trifluoroacetate (Aldrich, > 99%) was added to the polymer samples as cationization agent. The matrix was dissolved in THF at a concentration of 40 mg \cdot mL⁻¹. The potassium trifluoroacetate was dissolved in THF at a typical concentration of 1 mg \cdot mL⁻¹. Polymer was dissolved in THF at approximately 1 mg \cdot mL⁻¹. In a typical MALDI-ToF-MS analysis the matrix, potassium trifluoroacetate and the polymer solution were premixed in a ratio of 10:1:5. The premixed solutions were hand-spotted on the target well and left to dry. Spectra were recorded in both the linear and reflector mode.

4.4.3 High Throughput Experiments

The reactions were carried out in a custom made catalyst screening platform at Avantium Technologies. The system, which was specifically designed to avoid mass-transfer limitation issues, consists of modular blocks of twelve individual reactors (Figure 4-16) that after addition of the required components are sealed inside the glove box. The sealed blocks are transferred from the glove box to the reaction station (Figure 4-15), which consists of two beds, with 96 individually magnetically stirred positions. Each of the two beds can be operated at a different reaction temperature. The reaction time can be varied per block of twelve reactors by the modular feed-gas set-up or by inserting/removing blocks at a desired time.

For this feasibility study, one block of twelve reactors was used. Each stainless steel reactor was equipped with a Teflon insert, which reduced the maximum working volume to about 5 mL. The 96-position bed was heated by both electrical heating and by a circulating oil thermostat.



Figure 4-15. Reaction station with several blocks of twelve reactors connected to gas-inlet tubes.

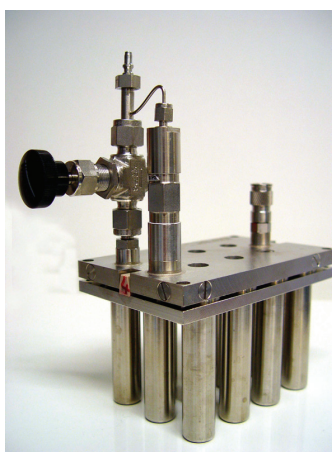


Figure 4-16. A block of twelve reactors which can be filled in the glove box.

Prior to use, the reactor block was heated to 70 °C for an hour and was left to cool under vacuum in the antechamber of the glove box for 10 min. After two more evacuation cycles the reactor block was transferred to the glove box and all reactors were equipped with a Teflon insert. The inserts were filled with 3 mL of CHO and 1 mL of the catalyst solution of the appropriate concentration in toluene. After filling, the reactor block was sealed and transferred outside the glove box to the heating jack. Once the reactors were placed in the reaction bed, the gas-lines were purged with CO₂ and the reactors were pressurized to 10 bar and heated to 50 °C, using a gas-on-demand (constant pressure) mode of operation. After 3 hours the reactors were cooled and depressurized. A sample from each reactor was taken for ¹H NMR analyses (300 MHz, CDCl₃) to determine the conversion. Conversions were determined by integration of the methine peaks in the ¹H NMR spectrograms: ¹H NMR (300 MHz, CDCl₃): δ 4.65 (br, CH (PCHC), 2H), 3.11 (s, CH (CHO), 2H). The samples for SEC analyses were prepared as follows: About 0.5 mL of each of the reaction

mixtures was added dropwise to a 10 fold excess of petroleum ether (40-70) upon which the poly(cyclohexene carbonate) (PCHC) precipitated. After separation and drying (vacuum, 60°C, 18h), the polymer was re-dissolved in the SEC eluent THF.

4.4.4 *Example of a typical polymerization using β -diketiminato zinc catalysts.*

(EtBDI)ZnOEt (194 mg, 295 μ mol, 0.06 mol-%) was dissolved in a mixture of CHO (50 mL, 495 mmol) and toluene (16.7 mL). After complete dissolution of the catalyst, the mixture was injected into a preheated (50°C) autoclave that was previously dried under vacuum at 100°C for 12 hours. The autoclave was pressurized to 9 bar with carbon dioxide and the polymerization commenced. At regular intervals, samples were collected (\pm 1 mL) via the bottom needle valve that was rinsed with THF after every sample to avoid cross-contamination. The samples were analyzed by ^1H NMR analyses (300 MHz, CDCl_3) to determine the conversion by integration of the methine peaks in the ^1H NMR spectra: ^1H NMR (300 MHz, CDCl_3): δ 4.65 (br, CH (PCHC), 2H), 3.11 (s, CH (CHO), 2H). The samples for SEC analyses were prepared as follows: about 0.5 mL of each of the reaction mixtures was added dropwise to a tenfold excess of petroleum-ether (40-70) upon which the poly(cyclohexene carbonate) (PCHC) precipitated. After separation and drying (vacuum, 60°C, 18h), the polymer was redissolved in the SEC eluent THF. Polymers needed for MALDI-ToF-MS analyses were prepared in a similar manner.

4.4.5 *Example of a typical polymerization using the bis(phenoxy) zinc catalyst.*

After a mixture of cyclohexene oxide (15 mL), toluene (35 mL) and catalyst (99 mg, 300 μ mol) was injected into the reactor, the reactor was heated to 30 °C and pressurized to 50 bar with carbon dioxide. All valves were closed and the reactor was further heated to 80°C, which resulted in a pressure of about 80 bar. Analyses and work-up procedures were similar to what is described above.

4.5 Acknowledgements

Avantium Technologies is kindly thanked for the use of their equipment and assistance (Niels Luchters) with the high throughput experiments.

4.6 References

- 1 Eberhardt, R.; Allmendinger, M.; Luinstra, G. A.; Rieger, B. *Organometallics* **2003**, *22*, 211.
- 2 Cheng, M.; Moore, D. R.; Reczek, J. J.; Chamberlain, B. M.; Lobkovsky, E. B.; Coates, G. W. *J. Am. Chem. Soc.* **2001**, *123*, 8738.
- 3 An even more active β -diketiminato zinc system was reported by: Moore, D. R.; Cheng, M.; Lobkovsky, E. B.; Coates, G. W. *Angew. Chem. Int. Edit. Engl.* **2002**, *41*, 2599.
- 4 Yokota, S.; Tachi, Y.; Itoh, S. *Inorg. Chem.* **2002**, *41*, 1342.
- 5 TOFs reported here are based on a longer reaction time than TOFs reported by Coates. Since the viscosity rapidly increases with increasing conversion, the TOF will drop with time and therefore the average TOF will consequently be lower.
- 6 Moore, D. R.; Cheng, M.; Lobkovsky, E. B.; Coates, G. W. *J. Am. Chem. Soc.* **2003**, *125*, 11911.
- 7 Allen, S. D.; Moore, D. R.; Lobkovsky, E. B.; Coates, G. W. *J. Am. Chem. Soc.* **2002**, *124*, 14284.
- 8 Darensbourg, D. J.; Rainey, P.; Yarbrough, J. C. *Inorg. Chem.* **2001**, *40*, 986.
- 9 Koning, C. E.; Wildeson, J.; Parton, R.; Plum, B.; Steeman, P.; Darensbourg, D. J. *Polymer* **2001**, *42*, 3995.
- 10 Samples were also prepared by removing all the volatiles under vacuum at 80°C for a night prior to dissolution in THF. Both methods were also applied after pre-treating the sample with a 10% HCl solution in water to ensure the disruption of catalyst-polymer chain interactions. All samples gave the same results in SEC and MALDI-ToF-MS.
- 11 Kobayashi, M.; Tang, Y.-L.; Tsuruta, T.; Inoue, S. *Makromol. Chem.* **1973**, *169*, 69.
- 12 Darensbourg, D. J.; Wildeson, J. R.; Yarbrough, J. C.; Reibenspies, J. H. *J. Am. Chem. Soc.* **2000**, *122*, 12487.
- 13 In a recently published artikel, Xiao et al. also detected the presence of cyclohexyl based end groups by means of MALDI-ToF-MS. Unfortunately the resolution of their spectra was too low to detect the presence of two overlapping isotope patterns. The linear mode used in this publication is unable to distinguish between separate isotope peaks, unlike the reflector mode MALDI-ToF-MS that was used for the spectra published here. Reference: Xiau, Y.; Wang, Z.; Ding, K. *Chem. Eur. J.* **2005**, *11*, 3668.

- 14 Polymerization was performed with TPPCrCl/DMAP using the following conditions: 15 mL of CHO, 35 mL of toluene, 300 μ mol of TPPCrCl, 3 mmol (10 eq.) of 4-dimethylaminopyridine (DMAP), 80 bar of CO₂, 80 °C, 24 hours. The same work-up procedure was followed as for a typical copolymerization with the [(2,6-F₂C₆H₃O)₂Zn·THF]₂ catalyst (see experimental section).
- 15 Epoxides can react with strong, non-nucleophilic bases by deprotonation in either the α - or the β -position. Abstraction of the α -hydrogen produces allylic alcohols and/or ketones. The β -deprotonation pathway on the other hand leads to exclusive formation of allylic alcohols.
- 16 For some recent papers see: (a) Magnus, A.; Bertilsson, S. K.; Andersson, P. G. *Chem. Soc. Rev.* **2002**, *31*, 223. (b) Crandall, J. K.; Chang, L.-H. *J. Org. Chem.* **1967**, *32*, 435. (c) Hodgson, D. M.; Lee, G. P.; Marriott, R. E.; Thompson, A. J.; Wisedale, R.; Witherington, J. *J. Chem. Soc., Perkin Trans. 1* **1998**, 2151.
- 17 Example of cyclohexene oxide rearrangements: Arata, K.; Tanabe, K. *Bull. Chem. Soc. Jpn.* **1980**, *53*, 299.
- 18 For some recent papers see: (a) Nishide, K.; Node, M. *Chirality* **2002**, *14*, 759. (b) de Graauw, C. F.; Peters, J. A.; van Bekkum, H.; Huskens, J. *Synthesis* **1994**, *10*, 1007. (c) Ooi, T.; Otsuka, H.; Miura, T.; Ichikawa, H.; Maruoka, K. *Org. Lett.* **2002**, *4*, 2669.
- 19 (a) Kehayova, D.; Kurtev, K.; Boneva, S. *Oxidation Communications* **1996**, *19*, 235-241. (b) TPC patent WO2003004448 to Kolomeyer, G. G.; Oyloe, J. S., Millenium speciality chemicals (2003).
- 20 Aida, T.; Inoue, S. *Acc. Chem. Res.* **1996**, *29*, 39.
- 21 See for example: Lopitiaux, G.; Ricart, G.; Faven, C.; Coqueret, X. *Macromol. Chem. Phys.* **2002**, *203*, 2560.
- 22 Soga, K.; Hyakkoku, K.; Ikeda, S. *Makromol. Chem.* **1978**, *179*, 2837.
- 23 Yu, K.; Jones, C.W. *J. Catal.* **2004**, *222*, 558.
- 24 Polymerization conditions: 15 mL of CHO, 35 mL of toluene, 50 °C, 9 bar of CO₂, 300 μ mol of catalyst and 10 eq. of ethanol.
- 25 Ivan, B. *Macromol. Symp.* **1994**, *88*, 201.
- 26 Darensbourg, D. J.; Wildeson, J. R.; Yarbrough, J. C.; Reibenspies, J. H. *J. Am. Chem. Soc.* **2000**, *122*, 12487.

- 27 (a) Ulmer, L.; Mattay, J.; Torres-Garcia, H. G.; Luftmann, H. *Eur. J. Mass Spectrom.* **2000**, *6*, 49. (b) Brown, T.; Clipston, N. L.; Simjee, N.; Luftmann, H.; HungerBühler, H.; Drewello, T. *Int. J. Mass Spectrom.* **2001**, *210/211*, 249.

This chapter was published in two parts: 1) van Meerendonk, W. J.; Duchateau, R.; Koning, C. E.; Gruter, G.-J. M. *Macrom. Rapid Commun.* **2004**, *25*, 382-386. 2) Meerendonk, W. J. van; Duchateau, R.; Koning, C. E.; Gruter, G.-J. M. *Macromolecules* **2005**, *38*, 7306-7313.

Chapter 5

Alternative monomers for polycarbonate synthesis

Abstract

The synthesis and use of a series of alternative monomers for the production of aliphatic polycarbonates is described in the present chapter. First, a series of cyclic oxiranes with different ring sizes (cyclopentene oxide, cyclohexene oxide, cycloheptene oxide and cyclooctene oxide) have been tested for their activity towards the copolymerization with CO₂. Three different catalysts were used, a bis(phenoxy) zinc, a β -diketiminato zinc and a porphyrinato chromium system. The commonly used cyclohexene oxide was by far the most active monomer and only the porphyrinato chromium catalyst was able to activate cyclopentene oxide and cycloheptene oxide, although in the latter case only the cyclic carbonate was formed. Subsequently, several 4-amide and 4-ester substituted cyclohexene oxide monomers were tested and copolymerized with CO₂. The ester functionalized monomers could be copolymerized with CO₂ using the very active β -diketiminato zinc catalyst under relatively mild conditions. Side reactions with the functional groups, although very interesting by themselves, limited the molecular weights that could be obtained. Difficulties with the purification and solubility of the amide substituted monomers led to low molecular weight polymers, limiting their practical applications. Finally, as a proof of concept, some long alkyl chain-modified epoxides were homo- and copolymerized with CO₂ leading to interesting polymer microstructures. Among the found microstructures, the formation of crown ethers by the cationic polymerization of octane oxide was detected by MALDI-ToF-MS.

5.1 Introduction

5.1.1 Potential polymer properties enhancing monomers

The currently known aliphatic polycarbonates are still of limited use as engineering plastics. The unique properties of the commercial poly(bisphenol-A carbonate) such as its high T_g and impact resistance are very difficult to obtain with aliphatic polycarbonates based on ethylene oxide (EO), propylene oxide (PO) and cyclohexene oxide (CHO). The first two monomers give polycarbonates with a T_g that is far too low and although the polycarbonate based on CHO has a higher T_g (around 116°C), it is still considerably lower than the T_g of poly(bisphenol-A carbonate)

(150°C). The fact that oxirane monomers are used for these copolymerizations limit the backbone to an aliphatic C2 bridge and since the T_g is related to the rigidity of the polymer chain,¹ preferably oxiranes should be chosen with substituents on both the α and β position. Two approaches were chosen. Firstly the effect of the ring size of oxiranes on the polymerization chemistry and on polymer properties was investigated with a series of oxirane monomers, ranging from a 5-membered ring to an 8-membered ring (Figure 5-1).

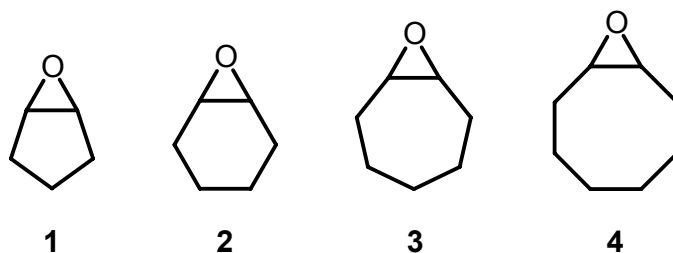


Figure 5-1. Several cyclic oxiranes.

Secondly, the effect of a modification of cyclohexene oxide, one of the most widely used monomers in oxirane – CO₂ copolymerizations, was investigated. With an ester or amide group on the 4-position, the reactivity is expected to be comparable to the standard cyclohexene oxide (**2**). It was argued that the additional functionality might have a positive influence on polymer properties and that it could also be used as a reactive group for post processing and modification. The amide groups have the potential of providing additional interchain interactions via hydrogen bonding, which is expected to result in an increase in T_g . In total four ester and amide functionalized monomers were synthesized (Figure 5-2).

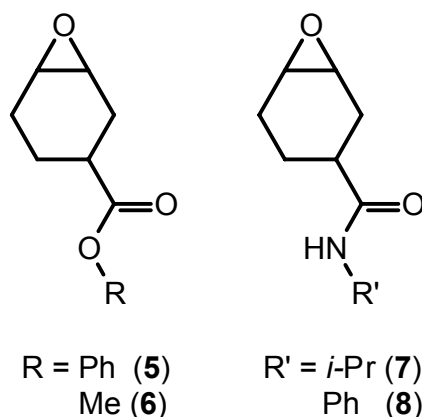
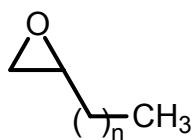


Figure 5-2. 4-Substituted cyclohexene monomers.

Two different aliphatic long chain epoxide monomers (Figure 5-3, octene oxide (**9**) and octadecene oxide (**10**)) were also tested for their activity in the homo- and copolymerization (with CO₂). In literature, very little is known about the synthesis of long alkyl chain substituted

polycarbonates or polyethers.² Although we do not expect improved physical properties by using these long alkyl chain epoxides, interesting surfactant-like structures can be prepared.



$$n = 5 \quad \mathbf{(9)}$$

$$15 \quad \mathbf{(10)}$$

Figure 5-3. Long chain aliphatic epoxide monomers.

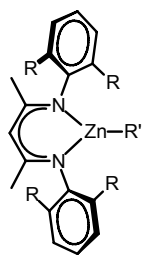
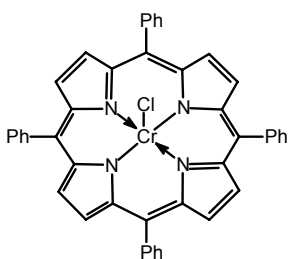
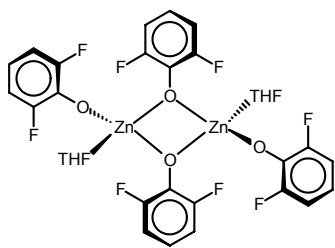
Three catalysts, representing three different classes, were selected from literature and used for the copolymerization of the different monomers with CO₂ (Table 5-1). The β -diketiminato zinc catalysts, already discussed in Chapter 4, form the most active class of catalysts for the copolymerization of CHO with CO₂. The bis(phenoxy) zinc and the porphyrinato chromium catalysts represent two other well-known classes. Although less active than the β -diketiminato zinc catalyst, the porphyrinato chromium system is less susceptible for the presence of H₂O, O₂ or functional groups than the zinc based catalysts.

5.2 Results and discussion

5.2.1 Synthesis and purification of the cyclic epoxides

Monomers **1**, **2** and **4** were purchased and dried by distillation from CaH₂. Monomer **3** however, is not readily available and was therefore synthesized by dehydrating of cycloheptanol to cycloheptene and the subsequent epoxidation to cycloheptene oxide. The dehydration step proceeded rapidly with the dropwise addition of the cycloheptanol to a molten excess of the anhydride (140°C). Since the boiling point of the cycloheptene is lower than of cycloheptanol, it could immediately be distilled out of the reaction mixture. The epoxidations were performed with *m*-chloroperbenzoic acid (CPBA) in dichloromethane (DCM).

Table 5-1. Different catalysts used in the (co)polymerization of monomers **1-9**.

Class	Catalyst	Abbreviation	Remarks
β -diketiminato zinc		11a : R=Et, R'=OMe (EtBDIZnOMe) 11b : R=Et, R'=OEt (EtBDIZnOEt)	
Porphyrinato chromium		12 : TPPCrCl	Cocatalyst required
Bis(phenoxy) zinc		13 : (F ₂ PhO) ₂ Zn	

5.2.2 Copolymerization results of cyclic epoxides

Monomers **1**, **3** and **4** were tested with three different catalytic systems for their activity towards copolymerization with CO₂. The results are summarized in Table 5-2, with more detailed information of the more successful runs in Table 5-3.

Table 5-2. Copolymerization results with different cyclic epoxides.

Catalyst \ Monomer	1 (C5)	2 (C6)	3 (C7)	4 (C8)
TPPCrCl / DMAP	Polymer (92%) ^{a)}	Polymer	Cyclic carbonate (14%) ^{a)}	-
(F ₂ PhO) ₂ Zn	-	Polymer	-	-
EtBDIZnOEt	-	Polymer	-	-

a) Conversion of the monomer.

From Table 5-2, it is clear that the use of different ring sizes in the cyclic epoxides monomers has a large influence on the reactivity of the oxirane. Only monomers **1** and **2** were successfully copolymerized with CO₂ and monomer. Surprisingly, conversions obtained with monomer **1** are twice as high as observed for monomer **2** (CHO) and the reactions went almost to completion. The low molecular weights indicate a large amount of chain transfer with water impurities and reliable T_g measurements could not be obtained. Furthermore, a significant amount of polyether linkages was observed. Monomer **3** was exclusively converted to the corresponding cyclic carbonate. Furthermore, only the TPPCrCl/DMAP system was able to activate monomers **1**, **2** and **3**. Both the (F₂PhO)₂Zn and the EtBDIZnOEt catalyst systems failed to catalyze either the copolymerization or cyclic carbonate formation of monomers **1**, **3** and **4** with CO₂. Therefore, it can be concluded that the TPPCrCl/DMAP catalyst seems to be the most versatile system with respect to monomer variation so far.

Table 5-3. Details of copolymerization of different cyclic epoxides with CO₂.

Entry ^{a)}	Monomer (mL)	Conversion to PCHC (%) ^{b)}	Cyclic carbonate (%)	Fraction CO ₂ (%)	\overline{M}_n (g · mol ⁻¹) ^{c)}	\overline{M}_w (g · mol ⁻¹) ^{c)}	$\overline{M}_w / \overline{M}_n$	Comments
1	1 (15)	92	0	72	2,600	7,910	3.0	polycarbonate
2	3 (15)	0	14	-	-	-	-	Only the cyclic carbonate was formed
3	2 (50)	46	0	> 99	5,080	9,300	1.8	polycarbonate

a) Polymerization conditions: 300 μmol of TPPCrCl catalyst, 3 mmol DMAP cocatalyst, 72 h, 80 bar, 80°C. b) Calculated from ¹H NMR integration of the methine peaks. c) PS equivalents.

The copolymer obtained from the copolymerization of monomer **1** and CO₂ (entry 1, Table 5-3) was analyzed by MALDI-ToF-MS. The spectrum (Figure 5-4) shows that one part of the polymer has one OH and one Cl end group while the other part has two OH end groups, which is the result of water initiation. Calculations show that 7-8 chains are formed per catalyst confirming some kind of chain transfer with water. Furthermore, the copolymer is not perfectly alternating, as can be seen by the mass differences of 44 (loss of CO₂).

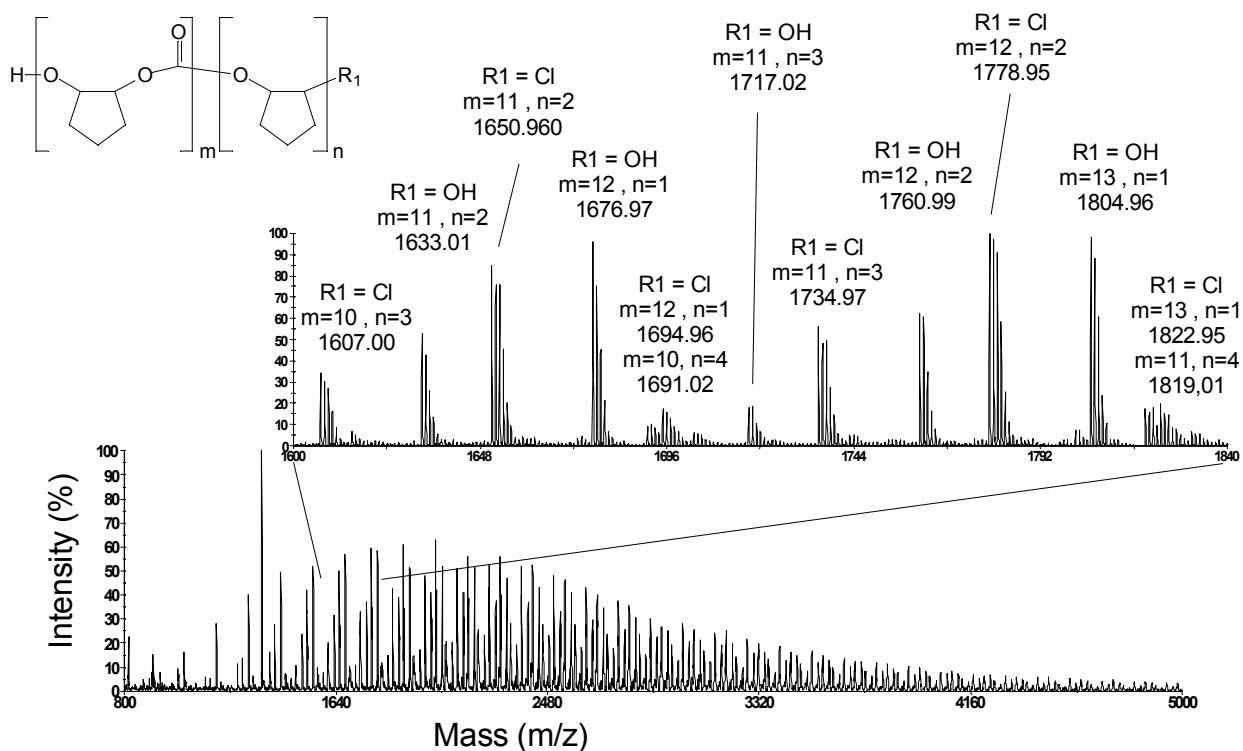


Figure 5-4. MALDI-ToF-MS spectrum of the polymer obtained in entry 1, Table 5-3 (cationization ion: K^+).

Furthermore, the results follow the trend observed by Bacsai et al. in their investigation of the reactivity order in the homopolymerization of monomers **1**, **2**, **3** and **4** to the corresponding polyethers with AlEt_3 as the initiator.³ The established reactivity order was found to be: cyclohexene oxide > cyclopentene oxide > cycloheptene oxide >> cyclooctene oxide.

These results seem to confirm the special character of the cyclohexene ring. Darensbourg et al. investigated the reactivity of 2,3-epoxy-1,2,3,4-tetrahydronaphthalene (Figure 5-5) with CO_2 , catalyzed by a TPPCrCl derivative.⁴ They were unable to copolymerize this interesting monomer and only the cyclic carbonate was formed instead. Although the monomer is basically a substituted CHO monomer, it seems as if the effect of the phenyl ring already renders this monomer inactive towards copolymerization. Darensbourg et al. postulated that electronic factors were the reason for this behavior.⁴

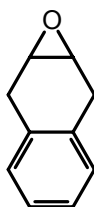
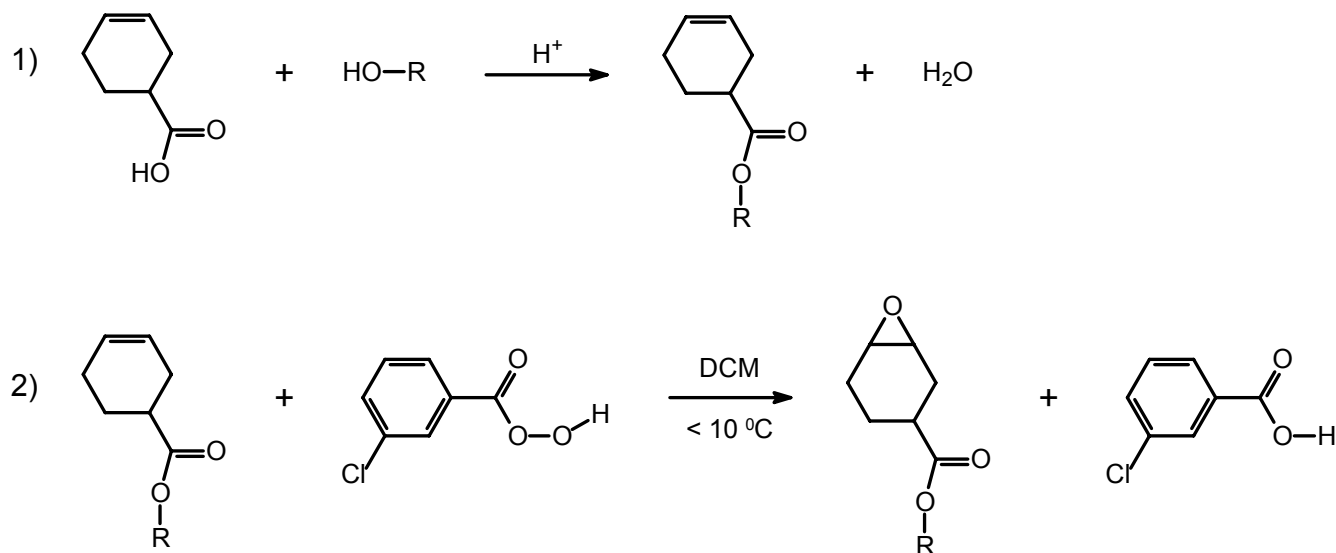


Figure 5-5. 2,3-Epoxy-1,2,3,4-tetrahydronaphthalene.⁴

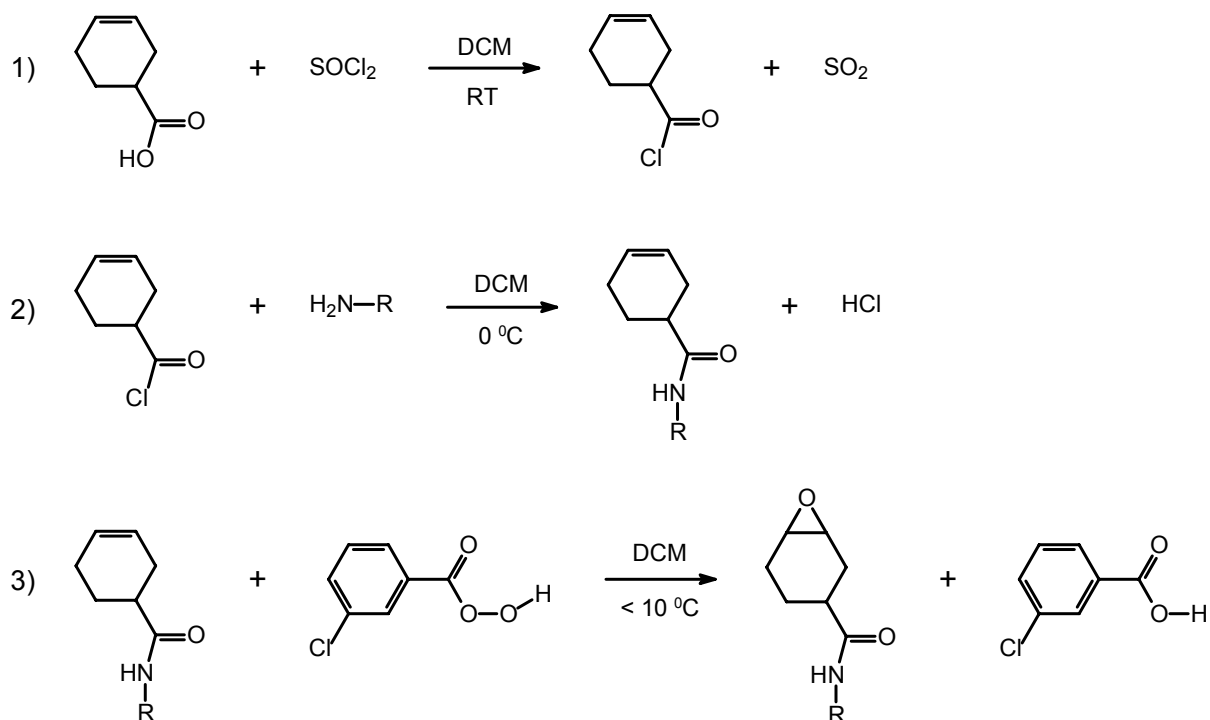
5.2.3 Synthesis of 4-substituted cyclohexene oxide monomers

The ester functionalized monomers **5** and **6** were synthesized from 3-cyclohexene-1-carboxylic acid in two steps (Scheme 5-1). The esterification reaction (step 1) proceeded rapidly in the presence of some sulfuric acid as a catalyst. The epoxidation of the double bond (step 2) with *m*-chloroperbenzoic acid was performed in dichloromethane (DCM) at temperatures below 10°C. Purification was performed by column chromatography using basic alumina.



Scheme 5-1. Synthesis of monomers **5** and **6** (R = Me, Ph respectively).

The amide functionalized monomers **7** and **8** were synthesized via a similar route as monomers **5** and **6** with one difference (Scheme 5-2): An intermediate conversion of the acid to the acid chloride (step 1) was performed to facilitate a faster reaction with the amine (step 2). Subsequently, a standard epoxidation of the double bond with *m*-chloroperbenzoic acid was performed in DCM. Purification of these monomers proved to be difficult due to the fact that the *m*-chlorobenzoic acid, which is formed after the epoxidation step, was difficult to remove. The basic alumina column was unfortunately not an option due to the affinity of the amide groups for the column material. However, most of the acid could be removed by extended washing with a 10% aqueous NaHCO₃ and an aqueous triethyl amine solution.



Scheme 5-2. Synthesis of monomers **7** and **8** (R = *i*-Pr, Ph respectively).

5.2.4 Lab scale copolymerizations of 3,4-cyclohexene-oxide-1-carboxylic acid methyl ester (**5**) and 3,4-cyclohexene-oxide-1-carboxylic acid phenyl ester (**6**) with CO₂.

Monomers **5** and **6** were copolymerized with the EtBDIZnOEt catalyst over a prolonged period of time and the results are summarized in Table 5-4.

Table 5-4. Result for the copolymerization of monomer **5** and **6**.

Entry ^{a)}	Monomer (g)	μmol catalyst	Time (h)	Toluene (mL)	Conversion to PCHC (%) ^{b)}	Cyclic carbonate (%)	Fraction CO ₂ (%)	\overline{M}_n (g · mol ⁻¹) ^{c)}	T _g	$\overline{M}_w / \overline{M}_n$
1	5 (10)	200	96	40	84	0	> 99	2,330	53.1	4.4
2	6 (7)	600	72	50	30	0	> 99	< 500	-	-

a) Polymerization conditions: Catalyst: EtBDIZnOEt (**11b**), 50°C, 10 bar CO₂. b) Calculated from 1H NMR integration of the methine peaks. c) PS equivalents.

The copolymerization of monomer **5** with CO₂ resulted in a polycarbonate with a low \overline{M}_n (2,330 g · mol⁻¹, Table 5-4, entry 1). Although the \overline{M}_n values are defined as PS equivalents, the

molecular weights observed with MALDI-ToF-MS (Figure 5-6) do not deviate greatly. Using the SEC values an estimated number of chains of thirteen was found per catalyst molecule. This indicates the presence of chain transfer reactions during the polymerization as was observed in chapter 4. MALDI-ToF-MS measurements were used to determine the end groups of the polymers and the spectrum is shown in Figure 5-6. The spectrum reveals a perfectly alternating copolymer as no loss of CO₂ could be observed (a mass difference of 44 g · mol⁻¹ between peaks indicates a loss of CO₂ unit).

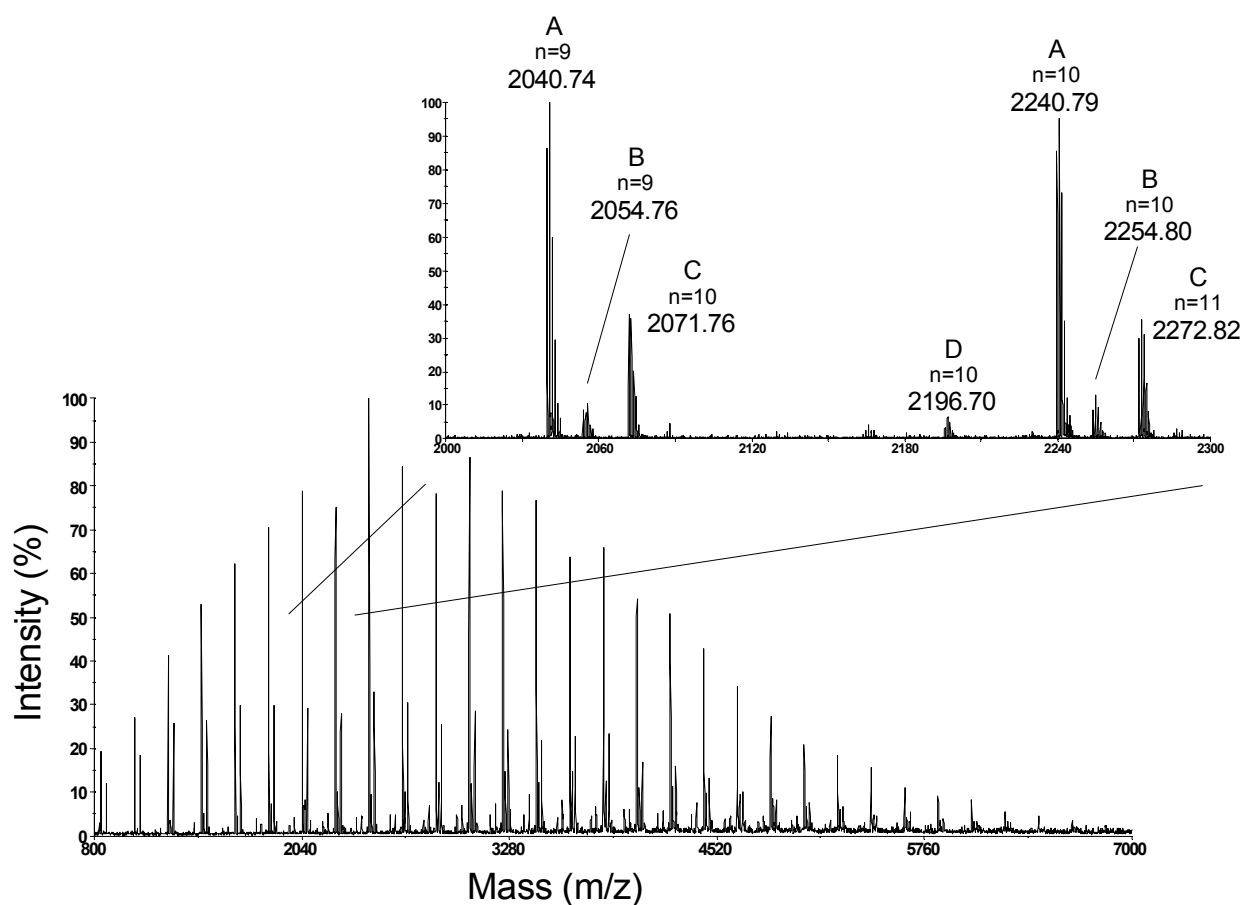


Figure 5-6. MALDI-ToF-MS spectrum of the polymer obtained in entry 1, Table 5-4 (cationization ion: K⁺). With ‘n’ the number of repeating units, of the corresponding polymer structure, is represented as given in Table 5-5.

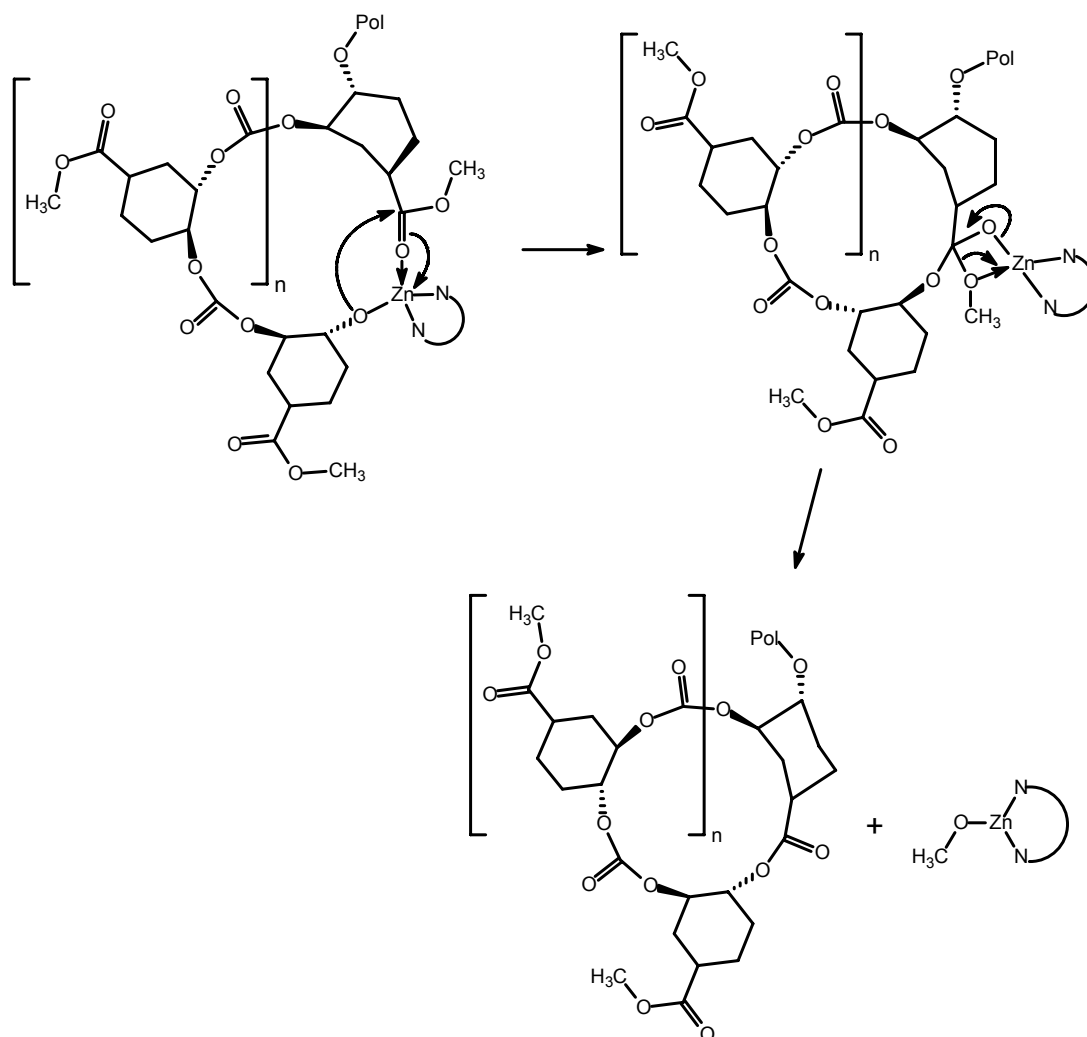
Taking a closer look at the MALDI-ToF-MS spectrum revealed some interesting chain structures, but the structure that would be expected under normal conditions in a polymerization with an EtBDIZnOEt (**11b**) catalyst, with one ethoxide end group and one OH end group, as seen in chapter 4, was not observed in Figure 5-6. All peaks are a clear indication of transesterification reactions, catalyzed by **11b**, leading to the formation of various loops, rings and coupling products. The proposed mechanism for these transesterification is shown in Scheme 5-3. An ester group, of a monomeric unit further in the chain, can coordinate to a cyclohexyloxide zinc species. Nucleophilic

attack of the cyclohexyloxide at the carbonyl of the ester group will lead to an intermediate structure (top right corner of Scheme 5-3), which can undergo a rearrangement to form a polymer loop and a new methoxide zinc species capable of initiating another chain. This mechanism also explains the formation of multiple chains for an intrinsically living catalyst. Similar transesterification reactions with zinc alkoxides were previously reported in the ring opening polymerization (ROP) of β -butyrolactone.⁵ Instead of chain transfer reactions with alcohols, as observed in the copolymerization of CHO with CO₂ catalyzed by EtBDIZnOEt (paragraph 4.2.4), chain transfer reactions now occur with the monomer. Furthermore the presence of peak A, where the initiating ethoxide group (from the catalyst) has been exchanged for a methoxide group (from the ester group of a monomer), supports this transesterification theory. This transesterification is of course not limited to monomer units in the same polymer chain (intramolecular transesterification), but can also occur with a free monomer or with a monomer unit of a different chain. In the case of a transesterification with a free monomer, a polymer structure with an epoxide end group should be formed and this structure can indeed be seen in Figure 5-6 (peak D). Of course this reactive end group can act as a macromonomer and can, on its turn, be further copolymerized with CO₂ leading to high amount of possible chain microstructures. In the case of transesterification of an ester group to a different polymer chain, chain coupling will occur. However, due to the similarity of the initiating groups and the condensation products of the transesterification reactions, the resulting structure will be a structural isomer to a normal linear chain, similar to the structure proposed for label C. In other words, the polymers could be highly branched or even a network could be formed. The use of other, more stable ester groups, like *t*-butyl ester, should reduce the influence of these side reactions.

Table 5-5. Possible structures for the peaks found in Figure 5-6 (entry 1, Table 5-4).

Label	n	Structure
A	9	
B	9	
C	10	
D	10	

a) The exact location of the monomer unit where the transesterification took place cannot be determined, so no discrimination can be made between rings or loops with dangling chain ends of different lengths.



Scheme 5-3. Proposed mechanism for the chain transfer and formation of loop or ring structures seen in the copolymerization of monomer 5.

The copolymerization of monomer 6 with CO_2 is slower than with monomer 5 as can be seen from the much lower conversion of 30% (entry 2, Table 5-4). SEC analysis showed a number of oligomers and no reliable \bar{M}_n and \bar{M}_w data could be obtained. The formed polymer was analyzed by MALDI-ToF-MS and the spectrum is shown in Figure 5-7.

The MALDI-ToF-MS spectrum shows three different peaks within a repeating unit. The polymer is almost completely alternating as can be seen from the maximum visible loss of only one CO_2 unit per chain (only from peak B to peak C a mass of $44 \text{ g} \cdot \text{mol}^{-1}$ can be found). Peaks B and C can be explained by the structures given in Table 5-6, but the origin of peak A is still unknown.

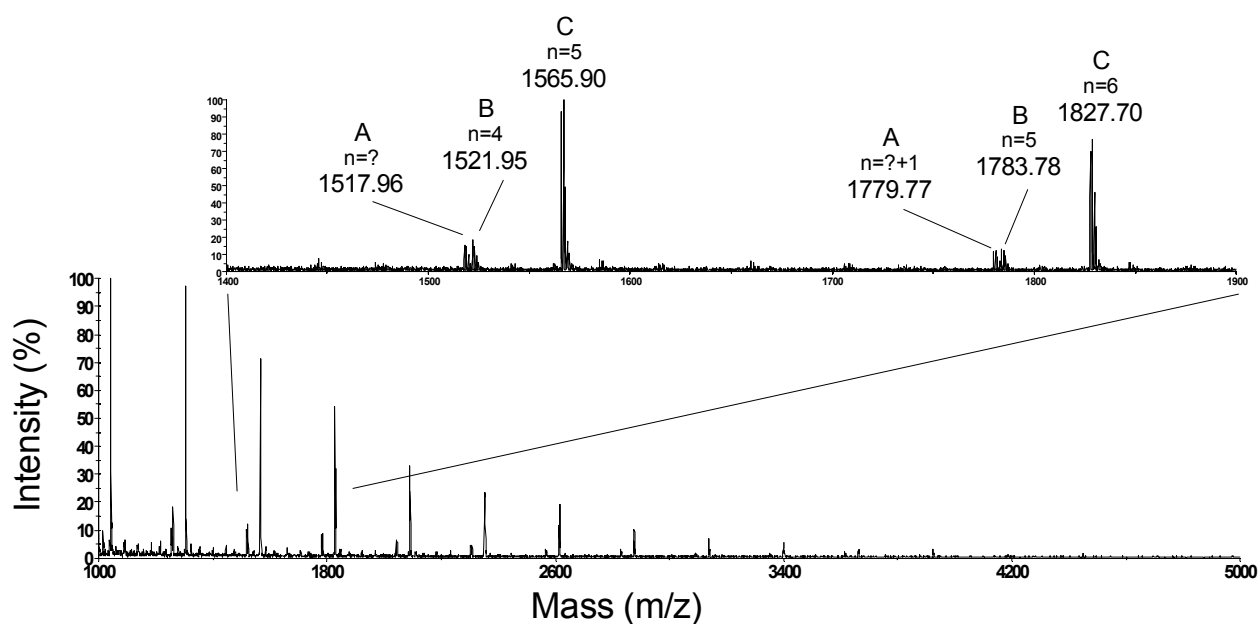


Figure 5-7. MALDI-ToF-MS spectrum of the polymer obtained in entry 2, Table 5-4. (cationization ion: K^+). With ‘n’ the number of repeating units, of the corresponding polymer structure, is represented as given in Table 5-6.

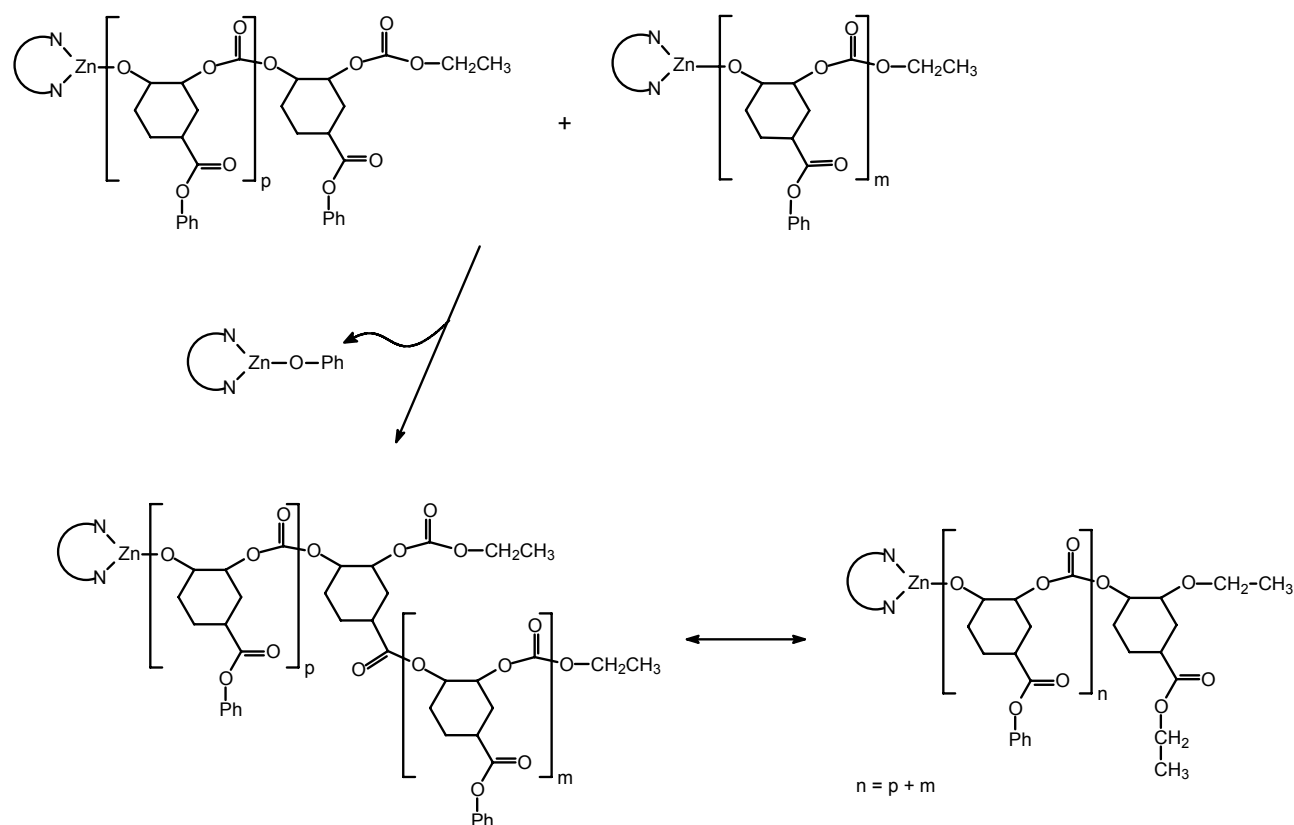
Table 5-6. Possible structures for the peaks displayed in Figure 5-7 (entry 2, Table 5-4).

Label	n	Structure
A		Unknown
B	4	
C	5	

Cationization ion is K^+ in all cases

Because the MALDI-ToF-MS spectra only provide information on the absolute mass of a given polymer chain, possible structural isomers cannot be distinguished. The suggested structures responsible for peaks B and C as given in Table 5-6 suggest an exchange between the ethoxide initiating groups of the catalysts and the phenyl esters of the monomers, similar to the case with the

polymer of monomer **5**. However, no polymer chains were observed with more ethoxide groups present. The transesterification reaction between an EtBDIZnOEt species and an ester group of the free monomer or polymer can therefore be excluded. Furthermore, the absence of phenoxide initiated polymer chains (i.e. without EtO groups) also excludes random transesterification between the catalyst and the monomers. A more plausible explanation for peak B is therefore the coupling of two individual chains by a transesterification reaction of a polymer chain on the ester functionality as displayed in Scheme 5-4. Apparently, the formed phenol molecule does not lead to chain transfer, since the presence of cyclic polymers, as was the case with monomer **5**, could not be detected by MALDI-ToF-MS. This was confirmed by a polymerization where 10 equivalents of phenol (with respect to the catalyst) were added after 3 hours polymerization time. The polymerization was continued for another 15 hours, but no increase in conversion was observed and the MALDI-ToF-MS spectrum was identical to the spectrum obtained from a sample after 3 hours (before phenol addition).⁶



Scheme 5-4. Coupling of two chains with the structural isomer of the coupling product at the bottom right.

Both monomers have been copolymerized with CO_2 in an almost completely alternating manner with only a maximum of 1 CO_2 unit missing. The introduced functionality did not affect the selectivity of the catalyst, but side reactions with the ester functionality were observed leading to chain transfer to the monomer in the case of monomer **5** and the formation of rings and chain coupling products. As a consequence of these side reactions, chain growth was severely limited.

When monomer **6** was used, the phenol formed in the chain coupling reaction inactivated the catalyst, hence the low conversions.

DSC measurements of the polymer obtained with monomer **5** showed a T_g of 53 °C ($\overline{M}_n = 2,330 \text{ g} \cdot \text{mol}^{-1}$). Since the molecular weight of the polymer, especially at lower molar masses, has a strong influence on the T_g , a direct comparison of the T_g found in literature of PCHC (around 116 °C) cannot be made.⁷ Two DSC measurements of low molecular weight PCHC were performed and for an \overline{M}_n of 1400 $\text{g} \cdot \text{mol}^{-1}$ a T_g of 52 °C was found and for an \overline{M}_n of 3500 $\text{g} \cdot \text{mol}^{-1}$ a T_g of 85 °C was found. This would indicate a relatively low T_g for the polymer obtained with monomer **5** in comparison to the PCHC samples. However, the exact relation between the \overline{M}_n and T_g for both polymers was not investigated in detail and one should be careful drawing conclusions from these measurements. For the polymer obtained with monomer **6** no T_g could be found (the \overline{M}_n was too low).

5.2.5 *NMR tube copolymerizations of N-isopropyl-3,4-epoxy-cyclohexyl-1-carboxamide (7) and N-phenyl-3,4-epoxy-cyclohexyl-1-carboxamide (8) with CO₂.*

Several preliminary copolymerization reactions were performed with monomer **7** in an NMR tube reactor but the solubility of the monomer proved to be a problem and no polymer was obtained when the solvents benzene-d₆, chloroform-d₁ or DCM were used. Of the tested solvents only DMSO-d₆ was capable of sufficiently dissolving monomers **7** and **8**. The β -diketiminato zinc catalysts EtBDIZnOMe proved unsuitable for the copolymerization of these amide substituted monomers. In the presence of amide groups the catalyst decomposed and formed several species, as was observed by ¹H NMR. A control experiment where ten equivalents of caprolactam were added to a normal CHO polymerization yielded only a fraction of the expected amount of PCHC (conversion < 2%).⁸

5.2.6 *Lab scale copolymerizations of N-isopropyl-3,4-epoxy-cyclohexyl-1-carboxamide (7) and N-phenyl-3,4-epoxy-cyclohexyl-1-carboxamide (8) with CO₂.*

With the results of the NMR-tube tests in mind, the lab scale polymerizations were mostly performed in DMSO, although the high boiling point makes it difficult to remove the solvent afterwards. Furthermore, only the TPPCrCl /DMAP catalyst system was used in the attempts to copolymerize monomers **7** and **8** with CO₂. All polymerizations were performed over prolonged

periods of time. A terpolymerization with monomers **2** (CHO) and **7** was also attempted and the results are shown in Table 5-7.

Table 5-7. Results of copolymerization reactions of monomer **7** and **8** using the TPPCrCl /DMAP catalyst system.

Entry ^{a)}	monomers (g)	solvent (50 mL)	conversion to PCHC (%) ^{b)}	\overline{M}_n (g · mol ⁻¹) ^{c)}	\overline{M}_w (g · mol ⁻¹) ^{c)}	$\overline{M}_w / \overline{M}_n$
1	7 (3 g)	DCM	41%	1039	1195	1.15
2	7 (6 g)	DMSO	82%	745	817	1.10
3	2 (8.7 g) + 7 (4.9 mL)	DMSO	91%	857	976	1.13

a) Polymerization conditions: 300 μmol of TPPCrCl, 10 eq. of DMAP, 72 hours, 80°C, 50 bar CO₂. b) Calculated from ¹H NMR integration of the methine peaks. c) PS equivalents.

When dichloromethane was used as a solvent, the solubility of the monomer was very poor, as was already observed in the NMR tube reactions, and only 3 grams of monomer could be solubilized (entry 1, Table 5-7). Overall yields are reasonable although the reaction itself is rather slow.

MALDI-ToF-MS spectra of the oligomers obtained from monomer **7** (entries 1 and 2, Table 5-7) showed isotope patterns that indicate the presence of chloride-containing polymer chains. The corresponding masses correspond to 3-chlorobenzoic acid initiated chains. Despite several attempts to purify the monomer, the acid was still present in quantities of 1-3%. Test reactions in an NMR tube of monomer **7** with 3-chlorobenzoic acid at room temperature did not show any reaction, but after heating for one night to 50°C, ¹H NMR spectra showed ring opening of the epoxides.⁹

Obtained molecular weights are low and the calculated number of chains per catalyst is very high (24 for entry 2), however, since the Mark-Houwink parameters are unknown this value is not very accurate. The high number of chains per catalyst is probably caused by the acid initiation, because evidence of chain-transfer reactions could not be found in the MALDI-ToF-MS spectra.

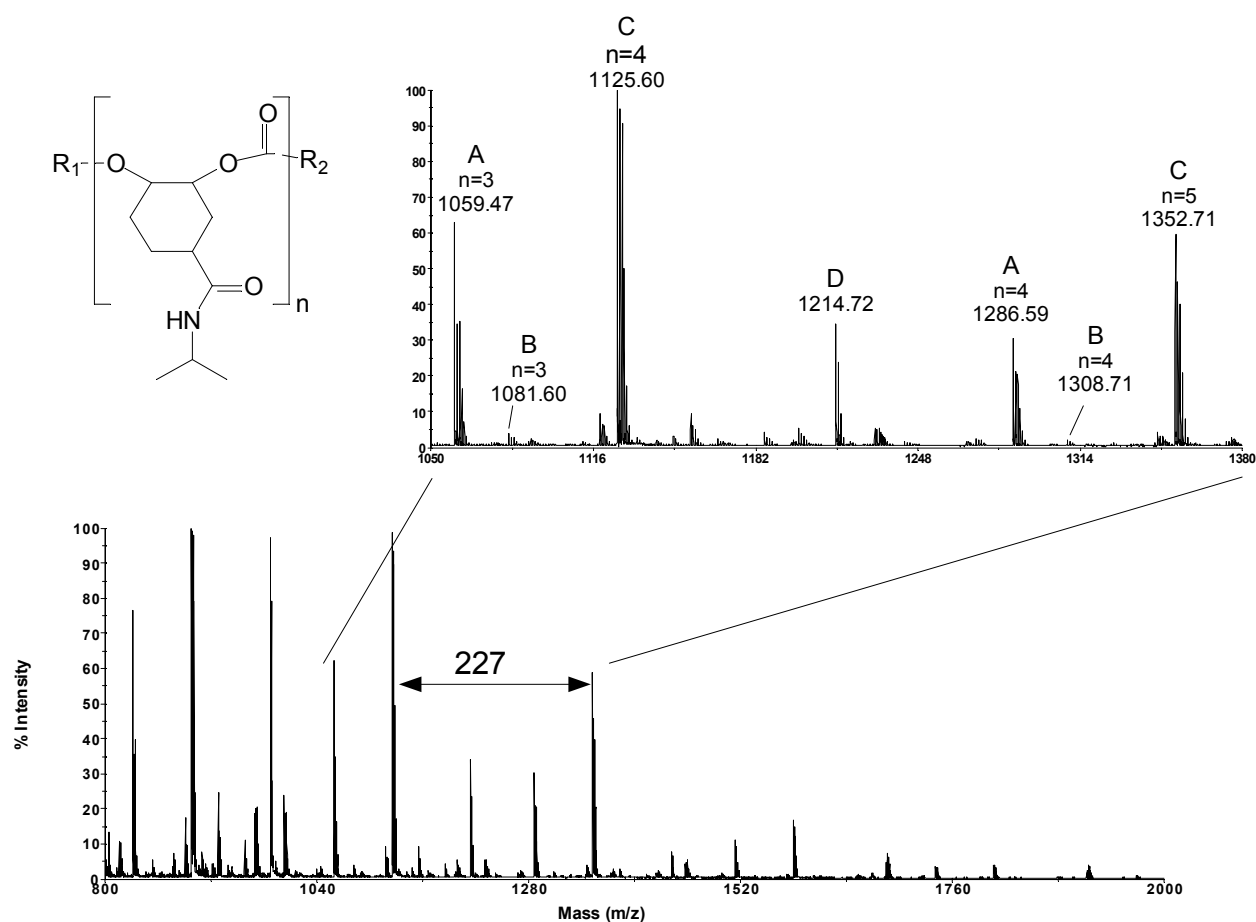
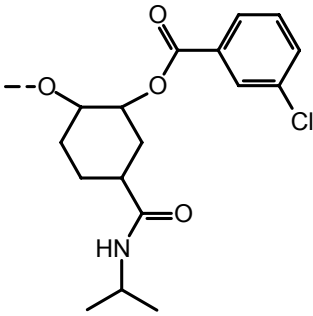
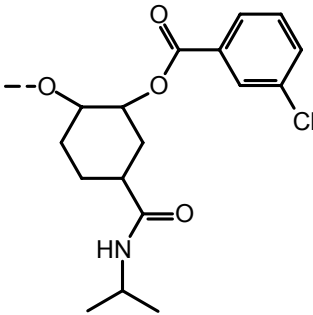
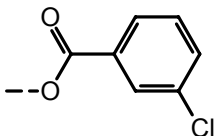


Figure 5-8. MALDI-ToF-MS spectrum of the polymer obtained in entry 1, Table 5-7 (cationization ion: K^+).

The proposed structures for the peaks displayed in Figure 5-8 are shown in Table 5-8. Structures for label B and C include an extra Na^+ , which probably exchanged with a H^+ from an alcohol end group or one of the amide groups in the polymer chain. Since no similar behavior was observed for other alcohol end groups, the amide groups are probably responsible for the increased affinity for sodium. Trace amounts of sodium in a MALDI-ToF-MS sample could often not be prevented due to its presence in glassware.

Table 5-8. Possible structures for the peaks found in Figure 5-8 (entry 1, Table 5-7).

Label	n	R1	R2
A	3	H	
B	3	Na	
C	4	Na	
D		Peak from matrix material	

A terpolymerization of CHO, monomer **7** and CO₂ was attempted in DMSO using the TPPCrCl / DMAP catalyst to test the flexibility of this system (entry 3, Table 5-7). MALDI-ToF-MS analysis (Figure 5-9) showed the formation of a terpolymer. The existence of a terpolymer could be ascertained by the observation that from a specific peak, corresponding peaks could be observed at lower masses with a difference of the mass of one repeating unit of either epoxide monomer. This indicates the presence of both epoxide monomers in a certain chain. A detailed end group analysis proved difficult. Two different end group masses (the sum of R₁ and R₂ was either 97 or 125 g · mol⁻¹) could be identified as shown in Figure 5-9, but since it cannot be excluded that the amide functionality is somehow involved in side reactions, these end group masses could be the result of too many different polymer micro structures. However, it is clear is that the monomeric units of all three monomers are present.

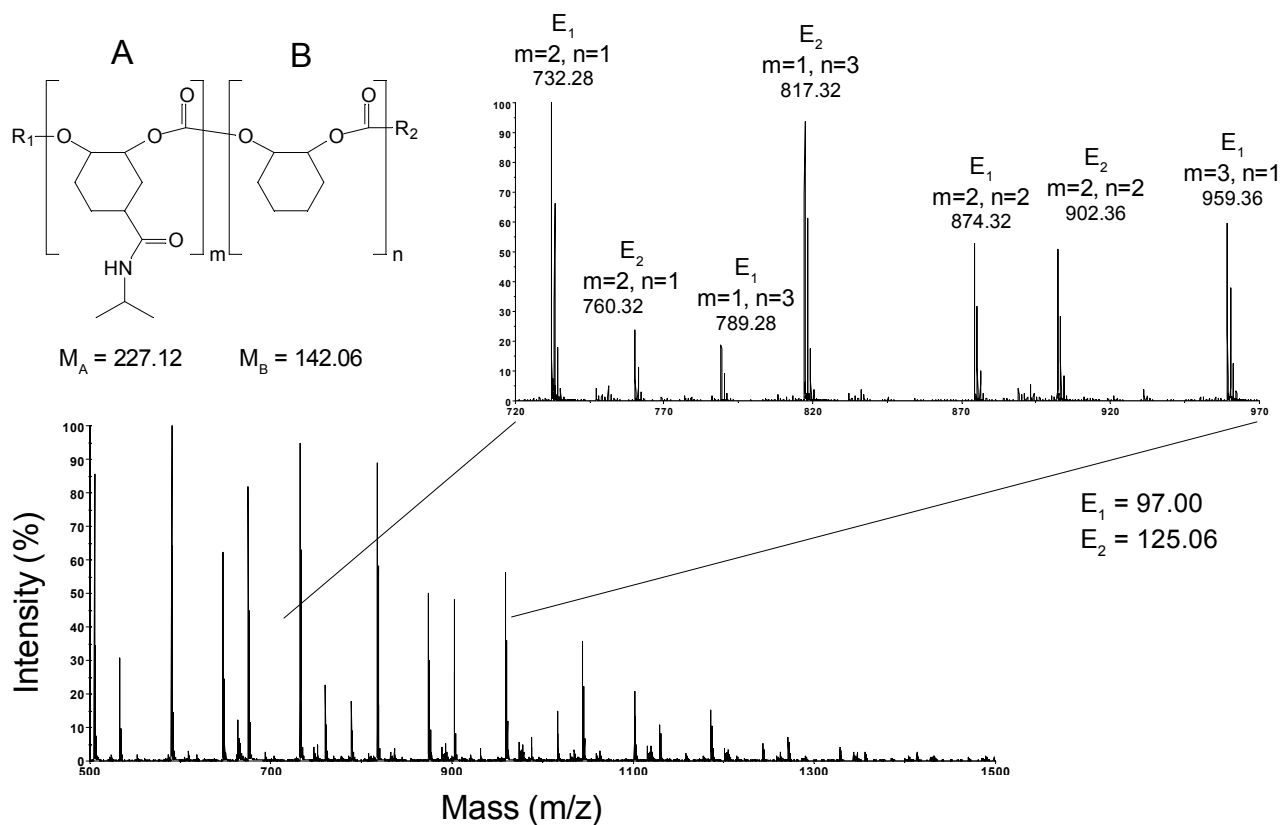


Figure 5-9. MALDI-ToF-MS spectrum of the polymer obtained in entry 3, Table 5-7 (cationization ion: K^+).

5.2.7 Polymer synthesis with octene oxide (9) and octadecene oxide (10)

The synthesis of polyethers with long alkyl side chains was attempted with both a cationic and an anionic initiator. The cationic initiator which was used was the cationic diazabutadiene zinc complex (**14**) shown in Figure 5-10 with a borate counter ion.¹⁰

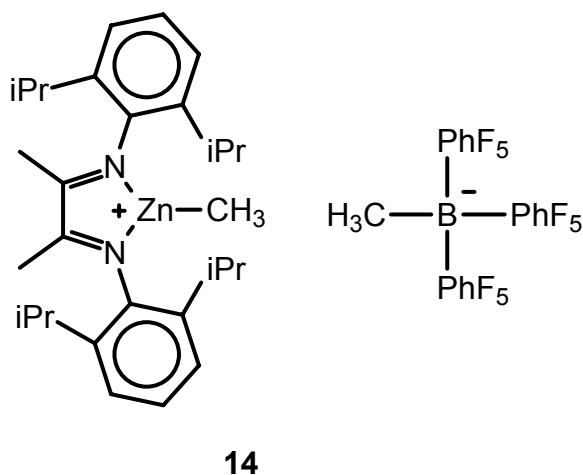


Figure 5-10. Structure of the cationic zinc complex $[(DAB)ZnMe]^+[MeB(Ar^{F5})_3]^-$ (**14**).

As an anionic homopolymerization catalyst butyl lithium was used (1 M solution in hexane). The results of the (co)polymerization experiments with monomers **9** and **10** are summarized in Table 5-9.

Table 5-9. Results of the (co)polymerization experiments with monomers **9** and **10**.

Entry	monomers (mL)	catalyst	solvent (mL)	Conversion to PCHC (%) ^{a)}	\overline{M}_n (g · mol ⁻¹) ^{b)}	\overline{M}_w (g · mol ⁻¹) ^{b)}	$\overline{M}_w / \overline{M}_n$	Remarks
1 ^{c)}	9 (1)	14 (± 5 µmol)	none	35	9,387	19,365	2.06	
2 ^{d)}	9 (2)	BuLi ^{e)} (1 mmol)	toluene (5)	25	503	518	1.03	
3 ^{d)}	10 (2)	BuLi ^{f)} (1 mmol)	toluene (5)	20	1,048	1,096	1.05	
4 ^{g)}	9 (100 mg)	11b (42 µmol)	C ₆ D ₆ (0.5)	12	554	701	1.26	copolymerization with 10 bar CO ₂

a) Calculated from ¹H NMR integration of the methine peaks. b) PS equivalents. c) Exothermic reaction, 10 min started at room temperature. d) Shortly heated to 80°C, total reaction time 10 min. e) 1 mL (1 M solution in hexane). f) 2 mL (1 M solution in hexane). g) Reaction performed in an NMR-tube: 44 µmol catalyst, 18 h, 60°C, 10 bar CO₂.

The values for the molecular weights found with SEC are probably not very accurate. With the relatively long side groups and low molecular weight, the radius of gyration of the polymer probably strongly deviates from that of the PS standard. Since the Mark-Houwink parameters for these polymers are unknown, the values in Table 5-9 should only be used as an indication of the real values. The low molecular weight of entries 2 and 3 in comparison to entry 1 is caused by the much larger amount of catalyst used. The polydispersities show a very different polymer distribution for the cationic versus the anionic polymerization mechanism (entry 1 versus entry 2, Table 5-9). The cationic polymerization with catalyst **14** leads to a Gaussian polymer distribution with a polydispersity of 2, while with the anionic mechanism (BuLi), a living system with a polymer dispersity close to unity is observed.

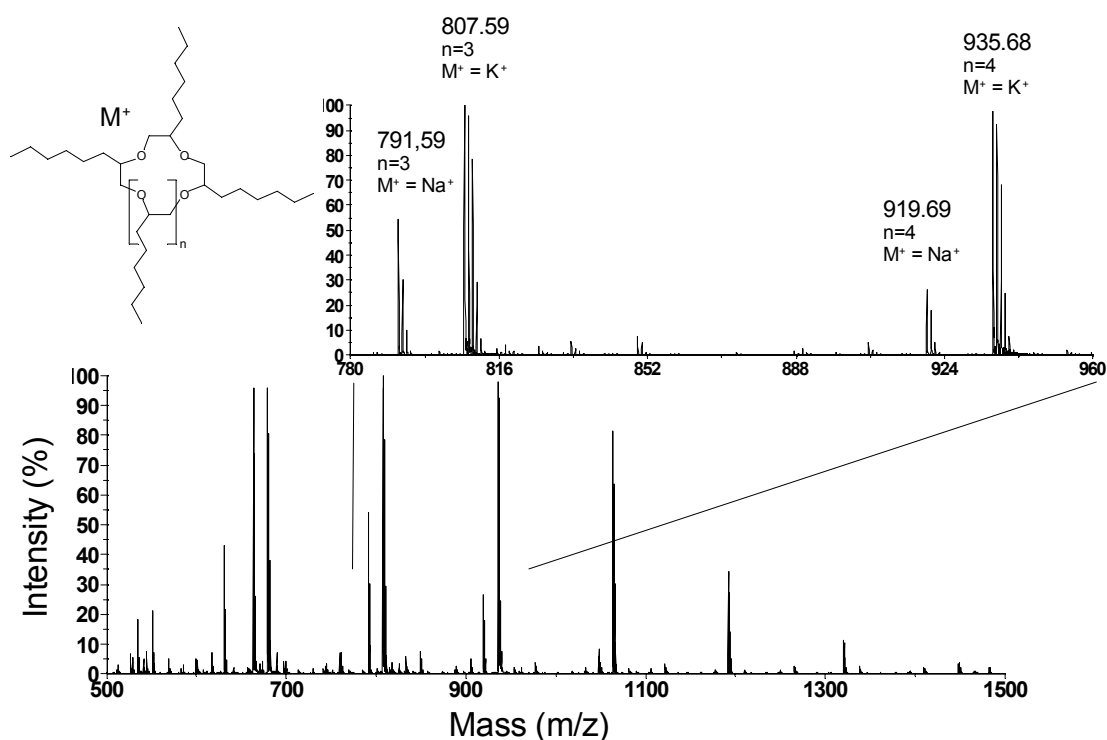
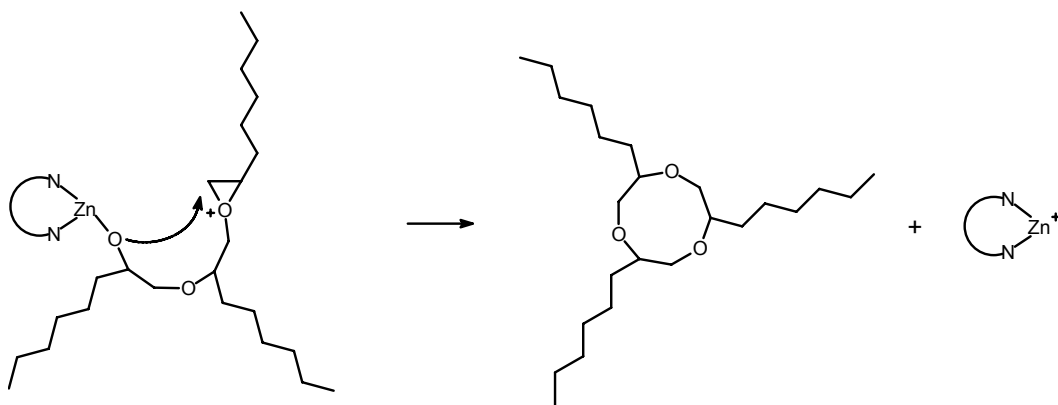


Figure 5-11. MALDI-ToF-MS spectrum of the polyether formed in entry 1, Table 5-9.

Interestingly, MALDI-ToF-MS analyses of the low molecular weight part of the polyether formed in entry 1 (Table 5-9) revealed the formation of cyclic ethers, and up to eight repeating units in a ring could be distinguished. Similar formation of cyclic polyethers, by cationic ROP by iodonium salts, was previously reported by Lie et al.¹¹ A possible mechanism for the formation of these macrocycles is shown in Scheme 5-5. The greater stability of the zinc cation in comparison to an alkyl cation is most likely the reason that the backbiting occurs at the zinc initiator site instead of randomly in a chain. This also explains the formation of only low molecular weight macrocycles. With increasing length of the polymer chain the chances of backbiting at the initiator site diminish rapidly.



Scheme 5-5. Possible mechanism for the formation of cyclic polyethers.

These crown ethers are easily cationized by potassium and sodium ions as can be seen in Figure 5-11. The large discrepancies in the observed molecular weights found with SEC and MALDI could be explained by the difference in ease of ionization between linear and cyclic polyethers. In Figure 5-12 a high molecular weight section of the same spectrum as shown in Figure 5-11 is displayed. Although the absolute intensities of these peaks are much lower than in Figure 5-11, this is probably the main distribution of polymer as was observed by SEC. This multitude of peaks, however, proved to be difficult to analyze and no satisfying microstructures could be assigned.

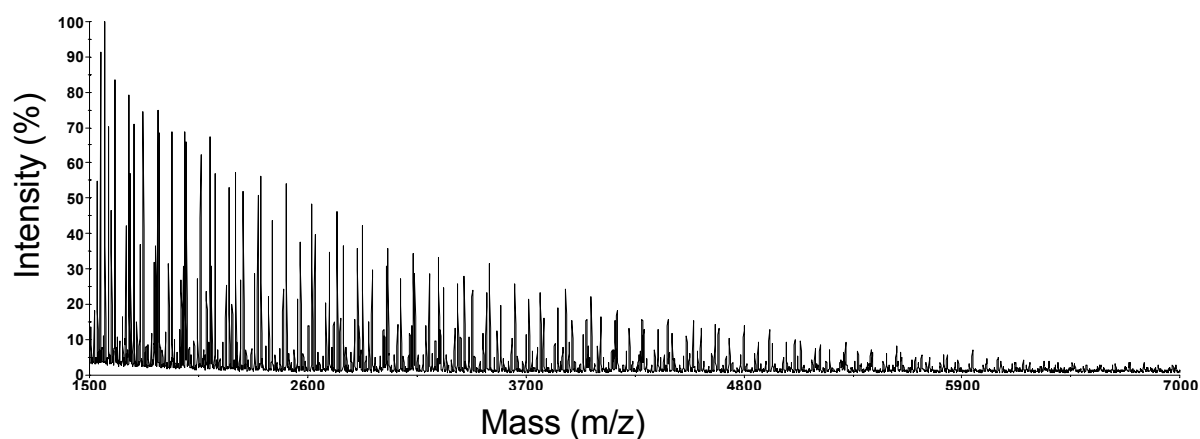


Figure 5-12. High molecular weight fraction of polyether from entry 1, Table 5-9 (see also Figure 5-11).

MALDI-ToF-MS analyses of the polymers obtained from entries 2 and 3 (Table 5-9) were not successful. The highly apolar linear polyethers¹² of monomer **9** and **10** are probably much harder to ionize and no suitable spectra could be obtained. ¹H NMR analyses, however, show the highly characteristic broad methine and methylene peaks for polyethers in the region between 3.5 and 4 ppm.

The polymer obtained from the NMR-tube copolymerization of monomer **9** and CO₂ was also analyzed by MALDI-ToF-MS and the spectrum is shown in Figure 5-13. From the mass of the repeating unit of 172 g · mol⁻¹, which corresponds to octene carbonate unit, it is obvious that an alternating copolymer is formed. Interestingly, the MALDI-ToF-MS spectrum also shows that the actual structure consists of a coupling product of two individual chains. This coupling was also observed for the NMR-tube copolymerization of CHO with CO₂ (Chapter 4, paragraph 4.2.5) with the same β -diketiminato zinc catalyst. The octene oxide analogues of the other polymer structures associated with the coupling mechanism (Scheme 4-4, structure D with loss of one CO₂ moiety and structure E) can be observed in Figure 5-13 although the resolution is too low for an accurate peak assignment. Since the coupling product is already found at relatively low conversions, the coupling

reaction is presumably faster, relative to the propagation reaction, than observed with the CHO/CO₂ copolymerization.

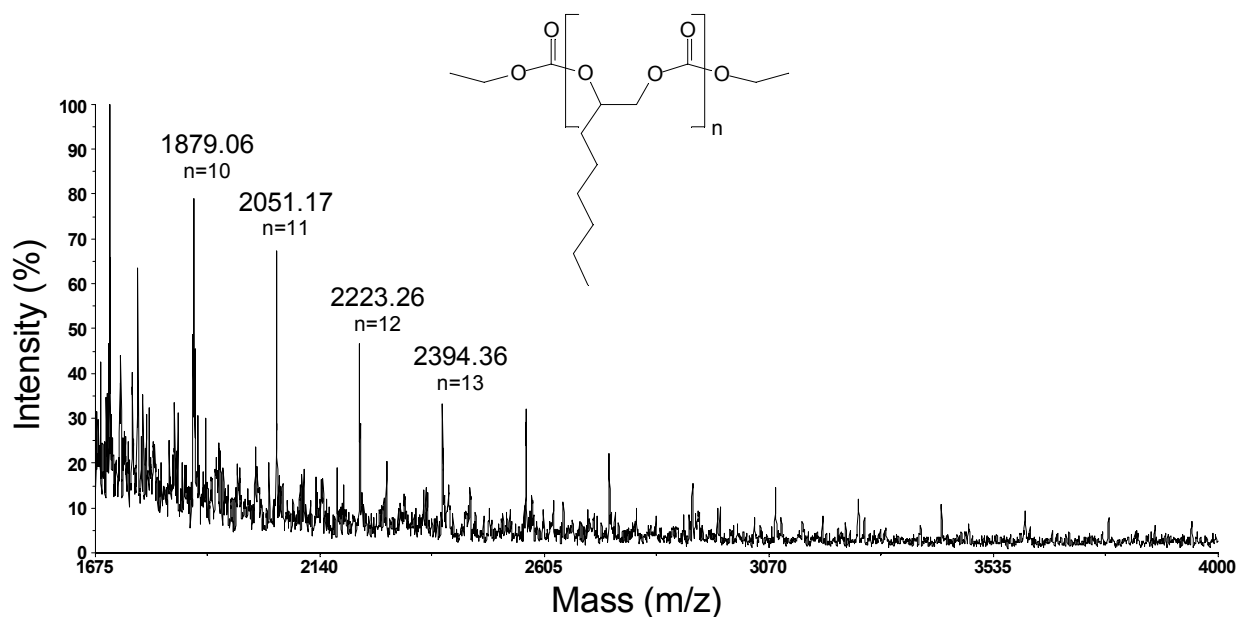


Figure 5-13. MALDI-ToF-MS spectrum of the polymer obtained in entry 4, Table 5-9 (cationization ion: K⁺).

5.3 Concluding remarks

Searching for alternative oxiranes for the production of aliphatic polycarbonates is a challenging task. The special electronic and steric properties of cyclohexene oxide make it a special and very suitable bis-1,2-substituted epoxide monomer for the copolymerization with CO₂. Small variations in the ring size were found to have a large negative influence on activity and selectivity. The 4-ester functionalized CHO monomers could be copolymerized with CO₂ using the β -diketiminato zinc catalysts under relatively mild conditions, but side reactions with the functional groups limited the molecular weights that could be obtained. These side reactions led to the formation of loops (or rings) as was seen by MALDI-ToF-MS spectra. The amide functionalized monomers were more difficult to purify and traces of *m*-chlorobenzoic acid led to a substantial amount of side-initiation. Also, the poor solubility of the amide functionalized monomers inhibited their practical use. The low molecular weights and the difficulty of isolating the polymers (no suitable solvent mixture for precipitation was found) implied that testing of actual physical properties was not possible.

As a proof of concept some long alkyl chain modified epoxides were homo and copolymerized with different catalysts leading to interesting polymer microstructures. When octene oxide was cationically homopolymerized, the formation of cyclic polyethers was detected. Furthermore, in the copolymerization of octene oxide with CO₂, novel chain coupling was observed

similar to what was found in Chapter 4. MALDI-ToF-MS proved, once again, to be a very good tool in the clarification of polymerization mechanisms.

5.4 Experimental section

5.4.1 Materials

Cyclopentene oxide (> 98%), cyclohexene oxide (98%), cyclooctene oxide (99%), 1-octene oxide (96%) and 1-octadecene oxide (85%) were purchased from Aldrich, dried over CaH₂, distilled and stored under argon on molecular sieves (4Å) in the refrigerator prior to use. Carbon dioxide 99.9993% pure was purchased from HoekLoos and used without further purification. Toluene (AR) and DMF (AR) were dried over an activated alumina column and stored on molsieves (4Å). Dimethylsulfoxide (DMSO, 99.5%) was dried over CaH₂ and distilled. 3-cyclohexene-1-carboxylic acid (> 98%) was bought from TCI Europe. 5,10,15,20-Tetraphenylporphyrine (TPPH₂, > 97%) was purchased from Aldrich and chromium(II)chloride (~ 90%) from VWR. Catalysts **11**¹³ and **13**¹⁴ were prepared according to literature methods. Catalyst **12** was prepared according to a slightly modified literature procedure as shown below.¹⁵ All other compounds and solvents were used without further purification.

5.4.2 Analytical techniques.

¹H NMR spectra were recorded on a Varian Gemini 2000 (300 MHz) and a Varian Mercury Vx (400 MHz) spectrometer. Size Exclusion Chromatography (SEC) traces were recorded on a Waters GPC equipped with a Waters model 510 pump and a model 410 differential refractometer (40 °C). THF was used as the eluent at a flow rate of 1.0 mL · min⁻¹. A set of two linear columns (Mixed C. Polymer Laboratories, 30 cm, 40 °C) was used. Molecular weights were calculated relative to polystyrene standards. Data acquisition and processing was performed using Waters Millennium32 software. THF was filtered twice (0.2 μ filter) and stabilized with BHT (4-Me-2,6-(*t*-Bu)₂C₆H₂OH). MALDI-ToF-MS analysis was carried out on a Voyager DE-STR from Applied Biosystems. The matrix, DCTB (*trans*-2-[3-(4-*t*-butylphenyl)-2-methyl-2-propenylidene]malononitrile) was synthesized according to literature procedures.¹⁶ Potassium trifluoroacetate (Aldrich, > 99%) was added to the polymer samples as cationization agent. The matrix was dissolved in THF at a concentration of 40 mg · mL⁻¹. The potassium trifluoroacetate was added to THF at a typical concentration of 1 mg · mL⁻¹. The polymer samples were dissolved in THF at approximately 1 mg · mL⁻¹. In a typical MALDI-ToF-MS analysis the matrix, potassium trifluoroacetate and the polymer solution were premixed in a ratio of 10:1:5. The premixed solutions

were hand-spotted on the target well and left to dry. Spectra were recorded in both the linear and reflector mode.

5.4.3 *Synthesis of 5,10,15,20-tetraphenylporphyrine chromium chloride (TPPCrCl, 12)*

Under argon a solution of 5,10,15,20-tetraphenylporphyrine (TPPH₂) (5 g, 8.1 mmol) and CrCl₂ (4 g, 32.5 mmol) in dimethylformamide (DMF, 100 mL) was refluxed for 3 hours. Next, the solution was allowed to cool to room temperature, opened to the air and allowed to stir overnight. The mixture was poured into water (200 mL) and solid impurities were removed by filtration. The TPPCrCl was separated from the residual chromium salts by extraction with diethylether (500 mL). The water layer was washed three times with diethylether (100 mL) and afterwards the combined organic layers were washed two times with brine (50 mL). The diethylether was removed by evaporation and the residual green solid was redissolved in a small amount of acetone. TPPCrCl was separated from TPPH₂ by chromatography over a column containing activated Al₂O₃, basic Brockmann I standard grade. First DCM was used as eluent to remove traces of TPPH₂. Switching to ethanol yielded the TPPCrCl. Yield: 4.8 g (6.85 mmol, 84%)

5.4.4 *Synthesis of cycloheptene oxide (3)*

Phthalic anhydride (296.2 g, 2.00 mol) was heated to 140°C before cycloheptanol (152.3 g, 1.33 mol) was added dropwise. During this addition the formed cycloheptene was immediately isolated by distillation. Cycloheptene (50.0 g, 0.52 mol) was dissolved in DCM (100 mL) and cooled down to 0°C. A solution of *m*-chloroperbenzoic acid (125.6 g, 0.55 mol) in DCM (800 mL) was added dropwise while keeping the temperature below 10°C. The mixture was stirred for 2 days at room temperature and the solids were removed by filtration. The filtrate was then washed with Na₂S₂O₃ (2 x 100 mL, 10% solution in water), NaHCO₃ (2 x 100 mL, 10% solution in water) and brine (100 mL). The solvents were removed on a rotary evaporator and the obtained product was further purified by distillation. The product was dried over CaH₂, distilled and stored under argon on molecular sieves (4 Å). Yield: 55.0 g (93%, 0.48 mol). ¹H NMR (300 MHz, CDCl₃): δ = 3.03 (br, 2H, *CHOCH*), 0.7-2.1 (br, multiple peaks, 10H, *CH*₂). ¹³C NMR (75 MHz, CDCl₃): δ = 55.92 (*CHOCH*), 30.91, 28.90, 24.33 (*CH*₂).

5.4.5 Synthesis of 3,4-cyclohexene-oxide-1-carboxylic acid methyl ester (5)

3-Cyclohexene-1-carboxylic acid (125 mL, 1.09 mol) and 2 drops of H₂SO₄ were dissolved in MeOH (200 mL) and refluxed overnight. The solvent was removed by distillation and 1,3-cyclohexene-1-carboxylic acid (50.0 g, 0.36 mol) was dissolved in DCM (150 mL) and cooled down to 0°C. A solution of *m*-chloroperbenzoic acid (86.0 g, 0.37 mol) in DCM (600 mL) was added dropwise while keeping the temperature below 10°C. The mixture was stirred for 2 days at room temperature and the solids were removed by filtration. The filtrate was then washed with Na₂S₂O₃ (2 x 100 mL, 10% solution in water), NaHCO₃ (2 x 100 mL, 10% solution in water) and brine (100 mL). The solvents were removed on a rotary evaporator and the obtained product was further purified by distillation. The product was dried over CaH₂, distilled and stored under argon on molecular sieves (4 Å). Yield: 47.1 g (84%, 0.30 mol). ¹H NMR (300 MHz, CDCl₃): δ = 3.65 (s, 3H, CH₃), 3.22, 3.14 (m, 2H, CHOCH), 2.49 (m, 1H, CHCO₂), 1.33-2.29 (m, 6H, CH₂). ¹³C NMR (75 MHz, CDCl₃): δ = 175.0 (CON), 51.42, 50.59 (CHOCH), 50.98 (CH₃), 35.15 (CHCON) 26.66, 22.33, 22.25 (CH₂).

5.4.6 Synthesis of 3,4-cyclohexene-oxide-1-carboxylic acid phenyl ester (6)

A solution of phenol (44.7 g, 0.475 mol) in DCM (100 mL) was added to a solution of 3-cyclohexene-1-carboxylic acid (50.0 g, 0.396 mol), dicyclohexylcarbodiimide (DCC) (122.67 g, 0.595 mol) and 4-*N,N*-6,7-dimethylaminopyridinium toluene-*p*-sulfonate (DPTS, 12.0 g, 0.040 mol) in DCM (400 mL). The mixture was stirred over night at room temperature. Next, the solution was concentrated under reduced pressure, dissolved in AcOEt and filtered through a Celite pad. The filtrate was evaporated and subjected to column chromatography on silica gel with a AcOEt:heptene eluents (2:9) to yield the 3,4-cyclohexene-oxide-1-carboxylic phenyl ester. 60.0 g (0.298 mol) of the ester was redissolved in DCM (150 mL) and cooled down to 0°C. Slowly a solution of *m*-chloroperbenzoic acid (86.0 g, 0.37 mol) in DCM (600 mL) was added dropwise while keeping the temperature below 10°C. The mixture was stirred for 2 days at room temperature and the solids were removed by filtration. The filtrate was then washed with Na₂S₂O₃ (5 x 100 mL, 10% solution in water), NaHCO₃ (5 x 100 mL, 10% solution in water) and brine (3 x 100 mL). The solvents were removed on a rotary evaporator and the obtained product was further purified by distillation. The product was dried over CaH₂, distilled and stored under argon on molecular sieves (4 Å). Yield: 38.2 g (59%, 0.175 mol). ¹H NMR (300 MHz, CDCl₃): δ = 3.65 (s, 5H, Ph-*H*), 3.22, 3.14 (m, 2H, CHOCH), 2.49 (m, 1H, CHCO₂), 1.33-2.29 (m, 6H, CH₂). ¹³C NMR (75 MHz, CDCl₃, mixture of isomers): δ = 173.63, 172.94 (CON), 150.55, 150.45 (Ph-C-OCO), 129.13, 129.00, 125.52, 125.46,

121.24, 121.17 (PhC), 51.79, 51.40, 51.06, 50.45 (CHOCH), 37.37, 35.78 (CHCOO) 26.86, 26.12, 23.24, 22.58, 22.47, 20.75 (CH₂).

5.4.7 Synthesis of *N*-isopropyl-3,4-epoxy-cyclohexyl-1-carboxamide (7)

3-Cyclohexene-1-carboxylic acid (100 g, 0.8 mol) was dissolved in DCM and a 5-fold excess of thionyl chloride (287 mL, 4 mol) was slowly added. The mixture was stirred at room temperature for 5 hours before the excess of thionyl chloride and solvent was removed by applying vacuum. The remaining liquid was redissolved in DCM and cooled to 0 °C before slowly isopropyl amine (200 mL, 2.33 mol) was added. The precipitated isopropyl amine·HCl salt was removed by filtration and the volatiles were removed by applying vacuum. About 100g (0.60 mol) of the amide was redissolved in DCM (500 mL) and the solution was cooled to 0°C. Slowly a solution of *m*-chloroperbenzoic acid (140 g, 0.814 mol) in DCM (1400 mL) was added dropwise, while keeping the temperature below 10 °C. Under stirring the mixture was allowed to warm up to room temperature and left for 5 hours. After the reaction was completed, the suspension (3-chlorobenzoic acid) was filtered off. The DCM solution was washed with Na₂S₂O₄ (100 mL, 10% solution in water) to reduce residual peroxides. Next, the solution was washed with NaHCO₃-solution (5 x 100 mL, 10% solution in water) and triethylamine-solution (3 x 50 mL, 2% solution in water) to remove residual 3-chlorobenzoic acid. The solvents were removed by rotary evaporation yielding a yellow solid which was washed with diethyl ether, resulting in a white powder. Yield: 25%. ¹H NMR (300 MHz, DMSO-d₆): δ = 1.04 (d, 6H, CH(CH₃)₂), 1.9-2.1 (m, 6H, CH₂), 2.3 (m, 1H, CHCO₂), 3.1 (dt, 2H, CHOCH), 3.7 (m, 1H, CH(CH₃)₂), 5.7 (s, 1H, NH). ¹³C NMR (75 MHz, DMSO-d₆): δ = 173.3 (CON), 64.82 (NCH(CH₃)₂), 50.87, 49.94 (CHOCH), 38.56 (CHCON) 25.87, 24.01, 21.69 (CH₂), 22.26 (CH(CH₃)₂).

5.4.8 Synthesis of *N*-phenyl-3,4-epoxy-cyclohexyl-1-carboxamide (CHO-Ph-amide, 8)

Monomer **8** was prepared by a similar procedure as used for the monomer **7**. Yield: 20%. ¹H NMR (300 MHz, DMSO-d₆): δ = 1.9-2.1 (m, 6H, CH₂), 2.3 (m, 1H, CH), 3.1 (dt, 2H, CHOCH), 7.3 (m, 1H, Ph-*H*), 7.6 (m, 1H, Ph-*H*), 7.8 (m, 1H, Ph-*H*), 7.9 (m, 1H, Ph-*H*), 8.1 (m, 1H, Ph-*H*), 9.3 (s, 1H, NH).

5.4.9 *Example of a NMR-tube reaction*

NMR tube reactions were performed in 3/8" SS-316 tubes equipped with a needle valve. An NMR-tube was filled with a solution of monomer **7** (33 mg, 180 μmol), catalyst **12** (15 mg, 21 μmol) and DMAP (13 mg, 107 μmol) in CDCl_3 (0.5 mL) and was sealed in the tube and put under pressure. The whole tube was put in an oven set to the desired temperature and left overnight.

5.4.10 *Example of a typical polymerization using β -diketiminato zinc catalysts*

The catalyst (295 μmol , 0.06 mol-%) was dissolved in a mixture of CHO (50 mL, 495 mmol) and toluene (16.7 mL). After complete dissolution of the catalyst, the mixture was injected into a preheated (50°C) autoclave that was previously dried under vacuum at 100 °C for 12 hours. The autoclave was pressurized to 9 bar with carbon dioxide and the polymerization started. The samples were analyzed by ^1H NMR (300 MHz, CDCl_3) to determine the conversion by integration of the methine peaks in the ^1H NMR spectra: ^1H NMR (300 MHz, CDCl_3): δ 4.65 (br, CH (PCHC), 2H), 3.11 (s, CH (CHO), 2H). The samples for SEC analyses were prepared as follows: About 0.5 mL of each of the reaction mixtures was added dropwise to a tenfold excess of petroleum-ether (40-70) upon which the poly(cyclohexene carbonate) (PCHC) precipitated. After separation and drying (vacuum, 18 h, 60°C), the polymer was redissolved in the SEC eluent THF. Polymer samples for MALDI-ToF-MS analyses were prepared in a similar manner.

5.4.11 *Example of a typical polymerization using the bis(phenoxy) zinc catalyst*

After injection of a mixture of cyclohexene oxide (15 mL), toluene (35 mL) and the catalyst (100 mg, 300 μmol) into the reactor, the reactor was heated to 30 °C and pressurized to 50 bar with carbon dioxide. All valves were closed and the reactor was further heated to 80 °C, resulting in a pressure of about 80 bar. Analyses and work-up procedures were similar as described above.

5.5 Acknowledgements

Latifa Yajjou en Rob Verlinden are kindly acknowledged for their contribution to this chapter. Prof.dr. Manfred Bochmann is kindly acknowledged for providing the cationic zinc initiator.

5.6 References

- 1 See for example: a) Scrivani, T.; Benavente, R.; Prez, E.; Perea, J. M. *Macromol. Chem. Phys.* **2001**, *202*, 2547. b) Shin, J. Y.; Park, J. Y.; Liu, C.; He J.; Kim, S.C. *Pure Appl. Chem.* **2005**, *77*, 801.
- 2 (a) U.S. Pat. US3409565 to Lal, J., Goodyear Tire & Rubber Company (1968). (b) Lal, J.; Trick, G. S. *J. Polym. Sci.; Part A-1* **1970**, *8*, 2339. (c) U.S. Pat. US3509068 to Lal, J., Goodyear Tire & Rubber Company (1970).
- 3 Bacskai, R. *J. of Polym. Sci.: Part A* **1963**, *1*, 2777 .
- 4 Darensbourg, D. J.; Fang, C. C.; Rodgers, J. L. *Organometallics* **2004**, *23*, 924 .
- 5 Rieth, L. R.; Moore, D. R.; Lobkovsky, E. B.; Coates, G. W. *J. Am. Chem. Soc.* **2002**, *124*, 15239 and references therein.
- 6 Polymerization conditions: 141 mg (300 μ mol) of EtBDIZnOEt / 15 mL of CHO / 35 mL of toluene / 50 °C. After 3 hours 10 equivalents phenol (3 mmol) was added in 10 mL of toluene and the polymerization was continued for another 15 hours.
- 7 Koning, C. E.; Wildeson, J.; Parton, R.; Plum, B.; Steeman, P.; Darensbourg, D. J. *Polymer* **2001**, *42*, 3995.
- 8 Polymerization conditions: 141 mg (300 μ mol) of EtBDIZnOEt / 15 mL of CHO / 1 g (8.84 mmol) of caprolactam / 35 mL of toluene / 50 °C / 3 hours. Conditions: 9 bar, 2 h, 50 °C. Result: almost no polymer (less than 2%).
- 9 Conditions: Monomer **7** (17 mg, 95 μ mol) and 3-chlorobenzoic acid (70 mg, 450 μ mol) was dissolved in 0.5 mL of CDCl₃.
- 10 Initiator was prepared in the group of Manfred Bochmann in the University of East Anglia, Norwich, UK. Details about the preparation are currently unknown to us.
- 11 Liu, B.; Chen, L.; Zhang, M. Yu, A. *Macromol. Rapid Commun.* **2002**, *23*, 881.
- 12 Ring formation with butyl anion initiating groups is very unlikely.
- 13 Cheng, M.; Moore, D. R.; Reczek, J. J.; Chamberlain, B. M.; Lobkovsky, E. B.; Coates, G. W. *J. Am. Chem. Soc.* **2001**, *123*, 8738.
- 14 Darensbourg, D. J.; Wildeson, J. R.; Yarbrough, J. C.; Reibenspies, J. H. *J. Am. Chem. Soc.* **2000**, *122*, 12487.

- 15 Mang, S.; Cooper, A. I.; Colclough, M. E.; Chauhan, N.; Holmes, A. B. *Macromolecules* **2000**, *33*, 303.
- 16 (a) Ulmer, L.; Mattay, J.; Torres-Garcia, H. G.; Luftmann, H. *Eur. J. Mass Spectrom.* **2000**, *6*, 49-52. (b) Brown, T.; Clipston, N. L.; Simjee, N.; Luftmann, H.; Hungerbühler, H.; Drewello, T. *Int. J. Mass Spectrom.* **2001**, *210/211*, 249.

Chapter 6

Physical properties of compression molded parts and coatings of aliphatic polycarbonates

Abstract

In this chapter several thermal and physical properties of two poly(cyclohexene carbonate) (PCHC) samples with different molecular weight distributions are discussed and compared to a commercial grade of poly(bisphenol-A carbonate) (BA-PC). The T_g and thermal stability of PCHC was much lower than BA-PC, but with respect to the modulus, scratch resistance and UV absorption, PCHC performed much better. Since these properties are especially interesting for coating applications, high molecular weight PCHC was degraded with a triol. The thus obtained low molecular weight PCHC was successfully cured with a caprolactam blocked triisocyanate on an aluminum substrate. Although the formulation needs to be improved, the initial results for these coatings look promising.

6.1 Introduction

Aliphatic polycarbonates are a relatively new and unexplored group of polymers with respect to potential industrial applications. One application area where aliphatic polycarbonates are currently of commercial importance is their use as sacrificial polymers in for example the production of microchannels.¹ Since poly(cyclohexene carbonate) is a brittle polymer, for the moment, it is of limited use as far as engineering plastics are concerned. Several studies have been undertaken to determine the shear rheology and the thermal and physical properties of a range of aliphatic polycarbonates.² Between the different aliphatic polycarbonates a large difference exists in their physical properties. For example, the T_g of poly(ethylene carbonate) (PEC) is below room temperature ($\pm 10^\circ\text{C}$) and at room temperature it behaves like an elastomer.^{2b} Poly(cyclohexene carbonate) (PCHC), on the other hand, has a T_g above 116°C and is, at room temperature, deep in the glassy state. This makes PCHC very brittle with a tensile strain at break of only 0.5% in contrast to tensile strain at break (at room temperature) of over 600% for PEC.^{2b} What has not been discussed in the literature is the effect of large differences in molecular weight distributions between structurally similar, but differently prepared polymers. In our studies, we looked at the differences

in T_g , modulus and yield stress between two compression molded PCHC samples, only differing in molecular weight distribution. For comparison, a sample of poly(bisphenol-A carbonate) (BA-PC) was analyzed in the same way. Finally, a preliminary investigation of the properties of PCHC-based coatings was performed.

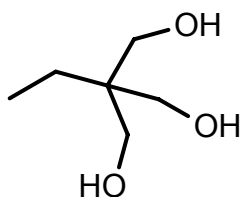
6.1.1 *Brittle versus tough behavior in polymers.*

All amorphous polymers are intrinsically tough as long as the polymeric chains are sufficiently long to make a substantial physical network of entanglements.³ On a macroscopic scale, however, strain softening can make polymers brittle when it occurs locally. For instance poly(bisphenol-A carbonate) behaves brittle when there is a notch or scratch at the stressed area. This results in local strain softening and failing of the entire sample (it breaks at the location of the notch or scratch). With tough polymers, after the initial strain softening, strain hardening of the polymer prevents the spreading of local defect. In the case of PCHC the \bar{M}_e or mass between entanglements was determined to be around $15,000 \text{ g} \cdot \text{mol}^{-1}$ indicating a rather stiff chain compared to BA-PC (\bar{M}_e is ca. $1,800 \text{ g} \cdot \text{mol}^{-1}$).^{2a} An \bar{M}_e of $15,000 \text{ g} \cdot \text{mol}^{-1}$ is quite high as the best physical properties are achieved if the \bar{M}_w is about 6-7 times larger as the \bar{M}_e . Only then, a sufficiently strong network of physical crosslinks is obtained. Most PCHC polymers obtained with the currently known catalysts, however, have \bar{M}_w values that are too low to achieve such a strong network (see chapter 2). Consequently, the strain at break for these PCHC samples is as low as 0.5%. Since for PCHC the yield point in a tensile test is located at higher strains than 0.5%, it is difficult to obtain the information about the strain hardening after the yield point has been reached. Hence, to get a somewhat better understanding of the brittle behavior of PCHC, several compression tests were performed, which usually provide more insight in post-yield stress-strain behavior.

6.1.2 *Poly(cyclohexene carbonate) for coating applications*

A possible alternative application area for aliphatic polycarbonates is their use in coatings. To investigate this potential, several coatings were prepared from poly(cyclohexene carbonate) and their properties are discussed. In order to be able to crosslink a certain polymer, at least two functional crosslinkable groups per molecular chain are required and the chains should not be too long ($\bar{M}_n \pm 3000 \text{ g} \cdot \text{mol}^{-1}$). For poly(cyclohexene carbonate), the functionality can only be achieved via the chain ends and as could be seen in chapter 3, after copolymerization of CHO with CO_2 most polymers have only one functional end group (OH). To introduce a higher degree of

functionality, high molecular weight PCHC was degraded in the presence of a triol (trimethylolpropane, Scheme 6-1).



Scheme 6-1. Trimethylolpropane used for the introduction of more functional groups.

Subsequently the functionalized PCHC polymer chains were cured with the crosslinking agent Vestagon B1530 and some properties of the cured coatings were tested.

6.2 Results and discussion

6.2.1 Properties of poly(cyclohexene carbonate)

Two types of poly(cyclohexene carbonate) samples were tested. The first sample has a very narrow distribution (PDI = 1.12) and was prepared with a β -diketiminato zinc catalyst. The second type has a very broad molar mass distribution (PDI = 9.65) and was prepared with a bis(phenoxy) zinc catalyst. The effect of this difference in molar mass distribution and PDI was investigated and the properties were compared to those of a BA-PC reference sample. A summary of the used samples and the used labeling system is displayed in Table 6-1.

Table 6-1. Sample information.

Polymer	Sample name of the polymer powder	Sample name of compression molded sample ^{b)}	\bar{M}_n (g · mol ⁻¹) ^{c)}	\bar{M}_w (g · mol ⁻¹) ^{c)}	\bar{M}_w / \bar{M}_n
PCHC	A	A'	27,300	30,660	1.12
PCHC	B	B'	20,880	201,390	9.65
poly(bisphenol-A carbonate) ^{a)}	C	C'	9,800 ^{d)}	20,790 ^{d)}	2.12

a) Grade PC-175 obtained from GE Advanced Materials (used in the production of Lexan® BA-PC). b) See paragraph 6.2.1.3 for preparation details. c) PS equivalents. d) Mark-Houwink parameters used: $a=0.67$ $K=4.9 \cdot 10^{-4}$ dL · g⁻¹.

6.2.1.1 Thermal properties

Since the glass transition temperatures (T_g) previously reported in literature were often based on polymer samples with very broad molecular weight distributions, the effect of the low molecular

weight samples on the T_g was investigated. The DSC thermograms for samples A, B and C are shown in Figure 6-1 and show only a marginal difference between the samples A and B with sample A having a slightly higher T_g than sample B. The observed value for BA-PC (sample C) is slightly lower than reported literature values for BA-PC. This can be understood, since the molar mass of Sample C is relatively low, whereas the reported literature values usually have been measured on high molar mass BA-PC.

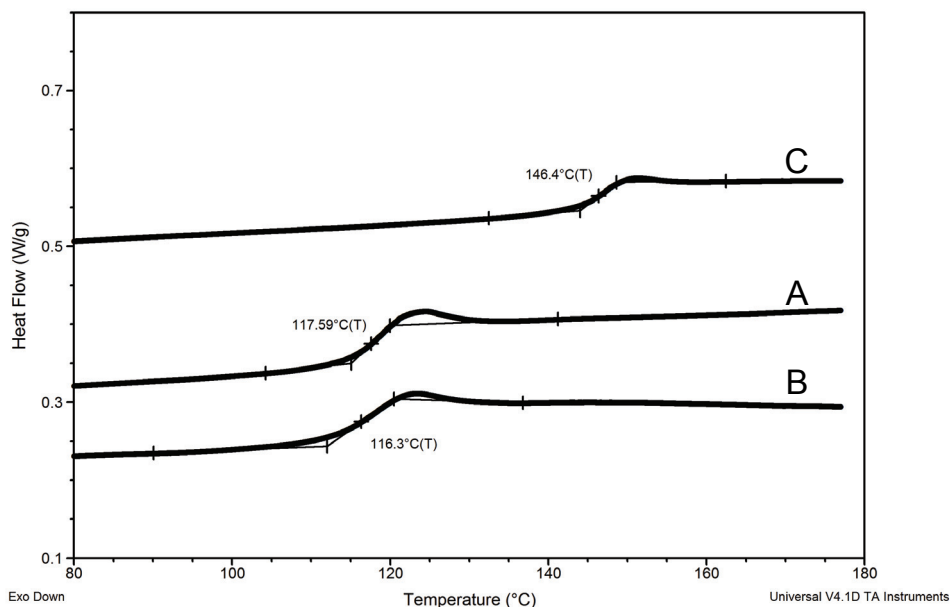


Figure 6-1. DSC curves for samples A, B and C with an offset of 0.1 W/g for the separate thermograms on the Y-axis. T_g values are calculated by the half extrapolated tangents method.

The thermal stability of the polycarbonate samples was measured under nitrogen with TGA and sample A and B both showed a 5% weight-loss around 218°C as can be seen in Figure 6-2. Sample C is much more stable and does not degrade below 350°C.

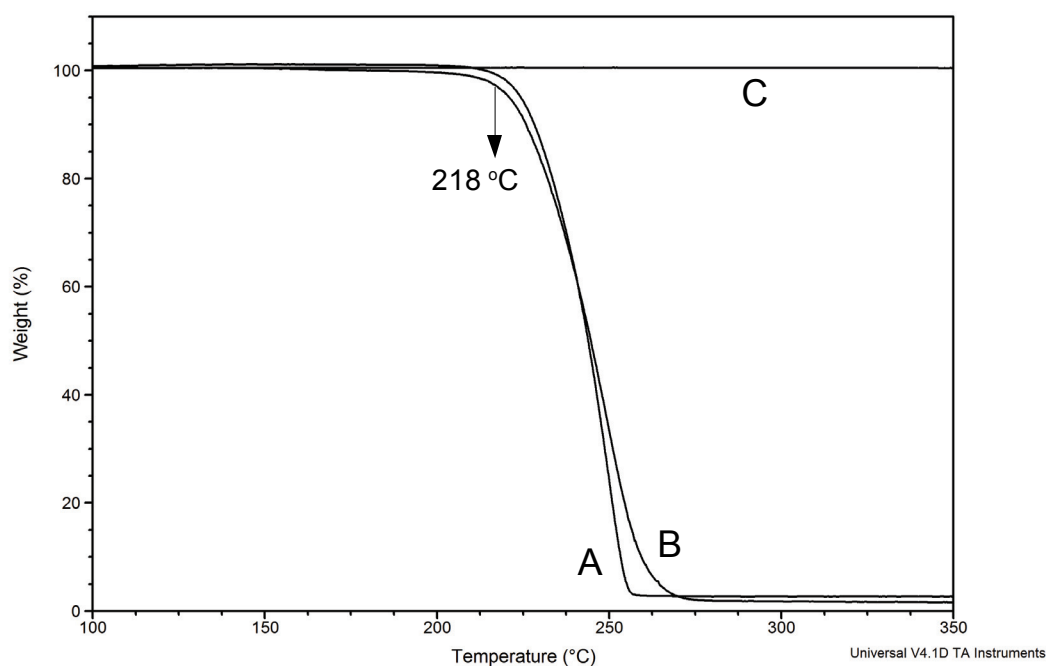
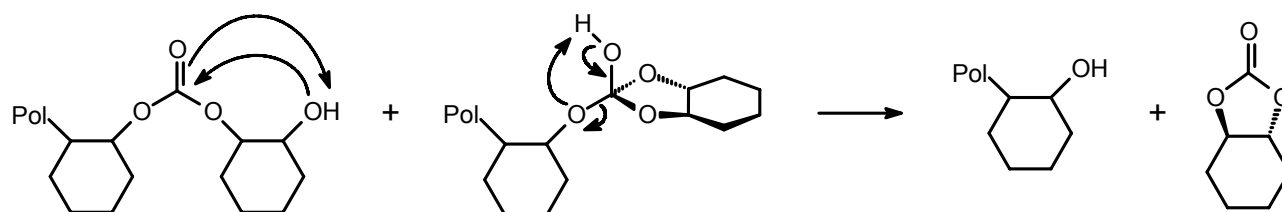


Figure 6-2. TGA curves for samples A, B and C.

Surprisingly, Mang et al. reported a much higher degradation stability of PCHC of up to 280°C.⁴ The lower values found here might be caused by residual catalyst traces, which enhance the degradation of the polymer, as was observed by Liu et al in the case of poly(propylene carbonate).⁵

The normal degradation pathway for PCHC is shown in Scheme 6-2. Backbiting of the alcoholic chain end leads to the formation of cyclic carbonates (see also chapter 2 paragraph 2.4.3). This unzipping process is very efficient so that can be used to obtain cyclic carbonates via distillation in good yield.⁶ During compression molding (paragraph 6.2.1.3) it was also observed that a small amount of CO₂ was liberated, probably by the same chain scission mechanism as described in chapter 3.



Scheme 6-2. Backbiting of the polymer chain end leading to the formation of cyclic carbonates.

6.2.1.2 Miscibility tests between samples B and C.

As already mentioned, a potential application area is in the field of coatings. In view of the modulus,^{2a} the scratch resistance of PCHC is expected to be much better than that of poly(bisphenol-A carbonate). To test the feasibility of having a PCHC coating on a BA-PC substrate, a solvent cast blend (1:1 from DCM) was analyzed by DSC (Figure 6-3), keeping in mind that the T_g values of both polymers are ca. 117°C for PCHC and ca. 146°C for BA-PC, respectively. The softening points of both polymers show only limited signs of convergence with a more pronounced decrease in T_g for sample C than an increase for sample B. Nevertheless, it is obvious that some PCHC is dissolved in the BA-PC phase, and a somewhat smaller amount of BA-PC is dissolved in the PCHC phase. In conclusion we can say that samples B and C are partially miscible, which assures a good adhesion of a PCHC coating on a BA-PC substrate.

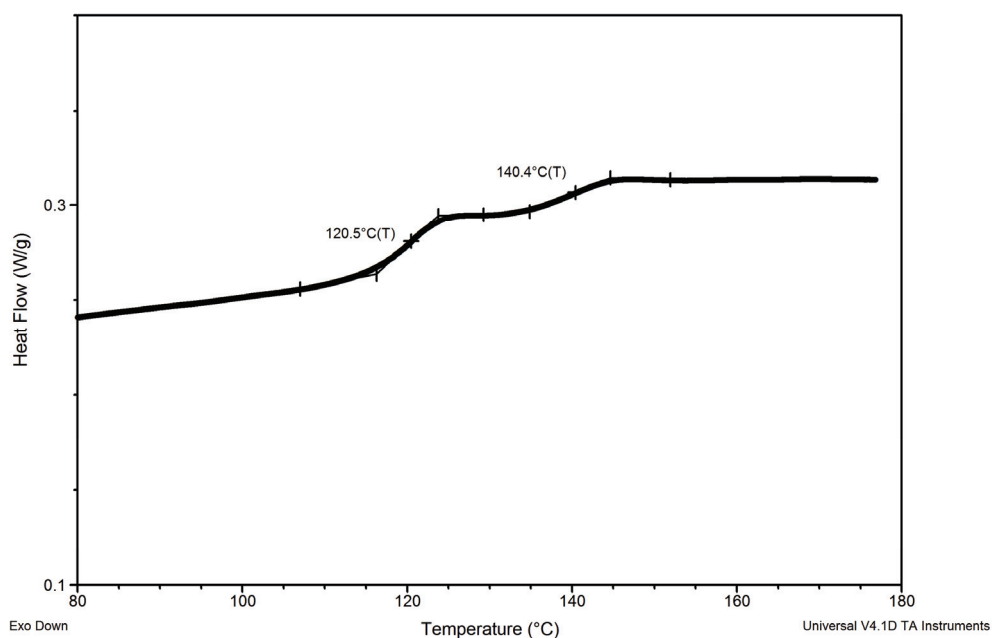


Figure 6-3. DSC analysis of a 1:1 blend of samples B and C.

6.2.1.3 Compression molding

For further testing samples A, B and C were pressed into spherical plates with a diameter of 25 mm and a thickness of 2 mm. Optimal temperature conditions were found at 195°C. It proved difficult to prepare samples A and B completely free of gas bubbles, which were probably formed from the slow thermal degradation of the sample during the molding. Unfortunately, the samples were too brittle for DMA analyses, but it was possible to machine smaller samples for compression tests (paragraph 6.2.1.6).

6.2.1.4 Hardness

The resistance of the molded samples A', B' and C' to indentation was measured with a shore-D indenter test. Although the method is not very accurate, it did indicate a hardness of PCHC similar to poly(bisphenol-A carbonate) as can be seen from Table 6-2.

Table 6-2. Shore-D hardness values.

Sample	Average Shore-D hardness
A'	25
B'	20
C'	25

6.2.1.5 Injection molding

Processing of samples A, B and C was attempted with a mini-injection molding setup (Figure 6-4) manufactured by DSM and located at the University of Liège.⁷ Optimal temperatures were found to be 70°C for the mold and 195°C for the sample compartment. After addition of the polymer sample, the polymer was allowed to melt for 5 minutes before the molten material was injected into the mold with a force of 10 bar.

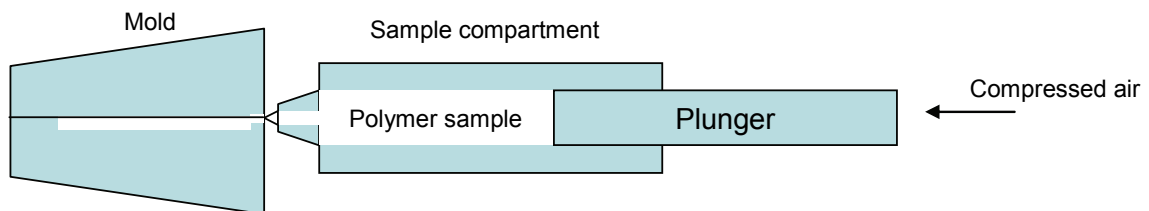


Figure 6-4. Schematic drawing of the used mini-injecting molding setup.

Unfortunately, the removal of the tensile bars from the mold proved extremely difficult due to the brittleness of the material which prevented the successful extraction of the bar without breaking it. Therefore, the modulus of the samples was determined by performing compression tests with samples that could be obtained by compression molding.

6.2.1.6 Compression test

Samples A', B' and C' were subjected to a series of compression tests to determine the modulus and strain hardening behavior. The results are shown in Figure 6-5, with the true strain defined in equation 6.1:

$$\text{True strain} = \ln(\lambda) \quad (6.1)$$

With λ defined as:

$$\lambda = 1 + \varepsilon \quad (6.2)$$

And ε is the strain defined as the displacement (ΔL) divided by the initial length (L_0) of the sample:

$$\varepsilon = \frac{\Delta L}{L_0} \quad (6.3)$$

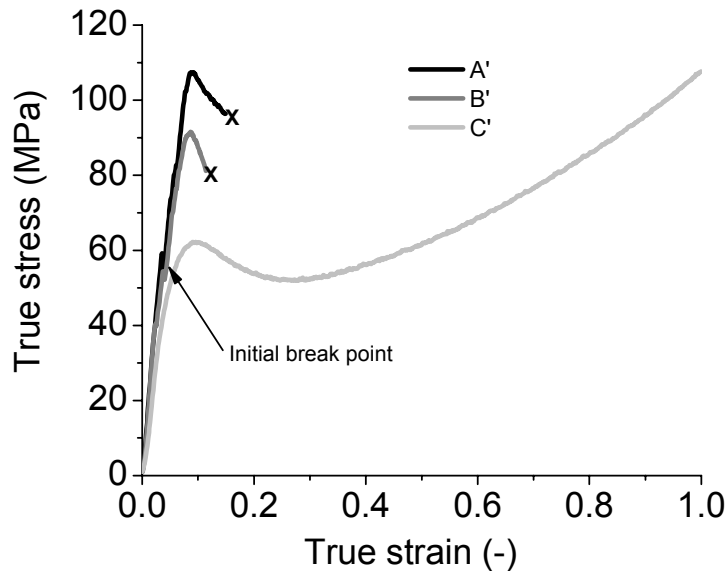


Figure 6-5. Compression tests of samples A', B' and C'.

In view of the steeper initial increase of the true stress with increasing true strain, samples A' and B' seem to have a somewhat higher modulus than the BA-PC sample. This is in agreement with the results reported by Koning et al,^{2a} who determined the moduli of PCHC and BA-PC by tensile tests. The very brittle nature of samples A' and B' is evident from Figure 6-5, which shows that an initial crack is formed around 55 MPa. Sample B' disintegrates at stresses above 90 MPa and sample A' disintegrates at stresses above 105 MPa. The (sharp) tops of the curves in Figure 6-5 do not represent the yield stress but merely the point at which the sample was pulverized. The sample with the narrow molar mass distribution (A') performed somewhat better than the sample with the very broad molecular weight distribution (B'). The Young's modulus can be calculated from the data obtained from the compression tests via equation 6.4.

$$\text{Young's Modulus (GPa)} = \frac{\text{Tensile stress (N/m}^2\text{)}}{\text{Tensile strain}} = \frac{\text{Force (N)} / \text{Area (m}^2\text{)}}{\text{Displacement} / \text{Initial length}} \quad (6.4)$$

For the Young's modulus calculations, a slope of the stress/strain curve of between 1% and 3% strain was used. The results are shown in Table 6-3 and indeed reveal a slightly higher modulus for the PCHC samples (A' and B') as compared to the PC sample (C'). Furthermore, sample A' performed better than B', thereby indicating a pronounced influence of the polymer distribution in favor of the lower polydispersity (Table 6-1). This can be explained by the fact that with a broad molecular weight distribution, the shorter chains cannot participate in the formation of a strong network and will act more as a plasticizer.

Table 6-3. Young modulus determined for samples A', B' and C'.

Sample	Young's Modulus (GPa)
A'	1.82
B'	1.59
C'	1.42

6.2.1.7 UV and Visible light transparency

The mechanical properties of poly(bisphenol-A carbonate) gradually degrade under exposure to sunlight. The absorption of light by the aromatic groups in the UV range leads to a number of reactions including the photo-Fries rearrangement.⁸ Apart from the yellowing effect of the products of these reactions, they also lead to a degradation of \overline{M}_n and \overline{M}_w by chain scission. Poly(cyclohexene carbonate) (sample B) does not have any aromatic groups and, as can be seen from Figure 6-6, the absorption in the UV range is far less than that of poly(bisphenol-A carbonate) (sample C). Accordingly, PCHC is expected to have better transparency and UV/VIS stability than BA-PC, both with respect to mechanical properties and discoloration (yellowing).

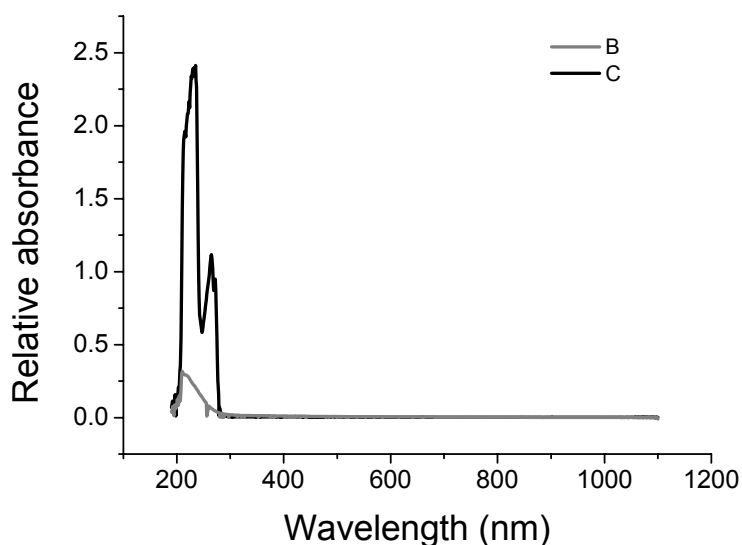


Figure 6-6. UV Spectra of samples B and C.

6.2.2 *Aliphatic polycarbonates for coating applications*

As expected, a preliminary coating test with a non-crosslinked sample A showed very brittle behavior when applied on an aluminum plate and, upon drying, the coating flakes off easily. The polymer samples available had molecular weights too high for effective crosslinking and, as already discussed in paragraph 6.1.2, an average functionality far below 2. To achieve lower molecular weights and to introduce more functionality, the polymers were degraded with a certain amount of trimethylolpropane in the melt at 195°C during a period of a several hours. The degradation process was followed over time by sampling and the decrease of the \bar{M}_n is shown in Figure 6-7. In around ten hours, the \bar{M}_n drops from over 37,000 g · mol⁻¹ to almost 1,000 g · mol⁻¹. Since only three data points were available no attempt was made to fit a kinetic model to the data points.

The more reactive primary alcohols of trimethylolpropane will react faster than the less reactive secondary cyclohexanol species already present as end groups in the PCHC. Subsequently, if an equilibrium is reached, a tripodal structures will be formed with three cyclohexanol end groups and the triol at the junction of the three arms.

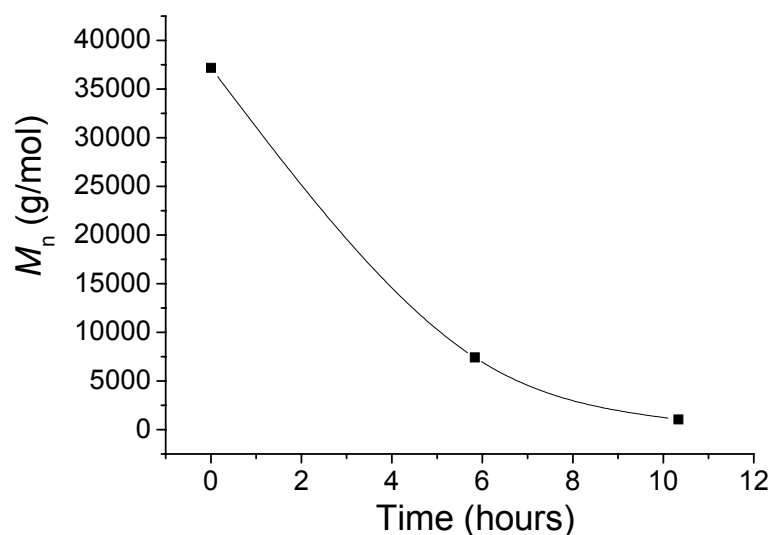


Figure 6-7. Degradation of PCHC sample with trimethylolpropane (the line is a spline interpolation of the sample points for clarification purposes only; The exact kinetics have not investigated)

After determining the OH value of the hydroxyl-functional polymers via titration, they were cured with the conventional polyisocyanate curing agent Vestagon B1530, an ϵ -caprolactam blocked trimer of isophorone diisocyanate (Figure 6-8).

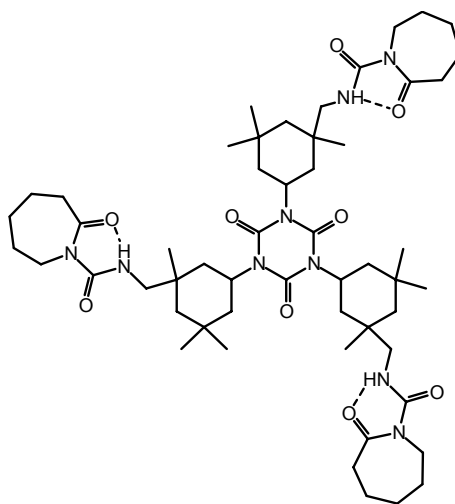


Figure 6-8. Vestagon B1530 crosslinker.

Above 170°C and upon reaction with the OH-functionalized PCHC molecules, ϵ -caprolactam is released and the network is formed (Figure 6-9).

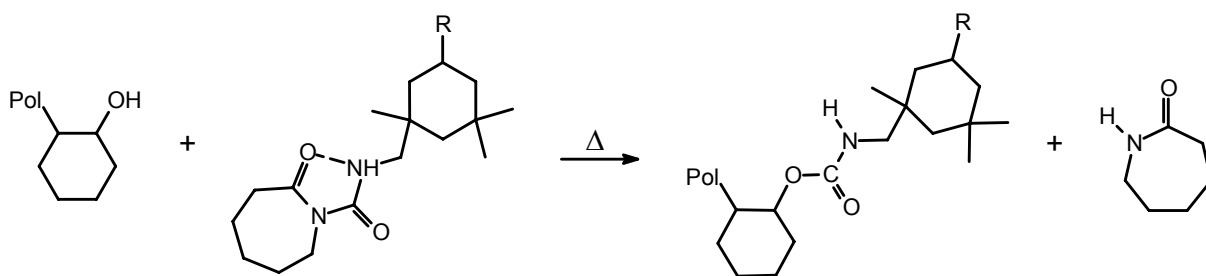


Figure 6-9. Crosslinking reaction of the blocked isocyanide with the polymer hydroxyl chain end.

Several coatings were prepared by solution casting on an aluminum substrate of a solution of PCHC and the crosslinker in NMP. The films were cured for 30 minutes at 200°C, producing a glossy and transparent film. The solvent resistance against acetone was determined to be around 50 double rubs before the coating was visibly damaged by the rubbing, indicating a reasonable solvent resistance. Impact tests and slow deformation tests showed the formation of cracks indicating a less than optimal crosslinking. Obviously, this as well as the solvent resistance can be further improved by optimizing the crosslinking procedure.

6.3 Concluding remarks

It is clear that PCHC cannot face a direct comparison with the commercially available BA-PC in the areas of thermal properties and toughness. The PCHC samples are simply too brittle to be used as engineering plastics without modification. The modulus, which was determined by compression tests, was higher for both PCHC samples than for the BA-PC sample as was the actual yield point (break point in the case of the PCHC samples). Moreover, the PCHC samples are more transparent than the BA-PC samples, especially in the low UV regions. Furthermore, it was possible to simultaneously degrade high molecular weight PCHC down to \bar{M}_n values around 2000-4000 g · mol⁻¹ and to introduce a hydroxyl functionality higher than two of the chains by reacting them with a triol. This allows the application of PCHC as a curable coating, as was demonstrated by the formation of several crosslinked films.

6.4 Experimental section

Analytical techniques.

¹H NMR spectra were recorded on a Varian Gemini 2000 (300 MHz) and a Varian Mercury Vx (400 MHz) spectrometer. Size Exclusion Chromatography (SEC) traces were recorded on a Waters GPC equipped with a Waters model 510 pump and a model 410 differential refractometer

(40 °C). THF was used as the eluent at a flow rate of $1.0 \text{ mL} \cdot \text{min}^{-1}$. A set of two linear columns (Mixed C. Polymer Laboratories, 30 cm, 40 °C) was used. Molecular weights were calculated relative to polystyrene standards. Data acquisition and processing was performed using Waters Millennium32 software. THF was filtered twice (0.2 μ filter) and stabilized with BHT (4-Me-2,6-(*t*-Bu)₂C₆H₂OH). MALDI-ToF-MS analysis was carried out on a Voyager DE-STR from Applied Biosystems. The matrix, DCTB (*trans*-2-[3-(4-*t*-butylphenyl)-2-methyl-2-propenyldene]malononitrile) was synthesized according to literature procedures.⁹ Potassium trifluoroacetate (Aldrich, > 99%) was added to the polymer samples as a cationization agent. The matrix was dissolved in THF at a concentration of $40 \text{ mg} \cdot \text{mL}^{-1}$. The potassium trifluoroacetate was added to THF at a typical concentration of $1 \text{ mg} \cdot \text{mL}^{-1}$. Polymer was dissolved in THF at approximately $1 \text{ mg} \cdot \text{mL}^{-1}$. In a typical MALDI-ToF-MS analysis the matrix, potassium trifluoroacetate and the polymer solution were premixed in a ratio of 10:1:5. The premixed solutions were hand-spotted on the target well and left to dry. Spectra were recorded in both the linear and reflector mode.

Compression tests

Cylindrical samples of approximately 5 mm diameter and 2 mm thickness were machined from a larger compression molded plate and tested on a servo-hydraulic MTS 831 Elastomer system. Samples were compressed at a speed of $10^{-3} \cdot \text{s}^{-1}$.

Determination of thermal properties.

Differential Scanning Calorimetry (DSC) was carried out on a TA Instruments Q100 DSC. Samples (2-5 mg) were heated twice from 50°C to 180°C at a rate of $10^\circ\text{C} \cdot \text{min}^{-1}$ and cooled down at the same rate to 50°C. The second heating cycle was used for data analysis.

Thermogravimetric analysis (TGA). The thermal stability of the polymer was measured using a Perkin-Elmer Pyris 6 TGA. Approximately 10 mg of polymer was heated from 40°C to 350°C at a heating rate of $10^\circ\text{C} \cdot \text{min}^{-1}$ with a N₂ flow of $20 \text{ mL} \cdot \text{min}^{-1}$. The results were analyzed using the Pyris 4.01 software.

UV measurements. UV spectra were recorded on a Hewlett Packard 8453 spectrometer. Spectra were recorded between 190 and 1100 nm. THF was used as a solvent (HPLC grade from Biosolve). Background spectrums were recorded with a sample cell filled with THF.

Degradation experiments

A mixture of PCHC (6 g, $\overline{M}_n = 38,000 \text{ g} \cdot \text{mol}^{-1}$, $1.6 \cdot 10^{-4} \text{ mol}$) and trimethylolpropane (0.26 g, $1.9 \cdot 10^{-3} \text{ mol}$) was heated to 210°C. After a homogeneous mixture was obtained the degradation was continued for 10 hours. During the degradation experiment, evolution and refluxing of a clear colorless liquid was observed (CHC).

Hydroxyl value determination

Approximately 1 g of sample was weighed precisely and dissolved in THF (30 mL). Subsequently, 15 mL of catalyst solution (10 g 4-(dimethylamino)pyridine in 1 L of THF) and 5.00 mL of acetylating solution (100 mL acetic anhydride in 1 L THF, $1.05 \text{ mol} \cdot \text{l}^{-1}$) was added and the solution was swirled and left to react for 15 minutes at room temperature. Then, 10 mL of hydrolysis solution (4 volume parts THF mixed with 1 volume part of water) was added and after complete mixing, the solution was allowed to react for 30 minutes at room temperature, while swirling the flask every 5 minutes. THF (30 mL) was added, after which the solution was potentiometrically titrated with a standard 0.5 M methanolic KOH solution. The device used was a Metrohm Titrino 785 DMP, fitted with an Ag titrode. The measurement was carried out in duplo.

Curing and characterization of coatings.

Curing. A solution of 0.25 – 0.5 g of polycarbonate resin and a 1.05 molar excess of the crosslinker (calculated from $^1\text{H-NMR}$ data) in 1 mL N-methyl-2-pyrrolidone (NMP) was prepared. Subsequently, a film of approximately 250 μm thickness was applied onto an aluminum panel, using a doctor blade. The film was left to dry at room temperature, followed by curing at 200°C during 30 minutes under N_2 flush.

Solvent resistance was determined by rubbing the coating with a cloth drenched in acetone, counting the number of double rubs needed to cause visible damage to the film.

Impact testing was performed according to ASTM norm D 2794-92 (resistance of organic coatings to the effects of rapid deformation).

Slow deformation was tested by the manually bending of the coated aluminum substrate.

6.5 Acknowledgements

Prof. R. Jérôme, Christophe Detrembleur and Jean-Michel Thomassin (Center for Education and Research on Macromolecules (CERM), Liège, Belgium) are kindly acknowledged for their help with the compression molding and injection molding experiments. Leon Govaert is kindly thanked for his help with the compression tests. Bart Noordover is kindly acknowledged for the help with the curing and coating tests.

6.6 References

- 1 Jayachandran, J. P.; Reed, H. A.; Zhen, H.; Rhodes, L. F. Henderson, C. L.; Allen, S. A. B.; Kohl, P. A. *J. Micromechan. Sys.* **2003**, *12*, 147.
- 2 (a) Koning, C. E.; Wildeson, J.; Parton, R.; Plum, B.; Steeman, P.; Darensbourg, D. J. *Polymer* **2001**, *42*, 3995. (b) Thorat, S. D.; Phillips, P. J.; Semenov, V.; Gakh, A. *J. Appl. Pol. Sci.* **2003**, *89*, 1163. (c) Thorat, S. D.; Phillips, P. J.; Semenov, V.; Gakh, A. *J. Appl. Pol. Sci.* **2004**, *93*, 534. (d) Li, X. H.; Meng, Y. Z.; Chen, G. Q.; Li, R. K. Y. *J. Appl. Pol. Sci.* **2004**, *94*, 711.
- 3 Mergler, Y. J.; van Kampen, R. J.; Nauta, W. J.; Schaake, R. P.; Raas, B.; van Greienvsven, J. G. H.; Meesters, C. J. M. *Wear* **2005**, *258*, 915.
- 4 Mang, S.; Cooper, A. I.; Colclough, M. E.; Chauhan, N.; Holmes, A. B. *Macromolecules* **2000**, *33*, 303.
- 5 Liu, B.; Chen, L.; Zhang, M.; Yu, A. *Macromol. Rapid Commun.* **2002**, *23*, 881.
- 6 Heating a poly(cyclohexane carbonate) sample under vacuum up to 260°C affords the *trans*-cyclohexene carbonate in good yield.
- 7 Center for Education and Research on Macromolecules (CERM), Liège, Belgium.
- 8 Rivaton, A.; Mailhot, B.; Soulestin, J.; Varghese, H.; Gardette, J. L. *Polym. Degrad. Stab.* **2002**, *75*, 17.
- 9 (a) Ulmer, L.; Mattay, J.; Torres-Garcia, H. G.; Luftmann, H. *Eur. J. Mass Spectrom.* **2000**, *6*, 49. (b) Brown, T.; Clipston, N. L.; Simjee, N.; Luftmann, H.; Hungerbühler, H.; Drewello, T. *Int. J. Mass Spectrom.* **2001**, *210/211*, 249.

Chapter 7

Epilogue and technology assessment

Today, many groups are active in the field of aliphatic polycarbonates and the literature provides evidence for a broad interest in this type of polymer. Research focuses mainly on finding more active and more selective catalysts for the copolymerization of CO₂ and several epoxides. Where TOFs between 1 and 10 h⁻¹ were reported a few decades ago, nowadays, with the development of highly active catalysts, TOFs of over 2000 h⁻¹ can be reached (mol monomer · mol catalyst⁻¹ · h⁻¹). However, as high as these values may seem, they pale in comparison with the current state of the art catalysts for polyolefin production, which exhibit activities generally two orders of magnitude higher. The development of more active catalysts for the copolymerization of oxiranes with CO₂ should increase the commercial potential of these aliphatic polycarbonates.

A more positive development is the reduction of the CO₂ pressures required for optimal activity and selectivity. Nowadays catalysts can operate highly efficient at a pressure of only 10 bar, compared to pressures up to 135 bar for earlier reported catalysts. Recently, even a catalyst that is active at ambient pressures has been mentioned. The research described in this thesis focuses on (i) the mechanistic aspects, (ii) the use of homogeneous model systems for silica surface silanol sites and (iii) the search for new monomers and application areas. As the reader probably observed reading this thesis, several ‘open ends’ are still present and the most obvious ones will be discussed next.

The silsesquioxane zinc complexes, described in chapter 3, form an interesting new class of catalysts and can be used as model compounds in developing silica-supported catalysts for the production of aliphatic polycarbonates. Several polymerizations were performed with ZnEt₂ modified silica particles, and \bar{M}_n and \bar{M}_w values were comparable to the polymers obtained with their homogeneous silsesquioxane zinc analogues. Some difficulties concerning the formation of sticky particles and relatively low conversions still need to be solved, but with this heterogeneous system a slurry-based process could be developed, in close collaboration with the Process Development Group at the TU/e. The preliminary results obtained using this process look promising for possible industrial applications. Of course, this is only becomes relevant when an useful commercial application for aliphatic polycarbonates is found.

As far as the mechanistic investigations on the synthesis of poly(cyclohexene carbonate) (PCHC) are concerned, we clearly demonstrated that things are often more complicated than originally anticipated (chapter 4 and 5). Side reactions, chain transfer reactions and even chain coupling reactions can, under specific circumstances, lead to a more complex polymerization behavior than predicted beforehand. The addition of functional groups to the oxirane monomers can lead to even more exotic behavior like the formation of rings or loops. A step was made in the identification of side reactions when β -diketiminato zinc complexes and bis(phenoxy) zinc catalysts were used. Although the exact nature of the species responsible for the formation of cyclopentyl, cyclohexyl and cyclohexenyl end groups is still unknown, the latter two end groups are most probably the result of a subtle interplay between a zinc catalyzed oxirane rearrangement reaction and a Meerwein-Ponndorf-Verley reduction/Oppenauer oxidation (MPVO) rearrangement.

Unfortunately, reports on the development of practical applications of aliphatic polycarbonates of the type studied in this thesis are rather scarce. As was demonstrated in chapter 6 the future of PCHC is probably not in the area of engineering plastics due to the brittleness of the polymer. On the other hand, the use of PCHC in coating applications looks promising, since physical properties that are important for coatings, such as modulus, scratch resistance and gloss are excellent. Glossy, transparent coatings with a high modulus could be obtained by crosslinking low molecular weight, alpha, omega hydroxy difunctionalized PCHC. As these were only preliminary results, optimization of the formulation and curing conditions should lead to further improvements as far as solvent and impact resistance are concerned. With respect to more common semi-aromatic polyester based coatings, the PCHC-based coatings are expected to exhibit a higher toughness and a better hydrolytic stability, as well as a better outdoor performance.

For all foreseen applications, the fact that the CO₂ monomer is cheap, non-toxic, readily available and, last but not least, renewable is a major advantage.

Appendix A

Lab scale reactor setup

A-1 Introduction

Most of the polymerizations carried out during this research project were performed in a Hastelloy reactor from Premex Reactor AG¹ with an internal volume of 380 mL (Figure A-1). The autoclave can withstand pressures up to 150 bar and temperatures up to 250 °C. One of the two available reactor vessels is equipped with sapphire windows to facilitate visual inspection during polymerizations. Both reactor vessels have a heavy duty needle valve located at the bottom, which allows sample collection during polymerization. Stirring is provided via a turbine stirrer with a hollow shaft. A separate vessel (40 mL) can be used for the injection of catalysts, monomers or other components at the beginning or during the polymerization, even when the reactor is pressurized.

The first part of this project involved the construction of the reactor, the supporting infrastructure and the development of a software environment for controlling and logging of the reactions parameters.

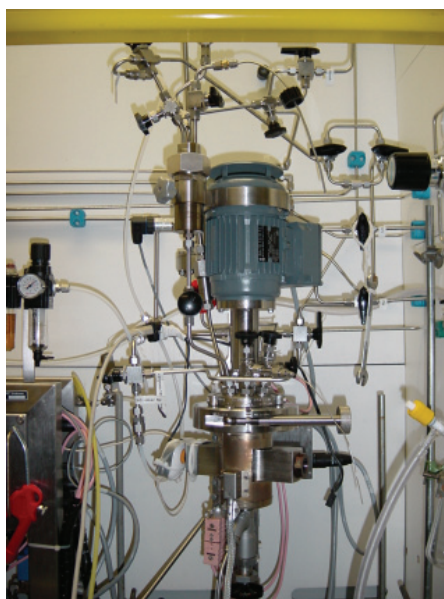


Figure A-1. Lab scale autoclave.

Two heating elements, one located in the reactor vessel and one in the lid, control the internal temperature. Vacuum is provided with an Edwards rotary oil pump (type 5). A schematic picture of

the reactor setup including the infrastructure for gasses (N₂ and CO₂) and vacuum lines is shown in (Figure A-2). A high pressure Sitec² pump is installed to provide pressures up to 150 bar.

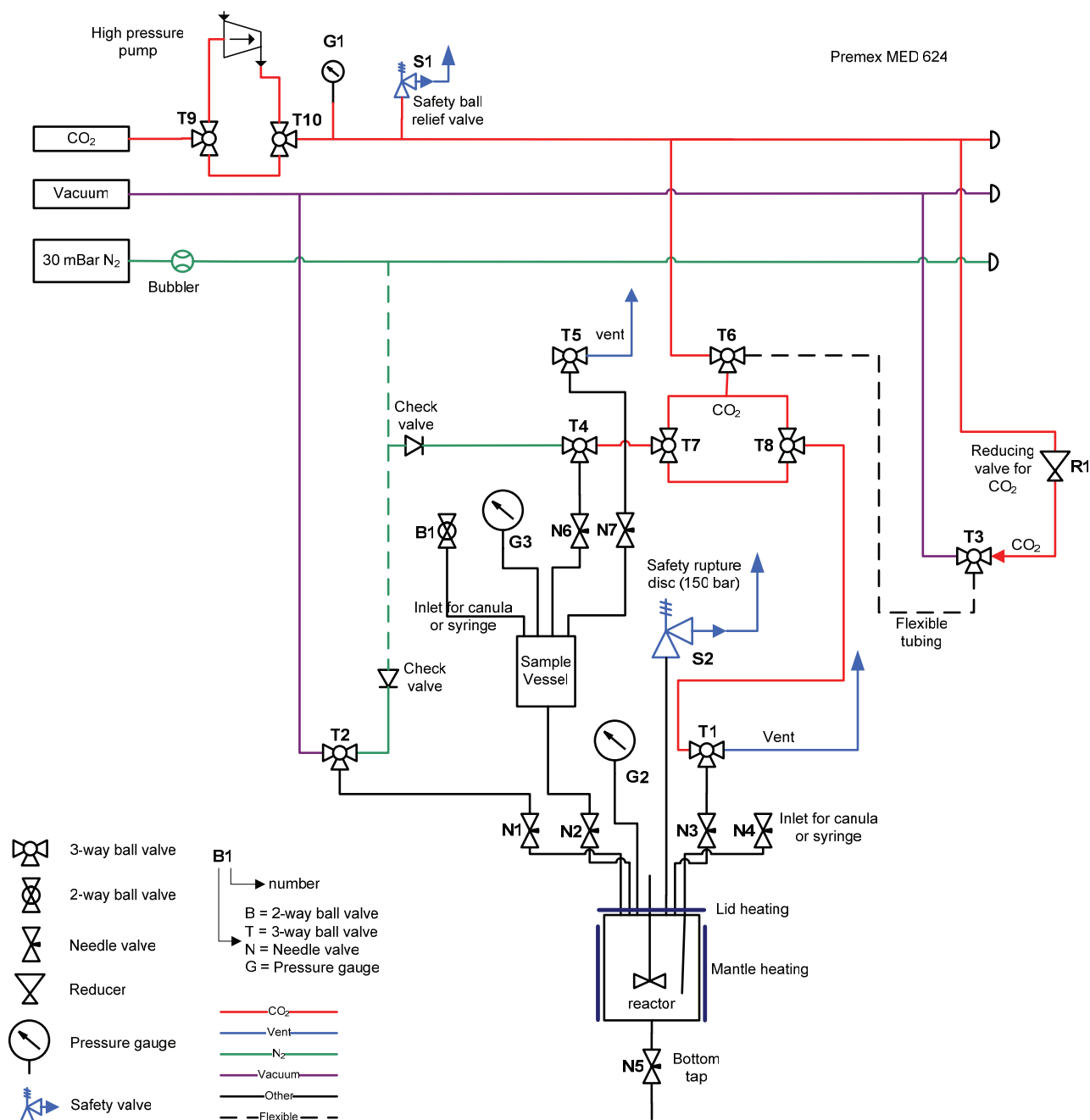
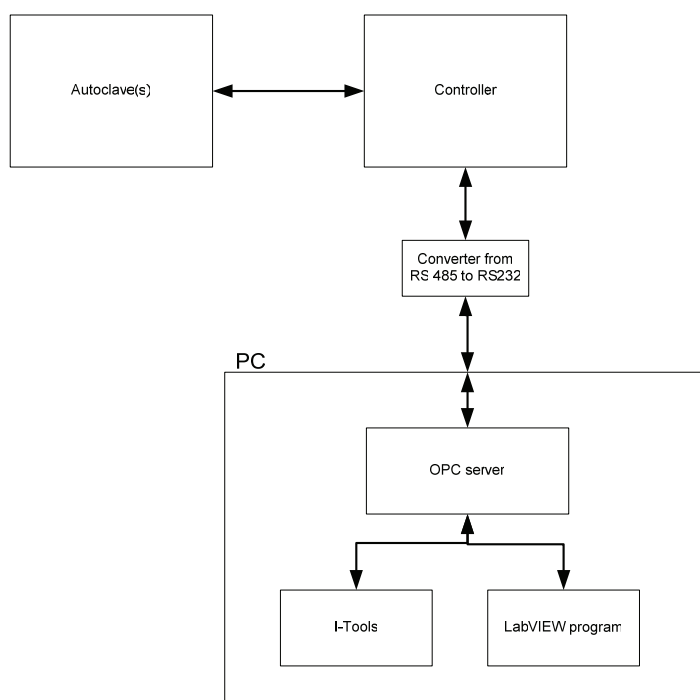


Figure A-2. Schematic representation of the reactor setup.

A-2 Communication and software setup

A schematic setup of the communication between reactor, controller and computer is depicted in Scheme A-1.



Scheme A-1. Schematic setup of communication between reactor controller and computer.

The reactor is primarily controlled with a controller build by ProControl³. The controller in turn is connected to a computer via a serial cable and a protocol adapter (conversion of RS-485 to RS-232). An OPC server⁴ included in the iTools software package⁵ and provides an easy interface for external programs to the controller.

A-3 LabVIEW

The graphical programming environment LabVIEW was used to create a user friendly interface with options for programming temperature profiles and the logging of reaction parameters (time, pressure and temperature). All logged data points can be imported easily in MSExcel via a visual basic macro. The functionality of the LabVIEW controller program is divided over 5 tabs and is described in Table A-1. As an example, a screenshot of the 'reactor' tab is shown in Figure A-3.

Table A-1. Overview of the different functions in the LabVIEW controller program.

Tab label	Description
Experiment	In this tab a user can enter experimental data like the amount of catalyst and monomer.
Programmer	In this tab different temperature profiles can be viewed and created
Control	Users can select a certain temperature profile and start/stop it. The logging options are also present in this tab
Reactor	A graphical representation of the most important parameters like temperature, pressure and stirring speed.
Graphs	Graphs including the temperature and pressure profile.

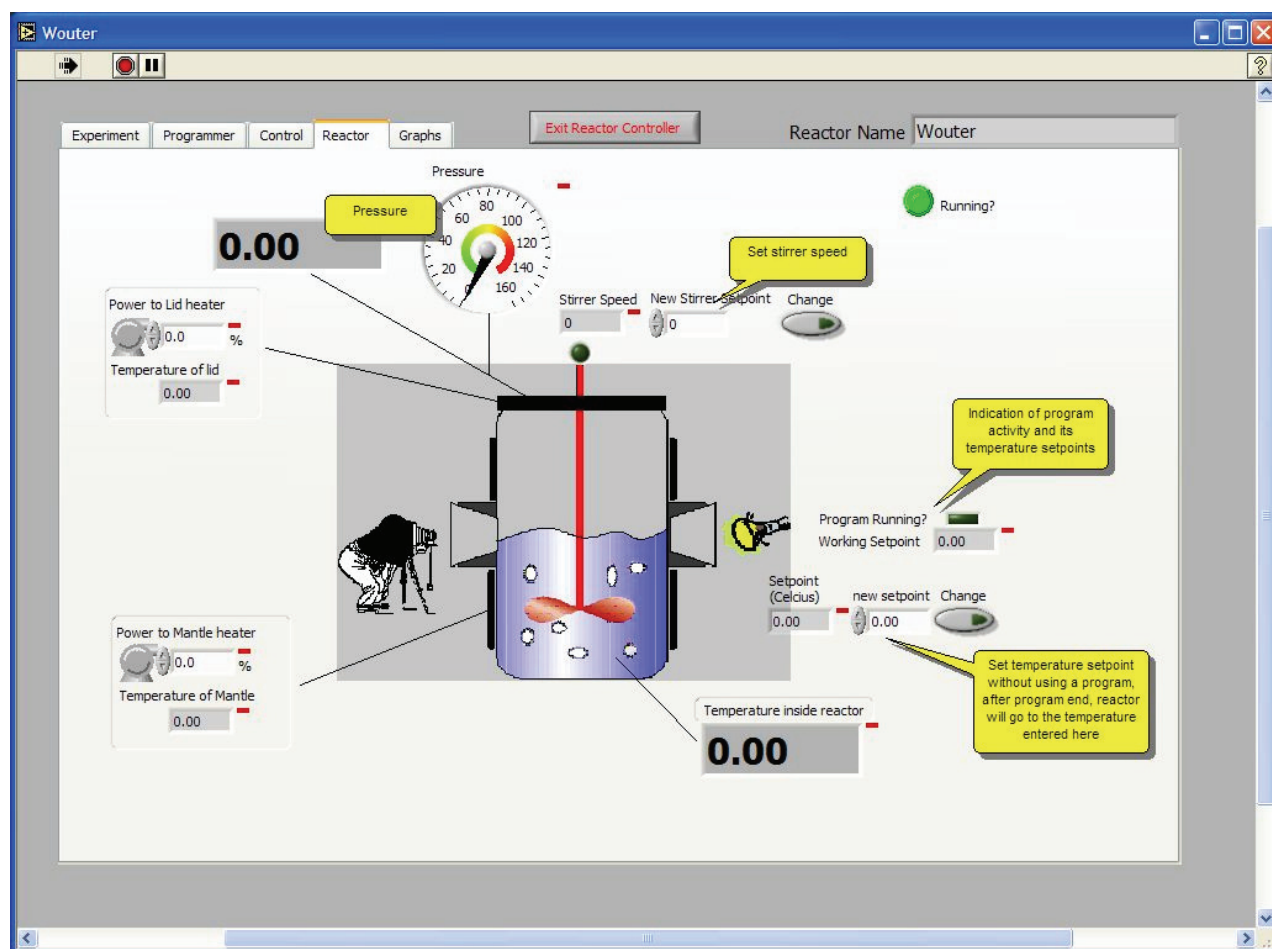


Figure A-3. Screenshot of the 'reactor' tab.

A-4 Webcam

A webcam can be mounted in front of the sapphire window to provide a visual monitoring tool that can be used to detect phase transitions or clouding of the reaction mixture during polymerizations.

A-5 References

- 1 De Heer B.V., C.L.A. de Heer, hebe@planet.nl, Tel: +31(0)72-5321733, Fax: 31(0)72-5337433.
- 2 SITEC-Sieber Engineering AG, <http://www.sitec-hp.ch/SITEC/index.htm>, sieber@sitec-hp.ch, Tel: +41 (0)1 982 2070, Fax: +41 (0)1 982 2079.
- 3 ProControl process automatisering, J. de Jong, procontrol@planet.nl, Tel: +31(0)75-6224791, Fax: +31(0)75-6226164.
- 4 OLE (Object Linking and Embedding) for Process Control.
- 5 Eurotherm BV Nederland, www.eurotherm.nl, info@eurotherm.nl, Tel. +31(0)172-411752, Fax: +31(0)172-417260.

Summary

The main goals of the work described in this thesis were (i) the development of a better insight into the mechanism of the oxirane-CO₂ copolymerization to aliphatic polycarbonates, (ii) to obtain polycarbonates with desirable physical properties by altering the oxirane-monomer and (iii) to attempt to develop a feasible process for this polymerization reaction in cooperation with the Process Development Group (TU/e). The copolymerization of carbon dioxide and cyclohexene oxide to poly(cyclohexene carbonate) (PCHC) was used to investigate the mechanistic aspects of the zinc catalyzed oxirane-CO₂ copolymerization. Despite the significant amount of research already done on copolymerizations of oxiranes and CO₂ (see chapter 2), several intriguing questions still remained unanswered. The lack of conformity in copolymerization behavior observed for the different classes of catalysts as well as the exact mechanism of copolymerization were both still puzzles waiting to be solved. With the work described in this thesis, a clarified picture of the copolymerization processes has evolved.

In chapter 3 the use of silsesquioxane zinc complexes for the copolymerization of CO₂ and cyclohexene oxide is described. This new class of catalysts was active and, under the right conditions, almost perfectly alternating PCHC could be obtained. These silsesquioxane zinc compounds are model compounds for silica supported catalysts and polymerizations with ZnEt₂-treated silica particles in a precipitation polymerization resulted in polymer particles with \overline{M}_n and \overline{M}_w values comparable to the polymers obtained with their homogeneous silsesquioxane zinc analogues. In a separate but related study performed in collaboration with Marcus van Schilt (Process Development Group, TU/e), it was further demonstrated that CO₂ consumption can be followed on-line by monitoring the decrease of system pressure during the reaction. CO₂ consumption was successfully interpreted in relation to both polycarbonate and cyclic carbonate formation (chapter 3).

As described in chapter 4, we initially looked at the use of high throughput equipment to assist us in our research. Two, reported living, β -diketiminato zinc complexes were tested for their activity at different catalyst concentrations using high throughput equipment. Molecular weights, polydispersities and activities were found to be comparable to literature values, but an unexpected deviation was discovered between the found \overline{M}_n development versus conversion and the calculated values, which initiated a thorough mechanistic study. The mechanistic investigation led to some surprising insights and initiation, propagation and termination reactions were identified by

analyzing the MALDI-ToF-MS spectra of the resulting polymers in detail. Furthermore, a very rapid reversible chain transfer mechanism (relative to propagation) with alcohols and/or hydroxyl terminated polymer chains was found, avoiding the limitation of the production of only one chain per catalyst.

In chapter 5 the search for alternative monomers for the production of aliphatic polycarbonates is described. Compared to the commonly used cyclohexene oxide, small variations in the ring size were found to have a large negative influence on activity and selectivity. Modifications of the cyclohexyl ring of the cyclohexene oxide monomer were performed with ester and amide groups and these new monomers were tested in copolymerization reactions with CO₂. The ester functionalized monomers could be copolymerized with CO₂, but side reactions with the functional groups limited the molecular weights that could be obtained. Interestingly, these side reactions, consisting of transesterification of the growing chain and the ester functionality, led to the formation of loops (or rings) and chain coupling, as was observed in MALDI-ToF-MS spectra. The amide functionalized monomers were more difficult to purify and traces of *m*-chlorobenzoic acid led to a substantial amount of side reactions. Also, some long alkyl chain modified epoxides were homo- and copolymerized with different catalysts leading to interesting polymer microstructures.

In chapter 6 a closer look was taken at the physical properties of PCHC. It is clear that PCHC cannot compete with the commercially available poly(bisphenol-A carbonate) (BA-PC) with respect to thermal properties and toughness. PCHC is simply too brittle to be used as an engineering plastic without modification. With respect to other physical properties, like modulus, yield point, scratch resistance and transparency, PCHC performed better than BA-PC. These properties make PCHC resins excellent coating precursors and several coatings were prepared by curing low molecular weight, difunctional hydroxyl end capped PCHC with a crosslinker. Glossy and transparent coatings were obtained, but a more thorough evaluation of their properties is still ongoing and could not be included in this thesis.

Finally, in chapter 7 the most important results obtained during this study are critically evaluated in the form of a technology assessment.

Samenvatting

De hoofddoelen van dit werk zoals beschreven in dit proefschrift zijn: (i) het ontwikkelen van een beter inzicht in het mechanisme van de copolymerisatie van oxiranen en CO₂ tot alifatische polycarbonaten, (ii) het verkrijgen van polycarbonaten met wenselijke fysische eigenschappen door het modificeren van het oxiraan monomeer en (iii) het proberen te ontwikkelen van een haalbaar proces voor deze polymerisatie reactie in samenwerking met de Process Development Group (TU/e). De copolymerisatie van koolstofdioxide en cyclohexeen oxide tot poly(cyclohexeen carbonaat) (PCHC) werd gebruikt om de mechanistische aspecten van de zink gekatalyseerde oxiraan – CO₂ copolymerisatie te onderzoeken. Ondanks het feit dat er al een aanzienlijke hoeveelheid onderzoek is gedaan op het gebied van copolymerisaties van oxiranen en CO₂ (zie hoofdstuk 2), bleven tot op heden verschillende intrigerende vragen onbeantwoord. Het gebrek aan eenheid in copolymerisatie gedrag gezien bij de verschillende katalysatorclassen, evenals het exacte mechanisme van copolymerisatie, waren beide puzzels die nog moesten worden opgelost. Met het werk zoals beschreven in dit proefschrift is er een duidelijker plaatje van de copolymerisatie processen ontstaan.

In hoofdstuk 3 wordt het gebruik van silsesquioxaan gebaseerde zinkcomplexen in de copolymerisatie van CO₂ en cyclohexeen oxide beschreven. Deze nieuwe katalysatorklasse was actief en, onder de juiste condities, kon bijna perfect alternerend PCHC worden verkregen. De silsesquioxaan zinkcomplexen zijn model verbindingen voor silica ondersteunde katalysatoren en polymerisaties met ZnEt₂ – bewerkte silicadeeltjes in precipitatiepolymerisaties resulteerden in polymeerdeeltjes met \overline{M}_n en \overline{M}_w waarden die vergelijkbaar zijn met de polymeren verkregen met behulp van hun homogene silsesquioxane zinkanalogen.

In een aparte maar gerelateerde studie die werd gedaan in samenwerking met Marcus van Schilt (Process Development Group (TU/e)) werd het verder aangetoond dat CO₂ consumptie online kan worden gevolgd door de systeemdrukvermindering tijdens de reactie te volgen. CO₂ consumptie werd succesvol vertaald naar een relatie met zowel de vorming van polycarbonaat als cyclisch carbonaat (hoofdstuk 3).

Zoals beschreven in hoofdstuk 4, hebben we in het begin gekeken naar het gebruik van high throughput apparatuur om ons te assisteren bij ons onderzoek. Twee, gerapporteerd levende, β -diketiminato zinkcomplexen werden getest op hun activiteit bij verschillende katalysatorconcentraties, gebruikmakend van high throughput apparatuur. Er werd gevonden dat molekulgewichten, polydispersiteiten en activiteiten vergelijkbaar zijn met literatuurwaarden, maar

een onverwachte afwijking werd gevonden tussen de waargenomen \overline{M}_n ontwikkeling versus conversie en de berekende waarden, wat uitmondde in een gedetailleerde mechanistische studie. Het mechanistische onderzoek leidde tot enkele onverwachte inzichten en naast de verwachte initiatie-, propagatie- en terminatiereacties werden enkele nevenreacties geïdentificeerd met behulp van een gedetailleerde analyse van de MALDI-ToF-MS spectra van de verkregen polymeren. Verder werd een zeer snel, reversibel ketenoverdachtsmechanisme (relatief ten opzichte van de propagatiereactie) met alcoholen en/of polymere ketens met eindstandige hydroxy groepen gevonden, wat de beperking van de productie van maar een keten per katalysator ophief.

In hoofdstuk 5 wordt de zoektocht naar alternatieve monomeren voor de productie van alifatische polycarbonaten beschreven. Er werd gevonden dat kleine variaties in de grootte van de ring een grote negatieve invloed hebben op activiteit en selectiviteit, vergeleken met het gewoonlijk gebruikte cyclohexeen oxide. Het cyclohexeenoxidemonomeer werd gemodificeerd door middel van het aanbrengen van ester en amide groepen op de cyclohexylring en deze nieuwe monomeren werden getest in copolymerisatiereacties met CO₂. De ester gefunctionaliseerde monomeren konden worden gecopolymeriseerd met CO₂, maar nevenreacties met de functionele groepen beperkten de molekulgewichten die konden worden gekregen. Interessant genoeg, leidde deze nevenreacties, bestaande uit omestering van de groeiende keten en de esterfunctionaliteit, leidde tot de vorming van lussen (of ringen) en ketenkoppeling, zoals werd gezien met behulp van MALDI-ToF-MS spectra. De amide gefunctionaliseerde monomeren waren moeilijker te zuiveren en sporen van *m*-chlorobenzoëzuur leidde tot een substantiële hoeveelheid nevenreacties. Ook werden enkele epoxiden die gemodificeerd waren met alkyl ketens gehomopolymeriseerd evenals gecopolymeriseerd met verschillende katalysatoren wat leidde interessante polymere microstructuren.

In hoofdstuk 6 werden de fysische eigenschappen van PCHC nader bekeken. Het is duidelijk dat PCHC, in een directe vergelijking wat betreft thermische eigenschappen en taaiheid, niet is opgewassen tegen het commercieel beschikbare poly(bisphenol-A carbonaat) (BA-PC). PCHC is eenvoudigweg te bros om zonder modificatie te worden gebruikt als een technische kunststof. Wat betreft de andere fysische eigenschappen zoals modulus, vloeipunt, krasvastheid en transparantie presteerde PCHC beter dan BA-PC. Deze eigenschappen maken dat PCHC harsen uitstekende uitgangsstoffen zijn voor coatings en verschillende coatings werden gemaakt door het uitharden van laag moleculair PCHC met aan beide uiteinden een hydroxy groep met een crosslinker. Glanzende en transparante coatings werden verkregen, maar een uitgebreidere evaluatie van hun eigenschappen wordt momenteel uitgevoerd en kon niet worden opgenomen in dit proefschrift.

Tot slot worden in hoofdstuk 7 de belangrijkste resultaten, die verkregen zijn tijdens deze studie, kritisch geëvalueerd in de vorm van een technologische beoordeling.

Dankwoord

Na iets meer dan 4 jaar is er (bijna) een einde gekomen aan dit Brabantse avontuur wat ongetwijfeld heel anders was afgelopen zonder de hulp van een heleboel mensen. Bij dezen zal ik een poging doen om iedereen te bedanken en ik hoop niemand te vergeten. Mocht dat wel zo zijn, dan ligt dat niet aan het feit dat ik ondankbaar ben, maar zegt het meer iets over mijn geheugen. Hierbij wil ik ook het Dutch Polymer Institute (DPI) bedanken voor de financiële steun en mijn industriële contactpersonen, tezamen met de overige DPI mensen, voor de nuttige tips en discussies bij de verschillende presentaties en bijeenkomsten. Ook NOVEM wil ik bedanken voor hun ondersteuning in dit samenwerkingsverband van DPI en NOVEM.

Als allereerste wil ik natuurlijk prof. Cor Koning bedanken voor de mogelijkheid om te kunnen promoveren in zijn groep. Cor, je hebt me geleerd met een nuchtere blik op de zaken te kijken en met de focus op het einddoel te voorkomen dat je te veel laat meeslepen in details. Ook mijn 2^e promotor, prof. Gert-Jan Gruter, wil ik hierbij bedanken, o.a. voor de mogelijkheid om bij Avantium de ‘high throughput’ proeven te kunnen doen.

Hierbij wil ook Rob Duchateau een grote veer geven voor de goede begeleiding tijdens het onderzoek. Rob, je nooit aflatende enthousiasme en je overvloed aan ideeën hebben een grote stempel op mezelf en het onderzoek gedrukt. Ik zal de vele discussies over de chemie, programmeren en andere zaken zeker missen al zullen we er in de toekomst nog vast wel gelegenheid toe hebben!

I would also like to thank the members of my reading committee: prof.dr. Cor Koning, dr. Rob Duchateau, prof.dr Gert-Jan Gruter, prof.dr.ir. Jos Keurentjes, prof.dr. Bart Hessen en prof.dr. Robert Jérôme.

I think I was very fortunate to be able to do my promotion in the SPC group! Everybody thanks for the good time. Of course I also want to mention and thank a long list of “office mates” with whom I had the pleasure to share the office over the last 4 years. Raf, Jesse, Rajan, Jens, Jelena, Rutger, Saskia, Nicolas, Jenny and David; thanks for the company, suggestions, discussion and sometimes outright hilarious moments in the office. I’ll never forget my first day, sitting quietly at my new desk when, suddenly, Raf shouts: “Stupid Indian”, while the Indian in question replies dryly: “stupid Belg”. Needless to say I was speechless....

I wil hier natuurlijk ook even stil staan bij mijn ‘partners in programming’ Maarten en Rob voor het database project en Robin en Bas voor de Maldy Analyse software. Vooral de database is een wat uit de hand gelopen hobby geworden met bijbehorende gevoelens van plezier (het maken),

frustraties (het debuggen) en voldoening (het dagelijks in gebruik zien en verkopen van het pakket). Ook de soms lange discussies en avonden met Bas om een werkbare versie van het Maldi Analyse programma voor elkaar te krijgen waren vaak plezierig en soms erg ‘uitdagend’.

Verder heb ik zeer prettig samengewerkt met Marcus van Schilt die de andere helft van dit project vormde. De mix van processkunde en chemie leverde altijd leuke discussies op! Samen met de andere leden van het CO₂ overleg (Rob, Cor, Jos, Maartje, Magda en Martin) hebben we altijd plezierig overlegd.

Of course I won't forget the people of the 'Cactus' lab! Jesse, John, Rachel, Kirti, Joep, Stéphanie, Soazig, Madri, Rafael, Rubin, Nilesh, Saeid, the occasional visitors and students; Thanks for the help and the great atmosphere in the lab!

Andere mensen die een special plekje hier krijgen voor de hulp bij het analyseren van de vele monsters zijn natuurlijk Wieb en Marion. Ook wil ik Bas en Robin hier bedanken voor de hulp bij de interpretatie van de MALDI-ToF-MS spectra. Ton Staring wordt bedankt voor de hulp bij de GC-MS analyses. Leon Govaert, Jules Kierkels, Peter Koets en Han Goossens wil ik hierbij bedanken voor de hulp en adviezen bij de fysische metingen. Ook wil ik hierbij Wouter Gerritsen (technische ondersteuning), Caroline, Helly en Pleunie (administratieve ondersteuning) bedanken.

Hierbij wil ook mijn twee studenten Rob Verlinden en Latifa Yajjou bedanken voor hun bijdrage aan hoofdstuk 5. Jullie hadden niet de makkelijkste projecten, maar het heeft uiteindelijk toch een leuk resultaat opgeleverd!

Ook mijn familie en verdere vrienden wil ik natuurlijk bedanken voor hun ondersteuning en begrip als ik weer eens wat te weinig aandacht voor jullie had. Ten slotte wil ik mijn lieve Renske hier bedanken. Wij hebben het niet altijd even gemakkelijk gehad de laatste jaren, jij met je octrooi-opleiding en ik met mijn promotie, maar samen zijn we er wel mooi doorheen gerold!

Wouter

Curriculum Vitae

Wouter van Meerendonk werd geboren op 1 mei 1977 te Amersfoort. Aan de scholengemeenschap De Waezenburg te Leek haalde hij in 1995 zijn VWO diploma waarna hij datzelfde jaar begon met de studie scheikunde aan de Rijksuniversiteit Groningen. In 2000 volgde een stage van 6 maanden bij Montell in Amsterdam en op 29 maart 2001 legde hij met succes het doctoraalexamen af. Per 1 juni 2001 startte hij zijn werkzaamheden als promovendus aan de Technische Universiteit Eindhoven onder de begeleiding van Prof. dr. C.E. Koning en dr. R. Duchateau.

Scientific papers

- van Meerendonk, W. J.; Schroder, K.; Brussee, E. A. C.; Meetsma, A.; Hessen, B.; Teuben, J. H. "Chloro- and alkyltitanium complexes of a new dianionic ancillary ligand: A linked amidinate-amide" *Eur. J. Inorg. Chem.* **2003**, 427-432.
- van Meerendonk, W. J.; Duchateau, R.; Koning, C. E.; Gruter, G.-J. M. "High-throughput automated parallel evaluation of zinc-based catalysts for the copolymerization of CHO and CO₂ to polycarbonates." *Macromol. Rapid Commun.* **2004**, 25, 382-386.
- van Schilt, M. A.; Wering, R. M.; van Meerendonk, W. J.; Kemmere, M. F.; Keurentjes, J. T. F.; Kleiner, M.; Sadowski, G.; de Loos, T. W. "High-Pressure Phase Behavior of the System PCHC-CHO-CO₂ for the Development of a Solvent-Free Alternative toward Polycarbonate Production." *Ind. Eng. Chem. Res.* **2005**, 44, 3363-3366.
- van Meerendonk, W. J.; Duchateau, R.; Koning, C. E.; Gruter, G.-J. M. "Unexpected Side Reactions and Chain Transfer for Zinc Catalyzed Copolymerization of Cyclohexene Oxide and Carbon Dioxide." *Macromolecules* **2005**, 38, 7306 – 7313.
- van Meerendonk, W. J.; Yajjou, L.; Duchateau, R.; Koning, C. E.; Gruter, G.-J. M. "Functionalized Cyclohexene Oxide Monomers in the Copolymerization of Cyclohexene Oxide and Carbon Dioxide." *to be submitted*.